

**THE MODIFICATION OF SUPPORTED  
PALLADIUM AND NICKEL CATALYSTS FOR  
ASYMMETRIC HYDROGENATION**

**BY**

**NICOLA C. YOUNG**

**A THESIS SUBMITTED FOR THE DEGREE OF DOCTOR OF  
PHILOSOPHY OF THE UNIVERSITY OF GLASGOW.**

**DEPARTMENT OF CHEMISTRY, OCTOBER 1995.**

© NICOLA YOUNG 1995.

ProQuest Number: 13833438

All rights reserved

INFORMATION TO ALL USERS

The quality of this reproduction is dependent upon the quality of the copy submitted.

In the unlikely event that the author did not send a complete manuscript and there are missing pages, these will be noted. Also, if material had to be removed, a note will indicate the deletion.



ProQuest 13833438

Published by ProQuest LLC (2019). Copyright of the Dissertation is held by the Author.

All rights reserved.

This work is protected against unauthorized copying under Title 17, United States Code  
Microform Edition © ProQuest LLC.

ProQuest LLC.  
789 East Eisenhower Parkway  
P.O. Box 1346  
Ann Arbor, MI 48106 – 1346

Theris  
10317  
Cup 1

TO  
MY FAMILY  
&  
ANDY



## ACKNOWLEDGEMENTS

With special thanks to Professor Webb for all his help, guidance and tolerance throughout the course of this research.

I am very grateful to the ICI/SRF/DTI Link scheme for providing the funding for this research and would like to thank all involved in this project, namely, Dr. E.Colvin, Mr.D.Hunter and Miss E.Allan at the University of Glasgow, Professor P.B.Wells, Dr.P.Johnston and Mr.S.R.Watson at the University of Hull, Dr. G.Robinson and Dr.W.Moss at Zeneca, Macclesfield, Dr.S.Korn at Zeneca, Huddersfield, Dr.A.Ibbotson, Dr.R.Sampson and, most importantly, Dr.S.D.Jackson at ICI Katalco, Billingham.

I am indebted to many members of staff and students at the University for their help and rapport, especially Vicky Yeats for all the electron micrographs and Rose Millar and David Kennedy for the splendid proof reading (and reviews). I would also like to thank my fellow students, past and present, for making my time at the University of Glasgow a most enjoyable experience.

Finally, thanks to all who I served alongside with on the 'Alchemist' council 1994-95 and what more can I say but 'Tequila'.

## SUMMARY

This thesis describes the study of asymmetric heterogeneous catalysis with the objective of developing new chiral solid surfaces which can be used to establish a more general framework for the generation of chiral centres on heterogeneous catalyst surfaces.

To this end the adsorption of a family of binaphthalene derivatives, namely R- and S-2,2'-dihydroxybinaphthalene, ( $\pm$ )-dimethoxybinaphthalene and R- and S-2,2'-diaminobinaphthalene, have been studied as potential chiral modifiers. The results show that the amount of modifier adsorbed is dependent on the initial concentration of the modifier in the modifying solution and the time of modification. Both the dihydroxybinaphthalene and diaminobinaphthalene modifiers are strongly adsorbed on to Ni/silica, Pd/silica and Pd/carbon catalysts. The extent of adsorption is different for the different modifiers and varies between the metals. The dimethoxybinaphthalene modifier was only adsorbed by the Pd/carbon catalyst. In separate experiments, using the support materials themselves, evidence has been obtained for the direct adsorption of the modifiers on to the carbon, but not on to the silica. From studies of the effects of washing, following the modification, it is apparent that a small proportion of the modifier that is adsorbed on the metal and most of the modifier which is adsorbed on the support is only weakly adsorbed. These results are interpreted as a strong dissociative adsorption via the O-H or the N-H groups on to the metal surfaces resulting in the binaphthyl modifiers being orientated on the surface in a 'near vertical' mode, with the naphthalene ring units directed up and away from the surface. It is proposed that adsorption on the carbon support is through a weak interaction between the naphthyl rings of the modifier and the support surface to orientate the binaphthyl molecule in a 'horizontal' mode.

All the catalysts modified with R- and S- forms of the dihydroxy and diaminobinaphthyls have been screened for enantioselectivity in the hydrogenation of methyl tiglate, tiglic acid and 3-coumaranone at atmospheric pressure and temperatures in the range 0 - 25°C. The palladium catalysts are active for the reduction of methyl tiglate, however, no enantiomeric excesses have been attained, although appreciable isomerisation of the methyl tiglate to methyl angelate was observed.

Tiglic acid and 3-coumaranone have been hydrogenated enantioselectivity over the R- and S-2,2'-diaminobinaphthyl modified palladium catalysts, with the two modifiers clearly directing the reaction in opposite directions. Enantiomeric excesses up to 13% and 19% were obtained for the respective substrates. Moderate enantioselectivity (7%) was also achieved for the hydrogenation of tiglic acid with the diaminobinaphthyl modified nickel/silica catalyst. Chiral direction is imparted to these reactions only when the diaminobinaphthyl modifier is present.

A mechanism is proposed in which the prochiral reactant is adsorbed at the modified surface by forming a surface complex with the diaminobinaphthalene modifier involving two recognition sites, namely a  $\pi$ - $\pi$  stacking interaction and hydrogen bonding. The  $\pi$ -system of the substrate is aligned over one naphthalene ring to allow a  $\pi$ - $\pi$  stacking interaction to occur, binding the reactant to the modifier. In addition, with the prochiral substrate in the correct orientation, an additional -N--H--O- hydrogen bonding interaction can be established between the substituent of the modifier and the C-O of the substrate to further stabilise the reactant. The steric influence only establishes the specific orientation of the co-adsorbed species. Subsequent hydrogenation is then controlled by orbital symmetry limitations which will only allow a *cis*-addition of the hydrogen to the open face of the unsaturated bond which results in the observed enantiodifferentiation.

## LIST OF CONTENTS

	<u>PAGE</u>
<b>CHAPTER 1: INTRODUCTION</b>	
1.1 HETEROGENEOUS CATALYSIS.	1
1.2 STEREOCHEMISTRY	8
1.3 IMPORTANCE OF CHIRALITY.	21
1.4 SYNTHESIS OF OPTICALLY ACTIVE COMPOUNDS.	22
1.5 CHIRAL ANALYSIS.	39
<b>CHAPTER 2: OBJECTIVES OF STUDY</b>	49
<b>CHAPTER 3: EXPERIMENTAL</b>	
3.1 INTRODUCTION.	51
3.2 PREPARATION	52
3.3 CHARACTERISATION	54
3.4 CATALYST ACTIVATION.	62
3.5 PRELIMINARY Ni/GRACE SILICA CATALYST WASH.	63
3.6 HIGH PERFORMANCE LIQUID CHROMATOGRAPHY.	64
3.7 ADSORPTION STUDIES.	71
3.8 POLARIMETRY.	72
3.9 HYDROGENATION.	73
3.10 CHIRAL GAS CHROMATOGRAPHY.	76
<b>CHAPTER 4: RESULTS.</b>	
4.1 INTRODUCTION	81
4.2 PREPARED CATALYSTS	81
4.3 CHARACTERISATION	84

	<u>PAGE</u>
4.4	ADSORPTION STUDIES. 89
4.5	ADSORPTION BY-PRODUCTS 127
4.6	RETENTION OF CHIRALITY. 138
4.7	COLOURATION OF MODIFIER SOLUTIONS. 138
4.8	CATALYST AGEING 140
4.9	REDUCTION PROBLEMS WITH Ni/GRACE SILICA CATALYSTS. 142
4.10	HYDROGENATION STUDIES. 143
4.11	BY-PRODUCTS FORMED DURING ESTER HYDROGENATIONS. 163
 <b>CHAPTER 5: DISCUSSION.</b>	
5.1	CHARACTERISATION 167
5.2	ADSORPTION STUDIES 172
5.3	ADSORPTION BY-PRODUCTS 185
5.4	COLOURATION OF MODIFIER SOLUTION 187
5.5	ASYMMETRIC HYDROGENATION 189
 <b>REFERENCES</b>	 204

---

**CHAPTER ONE**

**INTRODUCTION**

## 1.1: HETEROGENEOUS CATALYSIS

A great variety of hydrogenation reactions are carried out industrially with the aid of a heterogeneous catalyst. Such reactions range from large-scale, continuous catalytic operations in petroleum refineries, dealing with catalytic cracking, catalytic reforming and hydrodesulphurization, to small-scale batch operations in the pharmaceuticals and fine chemicals industry, where a very precise hydrogenation step is often desired. Asymmetric catalysis is a relatively small area in this large field of heterogeneous catalysis which is, however, a very important and rapidly advancing new area of research.

Even though there are a wide variety of enantioselective reactions promoted by chiral homogeneous catalysts, such reactions are not easily adapted to large scale liquid phase processes for use in industry. One of the problems is that the soluble catalyst must be separated from the product of the reaction, a process which frequently results in the destruction of the catalyst complex and the loss of the metal and chiral ligand, in addition to increased industrial costs through the incorporation of an additional processing stage. A solution to the separation problem is the use of heterogeneous catalysts which are normally much more robust, have better handling properties and can be removed from the reaction mixture by filtration or centrifugation and then, potentially reused. However when compared with a soluble chiral homogeneous system, with a molecularly defined catalytic species, a heterogeneous catalyst has an additional dimension that makes the system more complex. A homogeneous catalytic site is based on a single central metal atom, whereas a

heterogeneous catalyst has a non-uniform, extended metal surface which can have kinks, steps and other crystal imperfections. There is also the possible role of the support influencing the properties of the metal, a phenomenon called spillover, which will be discussed later.

For asymmetric activity, conventional supported metal catalysts, which possess no inherent chirality, can be modified to provide a chiral environment for subsequent asymmetric reactions. In general catalysis, in order to try and correlate catalyst behaviour with the specific properties of the catalyst, some methods of preliminary characterisation are required to provide an insight into the physical and chemical structure of the catalysts. Such techniques, mainly temperature programmed reduction, selective chemisorption and transmission electron microscopy, are commonly used for this purpose. Temperature-programmed reduction (TPR) has gained increasing importance since its first application by Robertson *et al.*<sup>1</sup> It is a highly sensitive technique which can be used to obtain the number of distinct, reducible species present in the catalyst, as well as information on the minimum temperature required to reduce the catalytic precursor. This reduction is often a very critical stage, because if it is not done correctly, the catalyst may sinter or may not reach its optimum state of reduction.

As chiral heterogeneous catalysts have been shown to be structure-sensitive, it is important to know the average particle sizes and the fraction of the metallic phase available for reaction. Traditionally metal catalysts were supported on an inert carrier, such as silica or alumina, to improve the metal dispersion and optimise the catalytic activity. However, with the best optical yields obtained with chiral heterogeneous

catalysts composed of large metal particles, a high dispersion was not necessary for this project. Selective chemisorption can be used to calculate the dispersion values and provide information on the number of surface metal sites. When a known volume of a sample gas is pulsed over an activated catalyst, a certain amount may be adsorbed. By calculating the amount of gas adsorbed, an indication of the number of surface metal sites can be obtained. This technique requires that the adsorbate forms a chemisorbed monolayer, that there is no significant contribution of the support to the chemisorption process and that a simple relationship exists between the number of molecules adsorbed and the number of surface atoms. Dispersion figures calculated by chemisorption methods are very fast, convenient, inexpensive and measure all particle sizes. However the drawbacks to this technique include a possible variation of adsorption stoichiometry with % dispersion, metal loading or preparation technique<sup>2</sup>, contamination<sup>3</sup> and adsorption suppression due to strong metal-support interactions.<sup>4</sup> Thus, as Farrauto pointed out<sup>5</sup>, a combination of chemisorption methods with at least one physical method, such as transmission electron microscopy (TEM), is necessary for an accurate determination of the metal particle size for a given catalyst system. TEM offers a means of directly observing the metal particles on the support and can provide particle size, size distribution and metal dispersion data for comparison with chemisorption measurements, which are essentially averaged data. In addition, particle shape can be examined as well as the spatial distribution of the particles throughout the support. The use of more than one characterisation method is essential for reliable conclusions.

Many other advanced techniques such as X-ray diffraction (XRD)

crystallography, to obtain information about the structure and composition of crystalline material, X-ray photoelectron spectroscopy (XPS), for information on elemental composition, and scanning electron microscopy (SEM), to examine the topology of the catalyst surface and the morphology of particles and crystals, to name but a few, are also available for a further, more detailed, catalyst characterisation but were outwith the main scope of this project.

Spillover can be a drawback during the characterisation of supported catalysts by selective chemisorption. Very often dihydrogen adsorption is used to determine surface areas, but if significant hydrogen spillover occurs then the amount of hydrogen adsorbed could give a false value for the surface area of the metallic component of the catalyst and the method becomes invalid. Hence  $H_2$  chemisorption should always be used in conjunction with an additional characterisation technique. Spillover involves the transport of an active species, adsorbed on an initial surface, on to another surface that would not normally adsorb this species under the same conditions.<sup>6</sup> Thus adsorbed species can gain access to a different phase (accepting surface) that is in contact with the original adsorbing and activating surface and as such spillover is an important phenomenon in adsorption and as a mechanistic step in heterogeneous catalysis. It is an additional process that is the result of a close interaction between the metal and the support of a catalyst. Dihydrogen can dissociatively adsorb on the metal phase and then surface diffuse across the metal particles as atomic hydrogen, to the interface with the support, where it can then spillover to this second surface and subsequently migrate across this surface also, figure 1.1.1. The support itself could not have independently adsorbed this hydrogen.

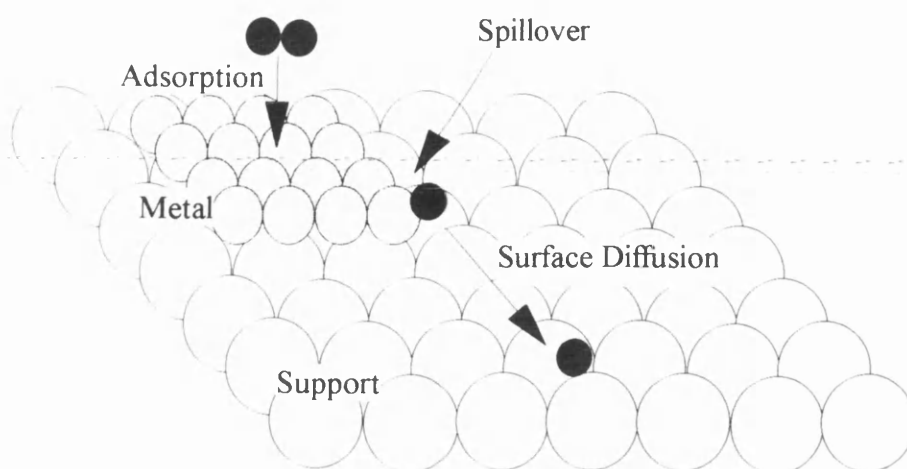


FIGURE 1.1.1. PROPOSED SCHEME FOR HYDROGEN SPILLOVER

In 1964 Khoobiar<sup>7</sup> showed that  $\text{WO}_3$  could be reduced to  $\text{H}_x\text{WO}_3$  with hydrogen at room temperature by mixing it mechanically with  $\text{Pt}/\text{Al}_2\text{O}_3$ . In the absence of  $\text{Pt}/\text{Al}_2\text{O}_3$ , temperatures above 500K were required. This brought attention to the process which was initially, chiefly observed using platinum or palladium as the metal and was predicted to be effective on other metals where hydrogen was not too strongly adsorbed. This is now known to be the case and a wide variety of transition metals have been investigated such as Rh, Ga and Zn.

Spillover occurs at the interface between adsorbing and accepting surfaces. This can be limited to the adjacent surface area of the accepting material or result in a long range effect. Surface diffusion of hydrogen is facilitated by hydroxyl groups on an

oxidic surface which help "pass" the hydrogen along.<sup>8</sup> Dramatic examples of such effects have been reported for spillover over millimetres or even centimetre distances.<sup>9</sup> Other workers have reported that the presence of water, alcohols and carbon could assist with the spillover process.<sup>10,11</sup> However no mechanism for transport between surfaces that are in physical contact has been clearly defined.

Several types of processes have been described that involve the participation of spillover in catalysis. The first systems that were detected were supported metals with hydrogen spillover from the metal to the support. Any hydrogen which spilled over was then able to reside on the surface of the support material for subsequent reaction or it could cause partial reduction of an oxidic support. In either of these states the spillover hydrogen had important implications and potential uses in catalysts. Other atomic species, specifically oxygen, were also found to spillover in a similar manner. The supports involved in this reaction have ranged from carbon surfaces to a wide variety of metal oxides, including ones such as  $\text{CeO}_2$  and  $\text{MnO}_3$ .

Although most studies of spillover have focused on H and O species, multiatom species have also been detected on supports as a result of spillover from a metal catalyst. Reactions of CO and  $\text{H}_2$  to form adsorbed species have been extensively studied because of the interest in methanation and Fischer-Tropsch synthesis. Infrared spectroscopy has been used to detect species such as formate ( $\text{CHOO}$ )<sup>12</sup> and methoxy ( $\text{CH}_3\text{O}$ )<sup>13</sup> that ended up on the support as a result of a spillover process when CO and  $\text{H}_2$  were present. Both these species were anchored via an oxygen substituent. The reaction of CO and NO on a metal catalyst forms isocyanate (NCO), which can also migrate to the support.<sup>14</sup> Once again infrared spectroscopy was used to distinguish between Pt-NCO and Si-NCO on a  $\text{Pt/SiO}_2$

catalyst. These studies have shown that molecular species can also be adsorbed on to additional support surfaces by a spillover mechanism, surfaces that would not normally have adsorbed such species independently. However the work in this area has been very limited and has not reported the spillover of any larger molecular entities.

Spillover is a reversible process, that is, a species that was residing on an accepting surface, and could not have been directly adsorbed, can diffuse back to and move on to the original source of spillover. This is termed 'reverse spillover' and indicates that once a molecular species has migrated to the support it can be returned, intact, to the metal phase, providing that it has not undergone a reaction. After reverse spillover, the species can recombine (if dissociated), react or desorb. Fujimoto<sup>15</sup> pointed out that during catalytic dehydrogenation on an oxidic surface H atoms form and, for the reaction to proceed, these atoms must be able to recombine and desorb as H<sub>2</sub>. For such a surface that could not directly adsorb dihydrogen this recombination and desorption may not take place or be very slow. It was shown that the addition of a metal, which was already known to adsorb H<sub>2</sub>, could accelerate the rate of dehydrogenation by providing sites for recombination and desorption via reverse spillover. Similarly, *iso*-pentane dehydrogenation to *iso*-pentenes or cyclohexane dehydrogenation to benzene on an active carbon surface can be accelerated by depositing a transition metal on the carbon surface.<sup>16</sup> At steady state, spillover involves competition between forward and reverse steps. If a change is made in the gas phase or solution such that the species spilling over is decreased in concentration or reacts with another species, then the concentration of activated species on the spillover source decreases and the concentration gradient is reversed. Reverse spillover will then act to re-establish an equilibrium.

## 1.2: STEREOCHEMISTRY

The science of organic chemistry is based on the relationship between molecular structure and properties. The area of science that deals with these structures in three dimensions is called stereochemistry.

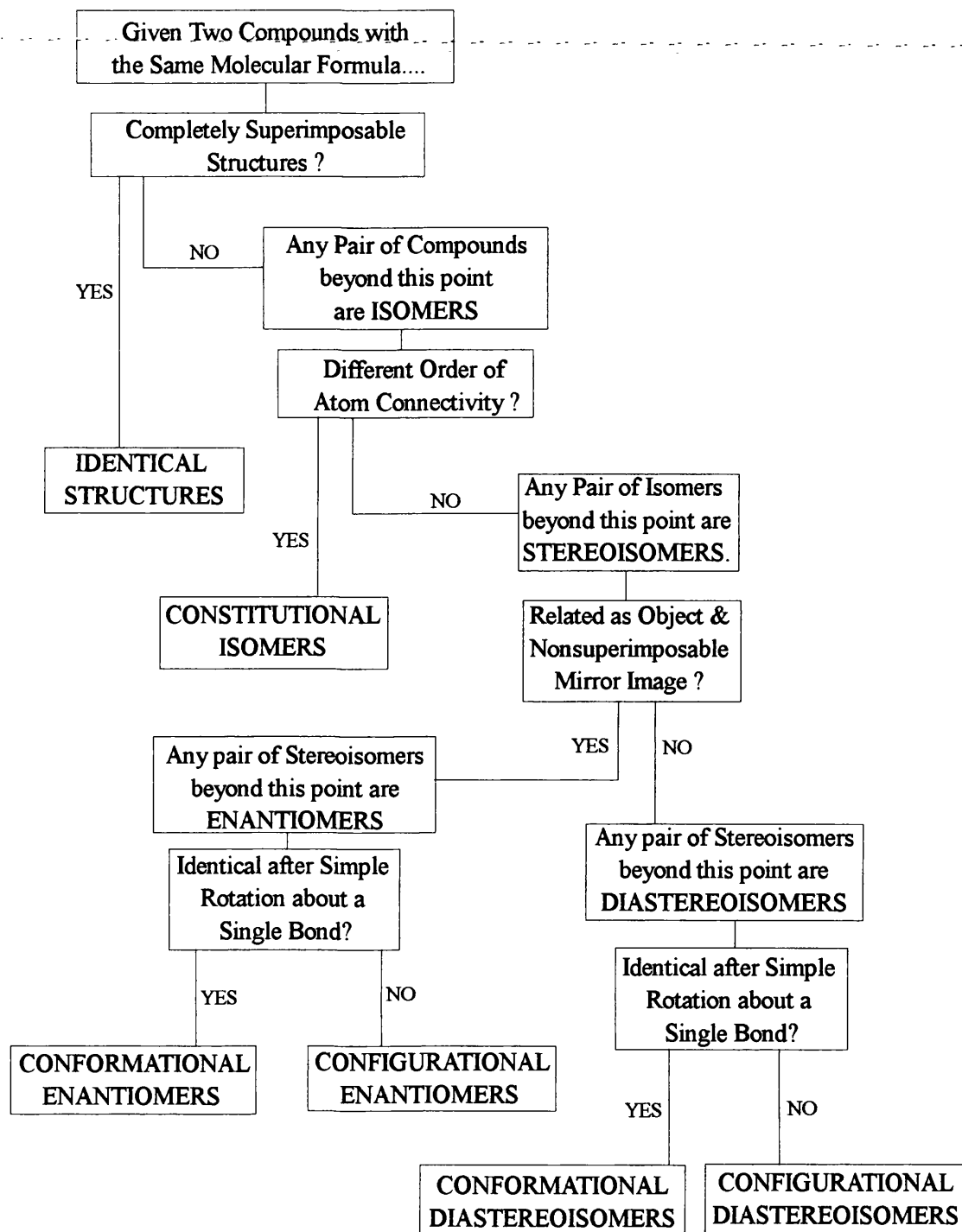
Isomers are different compounds that have the same molecular formula. Constitutional isomers are isomers that differ because their atoms are connected in a different way, for example, n-butane and isobutane. Stereoisomers are not constitutional isomers as their constituent atoms are connected in the same way. They differ only in the arrangement of their atoms in space, for example, cis- and trans-dichloroethene. Stereoisomers can be subdivided into two categories: enantiomers and diastereomers. Enantiomers are stereoisomers whose molecules are mirror images of each other and diastereomers are stereoisomers whose molecules are not mirror images of each other. Figure 1.2.1 summarises the relationship between different isomeric forms.

An object that is not superimposable on its mirror image is said to be *chiral* and to possess the property of *chirality*. The chiral molecule and its mirror image are enantiomers and the relationship between the mirror images is defined as enantiomeric. Chirality is a quality or character and as such cannot be measured or even quantified. The basis is quite simply that the object and its mirror image are not superimposable; it cannot be claimed that something is more chiral than something else. This 'handedness' of objects is a fundamental property of nature and such chirality can be observed at several levels<sup>17</sup>:

1. Macroscopic level: The gloves of a pair are mirror images of one another.

Single crystals of quartz are chiral even though the building block  $\text{SiO}_4$  is not

FIGURE 1.2.1: Isomeric Relationship Between Organic Compounds.



itself chiral in isolation.

2. Molecular assemblies: S-amino acids combine to form right-handed  $\alpha$ -helices.

D-ribose units ensure that nucleic acid helices are right-handed.

3. Molecular Chirality: Molecules can be non-superimposable on their mirror images.

4. Nuclear Chirality: The weak nuclear forces of matter and anti-matter are mirror images.

Objects (and molecules) that are identical with and thus superimposable on the mirror images are *achiral*.

Any molecule which has a plane of symmetry (also called a mirror plane) is not chiral and correspondingly the absence of such an imaginary plane can define a chiral molecule.

At the turn of the 19<sup>th</sup> century the Newtonian view of light as a beam of asymmetric particles was prevalent. However, to explain newly observed phenomena associated with reflections from an opaque or transparent body, Malus<sup>18</sup> in 1809 claimed that these particles were dipolar (like magnets); reflection caused these dipoles to become orientated to produce polarised light. This is the first recorded use of this term. Polarised light has a plane of polarisation. During the period 1812-18, Biot<sup>19</sup> demonstrated that many natural products, as liquids or solutions, rotate the plane of polarisation. This he consequently called *optical activity*, which he claimed was a molecular property. Subsequently, in 1838 Biot reported the expression defining specific rotation (Biot called this molecular rotatory power), equation 1.2.1:

$$[\alpha]_{\lambda}^T = \frac{\alpha}{lC}$$

where  $\alpha$  is the observed rotation in degrees,  $c$  is the concentration in  $\text{g cm}^{-3}$  and  $l$  is the pathlength in decimetres which, according to Biot, was chosen "*to avoid too many zeros*". He termed positive optical activity as the clockwise rotation of the plane of polarisation as viewed by the observer (down a polarimeter tube) with the light coming towards him from the light source, polarisers and sample. However Biot, a supporter of the particle theory of light, then abandoned the study of optical activity for about 15 years from 1818 until the wave theory of optical activity had become accepted and established in the 1830's. It was the work of Fresnel that established the modern held view of light waves in order to account for most of the optical phenomena then known, such as diffraction effects. In 1824, he turned his attention to optical activity. Plane polarised light was described as a transverse wave propagating in a single plane. Prisms made of certain crystalline substances, such as calcite, would only allow the passage of light waves with vectors in a single plane. The rotation of this plane was optical activity. Plane polarised light was considered to be the resultant of two in-phase components, one left circular, the other right circular. Optical rotation occurs as the result of the differential speeds of these mirror image components by optically active materials (nowadays chiral molecules).

Enantiomers have identical properties such as melting point, refractive index and solubility in common solvents, so how could they be distinguished? One easy observable difference was the way in which enantiomers differ in their behaviour towards plane polarised light. A chiral substance which rotates the plane of polarised

light in a clockwise direction is said to be dextrorotatory, (+), and the one that rotates the light to the left in a counterclockwise direction is said to be levorotatory, (-).

The discovery of molecular dissymmetry began with Pasteur<sup>20</sup> who was fascinated by the observation that mirror image crystals rotated the plane of linearly polarised light in opposite directions. He studied the case of a tartaric acid salt which could exist in two forms that rotated the plane of polarised light in opposite directions. optically active crystals could be produced from the solution of the racemate, which Pasteur carefully separated using tweezers under a microscope. He dissolved some of each kind of crystal separately in water and placed the solutions in turn in the path of the polarised light. What he discovered was that the left handed crystals rotated the polarised light to the left and the solution of right handed crystals rotated the polarised light to the right.

Pasteur was very fortuitous with the right choice of the salt of the acid, as the sodium ammonium tartrate was almost the only salt of the acid that crystallises in mirror image forms that a person can see are different and can separate mechanically, and with his cool working climate. In the hotter climes of Italy, Sacco was unable to reproduce Pasteur's results because at higher temperatures sodium ammonium tartrate crystallises as a racemate, with both the (+) and (-)-tartrate in a single lattice.

Thus, Pasteur was led to talk of molecular dissymmetry, as it became appreciated that there existed mirror image molecular structures with apparently identical physical properties except for optical rotation (Kelvin<sup>21</sup> coined the term *chirality* for this phenomenon in 1904). Thus the concept of molecular chirality was established by the 1870's. However, this was based essentially on the optical

phenomenon of optical rotation with, as yet, no correlation with shape and stereochemistry.

In 1874, Van't Hoff<sup>22</sup> and Le Bel<sup>23</sup> independently argued that mirror-image structures could only be supported if the four valent carbon atom was tetrahedral, figure 1.2.2. The presence of four different groups, a,b,c, and d led to the possibility of two structures which were non-superimposable mirror images of each other, that is enantiomers.

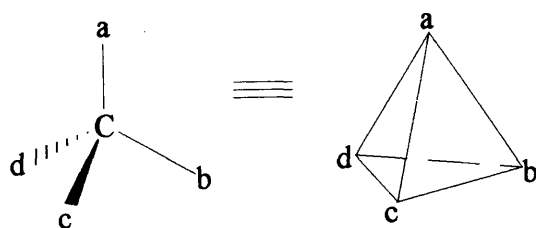


FIGURE 1.2.2: CHIRAL CENTRE

An important property of enantiomers was that interchanging any two groups at the tetrahedral atom that bears four different groups would convert one enantiomer into the other. The central tetrahedral atom is then known as the stereocentre. If all the tetrahedral atoms in a molecule have two or more groups attached that are the same, the molecule does not have a stereocentre and the molecule is achiral. However not all chiral molecules do possess such a centre and not all molecules possessing >1 tetrahedral stereocentre are chiral. However, the concept of chemical structure and molecular shape was now established and the existence of isomerism recognised, but the absolute stereochemistry of structures could still not be determined. This task was

first confronted by Fischer in 1891<sup>24</sup> during his studies of sugars. The (+)-glyceraldehyde molecule was given the D-configuration and arbitrarily drawn such that if the H atom is held away from the observer the grouping OH → CHO → CH<sub>2</sub>OH was clockwise. The (-)- isomer (the L-configuration) presented an anti-clockwise OH → CHO → CH<sub>2</sub>OH configuration. In 1951 Bijvoet *et al*<sup>25</sup> developed a special X-ray crystallographic method to determine the absolute configuration of molecules and it was found that fortune had shone on Fischer as it had on Pasteur; his arbitrarily chosen spatial orientation of the (+)-glyceraldehyde molecule was shown to be correct.

The D/L nomenclature was fraught with ambiguity and in 1966, three chemists, R.S.Cahn, C.K.Ingold and V.Prelog, developed an alternative nomenclature for describing enantiomers.<sup>26</sup> They devised a system of nomenclature that, when used in conjunction with the IUPAC system<sup>27</sup>, allowed chemists to clearly name individual enantiomers. According to this system, the enantiomers of 2-butanol, for example, should be separately designated either (S) or (R)-2-butanol. [ (S) and (R) are from the Latin words *sinister* and *rectus*, meaning left and right, respectively.] Based on three dimensional structures, as opposed to two dimensional Fischer projections, this system avoided the difficulties which arose when determining the absolute configuration of molecules with more than one chiral centre. This was done by ranking the groups around a tetrahedral chiral centre using an increasing priority order based on increasing atomic weights. The structure is then inspected from the side opposite the lowest ranking group. The sense of rotation of the descending order of the remaining groups was used to assign labels. For example, for a molecule X the sequence rule determined the priority order  $a > b > c > d$ . Thus viewing the molecule from the side remote from d, substituents a, b and c (decreasing order of priority) are either in

clockwise order, assigned as R, figure 1.2.3, or anti-clockwise and assigned as S. The advantages to this assignment was that for molecules with more than one chiral centre, the configuration of each chiral centre could be independently assigned. Versions of the same system also work for molecules which possess other forms of chirality.

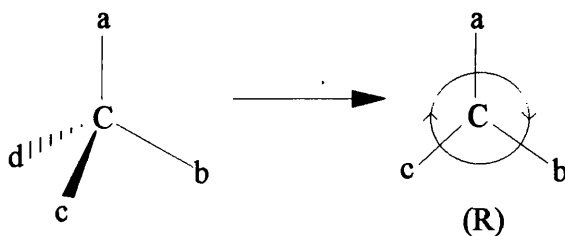


FIGURE 1.2.3: CHIRAL NOMENCLATURE

The direction of rotation of plane polarised light is also often incorporated into the names of optically active compounds, for example, (R)-(-)-2-butanol, however no obvious correlation between the enantiomeric configuration and the direction in which they rotate the plane of polarised light exists.

Many organic molecules possess more than one stereocentre, for example, a molecule such as cholesterol contains eight stereocentres. In compounds whose stereoisomerism is due to tetrahedral stereocentres, the total number of stereoisomers will not exceed  $2^n$  where  $n$  is the number of tetrahedral stereocentres. Looking at 2,3-dibromopentene, which has two stereocentres, there are four stereoisomers equivalent to  $2^2$ , figure 1.2.4, and each centre can be individually designated (R) or (S), using the

same rules as before. These structures are all different and cannot be superimposed on each other and, as such, any one of these structures would be optically active. If rotations of the structure itself or rotations about a single bond make one structure superimposable on another structure, then the two are not stereoisomers but different orientations or conformations of the same compound.

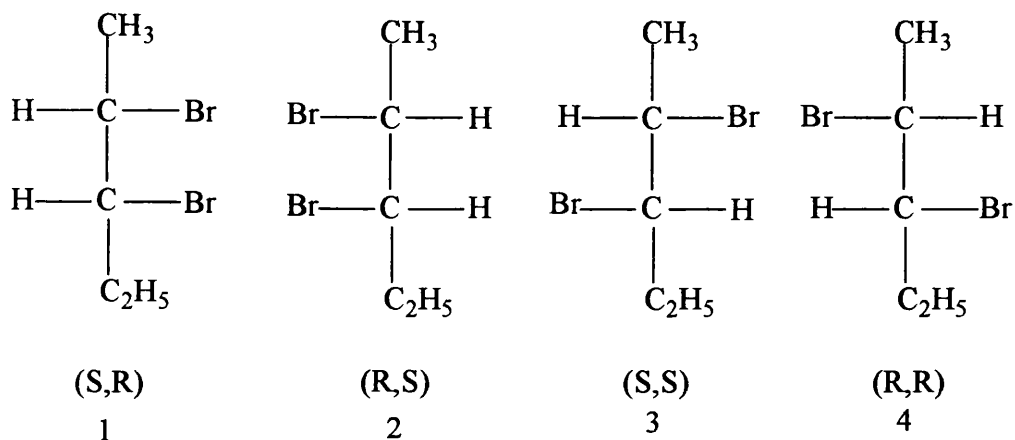


FIGURE 1.2.4: STEREOISOMERS OF 2,3-DIBROMOPENTANE

Looking at these four molecules of 2,3-dibromopentane, it can be seen that structures 1 and 2 represent a pair of enantiomers, likewise for structures 3 and 4. Structure 1 is not a mirror image of structure 3 and they are, therefore, diastereomers which would have different properties. If a molecule with >1 tetrahedral stereocentre has a plane of symmetry then, overall the molecule is classed as achiral and would be optically inactive, such as shown in figure 1.2.5 for 2,3-dibromobutane.

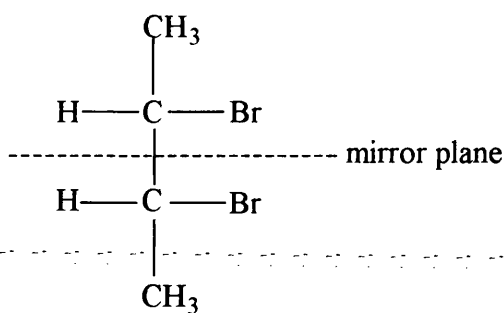


FIGURE 1.2.5: MESO FORM OR 2,3-DIBROMOBUTANE

The isomer of 2,3-dibromobutane represented, clearly has a plane of symmetry which would make it superimposable on its mirror image. Such molecules are called meso compounds. Hence all chiral structures must contain one or more stereogenic unit but not all molecules with such stereogenic units must be chiral. Chirality is a property of the molecule as a whole and can materialise in several different forms:

i) A chiral centre has been defined as an atom with a tetrahedral distribution of four different groups around the central atom and has concentrated mainly on asymmetric carbon. However other molecules can act as the chiral centre, such as shown in figure 1.2.6, including N, P and S.

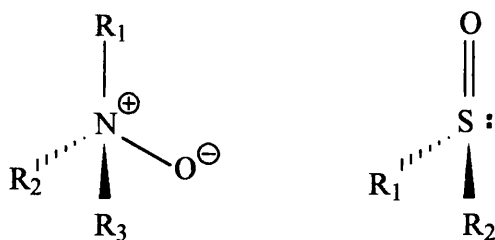


FIGURE 1.2.6: OTHER TETRAHEDRAL CHIRAL CENTRES

Sulfoxides can be classed as chiral as the separate enantiomers can maintain

the tetrahedral configuration up to  $\sim 200^{\circ}\text{C}$  before inversion occurs and resolution becomes impossible. A chiral centre is only one focus that will confer chirality on a molecule.

ii) Many other chiral molecules possessed another form of chirality, such a chiral axis. Here the tetrahedron has been distorted along one axis. Such compounds include allenes, cycloalkylidenes, biphenyls and binaphthyls, figure 1.2.7. Conformational isomerism occurs for biphenyls and binaphthyls as the barrier to inversion is large enough to prevent rotation and permit resolution. Axial chirality can be represented schematically as an elongated tetrahedron. In applying the sequence rule, the molecule is viewed along the chiral axis from one end to the other, figure 1.2.8. The two nearest groups are placed in the order a, b and the two further groups in the order c, d. the chirality rule is then applied as before.

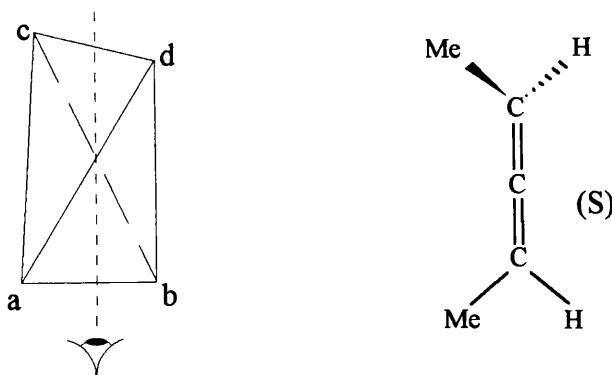


FIGURE 1.2.8: AXIAL CHIRALITY

iii) A chiral plane can also confer chirality in many different molecules. For hexahelicene, figure 1.2.9, an overlap of aromatic groups forces the molecule to twist to alleviate the overcrowding. This results in a helix form which can take a left or

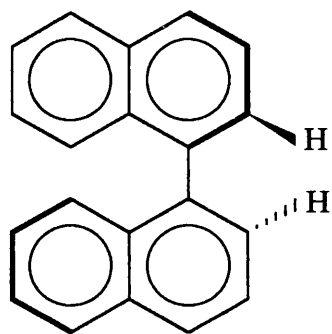
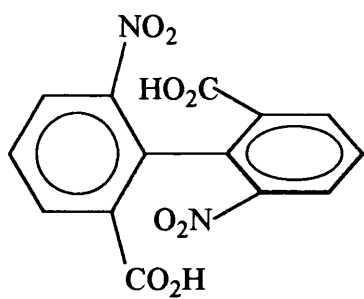
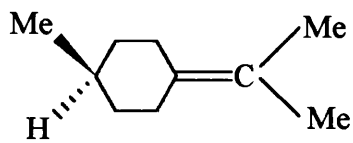
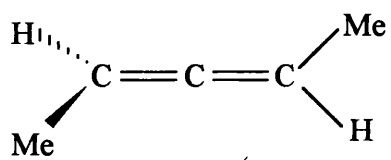


FIGURE 1.2.7: MOLECULES WITH AXIAL CHIRALITY

right handed form. Transcyclo-octene also has a chiral plane and can form two non-superimposable conformers which can be resolved. If however the "hole" in the ring increases, inversion becomes easier and chirality is lost.

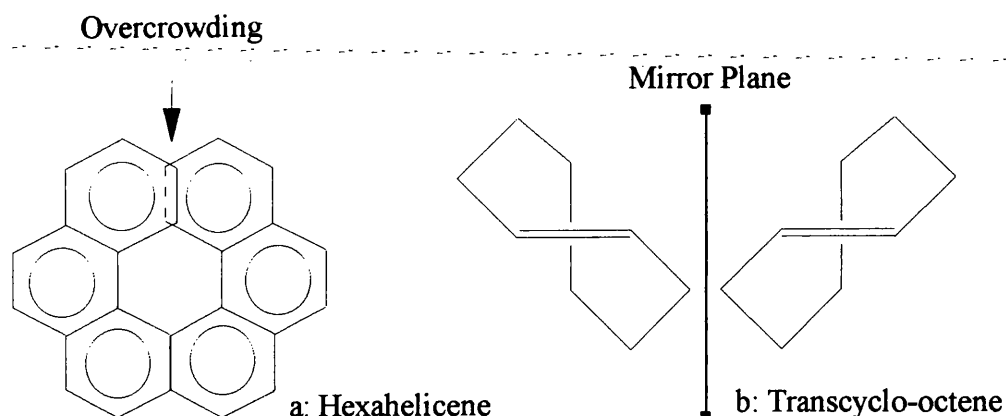


FIGURE 1.2.9: MOLECULES WITH A CHIRAL PLANE

An equimolar mixture of two enantiomers is called a racemic mixture or a racemate. Such a racemic mixture would show no resultant rotation of plane polarised light and would be classed as optically inactive and designated as ( $\pm$ ). A sample of an optically active substance that consists of a single enantiomer is said to be enantiomerically pure (or homochiral). Any sample which does not have an equimolar amount of each enantiomer has an enantiomeric purity  $<100\%$ . Thus the enantiomeric excess, e.e., can be defined as:

$$\% e.e. = \frac{[R] - [S]}{[R] + [S]} \times 100 \quad \text{Eq 1.2.2}$$

where [R] and [S] are the respective amounts of each enantiomer present in the sample. Hence if the e.e. of a mixture was 50% then there was 75% of one enantiomer present and only 25% of the opposite enantiomer.

If the addition of a substrate across a planar C=O bond leads to the formation of mirror image products, by an equal probability of the addition to either side of the plane, then the molecule is termed as having a prochiral face. Hence reaction at such enantiotopic faces can result in the production of enantiomers, with the C atom as a tetrahedral chiral centre. Both faces of the plane which contain the prochiral C=O group are named using the Cahn-Ingold-Prelog rules, figure 1.2.10; each group attached to the prochiral centre is given a priority, the face with the priorities decreasing in a clockwise direction is the re-face, and the other is the si-face.

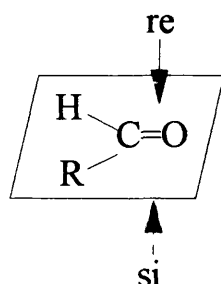


FIGURE 1.2.10: PROCHIRAL FACES OF C=O

Prochiral C=C groups are named in the same way, with the face at each separate carbon named individually, figure 1.2.11.

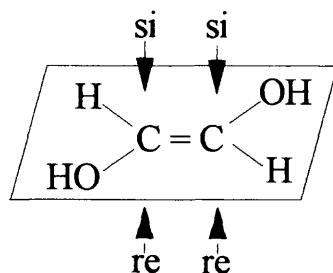


FIGURE 1.2.11: PROCHIRAL FACES OF C=C

Stereochemistry can have important effects on chemical reactivity. Two main factors control the stereoselectivity of a reaction. The first is a steric effect. For example, in figure 1.2.12, the approach of Y-Z to the prochiral face of C=O is retarded on one side by the bulkier substituent, and thus addition to the opposite face is preferential and results in the major product. Steric hindrance can thus control the resultant stereochemistry of the product.

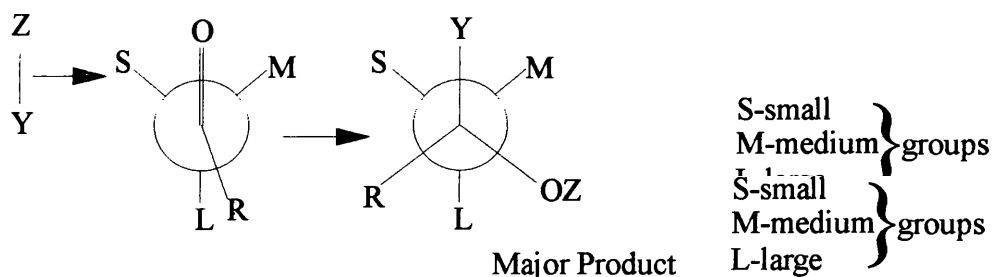


FIGURE 1.2.12: STERIC CONTROL DURING ADDITION OF Y-Z TO A PROCHIRAL C=O

The second controlling factor is a stereo-electronic effect and is much more subtle. The relative geometry of bonds made and broken in the transition stage can be critical. For example, figure 1.2.13 demonstrates that if the correct orbital alignment is not achieved then possible reaction can be diminished. Orbital control is very important in many types of reaction such as pericyclic reactions and 1,2 eliminations.

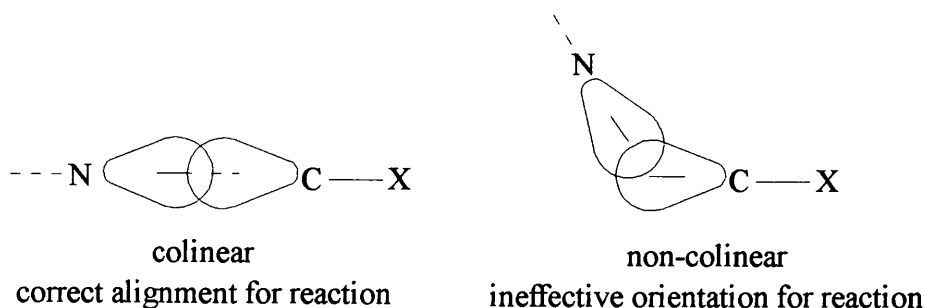


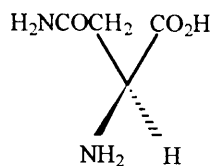
FIGURE 1.2.13: ORBITAL ALIGNMENT IN AN  $S_N$  REACTION

### 1.3: IMPORTANCE OF CHIRALITY

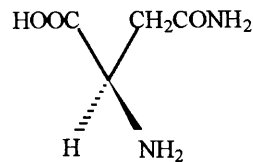
Synthesis of pure enantiomers has gained new impetus as a result of the increasing awareness of the importance of optical purity in the fields of food additives, pesticides, herbicides and, most importantly, pharmaceuticals.

That the shape of a molecule has considerable influence on its physiological action has been recognised for a long time. For example, in the early 1900's Cushny demonstrated that one member of a pair of optical isomers could exhibit greater pharmacological activity than the racemate: (-)-hyoscyamine was approximately twice as potent as the racemate in its effect on pupil nerve endings. Examples of property differentiation within enantiomers are numerous and often dramatic. A selection is given in figure 1.3.1, which emphasises the reason for commercial interest and the incentive for producing enantiomerically pure materials. Nature always makes the correct isomer of a molecule but many of the best selling drugs were racemates. In many cases this did not originally matter because, while one isomer had the desired therapeutic effect, the other isomer was inactive, such as the painkiller Ibuprofen. In other cases though, undesirable side-effects could be caused by the non-therapeutic isomer. One tragic and extreme case was the Thalidomide drug: one isomer had the desired effect of curing morning sickness but the other caused severe birth defects.

Since May 1992, America's Food and Drug Administration (FDA) has required chemical and biological information about both isomers of a chiral drug. It stated that: "... it is more important to evaluate both enantiomers clinically and consider developing only one when both enantiomers are pharmacologically active but differ significantly in potency, specificity of maximum effect...".<sup>28</sup> Hence even if the unneeded isomer is innocuous, the FDA wants to see it replaced with the single

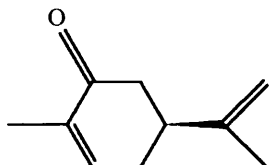


**Asparagine**



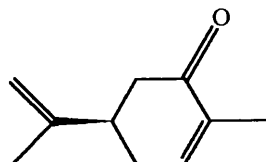
(S) bitter taste

(R) sweet taste

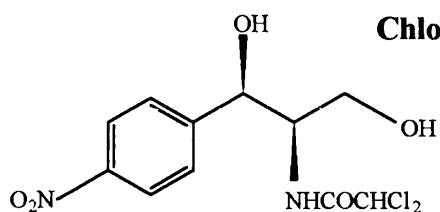


(S) caraway flavour

**Caravone**

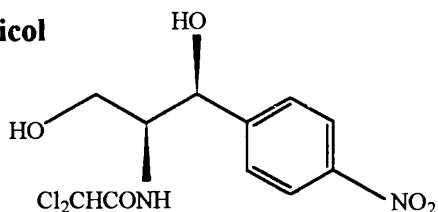


(R) spearmint flavour



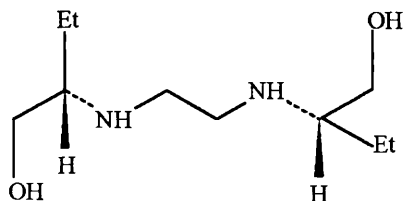
(R,R) antibacterial

**Chloramphenicol**

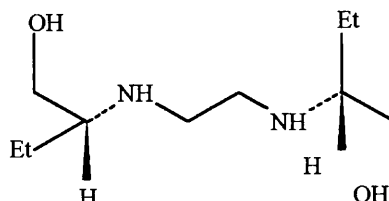


(S,S) inactive

**Ethambutol**

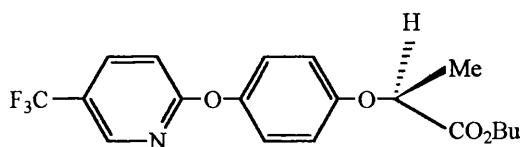


(S,S) tuberculostatic

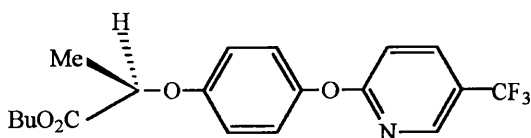


(R,R) causes blindness

**Fluazifop butyl**



(S) inactive



(R) herbicide

FIGURE 1.3.1: EFFECT OF CHIRAL MOLECULES

isomer version which would result in a more potent drug, being taken less frequently. For Ibuprofen mentioned earlier, the S-enantiomer is the active pain reliever and the R isomer is inactive, but the R form is slowly converted to the S enantiomer within the body. Thus taking pure S-Ibuprofen shortens the effective activation time required for pain relief by achieving higher blood levels of the chiral drug much quicker. With the technique of transdermal drug delivery (skin patches) only the active enantiomer diffuses through the skin. However, if a patch contains only the (S)-(-)-nicotine enantiomer there is much less skin irritation than with patches containing the racemate. The FDA's legislation also had an impact on other industries. For agrochemicals, this was an important environmental issue because such compounds are used on a much larger scale. The environmental damage caused by the racemate of a pesticide, where one enantiomer was inactive, was at least doubled compared to a homochiral formulation to gain a particular effect.

Chiral purity can also breath new life into old, discarded drugs. For example, there is currently a lot of research into redeveloping thalidomide in a chirally pure form for the treatment of leprosy and tuberculosis.

#### **1.4: SYNTHESIS OF OPTICALLY ACTIVE COMPOUNDS.**

One of the first methods to be used for the synthesis of optically active compounds was fermentation and it is still a very useful method for the synthesis of microbial metabolites such as L-amino acids, vitamins and hormones, from cheap raw materials such as sucrose. However, this method is limited to the production of 'natural' products which constitute microbial metabolites. Methods for the synthesis of 'unnatural' products can be divided into three classes, depending on the methodology

and starting materials:

- 1) -synthesis using the chiral pool materials,
- 2) -resolution of racemates
- 3) -creation from prochiral substrates.

The chiral pool refers to inexpensive, readily available, optically active natural products such as amino acids, lactic and tartaric acids, terpenes, alkaloids etc. These substrates can be used as building blocks and converted into optically active compounds via conventional organic synthesis involving retention or inversion of configuration or chirality transfer. For example, optically active carbapenem antibiotics have been developed which have, variously, utilised the chirality of L-glutamic acid<sup>29</sup> and L-aspartic acid.<sup>30</sup>

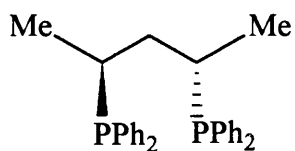
Resolution of a racemate involves the separation of the distinct enantiomers either by crystallisation or by kinetic resolution. Resolution via crystallisation depends on the preferential crystallisation either of diastereomeric salts, formed after reaction of the racemic mixture with an optically pure resolving agent, or alternatively, directly of the separate enantiomers at different rates. The success of kinetic resolution depends on the different rates of reaction of the two enantiomers with a chiral addend. Such methods of resolution are particularly attractive when accompanied by an *in situ* racemisation of the unwanted isomer which can act to increase the yield of the desired product.

It is more complicated to introduce the optical activity via asymmetric synthesis using chiral catalysts. However, chiral homogeneous, supported biphasic and heterogeneous catalytic systems, to name but a few techniques, have now been developed, with mixed success.

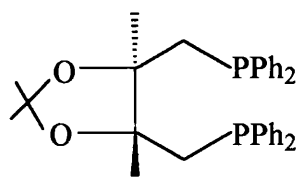
### 1.4.1: HOMOGENEOUS CATALYSIS.

The discovery by Wilkinson that tris(triphenylphosphine)rhodium chloride was a suitable catalyst for the asymmetric hydrogenation of olefins, led to a new branch of homogeneous catalysis with the potential for asymmetric induction. Figure 1.4.1 shows some of the most successful ligands developed. Early attempts using simple resolved chiral phosphines were not very impressive with enantiomeric excesses in the range 3 to 16%. The first major development was due to Kagan and Dang.<sup>31</sup> They demonstrated that the use of a chiral chelating biphosphine, (-) DIOP, gave good optical yields, particularly in the reduction of dehydroamino acid derivatives. A second development of considerable significance was due to Knowles, who developed the chelating biphosphine ligand called DIPAMP, which could effect optical yields of up to 95% for the catalytic hydrogenation of sterically hindered and multifunctional olefins.<sup>32</sup> Such chemistry is now the basis of several large scale processes, the most famous being the Monsanto process for the synthesis of L-Dopa. This was first commercialised in the mid 70's and used a Rh-DIPAMP catalyst, which was highly enantioselective and active for the hydrogenation of the dehydroamino acid derivative required.

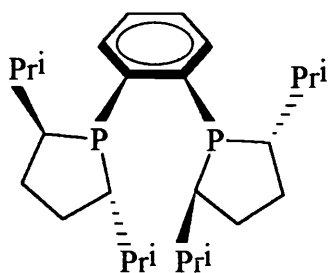
In asymmetric hydrogenation using (-)-DIOP-Rh catalysts, the different optical yields obtained for Z and E isomers of prochiral olefins, was interpreted to indicate that asymmetric induction takes place during or before the rhodium alkyl formation.<sup>33</sup> Almost without exception it was found that monophosphines were ineffective in asymmetric hydrogenation, and flexible chelate biphosphines gave rise to poor optical yields. X-ray studies were then used to show that the best chiral ligands were those that could to maintain conformational rigidity and chirality upon chelation, to achieve



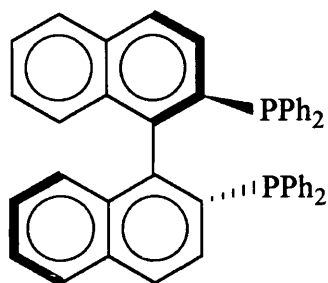
Bosnich 1978



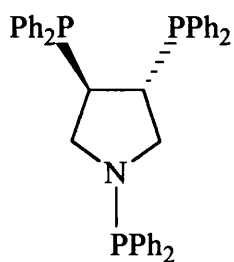
Kagan 1972  
DIOP



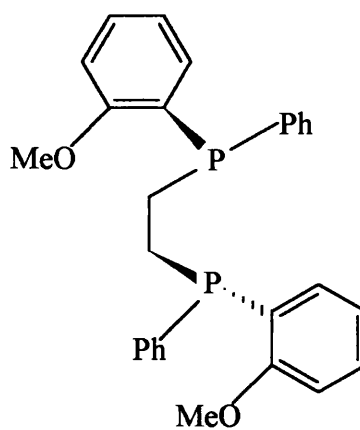
Burk 1990



Noyori, Otsuka 1980  
BINAP



Nagel 1983



Knowles 1975  
DIPAMP

FIGURE 1.4.1: HOMOGENEOUS MODIFIERS

a singular catalytic species. It was thus proposed that the ligands of the metals must have been endowed with suitable functionality, configuration and conformational rigidity to achieve an enantioselective catalyst. This led the work to the use of (R)-BINAP, a molecule which possessed only axial chirality. The BINAP ligand could accommodate a number of different transition metals, including Rh and Ru, by rotation about the binaphthyl C(1)-C(1') pivot and C(2 or 2')-P bonds without a serious increase in torsional strain.<sup>34</sup> A BINAP-Rh complex was able to enantioselectively hydrogenate prochiral olefins with up to 100% e.e.<sup>35</sup>, but the scope of this catalyst was not very wide. BINAP-Ru, on the other hand was much more versatile and was extended to include the hydrogenation of a wide range of carboxylic acids<sup>36</sup> and allylic alcohols<sup>37</sup>, as well as ketonic substrates, such as  $\beta$ -keto-esters<sup>38</sup> with enantiomeric excesses of up to 100% in both cases.

All the reactions described have involved Rh or Ru catalysts. However, in synthetic organic chemistry, the reduction of carbonyl groups by borohydride or aluminohydride reagents is much more common. Chiral catalytic analogues of these species are now emerging and are already becoming very important, for example, trichloromethyl ketones can be hydrogenated with enantiomeric excesses of up to 98% using such catalysts.<sup>39</sup>

Within all these homogeneous catalysts the metal site is a single metal atom, with the ligands relatively strongly complexed around the metal core. The rigid nature of the best chiral ligands results in a steric cleft. The reactant is then attracted to the metal centre through an electrostatic attraction and the orientation of which is directed by the ligands. Chiral discrimination can then occur through steric effects. As such systems do not rely on specific interactions between the modifier and the substrate,

these catalysts are not usually very substrate specific and can be used to promote a chiral reaction on a number of different types of substrates provided they respond favourably to the chiral environment in the vicinity of the active site.<sup>40</sup>

#### 1.4.2: SUPPORTED BIPHASIC SYSTEMS.

To avoid the problems of separation of products from catalyst in homogeneous catalysis, two-phase systems have been developed in which the catalytic complex (usually a water-soluble organometallic complex) remains in one (generally aqueous) phase while the products remain in a second, immiscible phase.<sup>41</sup> Catalysis then occurs at the interface between the two phases. Most of the work has concentrated on taking known homogeneous systems and trying to adapt them to two-phase systems and indeed two-phase catalysis is used commercially in the Rhurchemie-Rhone Poulenc process for the hydroformylation of propylene to butyraldehyde using a water-soluble rhodium triphenylphosphine trisulphonate catalyst.<sup>42</sup> More recently, Wan and Davis<sup>43</sup> have reported a heterogeneous catalyst that can successfully hydrogenate a prochiral carbonyl (2-(6'-methoxy-2'-naphthyl) acrylic acid) with an enantiomeric excess of 96%. In this system Ru-BINAP, previously discussed as an effective homogeneous catalyst, was sulphonated to ensure that the complex was soluble in the hydrophilic layer and served as the active catalytic chiral complex, figure 1.4.2.

Ethylene glycol was used in place of water in this system to avoid cleavage of the Ru-Cl bond in the chiral complex, which had been found to reduce enantioselectivity.<sup>44</sup> This phase was then supported on a hydrophilic silica, with a high surface area. The reactant and products were then retained in a hydrophobic chloroform/cyclohexane phase, fig 1.4.3. Catalytic hydrogenation then occurred at the

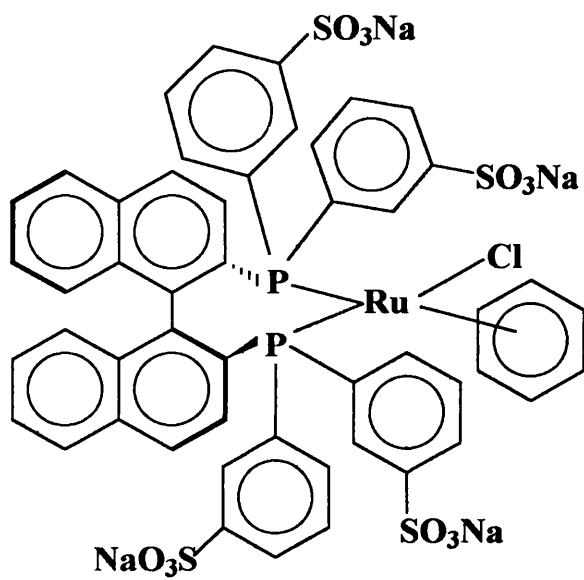


FIGURE 1.4.2: CHIRAL CATALYST

interface between the organic solvent and the supported phase. Maximising the available interfacial area by vigorous stirring, to induce bubbles, can improve the extent of reaction. Although the rate of reaction reported for the biphasic system was less than the comparable homogeneous catalyst, a further rate enhancement could possibly be achieved by the addition of a 'promoter ligand', which can bind the organometallic catalyst closer to the interface.<sup>45</sup>

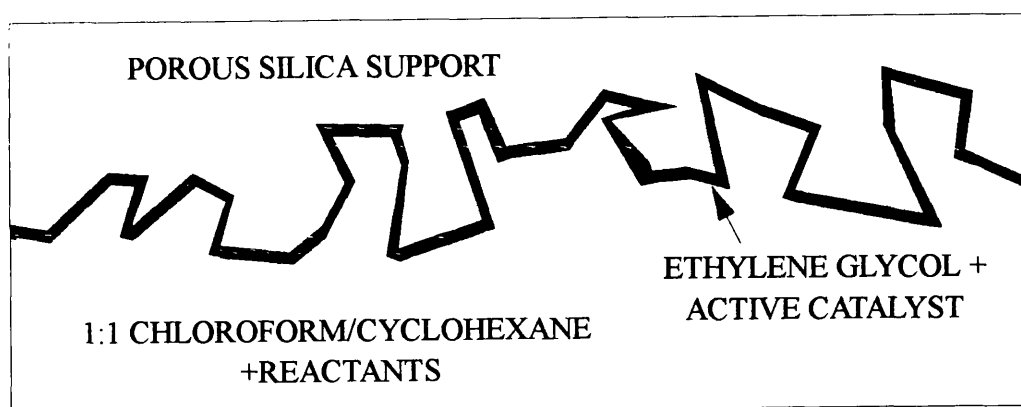


FIGURE 1.4.3: BI-PHASIC CATALYST

This method of restricting the chiral discriminator to a separate phase from the reactants and products, whilst maintaining the integrity of the organometallic complex (a major problem with the grafting of homogenous complexes on to supports), has meant the successful development of a chiral heterogeneous catalyst that was very similar to the homogeneous analogue.

## 1.4.2: HETEROGENEOUS CATALYSIS

The first chiral heterogeneous catalyst system was reported in 1932 by Schwab, before chiral homogeneous systems were developed. This initial work looked at metals supported on a chiral support and examined copper, nickel, palladium and platinum supported on quartz surfaces, which were used to dehydrogenate racemic 2-butanol.<sup>46</sup> At low conversions, a measurable optical rotation of the reaction solution indicated that one enantiomer of the substrate had preferentially reacted. As the left and right-handed forms of the quartz gave the opposite optical rotations it was deduced it was that the chiral support influenced the kinetic resolution, but the optical yields were low. A second technique was then introduced by Lipkin and Stewart who, in 1939, modified conventional heterogeneous catalysts by the addition of naturally occurring chiral molecules.<sup>47</sup> A Raney nickel catalyst, modified by glucose and a platinum catalyst modified by a cinchona alkaloid were both investigated and modest optical yields were achieved. This approach was advanced by Nakamura<sup>48</sup> and later Izumi<sup>49</sup> who chose chiral acids to modify both Pt- and Ni- catalysts. The work then briefly reverted to the original approach pioneered by Schwab, using a chiral support material to influence the enantioselectivity. Akabori and co-workers reported optical yields of up to 66% in the hydrogenation of C=N and C=C using a Pd/silk fibroin catalyst<sup>50</sup>, but these results were later found not to be reproducible<sup>49</sup> and the work in this field of catalysis again concentrated on the modification of conventional supported catalysts with chiral molecules.

While many systems have now been investigated, only two have been systematically studied. These are the hydrogenation of  $\alpha$ -ketoesters catalysed by Pt modified by cinchona alkaloids, and the hydrogenation of  $\beta$ -ketoesters catalysed with

Ni modified with optically active organic acids such as tartaric acid. Each of these has been studied in depth and developed into highly efficient heterogeneous asymmetric catalytic systems.

Since the initial report in the late 70's by Orito<sup>51,52</sup> concerning the asymmetric hydrogenation of  $\alpha$ -ketoesters, over supported platinum catalysts modified with cinchonidine, the system has been studied in great detail and e.e.'s of up to 95% have now been achieved.<sup>53</sup> The enantioselective hydrogenation of both methyl and ethyl pyruvate, figure 1.4.4, to the corresponding lactate products has been used to provide the most information on the cinchona modified platinum system and has illustrated several crucial factors necessary for enantioselective hydrogenation. The effect that variations in the type of catalyst, quantity and type of modifier, solvent, substrate concentration, temperature and H<sub>2</sub> pressure have on catalytic performance have all been investigated.

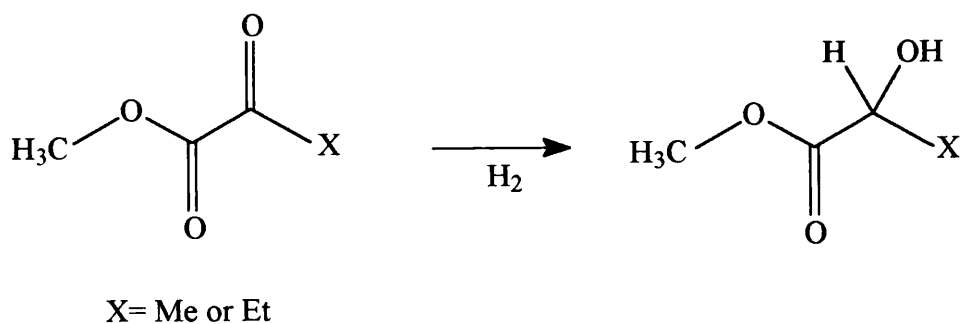


FIGURE 1.4.4: HYDROGENATION OF METHYL AND ETHYL PYRUVATE

A range of supported metal catalysts have been studied. Platinum<sup>52,54,55</sup> has been shown to be the most successful, while palladium<sup>56,57</sup> rhodium<sup>58</sup> and iridium<sup>59</sup> were all moderately suitable, but nickel and ruthenium were not effective.<sup>58</sup> These metals were

supported on a range of supports such as alumina, silica and carbon.<sup>54,58</sup> Figure 1.4.5 shows the structure of the cinchona alkaloids used. The most successful alkaloids studied are cinchonidine and cinchonine, although derivatives such as 10,11-dihydrocinchonidine<sup>58</sup>, have also been studied where similarly good or even better enantio-differentiation was observed. A small e.e. was also reported with some ephedrine derivatives, but these modifiers were not nearly as effective as the cinchona alkaloids.

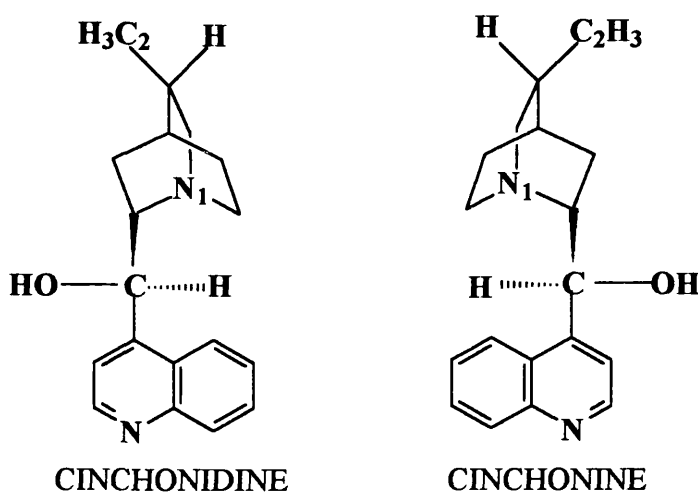


FIGURE 1.4.5: CINCHONA ALKALOIDS

Under reaction conditions, the modifier is adsorbed via an interaction between the  $\pi$ -electron system of the quinoline and the Pt surface.<sup>53</sup> By systematically varying the cinchona alkaloid structure, Blaser *et al*<sup>60</sup> were able to conclude that (1) if the N of the quinuclidine moiety is alkylated, optical induction is completely lost, whereas protonation enhanced the e.e., (2) changing the -OH substituent on C<sub>9</sub> for -OCH<sub>3</sub> did not influence the e.e. but substitution with -H significantly lowered the optical yield

and (3) lower enantioselectivity was observed with the hydrogenated quinoline nucleus. Hence, the enantio-differentiation of cinchona modified platinum catalysts are very sensitive to the exact structure of the modifier. In addition, these modifiers not only provide the chiral environment which the catalyst needs to promote enantioselective reactions, but they can also increase the rate of hydrogenation.

Catalyst preparation and structure have been shown to be important. Correlations have been found between the catalyst dispersion and the product e.e., such that low dispersions or large metal particles give the highest e.e.'s, making these reactions very structure sensitive. The activity and selectivity of the cinchonidine modified-platinum catalysts were found to depend primarily on the platinum salt used for impregnation, the best enantioselectivity was obtained by impregnation of alumina with chloroplatinic acid.<sup>55</sup> The size of the pores also affects the enantioselectivity, catalysts with larger pores affording better optical yields.<sup>60</sup>

Although most studies used ethanol or toluene as solvents, other reaction mediums have also been investigated. The rate of ethyl pyruvate hydrogenation and the optical yield decrease with increasing polarity of the solvent. Good results are obtained in apolar solvents. Alcohols and acids allow high optical yields, but a solvent interaction can be detected with the modifier or reactant. Although acidic solvents give high optical yields, basic solvents give lower e.e.'s. The best results have been reported in acetic acid (95% e.e. for ethyl pyruvate hydrogenation).<sup>61</sup> The presence of amines or weak acids as additives can influence both the activity and enantioselectivity.

Temperatures between 20-50°C and dihydrogen pressures > 10bar give good enantioselectivities. Higher pressures usually lead to slightly higher e.e.'s and an increase in rate, while an increase in temperature also leads to higher rates but to a

lower selectivity possibly due to the thermal desorption of the modifier from the catalyst at elevated temperatures.<sup>62,63</sup>

An initial model was proposed by Wells and coworkers<sup>54</sup> which successfully accounted for the sense of the observed enantioselectivity, during the hydrogenation of methyl pyruvate to methyl lactate. The 'template model', as it was called, relied on adsorption of the alkaloid modifier as an ordered, non-close packed array, which left exposed, shaped ensembles of platinum atoms at which configurational selection occurred during the adsorption of the reactant. Thus adsorption of the alkaloid molecules created a chiral environment around the active site on which the reaction then took place. However, evidence for the ordered adsorption of cinchona molecules was unfounded. This model would have required moderate surface coverages of alkaloid before fully templated sites were created, but experimental evidence showed that high enantioselectivity could be achieved even with low coverages.<sup>64</sup> Thus a 1:1 interaction between the modifier and the prochiral reactant in association with an ensemble of surface Pt particles was developed as the active chiral site.<sup>65,66</sup> In this model the modifier not only interacted with the catalyst surface but also with the reaction substrate, such that the chiral environment is enhanced by specific chiral interactions between the modifier and the substrate.

Augustine *et al*<sup>63</sup> proposed a model which relied upon the N of the quinuclidine being adjacent to the hydroxyl group ( in N<sub>1</sub>-C<sub>8</sub>-C<sub>9</sub>-O position , figure 1.4.5) to enable the formation of a "six-membered ring interaction" between the quinuclidine nitrogen and the keto carbon, as well as the C<sub>9</sub> oxygen and the ester carbon. However, this assumption is not in agreement with the experimental evidence that substitution of the -OH group by -OCH<sub>3</sub>, does not reduce the optical yield. Theoretical studies using

quantum chemistry<sup>66,67</sup> have also been used to rationalise the 1:1 interaction between the modifier and the substrate. Calculations showed, that in cases where the quinuclidine nitrogen of the cinchonidine alkaloid could be protonated, a favourable interaction between the modifier and the substrate was established. Thus, molecular modelling was able to account for the opposite enantiomers of the lactate product produced by the cinchonidine and cinchonine modifier enantiomers due to steric interactions, and, in general, was able to provide a reasonable explanation of the 1:1 interaction model. However, this approach was simplified and did not take into account solvent effects, mode and conformation of the adsorbed modifier or the mechanism of hydrogen transfer.

The second well studied system is the modification of nickel catalysts, by  $\alpha$ -hydroxy or  $\alpha$ -amino acids. Figure 1.4.6 shows the various substrates that have been enantioselectively hydrogenated by the tartrate modified nickel systems.

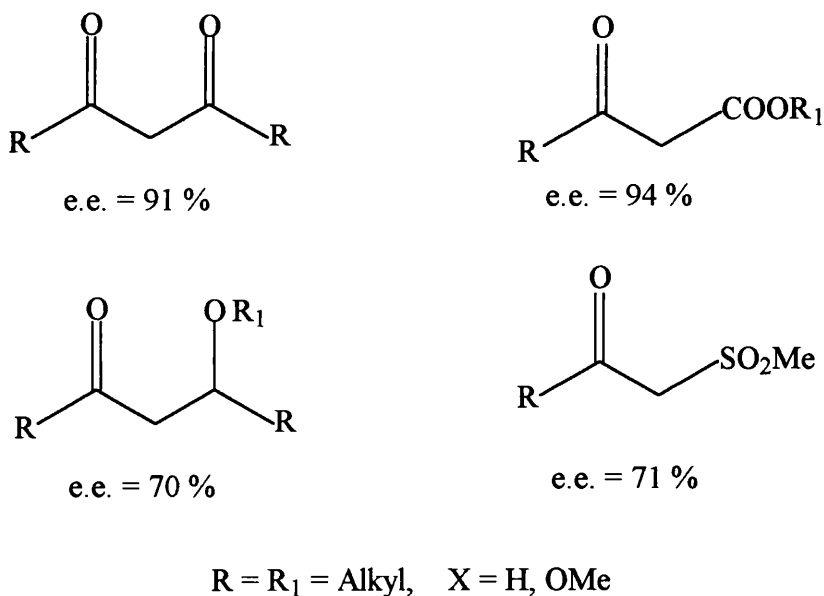


FIGURE 1.4.6: ASYMMETRIC HYDROGENATION WITH MODIFIED Ni CATALYSTS

The highest optical yields have been obtained for  $\beta$ -ketoesters and  $\beta$ -diketones. However, most investigations were carried out with methyl acetoacetate (MAA) as the substrate, figure 1.4.7. As with the cinchona modified platinum catalyst system, many factors influence the catalytic performance.

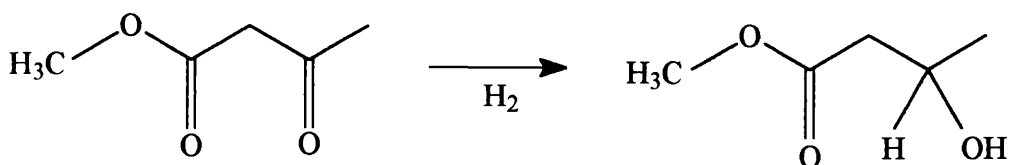


FIGURE 1.4.7: HYDROGENATION OF METHYL ACETOACETATE

Raney nickel and nickel powder systems have been the most extensively studied using a range of modifiers<sup>49,68</sup> although successful supported metal catalysts have now been reported, both by Sachtler *et al.*<sup>69,70</sup> and Nitta *et al.*<sup>71,72</sup> Klabunovskii *et al.* examined the enantiodifferentiation ability of different metal catalysts (Raney-Co, -Fe, -Cu and -Ru) in the hydrogenation of MAA and found that a nickel catalyst was most successful.<sup>73,74</sup>

The preferred structure of the modifier is  $RCHXCOOH$  ( $X = OH$  or  $NH_2$ ) and molecules containing two chiral centres were better than those with only one. In general, (S)- $\alpha$ -amino acids and (S)- $\alpha$ -hydroxy acids give opposite enantiomeric products in the hydrogenation of MAA. Tartaric acid was superior to other  $\alpha$ -hydroxy acids under optimum reaction conditions as a chiral modifier for nickel catalysts. A systematic alteration of the tartaric acid structure, figure 1.4.8, has shown that the two carboxyl groups and at least one of the hydroxyl groups are necessary to create an effective modifier.<sup>49,75,76</sup>

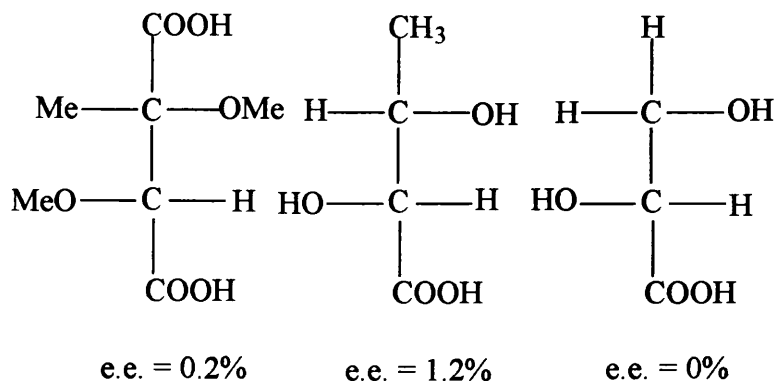
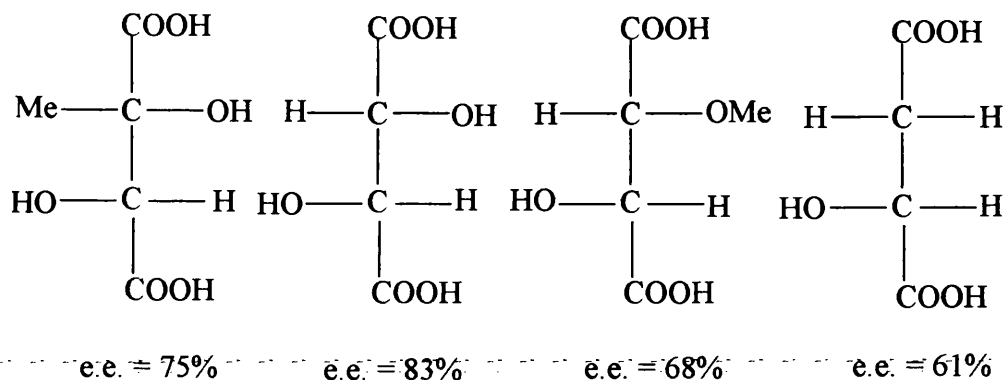


FIGURE 1.4.8: EFFECTIVE NICKEL CATALYST MODIFIER

Keane and Webb<sup>77</sup> have now shown that better enantioselectivities can be achieved with Ni/silica catalysts modified with L-alanine than tartaric acid for the hydrogenation of methyl acetoacetate. Modifier concentration, pH, temperature, time and sometimes modification procedure are crucial for a good catalyst performance. Tai *et al*<sup>78</sup> recently reported that treating the modified catalyst with ultra sound leads to enhanced activity and enantioselectivity for the hydrogenation of  $\alpha$ -ketoesters and  $\alpha$ -diketones with enantiomeric excesses of up to 94%. The modification of the nickel catalysts with tartaric acid is a corrosive procedure and nickel is leached in to solution.<sup>77,79</sup> Keane and Webb<sup>77,80,81</sup> have detailed the effects of the modification procedure on the catalytic properties of the nickel/silica system modified with tartaric acid and amino acids.

The solvent and additives employed in the reaction system have a significant influence on the optical yield. In the early work with TA-MRNi, it was reported that the use of a polar protic solvent such as methanol, ethanol or isopropanol increased the optical yield.<sup>82</sup> More recent work has shown that aprotic semipolar solvents, especially methyl propionate<sup>49</sup>, give the highest e.e.'s, but other trends have also been reported. Webb<sup>83</sup> has given the following sequence: n-alcohols > methyl propionate ~ ethyl acetate >> THF >> toluene ~ acetonitrile. The optical yield can also be increased appreciably by the addition of carboxylic acids, particularly pivalic acid in the hydrogenation of methyl ketones.<sup>84</sup> The addition of water is detrimental.<sup>49</sup> Sodium halide co-modifiers generally increase the enantioselectivity, although there is still considerable debate regarding the nature of this effect. Harada and Izumi<sup>85</sup> have claimed that the ionic species preferentially blocks sites on the surface which are non-differentiating, whilst Bostelaar and Sachtler<sup>86</sup> have ascribed the effects to modification of the stereochemistry of the product-determining surface complex.

There is still no general consensus of opinion as to the nature of the enantiodifferentiation. The nature of the surface complex produced by modification is still a point of debate, with ideas ranging from the formation of an adsorbed species capable of forming a complex with the reactant molecule<sup>87</sup> to the formation of Na-Ni-tartrate Ni complexes on the catalyst, through the formation of heteroligand chelate complexes of the type  $NiL_1L_2$  ( $L_1$  and  $L_2$  are substrate and modifier complexes respectively).<sup>88</sup> Izumi's<sup>49</sup> group proposed a mechanism for the enantioselective hydrogenation based on an interaction between the adsorbed substrate and the tartrate via hydrogen bonding, which controls the orientation of substrate adsorption. The importance of the NaX was then explained as the blocking of unmodified sites and,

since the ratio of unmodified to modified sites determines the optical yield, the e.e. increases. Sachtler<sup>89</sup> proposed a mechanism where dihydrogen is dissociated on the nickel surface and then migrates to the substrate which is coordinated to the adsorbed dimeric nickel-tartrate species. Neither of these models considered the corrosive effects of the acid modifier. It has been shown recently<sup>90</sup> that the nickel (II) tartrate complex and the complex leached during the modification procedure can catalyse the hydrogenation of MAA and exhibit enantioselectivities. However, the enantioselectivities were substantially less than those observed with a TA-modified Ni/silica catalyst.

Webb<sup>90</sup> has concluded that optimum activity and enantioselectivity is associated with conditions under which a 1:1 interaction between the adsorbed modifier and the reactant can occur. High modifier surface concentrations result in a decrease in enantioselectivity, as the adsorbed reactant can interact with more than one adsorbed modifier molecule. Thus nickel catalysts modified with  $\alpha$ -hydroxy or  $\alpha$ -amino acids can be used to achieve high optical yields in the hydrogenation of MAA but the nature of the chiral catalyst is very complex.

Both these systems have concentrated on the reduction of C=O, whereas research into the hydrogenation of C=C, with the exception of the work by Akabori and co-workers previously mentioned<sup>50,91</sup>, has been much more restricted. Perez *et al*<sup>92</sup> reported the first successful asymmetric hydrogenation of  $\alpha$ - or  $\beta$ -substituted cinnamic acids over a Pd/carbon catalyst modified with the cinchona alkaloids and were able to achieve maximum optical yields of 30%. Bartok *et al*<sup>93</sup> have investigated the hydrogenation of the sodium salts of substituted cinnamic acids over Raney-Ni modified with tartaric acid and achieved an enantiomeric excess of 17%.

Hydrogenation of the respective acids or esters gave no optical yield due, respectively, to a chemical reaction between the acids and the catalyst which prevented transformation of these reactants and a lack of sufficient interactions between the adsorbed tartaric acid and the esters to influence the ratio of enantiomers formed. Nitta and co-workers<sup>94</sup> expanded this field by examining several reaction variables associated with the hydrogenation of  $\alpha$ -phenyl cinnamic acid over Pd/carbon catalysts. The rate of reaction and the enantioselectivity were both observed to be very dependent on the method of preparation, which was attributed to detrimental effects from residual surface chloride retained during impregnation. The reaction solvent was also found to have a substantial effect on the enantioselectivity observed during the hydrogenation of  $\alpha$ -phenyl cinnamic acid, with a maximum optical yield of 53% was reported using a 9:1 N,N'-dimethyl formamide/water composition as the solvent.<sup>95</sup> Obviously the successful asymmetric reduction of prochiral C=C using chirally modified heterogeneous catalysts is not as advanced as that of C=O, but the stereoselective reduction of both functionalities is very important in organic chemistry.

The main drawback to these systems is the sensitivity and specificity of the modified catalyst, which is often only enantioselective for the hydrogenation of one prochiral substrate and by varying either the substrate, modifier, metal or support any enantioselectivity can easily be reduced or even eliminated.. Thus all these heterogeneous asymmetric catalytic systems are very complex, with the catalysts required to have high activity and regioselectivity, as well as stereoselectivity.

## **1.5: CHIRAL ANALYSIS.**

Highly effective methods are now needed to quantify the degree of optical purity in chiral drug molecules. Indeed the efficiency of modern methods for asymmetric organic synthesis are now pushing chiral analysis to its limits.

### **1.5.1: FUNDAMENTALS OF CHIRAL RECOGNITION.**

Traditionally, the enantiomeric purity of a chiral molecule was assessed by a chiroptical method such as polarimetry. This involved measuring the optical rotation of plane polarised light by a sample under defined conditions of temperature, solvent and concentration. This value was then compared to the known rotation for an enantiomerically pure sample of the compound, measured under identical conditions. However, the accuracy of this technique is not sensitive enough for the control of optical purity, especially within the pharmaceutical industry. In addition, large samples are required and the results can be very susceptible to traces of optically active impurities. The calculation of enantiomeric excess from the optical rotation may also be impossible, because the specific rotation of the pure enantiomer is unknown or wrong due to impurities. Hence, although such a technique is a very convenient method it is a rather unsatisfactory method for determining accurate enantiomeric purity unless stringent conditions are followed.

Given these limitations it can be necessary to use an independent method of analysis when assaying enantiomeric purity with such an alternative being nuclear magnetic resonance (NMR) spectroscopy. Although enantiomers cannot be distinguished in an achiral medium, since the resonances of enantiotopic nuclei are isochronous, diastereomers may be distinguished because the resonances (of certain diastereotopic nuclei) are anisochronous.<sup>96</sup> The determination of enantiomeric purity using NMR

therefore requires the use of a chiral auxiliary that converts the mixture of enantiomers into a diastereomeric mixture. There are three types of chiral auxiliary that are used.<sup>97</sup> Chiral lanthanide shift reagents<sup>98</sup> and chiral solvating agents<sup>99</sup> form diastereomeric complexes *in situ* with the substrate enantiomers and may be used directly. Chiral derivatising agents<sup>100</sup> require the separate formation of discrete diastereomers prior to analysis, and care has to be taken to ensure that neither kinetic resolution nor racemisation of the derivatising agent occurs during derivatisation. However chiral NMR is expensive and again requires strict conditions. Chromatographic techniques are now preferred for quality control in pharmaceutical and fine chemical applications, being more precise than NMR-based methods.

#### 1.5.2: CHROMATOGRAPHIC SEPARATIONS.

For small scale reactions, preparative separations are not feasible and for these reasons direct analysis is preferred, for example, chromatographic analytical procedures. Such techniques have been at the forefront of development in chiral analysis over the last 20 years with a particular emphasis on gas-liquid chromatography (GC) and high performance liquid chromatography (HPLC).

Chiral recognition fundamentally relies on reaction with a second chiral molecule, whereby the two enantiomers of interest will interact in a different fashion with a homochiral substance. This can be achieved in different ways:

- 1) Precolumn derivatisation with chiral reagents produces diastereomers which can be separated by non-chiral chromatographic techniques. However, for the determination of the enantiomeric excess, this procedure can cause problems as diastereomers may have different detector responses and the derivatisation stage requires a pure chiral reagent, to avoid the misleading formation of interfering

diastereomeric pairs. Further chemical treatment may also be necessary if the starting enantiomers are to be recovered.

2) Relative separation by interaction with a chiral solvent or chiral additive to the mobile phase. These can induce temporary diastereoisomerism between enantiomers for separation with non-chiral stationary phases. Of course, this method is only applicable for liquid mobile phases. The disadvantages to this system include that the additive may interfere with detection, the optical purity of this additive or the solvent must be very high to obtain a reliable measure of e.e. and the technique can be expensive.

3) Chiral stationary phases allow direct separation of optical isomers, often without derivatisation, or with achiral derivatising agents. For this reason they are preferred for control of optical purity or determination of e.e. values. If the chiral support was only 99.75% optically pure the two isomers will still travel down the chromatography column at different rates, because the major enantiomer of the support will dominate in retaining the slower-moving enantiomer of the analyte. Peak areas and hence e.e. can still be determined. The separation would be less efficient, and may require longer retention times with consequent peak broadening, but although the detection limit of the minor enantiomer will be reduced if the optical purity of the chiral support is not complete, it does not prevent a reliable analysis.

In both these cases resolution is achieved by formation on column of transient diastereomers. The resolution resulting from different stabilities between the chiral selector (immobilised on the stationary phase or present in the mobile phase) and elution order based on the weakest diastereomer formation, figure 1.5.1. If the C---C' interaction is attractive then that would be the most retained enantiomer, and if the

interaction was repulsive then that would be the least retained enantiomer which would elute first.

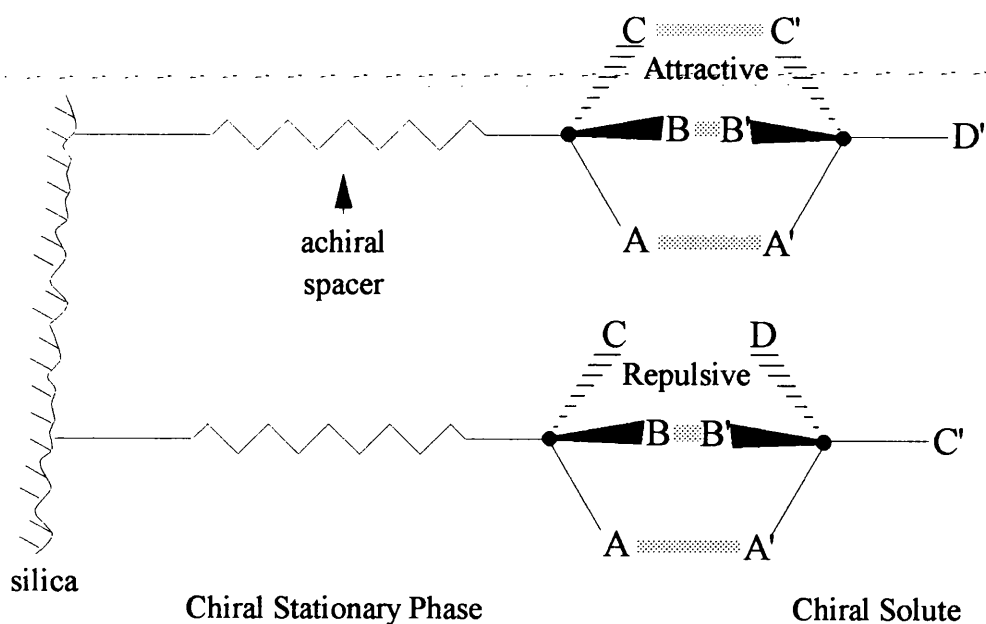


FIGURE 1.5.1: CHIRAL STATIONARY PHASES

### 1.5.3: CHIRAL STATIONARY PHASES (CSP).

Unfortunately there is no universal chiral stationary phase for resolving all enantiomeric substances. However, chiral column technology is a rapidly expanding field and in 1987, Wainer<sup>101</sup> classified the available phases developed for high performance liquid chromatography (HPLC) into the following five categories according to their chiral recognition mechanisms:

Type I - in which the solute-CSP complexes are formed by mechanisms such as attractive interactions, hydrogen bonding, dipole stacking and  $\pi$ - $\pi$  interactions.

Type II - in which the primary mechanism for the formation of solute-CSP

complexes is through attractive interactions, but where inclusion complexes also play an important role.

Type III - in which the solute enters in to chiral cavities within the CSP to form inclusion complexes.

Type IV - in which the solute forms part of a metal diastereomeric complex, also known as chiral ligand exchange chromatography.

Type V - in which the CSP is a protein and the solute-CSP complexes are based on combinations of polar and hydrophobic interactions.

The "three-point interactive rule" of chiral recognition, first proposed by Dalglish<sup>102</sup> for paper chromatographic separations of amino acids, was later extended to HPLC and verified by Baczuk *et al.*<sup>103</sup> Pirkle and his coworkers, however, began the first rational approach to the design of CSPs for HPLC using various optically active  $\pi$ -acids and  $\pi$ -bases and proved their wide utility.<sup>104</sup> Hence Type I CSPs are often referred to as 'Pirkle Phases' after their inventor. In 1981 the first column became commercially available, which consisted of dinitrobenzoylphenylglycine bonded to a silica support. With this phase and its analogues, Pirkle was able to suggest the mechanisms which led to enantiomeric resolution. The greater the number of specific, discrete, simultaneous interactions between the chiral solute molecules and a chiral locus on the stationary phase then the greater the likelihood of effective chiral discrimination, and hence chromatographic resolution of enantiomeric solutes. Hence a CSP should contain, at least, one each of three types of functional groups near the chiral centre, figure 1.5.2.

- i)  $\pi$ -acidic or  $\pi$ -basic aromatic groups, capable of donor-acceptor interaction (charge-transfer complexation).
- ii) polar hydrogen-bonds and /or stacking sites.
- iii) bulky non-polar groups, providing steric repulsion, van der waals interaction, and/or conformational control.

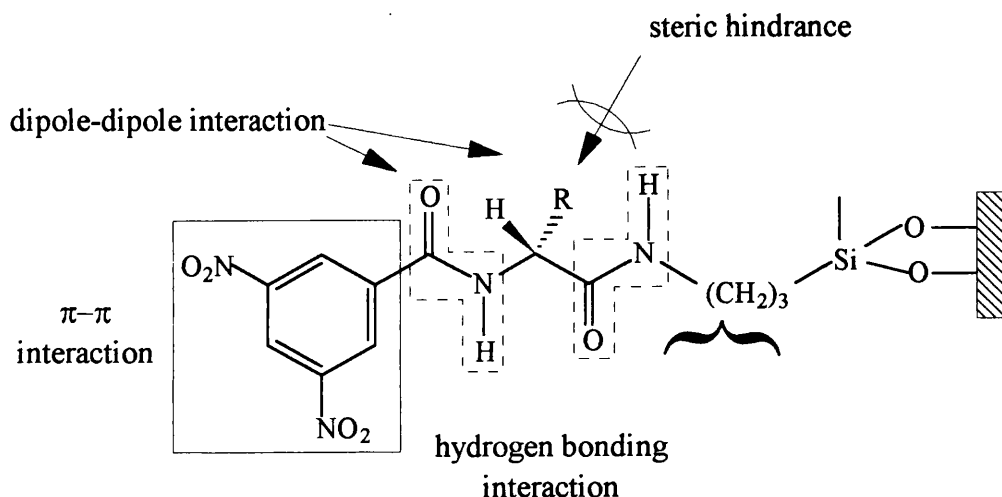


FIGURE 1.5.2: AN EXAMPLE OF A TYPE I CSP

As an extension to the programme in Pirkle's group it was demonstrated that if resolution could be achieved with one chiral selector immobilised for a group of compounds, then it should be possible to reverse the selector with the analyte molecule and again achieve resolution. This was termed the "principle of reciprocity" and allowed the generation of many new CSPs to evolve by analogy. The advantages to Type I phases include their high applicability and efficiencies, and for trace analysis the ability to select the (R) or (S) configuration of the CSP in which the trace component elutes first, hence increasing sensitivity.

For Type II (polysaccharide) phases amylose and cellulose were first exploited in chiral separations 20 years ago. They are both polymers of D-glucose units, where helical structure formation can lead to a degree of inclusion. For these naturally occurring polymers, although they were shown to give resolution of a number of compounds, generally this was somewhat limited and the chromatographic peak shapes were broad. Nowadays these CSPs are often based on modified cellulose generally coated on to silica. The separations occur due to:

- i) The formation of diastereomeric solute CSP complexes through hydrogen bonding via either the polar ether or carbamate.
- ii) The stabilisation of this complex through the insertion of the aromatic portion of the solute into a chiral cavity of the CSP.
- iii) Chiral discrimination between enantiomeric solutes due to differences in their steric fit within the chiral cavity and the environment just outside this cavity.

Examples of such CSPs are shown in figure 1.5.3. There are limitations in use, relating to solvents, which can strip the polymer coating away from the phase, but generally they are robust, if slightly expensive.

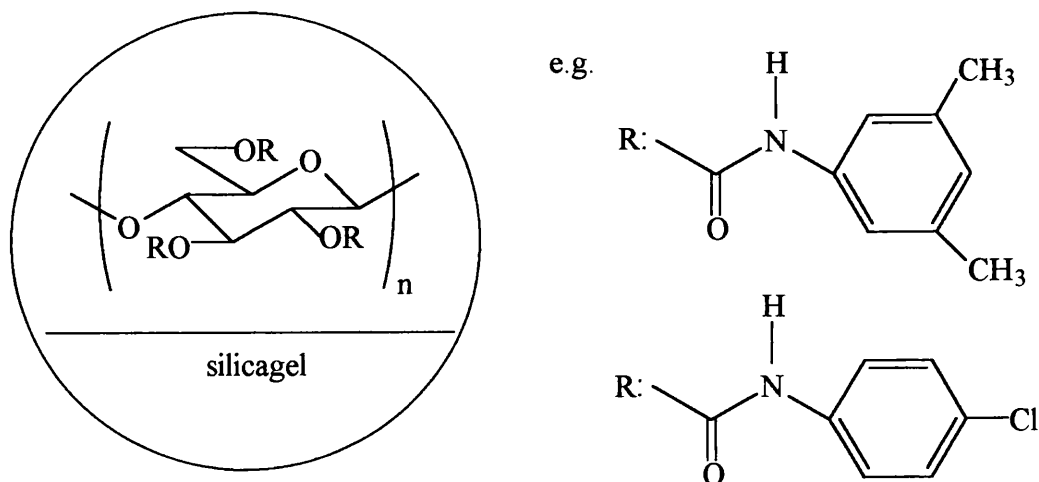


FIGURE 1.5.3 CELLULOSE CARBAMATE COATED ON SILICA GEL

Type III CSPs are inclusion type, in which the host (the CSP) includes partially or completely the guest (the solute) molecule. For an enantiomeric separation to occur, there must be a difference in stability of the inclusion complexes formed for each isomer of the solute. Such CSPs are prepared by covalently binding cyclodextrins to silica. Cyclodextrins consist of glucose units bonded through  $\alpha$ -(1,4) linkages forming a truncated cone shaped molecule figure 1.5.4, with the wider side formed by the secondary 2- and 3-hydroxyl groups and the narrower side by the primary 6-hydroxyl. The number of glucose units determines the dimensions and size of the cavity. This cavity is lined by the hydrogen atoms and the glycosidic oxygen bridges. The non-bonding electron pairs of the glycosidic oxygen bridges are directed toward the inside of the cavity, producing a high electron density and lending it some Lewis base character. As a result of this special arrangement of the functional groups in the cyclodextrin molecules, the cavity is relatively hydrophobic, while the external faces are hydrophilic. Resolution is mainly dependent on a tight fit of the solute in the cavity, and on the interactions between the solute and the secondary hydroxyls. An outer rim of hydroxyl groups can be derivatised in a number of ways, such as acetylated. These derivatised phases allow chiral interactions to take place, where previously the solute would have projected well above the cyclodextrin. At present there are few applications on the  $\alpha$ - and  $\gamma$ -cyclodextrin phases. Whereas  $\beta$ -cyclodextrin phases have a wide range of chiral applications.

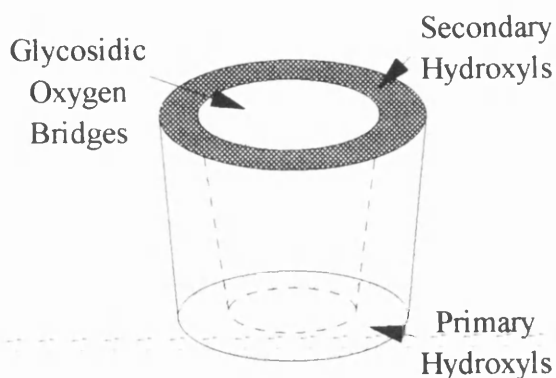


FIGURE 1.5.4: FUNCTIONAL STRUCTURAL SCHEME OF CYCLODEXTRIN

Type IV CSPs are often called chiral ligand exchange phases. They consist of a chiral chelating agent, typically an amino acid or a modified amino acid, linked via an aliphatic spacer arm to silica, which is loaded with  $\text{Cu}^{2+}$ . The separation requires the analyte (mobile ligand) to form an enantioselective complex with the amino acid (fixed ligand) and copper ion, figure 1.5.5. If the complexes formed with the enantiomers of the analyte have different stabilities a chiral separation can be achieved. In order to form such a complex the analyte must have two polar functional groups with the correct spacing, which can simultaneously act as ligands for the copper ion. This limits the technique to the separation of amino acids and their derivatives, dipeptides and 2-hydroxycarboxylic acids.

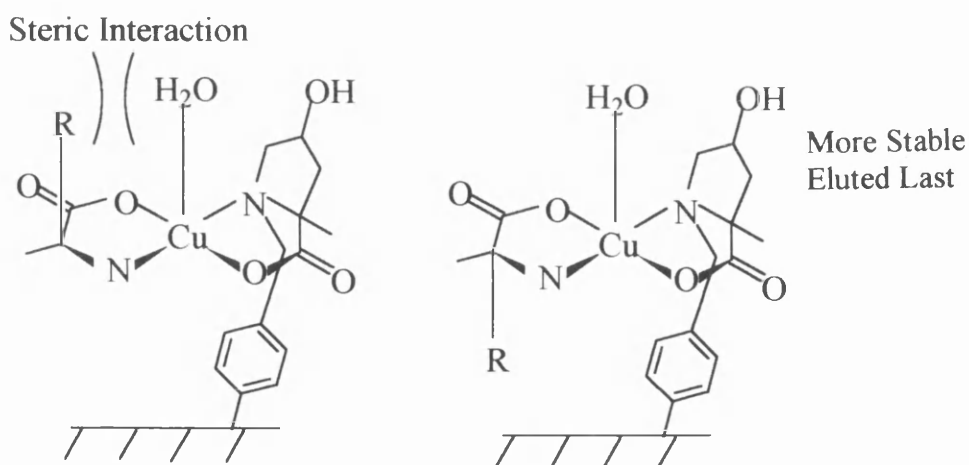


FIGURE 1.5.5: TYPE IV CSP

The final class of CSP consist of proteins. The two most useful at present are based on human  $\alpha$ -acid glycoprotein and bovine serum albumin. Due to the complex nature of these proteins utilised, the chiral recognition mechanism is largely unknown, but involves mainly hydrophobic and electrostatic interactions, although hydrogen bonding and charge transfer interactions can play a significant role. Such CSPs have a wide applicability in the field of drug bioanalysis, as they undergo stereoselective interactions with a large number of pharmacologically active compounds.

Hence with such a wide range of chiral columns being developed with substantial improvements in column lifetime and performance, HPLC methods are being used to an increasing extent.

Due to the high efficiency, sensitivity and speed of chiral separation by high-resolution capillary gas chromatography, GC also represents a versatile and attractive method for enantiomeric analysis. However the prerequisite of this method is the volatility, thermal stability and resolvability of the chiral analyte, restricting universal use of the technique. Enantiomeric separation by GC is mainly performed on three types of CSP<sup>105</sup>: 1) on chiral amino acid derivatives mainly via hydrogen-bonding<sup>106</sup>, 2) on chiral metal coordination compounds via complexation<sup>107</sup> and 3) on cyclodextrin derivatives via inclusion,<sup>108</sup> which all operate through very similar mechanisms as previously described for HPLC. These CSPs can be immobilised on the inner wall of fused-silica capillary columns by crosslinking, thus affording high-resolution capillary columns with an extended range of operating temperatures. Thus, where applicable, GC has become the preferred analytical technique within the pharmaceutical and fine chemical industries due to the precision afforded by this method.

**CHAPTER TWO**  
**OBJECTIVES OF STUDY**

The use of heterogeneous supported metal catalysts to bring about the enantioselective hydrogenation of prochiral organic compounds is an important field of catalysis that is rapidly advancing, particularly in the pharmaceuticals industry where the decision to produce single isomerically pure compounds has been taken. A necessary pre-requisite for the use of such supported metal catalysts as asymmetric hydrogenation catalysts, is their modification by adsorption of a specific chiral molecule, since supported metal catalysts possess no inherent chiral directing properties, and it is the chemistry of such supported systems that is the subject of this work. Such catalyst/modifier systems have been shown to be very highly specific, not only with respect to suitable modifiers, but also to the reaction which can be analysed. The vast majority of research in this field has concentrated on optimising the enantioselectivity of the two established systems, namely the Pt/cinchonidine/ $\alpha$ -ketoester and Ni/tartaric acid/ $\beta$ -ketoesters, by incrementally altering the system variables, such as pressure, temperature and pH, to name but a few.

This work aims to develop entirely new chiral catalysts with the main objective of establishing a more general understanding of the generation of chiral centres on heterogeneous catalyst surfaces.

In the vast majority of previously researched systems, there has been little attempt to investigate the amount of modifier species on the catalyst surface, which has meant that any quantitative aspect of catalyst/modifier/substrate interactions cannot be defined. This work began adsorption studies with 2,2'-dihydroxy-1,1'-binaphthalene, 2,2'-diamino-1,1'-binaphthalene, 2,2'-dimethoxy-1,1'-binaphthalene, 2-hydroxy-2'-methoxy-1,1'-binaphthalene and 2,2',7,7'-tetrahydroxy-1,1'-binaphthalene, as chiral binaphthalene derivatives have already been shown to be very successful chiral

substrates for asymmetric homogeneous catalysts.<sup>35,36</sup> Detailed adsorption studies were carried out to ascertain;

- the extent of the modifier adsorption on the catalyst surface.
- the nature of the interaction between the catalyst and the modifier (for example, is it a strong or weak interaction)
- the mode of adsorption of the modifier molecules.

The potential of these modified catalysts for asymmetric hydrogenation was then studied with respect to a range of prochiral reactants, which have different spatial and chemical requirements, namely;

- Methyl tiglate and 4-Trifluoro, 2-methyl, 2-butenic acid ethyl ester  
- $\alpha,\beta$  unsaturated esters.
- Tiglic acid - an  $\alpha,\beta$  unsaturated carboxylic acid
- 3-Coumaranone - an isolated ketone.

These prochiral reactants allow investigation into the regioselectivity as well as the specific site requirements for enantioselectivity in the modified catalysts.

The catalysts used in this study were 10% w/w Ni supported on Grace silica and Cab-O-Sil silica, 2% w/w Pd supported on Grace silica and carbon and 1% w/w Pd supported on Cab-O-Sil silica. These catalysts were each characterised by temperature programmed, selective chemisorption and transmission electron microscopy techniques prior to the study of their reaction chemistry.

## **CHAPTER THREE**

### **EXPERIMENTAL**

### **3.1: INTRODUCTION**

A series of catalysts were prepared with either palladium or nickel salts on a range of silicas and carbon supports. Thus results could be examined for evidence of effects arising from differences in support and active metal.

Characterisation techniques included temperature programmed reduction, carbon monoxide and dioxygen chemisorption, transmission electron microscopy and atomic absorption.

Although such supported heterogeneous catalysts do not possess any inherent chiral quality, it has been shown that enantiodifferentiating abilities can be induced by the adsorption of a chiral adlayer on to the prepared catalysts. Several chiral substances were used as modifiers, using two different approaches:

i)- Detailed adsorption studies were performed with several chiral molecules in an attempt to understand the nature of the chiral adlayer prior to hydrogenation.

ii)- A second set of chiral molecules were used to directly modify the catalyst surfaces before use as possible enantioselective catalysts. No previous investigations into the amounts adsorbed preceded the hydrogenation reactions.

The resultant chiral catalysts were then all tested for enantioselectivity against a series of prochiral C=C and C=O test reactants. Using such a variety of catalysts, modifiers and test reactants would allow an investigation onto the necessary requirements of enantioselective hydrogenation, through site geometry, electronic effects and chemical selectivity.

## 3.2: CATALYST PREPARATION

### 3.2.1 : WET IMPREGNATION

Four catalysts were prepared by wet impregnation, namely 2% Pd/Carbon, 2% Pd/Silica and two 10% Ni/Silica catalysts. The Pd catalysts were prepared on the 250g scale and the Ni on a 500g scale. The supports used were: Carbon Norit RX3 Extra which was a pellet form and Grace Silica C30 and C10 beads.

A round bottom flask was charged with the blank support and a solution of the required metal nitrate was added. For the nickel solution 247.75g of  $\text{Ni}(\text{NO}_3)_2 \cdot 6\text{H}_2\text{O}$  was directly dissolved in 850 mls of deionized water. The palladium nitrate was not as soluble. Initially 10.81g  $\text{Pd}(\text{NO}_3)_2 \cdot x\text{H}_2\text{O}$ ,  $x \sim 1$ , (Johnson Matthey) was added to 470mls of deionized water and 25ml concentrated nitric acid. This solution was then stirred on a hot plate for 2 hours. Any remaining undissolved Pd residue was filtered and the mass recorded to allow a determination of the nominal % w/w Pd/support. The flask was attached to a Buchi rotary evaporator with a dinitrogen purge system and the water evaporated from the catalyst samples. The precursor beads or pellets were then air dried in an oven: Pd samples were dried at 60°C for 18 hours followed by 2 hours at 120°C. The nickel catalysts underwent a similar procedure at 100°C for 16½ hours and 3½ hours at 120°C.

Each precursor species was calcined in air in a muffle furnace. The temperature was slowly ramped to the required calcination temperature, 250°C for Pd and 450°C for Ni, and held at this value for 2 hours after which the catalysts were allowed to cool to ambient temperature. Calcination resulted in the homogeneous decomposition of the metal nitrates to the oxides. This procedure resulted in metal oxides dispersed on the porous support surfaces.

An additional 1% Pd/Cab-O-Sil silica catalyst was prepared at a later date by the same wet impregnation and calcination procedure by ICI Katalco.

Activation of the catalysts was achieved by reduction of the supported oxide in a flow of dihydrogen as discussed in Section 3.4.

### 3.2.2: HOMOGENEOUS PRECIPITATION/DEPOSITION.

In this process all the ingredients are present in the reaction vessel at the start of the precipitation: nickel nitrate and urea, each dissolved in a specified volume of water and the silica support, suspended in the aqueous medium. The essence of the method is that the precipitating agent, hydroxyl ions- is generated gradually throughout the solution by hydrolysis of urea upon heating of the reaction mixture to 90°C.

One catalyst was prepared by the homogeneous precipitation/deposition of nickel on to a non-porous microspheroidal Cab-O-Sil 5M silica of surface area 194 m<sup>2</sup>g<sup>-1</sup>. 150g of the silica was stirred into a slurry with 150ml deionized water in a 2l three necked round bottomed flask fitted with an overhead Citenco motor driven stirrer and a thermometer in one side arm. 400ml of nickel nitrate solution containing 74.52g Ni(NO<sub>3</sub>)<sub>2</sub>·6H<sub>2</sub>O (Aldrich 99.999%) was then added. Temperature control was maintained using an oil bath equipped with a heating element.

42.61g of urea (B.D.H. 99.5%), corresponding to a molar ratio of Ni(NO<sub>3</sub>)<sub>2</sub>·6H<sub>2</sub>O / H<sub>2</sub>NCONH<sub>2</sub> = 0.36, was dissolved in 50ml deionized water and subsequently added to the precipitation vessel. Dilute nitric acid was added to adjust

the initial pH prior to reduction from 4.1 to 2.4 to prevent premature hydrolysis. The reaction vessel was heated slowly to  $90 \pm 3^\circ\text{C}$  and stirred continuously for a 5 hour period. The suspension was then filtered through a Pyrex No. 4 sinter, the filtrate washed with 4 x 100ml portions of warm deionized water and air dried in an oven for 22 hours at  $114^\circ\text{C}$ .

Calcination of this catalyst was not necessary as direct reduction of the hydroxide precursor to the metal could easily be achieved. However, after drying, the catalyst appeared to have also partially calcined to the oxide. Therefore an additional calcination stage at  $450^\circ\text{C}$  for 5 hours was incorporated to calcine the entire sample and remove any hydroxide precursor. The resultant catalyst was sieved in the mesh range 150 - 250  $\mu\text{m}$ .

### **3.3: CATALYST CHARACTERISATION.**

#### **3.3.1: TEMPERATURE PROGRAMMED REDUCTION.**

When a catalyst precursor, e.g. NiO/Silica, is submitted to a programmed temperature rise whilst a reducing gas mixture is flowed over it, dihydrogen is adsorbed as a function of the temperature-reactivity relationship of the oxidised species. This technique is known as temperature-programmed reduction (T.P.R.). The rate of reaction is continuously measured by monitoring the composition of the reducing gas at the outlet of the reactor.

TPR is a highly sensitive technique which does not depend on any specific property of the catalysts other than that the species under study is in a reducible

condition, that is; the species need not be in a crystalline form nor have any particular properties such as paramagnetism.

The experiments were carried out in a closed system, with a flow through fixed bed reactor vessel. Figure 3.3.1 shows a schematic diagram of the system used. The catalyst sample vessel was surrounded by an electric furnace, which permitted the temperature to be increased linearly over the range 0 - 700°C. Approximately 0.2g of catalyst was placed in the reactor and the entire system purged with He, 80 ml min<sup>-1</sup>, until a steady baseline was achieved on the chart recorder.

During TPR the reducing gas stream consisted of a low concentration of dihydrogen in dinitrogen, 6% H<sub>2</sub>/N<sub>2</sub>, which was purified by passing through a deoxygenating catalyst, 1% Pd/WO<sub>3</sub>, and dried by passing through a trap containing Linde 5Å molecular sieve. Dihydrogen uptake can then be measured by the difference in the thermal conductivity of the gas before and after reaction. A cold trap (dry ice/acetone), was incorporated after the reactor vessel and before the T.C.D. to remove any reduction products from the gas stream which may be harmful to the tungsten/rhodium filaments of the T.C.D.

The reducing gas, 40 ml min<sup>-1</sup>, was brought on line at a sufficiently low temperature to prevent reaction and the baseline on the chart recorder allowed to settle. Once a steady level plot was obtained the reactor temperature was steadily ramped at a linear rate of 5°C min<sup>-1</sup>. As the reduction temperature of a specific species was reached, consumption of dihydrogen occurred and the corresponding compositional

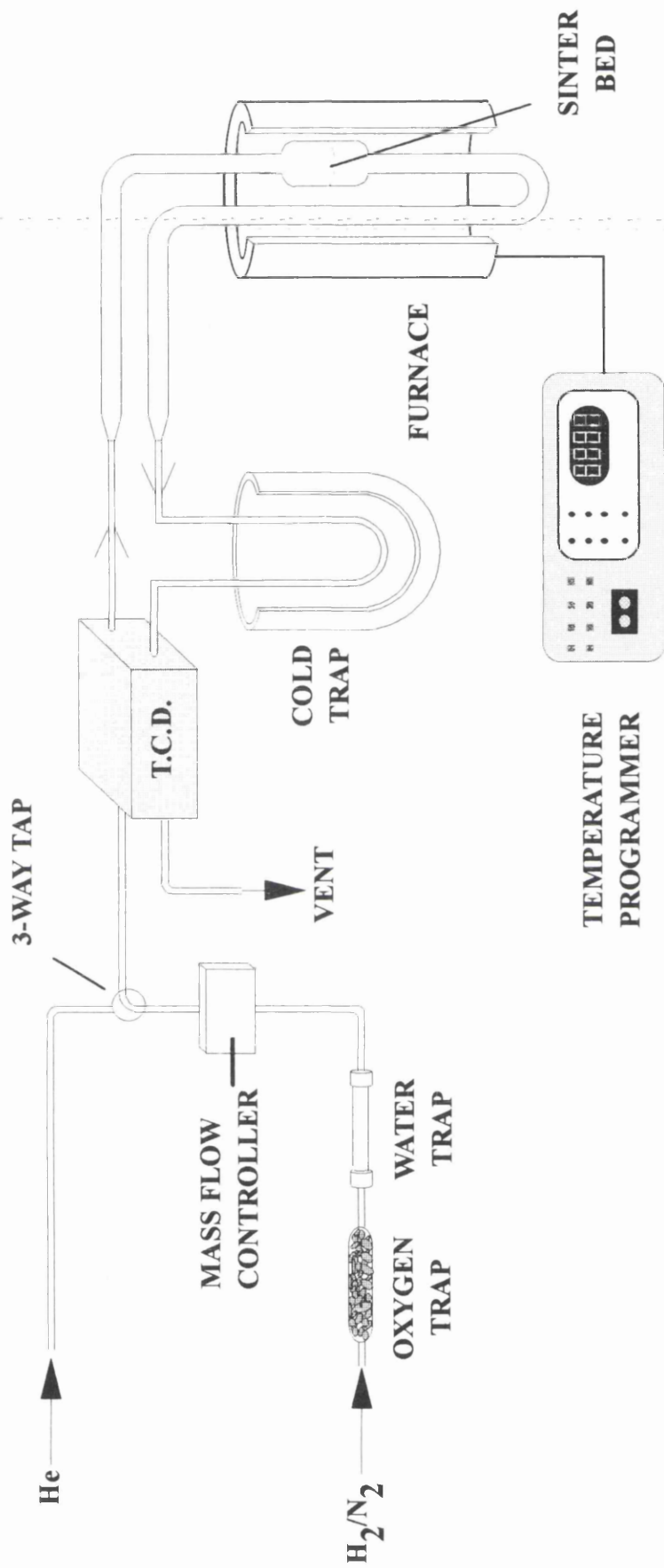


FIGURE 3.3.1 SCHEMATIC DIAGRAM OF THE T.P.R. APPARATUS

change of the effluent gas was monitored by the T.C.D. Distinct reduction processes in the sample show up as peaks in the reduction profile, (see figure 3.3.2) where there is a direct correlation between the time axis and temperature. As such, a characteristic reduction profile for each individual catalyst can be established, providing information on the number of distinct species present, as well as the minimum reduction temperature required to reduce the catalyst before use in subsequent reactions.

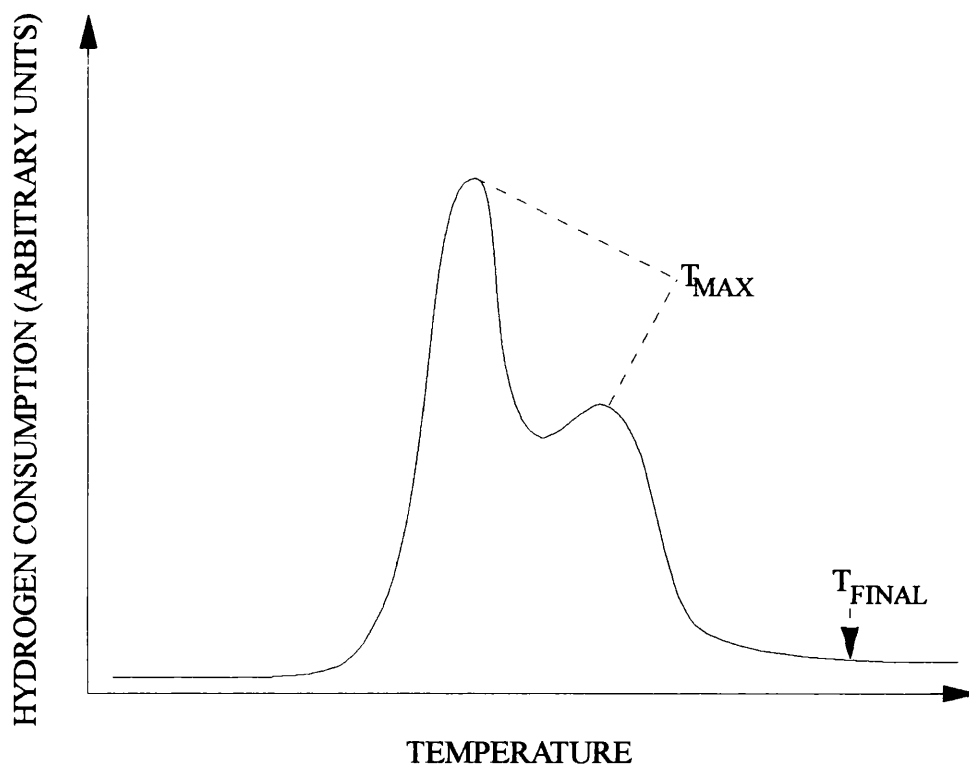


FIGURE 3.3.2: TYPICAL TPR TRACE

### 3.3.2: ATOMIC ABSORPTION

#### 3.3.2.1: Determination of Metal Content.

The metal loading of each catalyst precursor was determined by atomic absorption spectrometry using a Perkin Elmer 1100B Spectrophotometer, fitted with a suitable Cathodean Ltd hollow cathode lamp, to detect either palladium or nickel. Palladium absorption was measured at 247 nm and nickel at 232 nm.

Calibration curves were constructed by preparing standard solutions from initial 1000ppm standards (B.D.H Ltd, Spectrosol stock solution) containing 5% by volume concentrated nitric acid. The linear region for Pd measurements was within the range 0 - 10ppm and 0 - 5ppm for Ni. The calibration graphs are shown in figures 3.3.3 and 3.3.4, where absorption (arbitrary units) is plotted against p.p.m. metal

Catalyst samples of a known weight (ca. 0.1g) were treated with 5ml nitric acid and left overnight. The resultant solution was then filtered from the support and made up to 100ml with deionised water. The sample solutions were diluted so that the absorbance of the solution fell within the calibrated regions.

#### 3.3.2.2: Determination of Metal Content within Modifier Solutions.

Atomic absorption was also used, in conjunction with UV-Vis spectroscopy, to determine the nature of the colouration, resultant in the diol modifier solutions after contact with both the palladium and nickel/Grace silica catalysts. It was possible that the colour arose from metal lost from the catalyst as a complex in solution.

After a single adsorption study (see Section 3.6) the coloured modifier solution was decanted and transferred to a volumetric flask. The flask was warmed on a hot plate to evaporate the solvent. This left a thick yellow/brown mud-like product. The volumetric flask was then made up to the mark with deionised water and 5% by volume nitric acid, in line with the standards previously prepared. A small amount of precipitate formed, possibly residual diol which was insoluble in water, was filtered from the solution and the sample volume adjusted. The metal content was then analysed by atomic absorption.

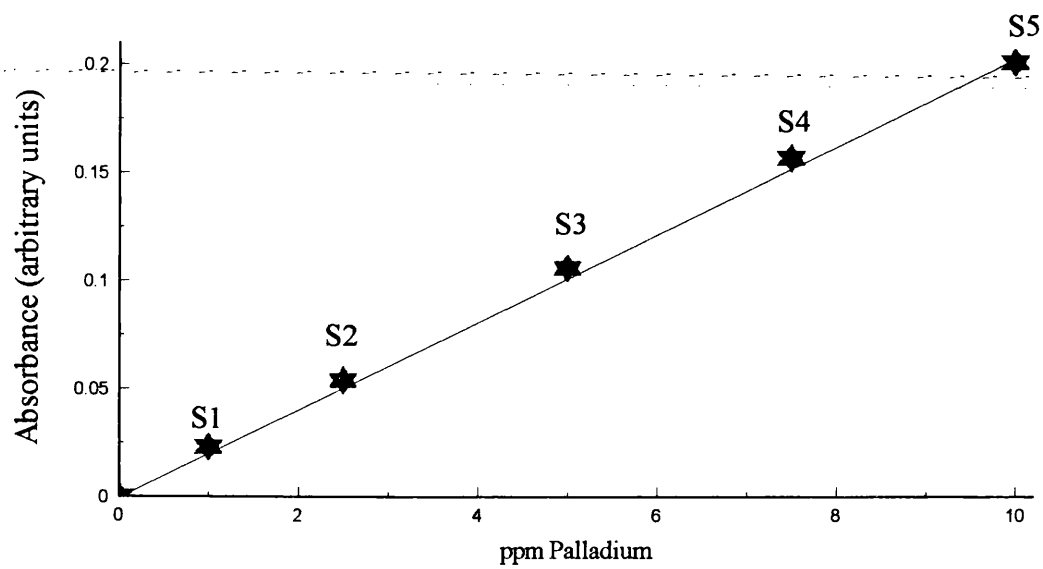


FIGURE 3.3.3: Pd A.A.CALIBRATION GRAPH

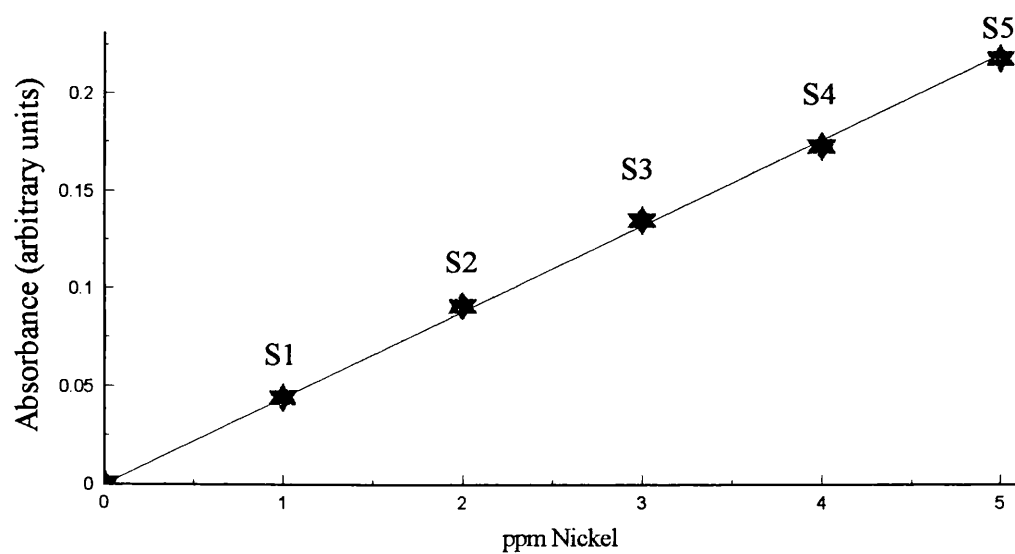


FIGURE 3.3.4: Ni A.A.CALIBRATION GRAPH

### 3.3.3: CHEMISORPTION.

For a through understanding of the behaviour of supported metal catalysts it is necessary to know the degree of dispersion of the metal. The dispersion,  $D$ , which can be defined as the fraction of the total number of metal atoms which are at the surface of the metal particles, equation 3.3.1, is of considerable practical value in measuring the number of surface sites available for the catalysed reaction and also provides a determination of the metal particle sizes.

$$\% \text{ Dispersion} = \frac{\text{No. Metal Atoms on Surface}}{\text{Total No. Metal Atoms per Sample}} \quad \text{Eq.3.3.1}$$

When a known volume of a sample gas is pulsed over an activated catalyst, a certain amount may be adsorbed. By calculating the amount of gas adsorbed, an indication of the number of surface metal sites can be obtained. This technique requires that the adsorbate forms a chemisorbed monolayer, that there is no significant contribution of the support to the chemisorption process and that a simple relationship exists between the number of molecules adsorbed and the number of surface atoms.

Of all the adsorbates, dihydrogen, dioxygen and carbon monoxide are the most frequently used in determining crystallite dimensions of supported metals. However, when dihydrogen is passed over palladium catalysts, difficulties arise in that not only does chemisorption take place, but dihydrogen is also taken up in the bulk of the metal.<sup>109</sup> This additional absorption can result in large uncertainties in the final surface area. Hence the adsorption of dioxygen and carbon monoxide was investigated for both palladium and nickel catalysts.

Figure 3.3.5 shows, schematically, the pulse flow, gas adsorption apparatus used. The vacuum system was maintained at a pressure of  $10^{-4}$  Torr or better by means of a mercury diffusion pump backed by a rotary oil pump. A cold trap, containing liquid nitrogen, was employed for two functions; 1) to prevent the rotary oil pump being polluted by any condensable reaction gases, 2) to prohibit any mercury vapour reaching the catalyst, where it could act as a permanent poison.<sup>110</sup>

For the standard reduction of the catalyst, a Watlow furnace was controlled using a Variac transformer, the temperature being monitored by a thermocouple in contact with the catalyst vessel.

The adsorbate gases were stored in bulbs attached to the line via a manifold at the head of the system. Gas samples could then be admitted to the fixed volume loop and the pressure measured by a mercury manometer. Pulses of gas were then injected on to the reduced catalyst sample in the reactor vessel in a constant flow of helium carrier gas. A T.C.D., placed down line of the reactor, attached to an amplifier and chart recorder, was used to detect any resultant changes in gas composition.

Approximately 0.1g of catalyst was reduced *in situ* in a flow of dihydrogen, as described in Section 3.4. In this reduced state, the catalyst was activated and chemisorption could readily occur at the surface metal sites. The dihydrogen was replaced by helium, the inert carrier gas, and the sample allowed to cool. Both the dihydrogen and the helium were purified over a deoxygenating catalyst, 1% Pd/WO<sub>3</sub>, and dried by passing through a trap containing Linde 5Å molecular sieve. Before any

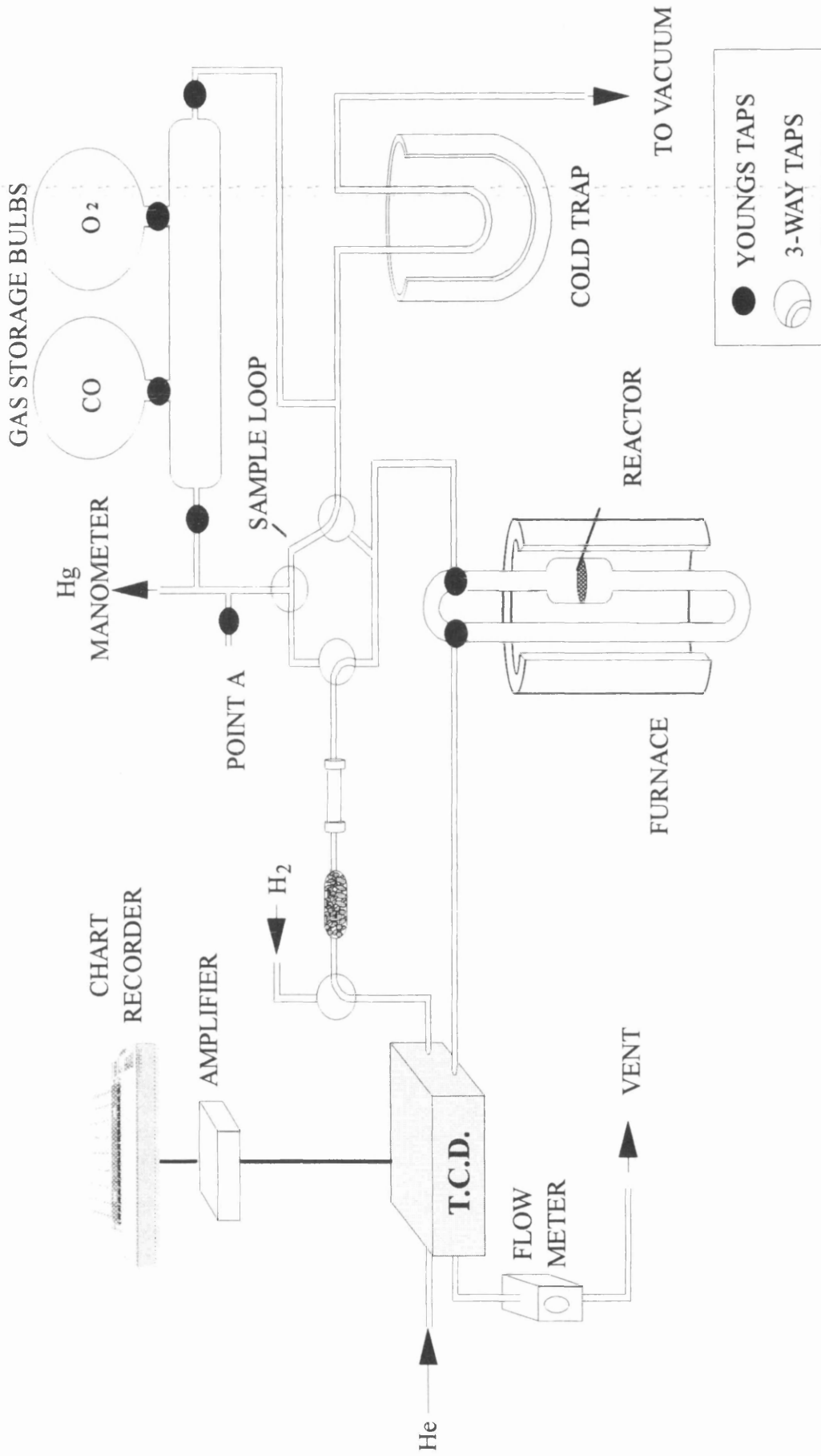


FIGURE 3.3.5: SCHEMATIC OF CHEMISORPTION APPARATUS

adsorbate gas could be pulsed over the active catalyst, the system was standardised. The catalyst sample vessel was isolated and standard pulses of the adsorbate were injected into the helium flow. These samples by-passed the reactor, flowed through the detector and resulted in peaks on the chart recorder. Once three sequential, identical standard peaks were obtained on by-pass, pulses of a known volume and pressure, (approximately 5 mmol), were passed over the catalyst sample. The amount adsorbed was determined as the difference between the areas of the eluted peak and a standard peak, where no adsorption had occurred. Figure 3.3.6. shows a typical plot. Pulsing was continued until three standard peaks of an identical height were obtained, indicating that no more gas was irreversibly adsorbed on to the surface.

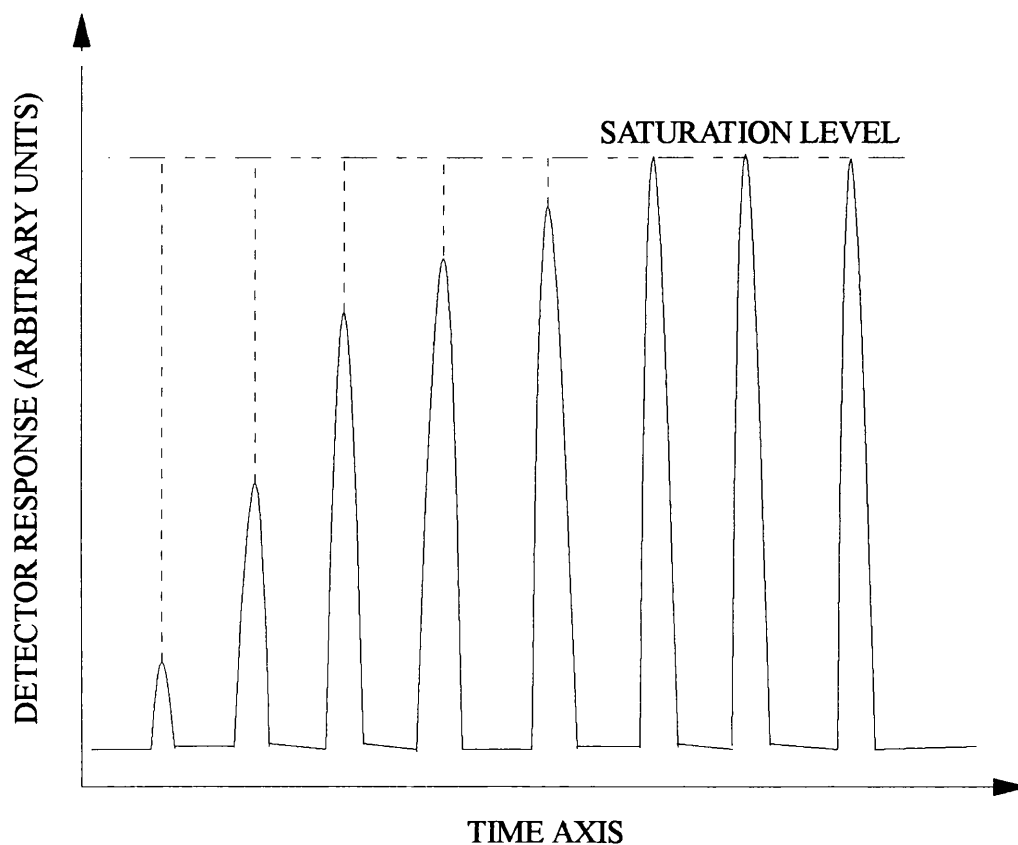


FIGURE 3.3.6: TYPICAL CHEMISORPTION TRACE

The volume of the gas sample loop was determined experimentally using Boyle's Law, equation 3.3.2, which states that :

$$V \propto \frac{1}{P} \quad \text{Eq: 3.3.2}$$

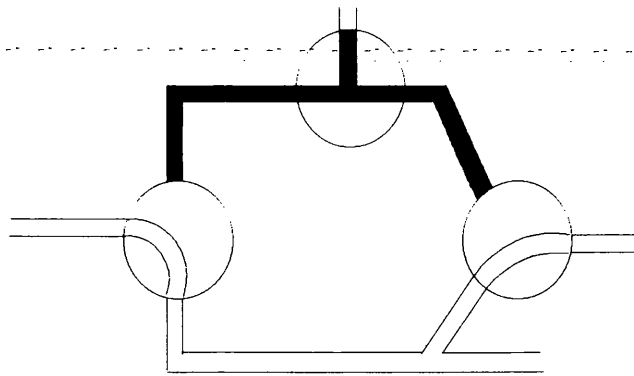
therefore, under ambient temperature conditions, it can be assumed that:

$$p_1 V_1 = p_2 V_2 = p_3 V_3 \quad \text{Eq: 3.3.3}$$

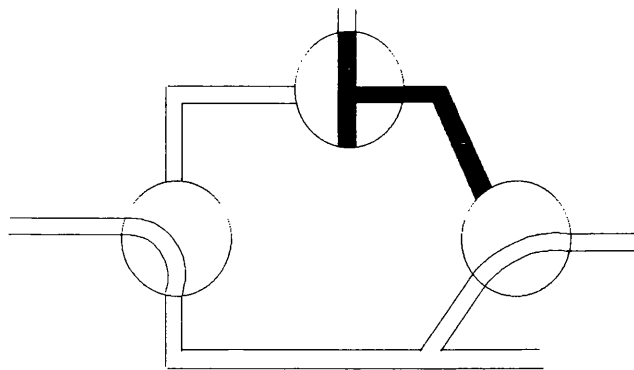
A standard volume flask, ( $V_1=174.25 \text{ cm}^3$ ), was attached to the line at point A on figure 3.3.5, and filled with air to a known pressure,  $p_1$ . The flask was then isolated and the line evacuated. The air in the flask was then expanded through the line, into the sample loop, to provide  $p_2$  and  $V_2$ . By a further expansion into the loop itself, the third pressure and volume,  $p_3$  and  $V_3$ , could be measured. Small pressure changes were accurately measured using a pressure transducer, (Edwards medium vacuum control unit 251, Edwards High Vacuum International). Knowing  $p_1$ ,  $p_2$ ,  $p_3$  and  $V_1$ , the volume of the loop can be calculated using the relationship in equation 3.3.4.

$$\text{Loop Volume} = V_3 - V_2 = p_1 V_1 \left( \frac{1}{p_3} - \frac{1}{p_2} \right) \quad \text{Eq: 3.3.4}$$

By filling either the entire sample loop or alternatively only half the volume, see figure 3.3.7, two different volumes could be used during the pulse flow work.



a: Full Loop Size



b: Half Loop Size

**■** : Volume filled with sample gas

FIGURE 3.3.7: CHEMISORPTION SAMPLE LOOP

### 3.3.4: TRANSMISSION ELECTRON MICROSCOPY.

Electron microscopy was used as a technique to provide information on the particle sizes and the metal dispersions of each catalyst by direct observation of the metal particles on the support.

Finely ground catalyst, having been reduced and passivated, to allow handling in air, was suspended in distilled water and ultrasonically dispersed for 10 mins. A drop of the fine suspension was then placed on a 300 square mesh, carbon coated copper grid (3.05 mm) and placed in an oven at 40°C overnight to permit the droplet to evaporate.

The impregnated grid was placed in the microscope and T.E.M. measurements were conducted using a Phillips 1200 electron microscope.

### 3.4 CATALYST ACTIVATION

An *in situ* isothermal reduction was performed prior to every adsorption and catalytic study. A sample of the calcined catalyst precursor was loaded on to the silica sinter in the reactor vessel and reduced in a 50 cm<sup>3</sup> min<sup>-1</sup> flow of dihydrogen (for Pd) or 150 cm<sup>3</sup> min<sup>-1</sup> (for Ni), which was passed through the catalyst in a downward direction, to prevent any carry over of catalyst particles. The reactor bed was heated to the predetermined reduction temperature, 450°C for each of the nickel catalysts, 250°C for both Pd/Carbon and 2% Pd/silica and ambient temperature for the 1% Pd/silica. These conditions were maintained for either three or two hours for all the Ni or Pd catalysts respectively. After this reduction the reactor vessel was purged with a flow of an inert gas, (dinitrogen or helium), and the catalyst allowed to cool to ambient temperature for 30 min before subsequent use. If the sample had been left to cool in a flow of dihydrogen there would have been the possibility of dissociative

adsorption of the dihydrogen on to the surface which would have eclipsed metal sites and hindered subsequent processes. The temperature was monitored by means of a Cr/Al thermocouple, attached to a Comark electronic thermometer, inserted in a well within the reactor, in contact with the sinter bed. The gas flow was monitored via a bubble flow meter attached to the effluent gas stream and could be finely adjusted using a Nuprox needle valve.

The reduction gases used were either H<sub>2</sub> (BOC, 99.9%) or D<sub>2</sub> (B.D.H. Ltd., 99.5% pure)

### **3.5: PRELIMINARY NICKEL/GRACE SILICA**

#### **CATALYST WASH.**

Within both the Ni/Grace silica-C30 and C10 catalyst systems, agitation of the particles within the reactors proved to be abrasive and as such the catalysts appeared to degrade when simply stirred, to result in visible particles suspended within the modifier solutions. This effect was predominant within the C30 system but was also apparent with the C10. This meant that the catalysts were unacceptable in their prepared state. The alternatives were to either i) change the silica support, ii) prepare a new series of catalysts by an alternative method to wet impregnation such as homogeneous deposition/ precipitation or iii) alter the current catalysts. However the Grace silica support was of considerable interest at the start of the project and the idea of changing these catalysts, already prepared by wet impregnation, also meant that comparisons could be drawn against the Pd/Grace silica catalyst, prepared by the same route, without the additional variables of catalyst preparation technique and the nature of the silica support. Thus, the third proposal was the most favourable and as such a basic preliminary wash stage was adopted for both the catalyst samples. This was

achieved as follows: 10g samples of the catalyst were reduced at 450°C in pure dihydrogen for three hours. These samples were then cooled to room temperature in a flow of 1% dioxygen diluted in dinitrogen. Passivation of the catalyst in this gas flow ensured that only a surface nickel oxide coating was formed which protected the metal from complete oxidation upon exposure to the atmosphere, a highly pyrophoric reaction.<sup>111</sup> The reduced catalysts were stirred vigorously in a conical flask with 30ml of pure THF for one hour. The catalyst beads were then decanted from the solution and the solvent left to evaporate. This left a black powdery residue which was stored for atomic absorption analysis to determine the amount of nickel removed by this process. The remaining number of surface nickel atoms in the catalysts were analysed by chemisorption. These "washed" catalysts were then used throughout the project.

## **3.6: HIGH PERFORMANCE LIQUID CHROMATOGRAPHY**

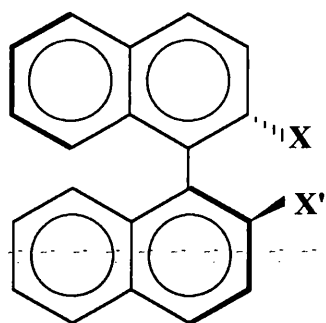
### **(HPLC)**

#### **3.6.1: MATERIALS.**

Table 3.6.1 shows a list of modifier species used in the detailed adsorption studies. The structures are all shown in figures 3.6.1 and 3.6.2. These molecules were used to modify the catalyst surface before enantioselective hydrogenation. Included are the associated molecules that were also investigated to help provide information on the modes of adsorption. Materials that were not available commercially were synthesised by an organic chemist<sup>112</sup>, (OC), to a level of high purity.

TABLE 3.6.1: MODIFIER MATERIALS.

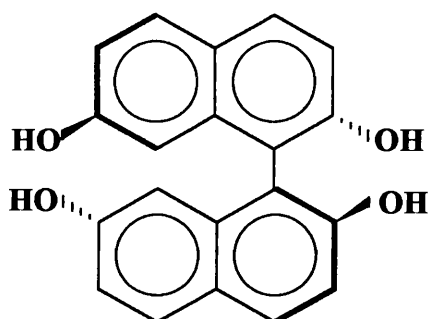
CHEMICAL	SOURCE	% PURITY	ABBREVIATION
± 2,2'-Dihydroxy-1,1'-binaphthalene	Fluka	>99	±-DIOL
R(+)-2,2'-Dihydroxy-1,1'-binaphthalene	Aldrich	99	R-DIOL
S(-)-2,2'-Dihydroxy-1,1'-binaphthalene	Lancaster	99	S-DIOL
(±)-2,2'-Diamino-1,1'-binaphthalene	OC	/	±-DIAMINE
R(+)-2,2'-Diamino-1,1'-binaphthalene	Fluka	>99.5	R-DIAMINE
S(-)-2,2'-Diamino-1,1'-binaphthalene	Fluka	>99.5	S-DIAMINE
(±)-2-Hydroxy-2'-amino-1,1'-binaphthalene	OC	/	AMINOL
(±)-2,2'-Dimethoxy-1,1'-binaphthalene	OC	/	DIMETHOXY
(±)-2-Hydroxy-2'-Methoxy-1,1'-Binaphthalene	OC	/	HYDROXY METHOXY
S(-)-2,2',7,7'-Tetrahydroxy-1,1'-binaphthalene	OC	/	TETRAOL
R(-)-1-(9-Anthryl)-2,2,2-trifluoroethanol	Fluka	>98	TFAE
(CH <sub>2</sub> ) <sub>6</sub> bridged, pyridine based macrocycle	OC	/	C <sub>6</sub> -MACRO
(CH <sub>2</sub> ) <sub>5</sub> bridged, pyridine based macrocycle	OC	/	C <sub>5</sub> -MACRO



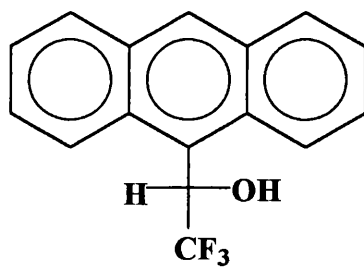
**BINAPHTHYL**

$X = X'$   $\longrightarrow$  **DIOL, DIAMINE, DIMETHOXY.**

$X \neq X'$   $\longrightarrow$  **AMINOL, HYDROXY METHOXY**

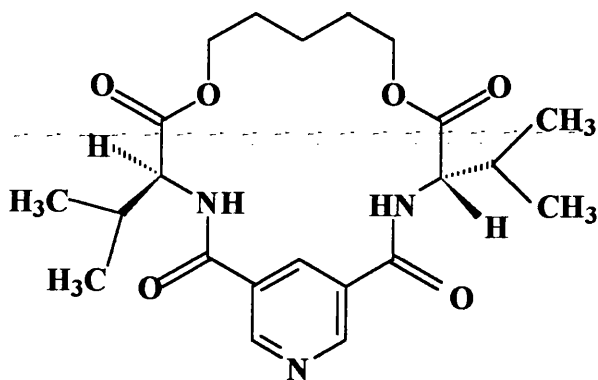


**TETRAOL**

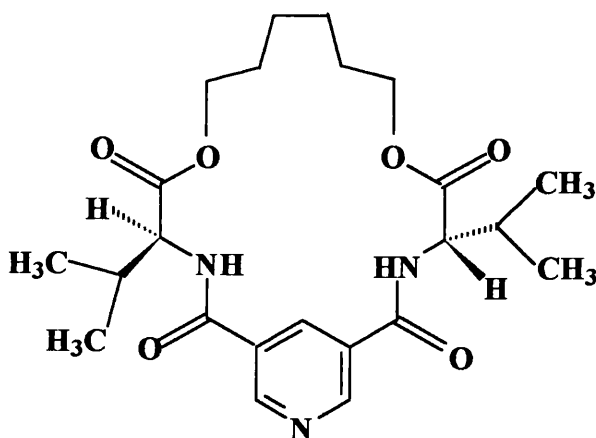
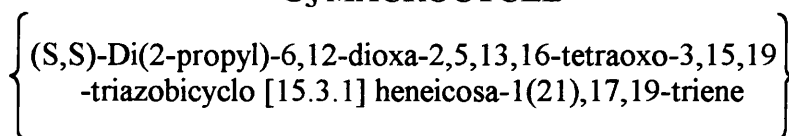


**TFAE**

FIGURE 3.6.1: BINAPHTHYL RELATED MODIFIERS



**C<sub>5</sub> MACROCYCLE**



**C<sub>6</sub> MACROCYCLE**

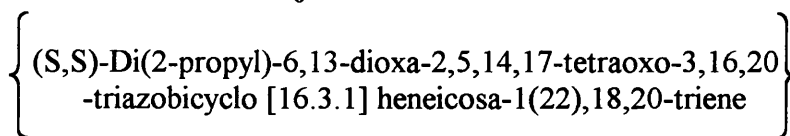


FIGURE 3.6.2: UNCHELATED MACROCYCLE STRUCTURES

Also shown are the abbreviated names and acronyms by which each modifier will be referred to in the following sections.

Adsorption studies were concentrated on the binaphthyl derivatives, the macrocycles and TFAE. Detailed adsorption studies were performed with these modifiers to try and examine the extent and mode of adsorption before use as hydrogenation catalysts.

### 3.6.2: QUANTITATIVE ANALYSIS

A quantitative HPLC technique was used to evaluate the extent of modifier adsorption. The system, shown schematically in figure 3.6.3, consisted of several components:

- 1) A solvent reservoir that contained the mobile phase.
- 2) A reciprocating, dual piston that pushed the solvent, at high pressure, through the column.
- 3) A pressure transducer that monitored the pump pressure before the column and controlled the piston motors to maintain a constant pressure. If the pressure had risen above a maximum value the system would have automatically shut down.
- 4) A Rheodyne injector system and sample loop, that introduced the sample solution into the moving mobile phase.
- 5) The column - a narrow stainless steel tube, tightly packed with small particles of the material used to effect the separation.
- 6) A Spectra 100 UV-Vis detector with a standard deuterium lamp that measured the concentration of the sample components as they eluted from the column.

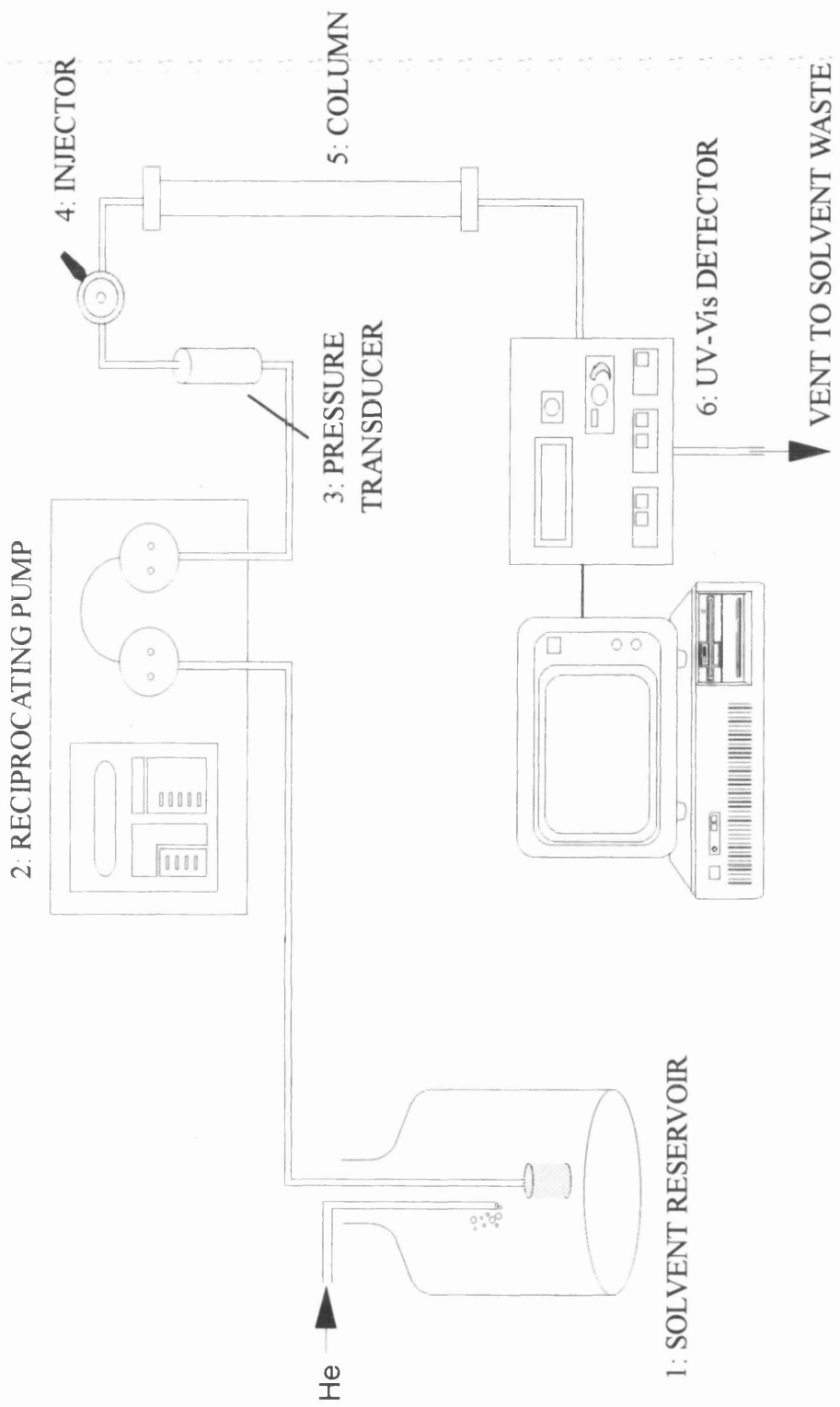


FIGURE 3.6.3: SCHEMATIC OF HPLC SYSTEM

- 7) A personal computer with 'NINA' data acquisition, integration and evaluation system to record the chromatogram or alternatively a Pye Unicam PU4810 computing integrator.

The analysis was performed on a Spherisorb (5 $\mu$ m) C8-SB5 column (200 x 4.6 mm). This column, for reversed phase chromatography, had C8 hydrocarbon chains grafted on to the silica packing material, which reduced the polarity of the stationary phase. As such, more polar molecules were expected to elute first. Isocratic elution was achieved with a mobile phase of 60% acetonitrile / 40% water (by volume), which was vigorously sparged with helium for 5 min prior to use to remove dissolved air. The flow rate was maintained at 1 ml min<sup>-1</sup>. All HPLC grade solvents were supplied by Rathburn Chemicals.

For each injection, 25 $\mu$ l of solvent were introduced to the 10 $\mu$ l sample loop. This excess of solution filled the loop and also flushed any previously retained residue out through the vent. Alternative injection volumes of 15 $\mu$ l and 20 $\mu$ l were also investigated. However, 25 $\mu$ l samples had the greatest reproducibility and smallest error,  $\pm 2\%$ , and this volume was adopted as the standard injection volume throughout.

As the sample eluted from the column, it passed through a small flow cell held in the radiation beam of the UV-Vis detector. The Beer-Lambert Law (equation 3.6.1) states that the UV absorbance of a species is proportional to the concentration of that species.

$$A = \epsilon c l$$

Eq: 3.6.1

$\epsilon$  = Extinction coefficient

$c$  = Concentration

$l$  = Path length

However, for some systems concentration may not be linearly proportional to the measured absorbency owing to a variety of factors such as hydrogen bonding, ion-pair formation, solvation and instrumental factors which can cause incorrect calculations of sample concentration in the solvent medium. Calibration curves were constructed from chromatograms to ensure that the absorbance values of the concentrations of modifier in tetrahydrofuran were obtained within a linear region. As each modifier had a different extinction coefficient separate calibration curves were obtained. Figures 3.6.4 and 3.6.5 show the calibration curves of the diol and diamine as examples.

After removal from the modifier reactor, each solution was purified through a self-contained disposable filter (0.45 $\mu$ m, Gelman Sciences Ltd) to prevent contamination of the HPLC system. The initial starting solution, of a known concentration, and the sample were each then analysed three times by HPLC to reduce errors. As HPLC is sensitive to changes in chromatographic conditions e.g. slight variations in the mobile phase composition, the initial starting solution was used as an external standard. The resultant chromatogram provided retention times, to identify the peak, and peak areas that were used for the quantitative analysis. The amount,  $X$ , of the sample compound was calculated as follows:

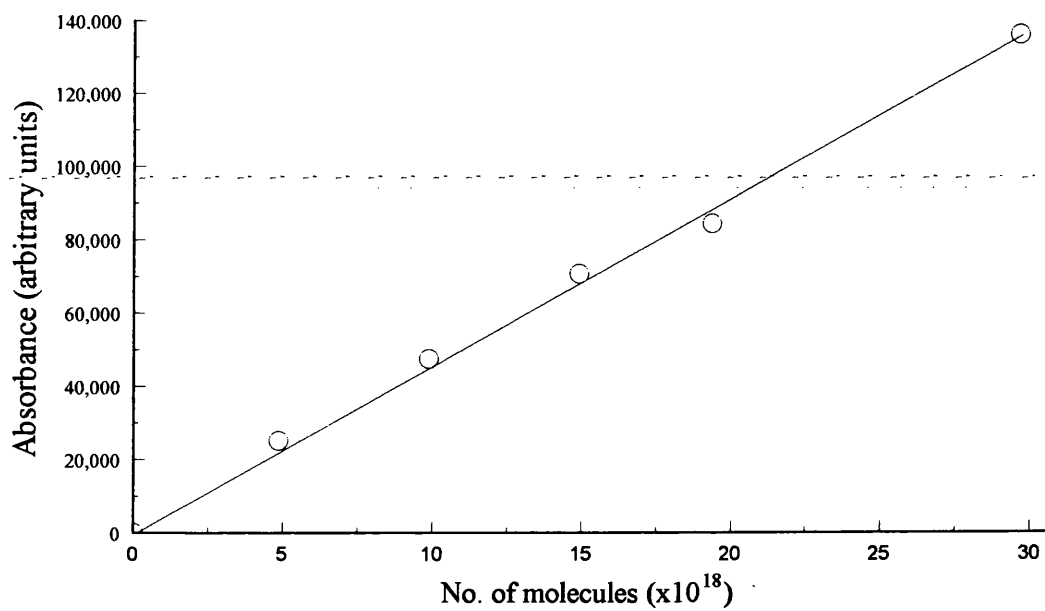


FIGURE 3.6.4: DIOL HPLC CALIBRATION

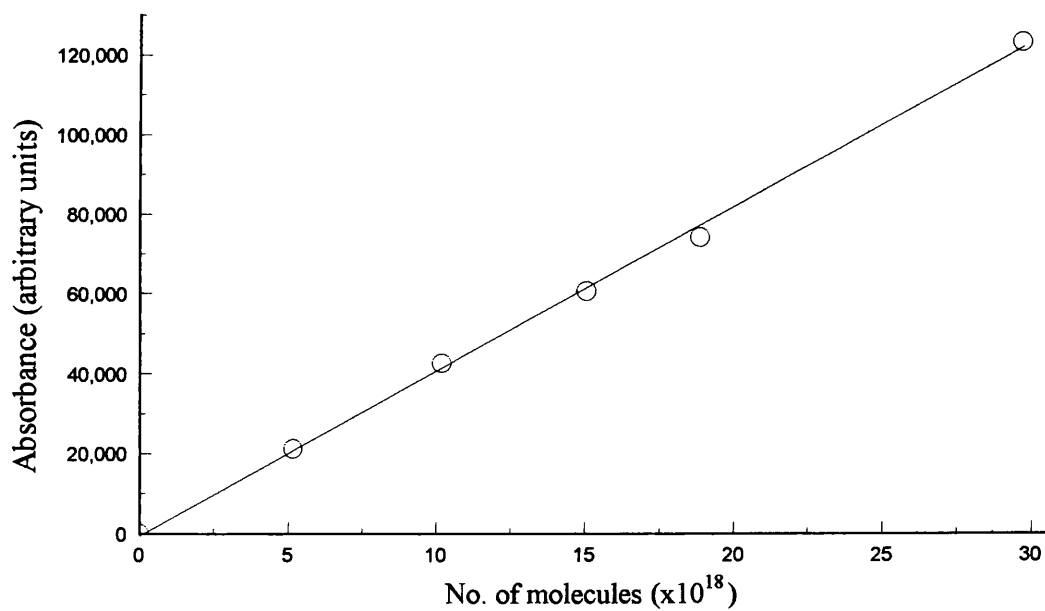


FIGURE 3.6.5: DIAMINE HPLC CALIBRATION

$$\text{No. Molecules } X = \frac{\text{Area } X \times \text{No. Molecules Standard}}{\text{Area Standard}} \quad \text{Eq: 3.6.2}$$

The UV spectra of each modifier in THF was recorded before HPLC analysis to predetermine the optimum UV wavelength for detection. The retention times on the column and the UV detector wavelengths for each of the main modifier molecules analysed by this technique are shown in table 3.6.2.

HPLC is very effective when a strong absorbing UV chromophore is present in the modifier molecule. The presence of poly-aromatic systems enabled easy UV detection above 280 nm to avoid solvent impurity peaks. Table 3.6.3 shows the UV cut off values for the solvent and mobile phase components.

TABLE 3.6.3 : SOLVENT PROPERTIES	
Solvent	UV Cut Off (nm)
Acetonitrile	210
Tetrahydrofuran	280
Water	200

Unfortunately the UV absorbance for the macrocycles was optimum at 240nm which meant that an additional THF peak was also present on the HPLC trace. However, under the HPLC conditions used, these peaks were totally resolved and as such the solvent did not present any analytical problems.

**TABLE 3.6.2: RETENTION TIMES OF MODIFIER MOLECULES**

Modifier	Retention Times (min)	UV Wavelength (nm)
Diol	6.5	340
Diamine	8.3	340
Dimethoxy	13.4	340
Tetraol	3.5	340
Hydroxymethoxy	8.5	340
Aminol	7.6	340
TriFluoroAnthrylEthanol	9.12	340
C <sub>5</sub> -Macrocycle	3.94	240
C <sub>6</sub> -Macrocycle	4.11	240

### 3.6.3: HPLC-MS

As in the case of all other chromatographic methods, HPLC is a poor identifier. Other instruments, such as a mass spectrometer, must be employed to aid positive identification of any unknown peaks. This is particularly of interest because of the high specificity and universal applicability of HPLC-MS. However, for a long time the main obstacle to the connection of HPLC and mass spectrometry was the problem of surplus solvent. This obstacle has now been overcome and it is possible to link liquid chromatography on-line to a mass spectrometer.

Analyses were carried out at Zeneca, Macclesfield with a 'Quattro' Mass Spectrometer, (Fisons Scientific Instruments) for electrospray ionisation, in conjunction with the HPLC system. In this technique the whole eluent is sprayed into the source of the MS where the ions are then separated at right angles. The eluate is initially transported through a heated capillary and ionised. After addition of ammonium salts (acetate) non-volatile compounds can be ionized, emphasizing the  $MH^+$  peak. The liquid chromatography conditions were identical to those at Glasgow, with the sole exception that a C18 column was used to effect component separation in place of the C8. The analyses were carried out over the mass range  $m/z = 100 - 1200$ .

### 3.7: ADSORPTION STUDIES.

After catalyst activation the reduced catalyst was cooled to reaction temperature in a flow of dinitrogen. Once cool the reactor vessel, figure 3.7.1, was isolated from the gas stream and inverted. This resulted in the catalyst resting in the bottom well under a positive pressure of dinitrogen.

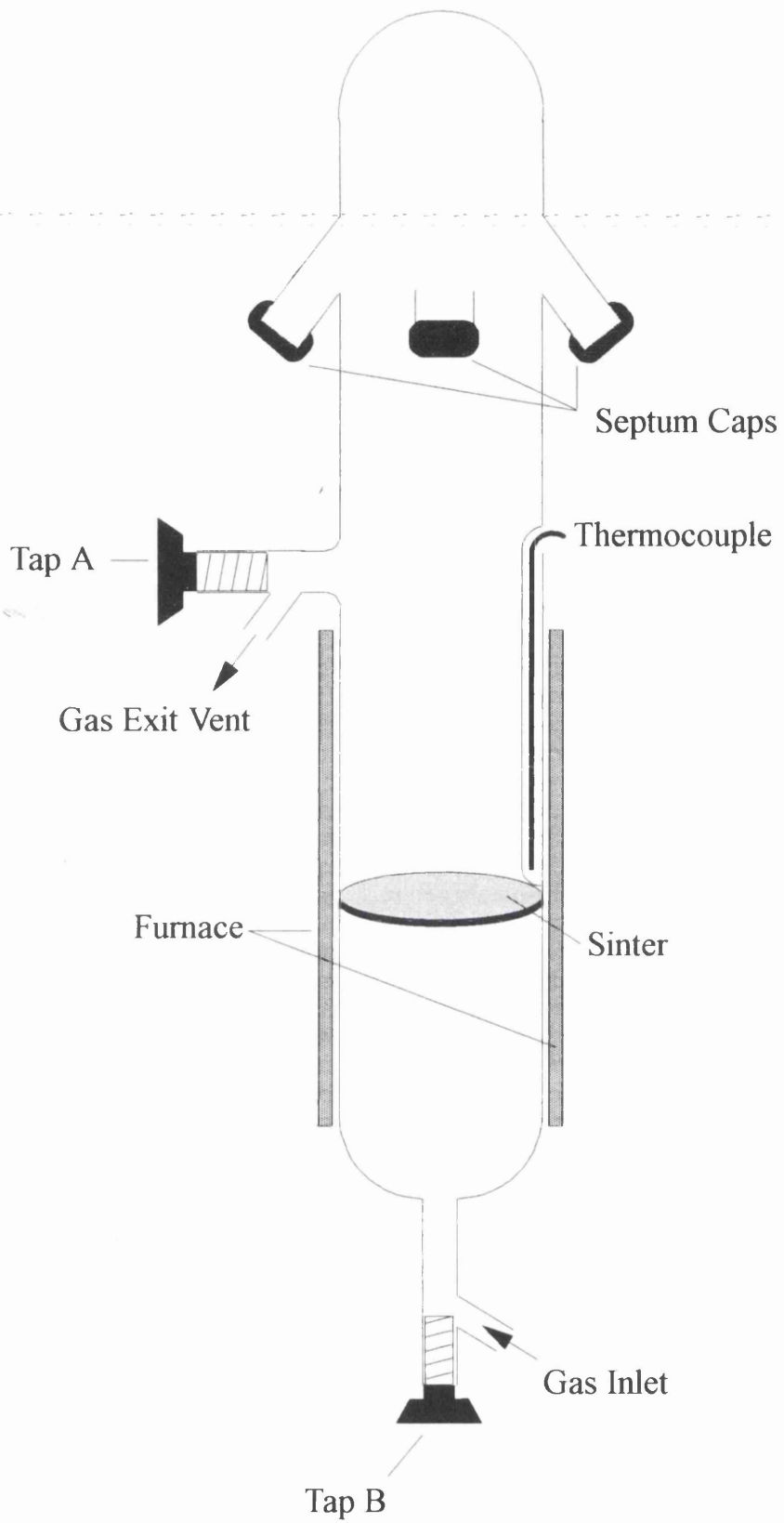


**FIGURE 3.7.1: ADSORPTION REACTOR**

Known concentrations of the selected modifier molecule were prepared in volumetric flasks with tetrahydrofuran (THF) as the solvent. The THF (HPLC Grade, Rathburn Chemicals) was stored under a positive pressure of dinitrogen. Modifier solutions, 10ml, were then injected into the reactor vessel via one of the side arms, which were sealed with B10 septum caps.

The standard modification thus proceeded under an inert dinitrogen atmosphere with constant stirring, using a magnetic bar, for a 24 hour period at the desired temperature. Temperature control was attained by the incorporation of either an oil bath or a Dewar flask, containing ice, surrounding the reactor well.

After modification the concentration of the post-modification solution was analysed by quantitative HPLC, as previously described in Section 3.6. Adsorption isotherms were constructed by periodically removing small aliquots of modifier solution (~0.15 ml) for analysis by HPLC to determine the amount of modifier retained on solution.

### **3.8: POLARIMETRY**

Polarimetry was used to investigate whether or not the individual binaphthyl modifier molecules retained their inherent chirality once they had contacted the catalyst surfaces. This technique was used as the binaphthyl modifiers were not sufficiently volatile for chiral G.C. analysis and were unsuitable for separation by the available chiral HPLC columns. Optical rotation values were measured with an AA-100 Polarimeter, Optical Activity Ltd, (sensitivity  $\pm 1$  millidegree). All measurements were made at a temperature of  $25 \pm 3^{\circ}\text{C}$  using the sodium D-line (wavelength = 589.3 nm).

The polarimeter cell, (volume = 1cm<sup>3</sup> and path length = 10cm), was filled with T.H.F. and the polarimeter was zeroed against this solvent. The cell was then washed with acetone and thoroughly dried. Standard solutions were then analysed over the range  $c = 0 - 1$ , where  $c$  was the concentration of solute expressed as g per 100ml, and a calibration graph was obtained, as shown in figures 3.8.1 and 3.8.2

Solutions of the chiral binaphthalene derivatives were injected over the activated catalysts and the systems left to equilibrate for 20 hrs. The post-modification solutions were transferred to the polarimeter cell and the optical rotation measured. The resultant corresponding concentration was determined from HPLC.

The modified catalysts were then washed and the final solutions were also analysed by this technique.

### **3.9: HYDROGENATION.**

After adsorption studies with the binaphthyl derivatives, TFAE or unchelated macrocycles, the modified catalysts were then investigated for enantioselective hydrogenation.

Several additional modifier species were also introduced at this stage, table 3.9.1, which were collectively referred to as the 'alternative modifiers'. They were all similar in that they possessed an aromatic moiety with an attached chiral arm, containing a variety of hydroxide and amine substituents, figure 3.9.1. These molecules were used to modify the catalyst surface in the same way, Section 3.7, but the extent of modification was not analysed and as such the amount of modifier adsorbed on the surface was not detailed.

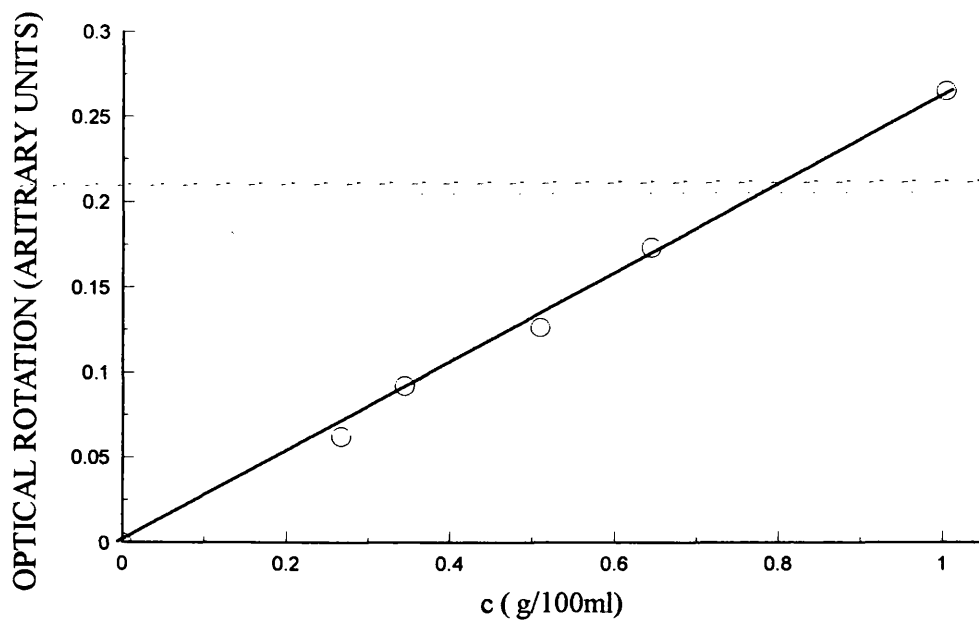


FIGURE 3.8.1: DIOL POLARIMETER CALIBRATION

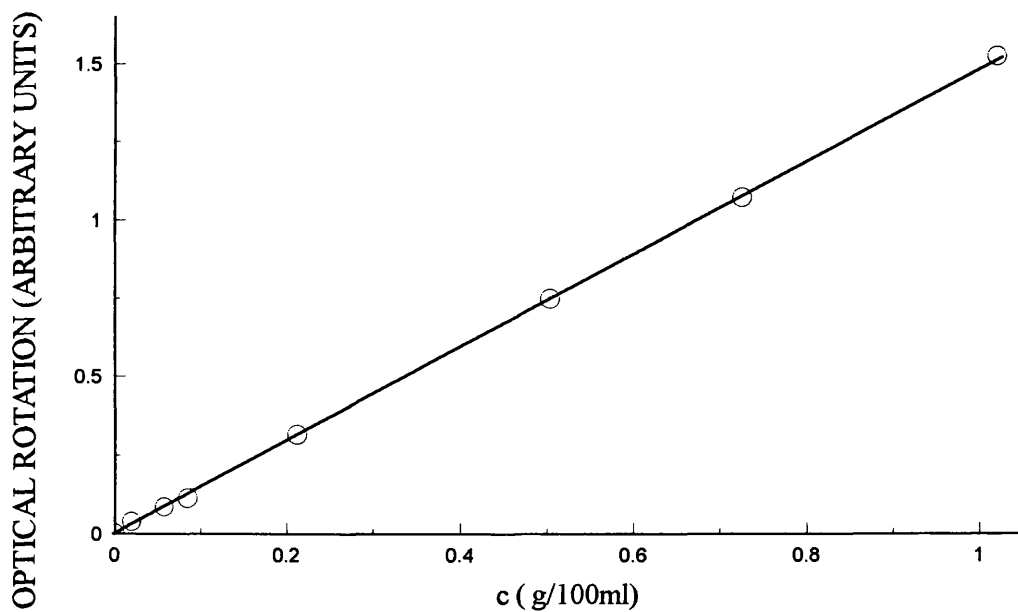
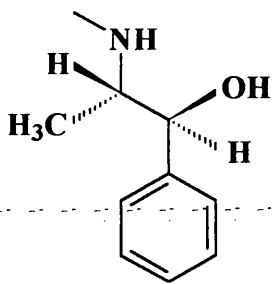
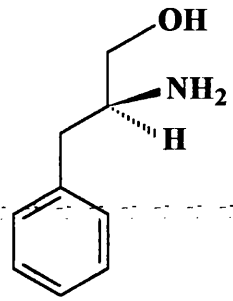


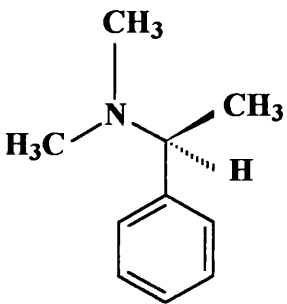
FIGURE 3.8.2: DIAMINE POLARIMETER CALIBRATION



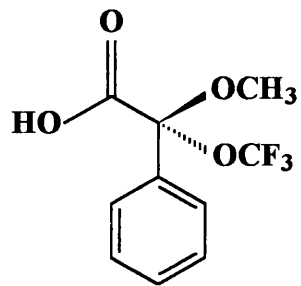
**Pseudo**



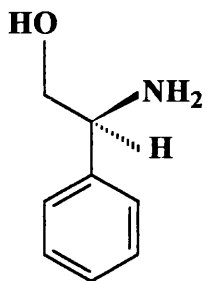
**PhAla**



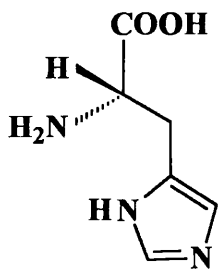
**DMPEA**



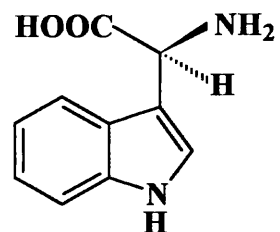
**MTFMPAA**



**PhGly**



**His**



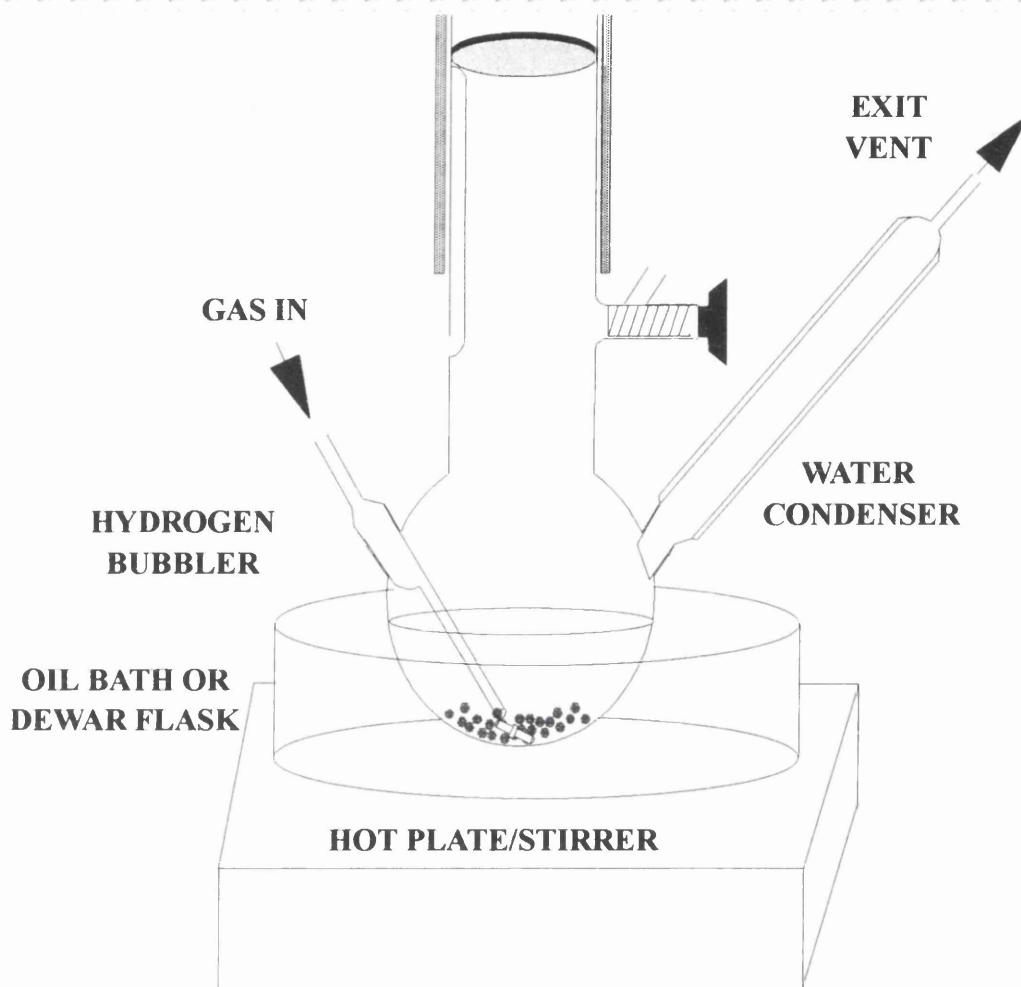
**Trp**

FIGURE 3.9.1: ALTERNATIVE MODIFIER STRUCTURES

TABLE 3.9.1: ALTERNATIVE MODIFIER MATERIALS.

CHEMICAL	SOURCE	% PURITY	ABBREVIATION
S(-)-2-Amino-1,1'-diphenyl-1-propanol	Fluka	99	DiPhAla
(+)-Pseudoephedrine	Fluka	~98	Pseudoeph
L-Phenylalaninol	Fluka	~99	PhAla
R(+)-N,N-dimethyl-1-phenylethylamine	Fluka	/	DMPEA
R-(+)- $\alpha$ -Methoxy- $\alpha$ -trifluoromethylphenylacetic Acid	Fluka	>99	MTFMCAA
L-(+)-Phenylglycinol	Fluka	/	PhGly
L-Histidine	Fluka	>99	His
L-Tryptophan	Fluka	>99	Trp

Hydrogenation of both the prochiral C=O and C=C reactants was performed in the liquid phase at atmospheric pressure. The reaction vessel used was an adaption of the initial modification reactor, where the bottom well had an increased capacity and three larger side arms to carry the water condenser and gas bubbler used for hydrogenation studies. After an *in situ* modification the final post modification solution was removed by syringe and a fresh 15ml of THF added. With the freshly modified catalyst stored under solvent, the two septum caps were removed and the water condenser and dihydrogen bubbler attached to the reactor, (figure 3.9.2). Dihydrogen was bubbled through the catalyst/solvent system at a rate of 5 ml min<sup>-1</sup> for an initial 5 min. before the reactant was introduced. This bubbling technique ensured that the dihydrogen was



**FIGURE 3.9.2: HYDROGENATION APPARATUS**

kept in close contact with the active surface. The reactant, either 0.5g Tiglic Acid or 0.5g 3-Coumaranone in 5ml THF or 2ml Methyl Tiglate or 4-Trifluoro, 2-methyl, 2-butenic acid ethyl ester, was then added by syringe through the third septum cap. The reaction proceeded, with constant agitation, for 20 hours, unless otherwise stated. After this time the reactants and products were analysed directly by chiral gas chromatography.

The test reactants analysed by this process were:

- 1)- Methyl Tiglate, (Avocado Ltd. 98%) - an  $\alpha,\beta$  unsaturated ester for prochiral C=C hydrogenation,  $\text{CH}_3\text{CHC}(\text{CH}_3)\text{COOMe}$
- 2)- 4-Trifluoro, 2-methyl, 2-butenic acid ethyl ester,(OC), a trifluorinated derivative of methyl tiglate,  $\text{CH}_3\text{CHC}(\text{CF}_3)\text{COOEt}$
- 3)- Tiglic Acid,(Lancaster 98+%),  $\text{CH}_3\text{CHC}(\text{CH}_3)\text{COOH}$
- 4)- 3-Coumaranone, (Lancaster 97%), a prochiral ketone for the hydrogenation of C=O,  $\text{C}_8\text{O}_2\text{H}_6$

To ensure that racemisation of any of the enantiomeric products could not simply be induced by the catalysts, a single enantiomer of the product was injected over the active catalyst and the reaction monitored by G.C. Only a singular peak was measured throughout indicating that no racemisation had occurred.

### 3.10:CHIRAL GAS CHROMATOGRAPHY

#### 3.10.1: PRODUCT ANALYSIS

The separation of enantiomers by gas chromatography (GC), can be performed in two modes: (1) *indirect method*: off-column conversion of enantiomers into diastereomeric derivatives by complete chemical reaction with an enantiomerically pure resolving agent and subsequent gas chromatographic separation of the diastereomers on a conventional non-chiral stationary phase, and (2) *direct method*: gas chromatographic separation of the enantiomers on a chiral stationary phase containing a resolving agent of high enantiomeric purity. Method 2, chiral chromatography, is especially useful for e.e. determination as no sample derivatisation is required, for example, volatile enantiomers can be analysed directly with small amounts of vapour. Owing to the large separation power of gas chromatography in the high-resolution capillary columns, contaminants and impurities are usually separated from the analytes and simultaneous analysis of e.e. and % conversion of the starting material is feasible in one analytical run.

Analyses were performed with a CP9000 Gas Chromatograph fitted with a flame ionisation detector, (FID), and an HP3395 integrator. Resolution of the enantiomeric products, as well as separation of the solvent and prochiral starting material was achieved using a CP Cyclodex-B fused silica WCOT column, (25 m x 0.25 mm,  $d_f = 0.25 \mu\text{m}$  : Chrompack). This wall-coated open tubular column (WCOT) has a chiral  $\beta$ -cyclodextrin liquid phase coated as a thin film on the inside surface of the column. Enantiomeric separation by this technique involves the rapid and reversible diastereomeric association between the chiral stationary phase and the analyte via inclusion.

The injector was operated in splitflow mode with a split ratio of 50:1. The split ratio is defined as:

$$SPLIT\ RATIO = \frac{SPLIT\ FLOW}{COLUMN\ FLOW} \quad \text{Eq: 3.10.1}$$

where split flow =(flow delivered by mass flow controller) - (column flow) = flow measured at the vent on the flow control panel.

An achiral detection device responds equally to enantiomers, irrespective of their molecular configuration and as such a comparison of the relative peak areas provides an unambiguous measure of the enantiomeric ratio from which e.e. can be calculated, provided that the detector is employed within its linear range. FID is considered to provide a linear response over several orders of magnitude and was selected as the detector. Another advantage was that FID lacks any response to air and water. This is useful in that these need not be removed from the samples when they are not components of interest. A post-column purge flow of make-up gas (helium), was required to optimise detector performance. The flow rates used throughout are shown in table 3.10.1.

Gas	Flow Rate (ml min <sup>-1</sup> )
He	30
H <sub>2</sub>	30
Air	250

Table 3.10.2 below shows the specific GC operating conditions for each of the reactants.

REACTANT	Injector & Detector Temperature (°C)	Column Head Pressure (kPa)	Column Conditions
Methyl Tiglate	150	130	Isothermal elution at 36°C
4-Trifluoro, 2-methyl, 2-butenic acid ethyl ester	150	130	Isothermal elution at 36°C
3-Coumaranone	180	100	Programmed elution: 110°C (10 mins) to 140°C at 1°C min <sup>-1</sup>

Resolution of the Tiglic Acid hydrogenated products could not be effected by this column. Subsequent analyses were performed at the University of Hull, also using a split flow capillary injection system. Chiral separations were achieved on a Cyclodex

column (SGE Ltd) with a helium carrier gas flow. The column temperature was isothermal at 90°C with the injector port at 200°C.

A good baseline resolution of the enantiomers of each of the hydrogenation products was achieved. Table 3.10.3 shows the retention times of each species on the chiral column and the relative orders of elution, along with figures 3.10.1 - 3.10.3 which show typical chromatograms.

TABLE 3.10.3: GC RETENTION TIMES			
REACTANT	RETENTION TIMES (MINS)		
	Starting Material	1 <sup>st</sup> Enantiomer	2 <sup>nd</sup> Enantiomer
Methyl Tiglate	18.2	13.3	13.9
4-Trifluoro, 2-methyl, 2-butenic acid ethyl ester	18.5	14.0	17.1
3-Coumaranone	14.0	28.4	28.7

The GC was calibrated for each reactant by analysis of several standard mixtures consisting of known mole fractions of each reactant and products. The graph of mole fraction against percentage area was then plotted for each component. For example, figures 3.10.4 and 3.10.5 show the typical results obtained for Methyl tiglate and the hydrogenated product 2-Methyl Butyric Acid Methyl Ester. For each component there was a direct linear correlation between the % area on the integrator and the mole fraction (MF), hence the extent of reaction could be determined by:

$$\% \text{ CONVERSION} = (1 - \text{MF STARTING MATERIAL}) \times 100 \quad \text{Eq 3.10.2}$$

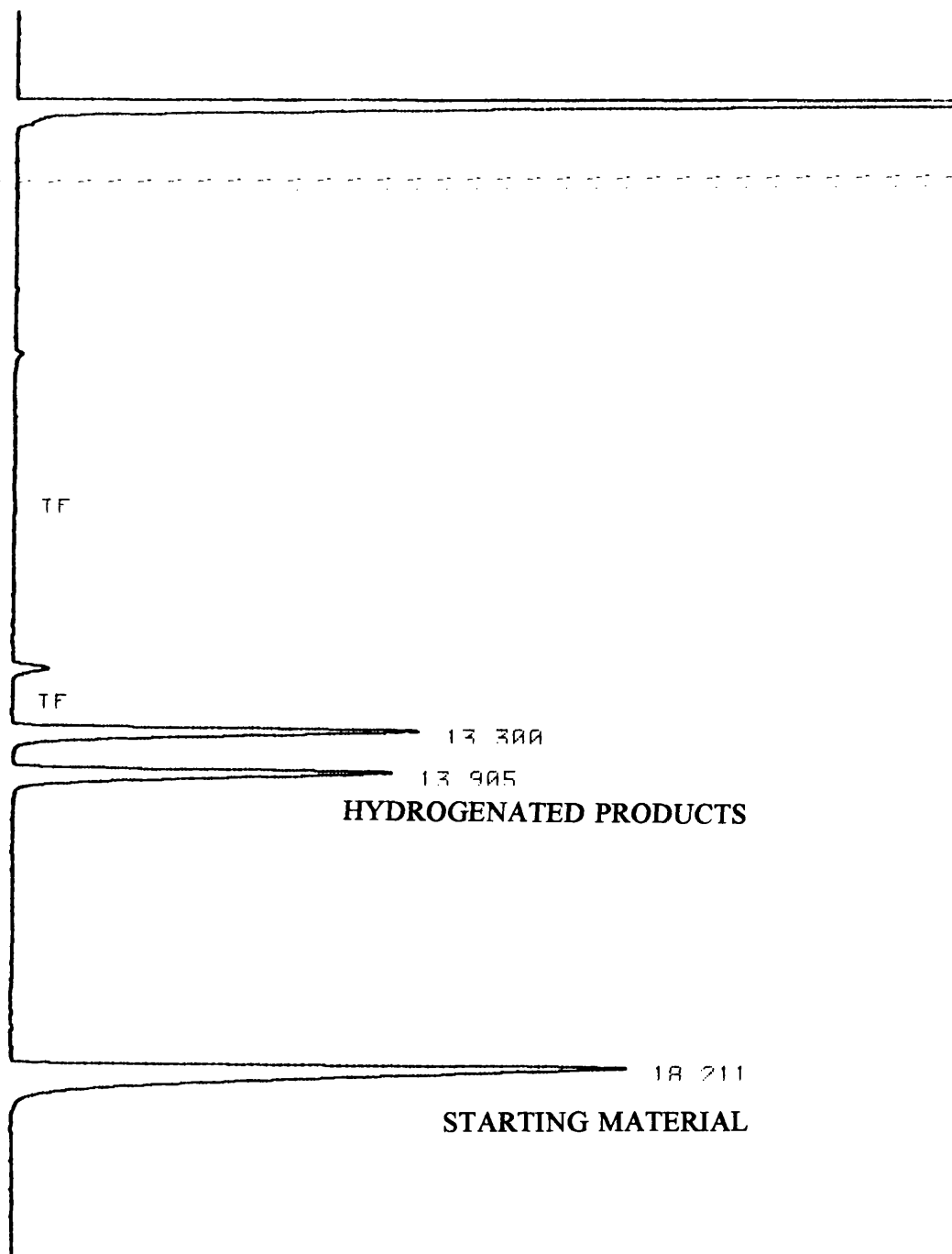


FIGURE 3.10.1: TYPICAL CHROMATOGRAPH OF METHYL TIGLATE.

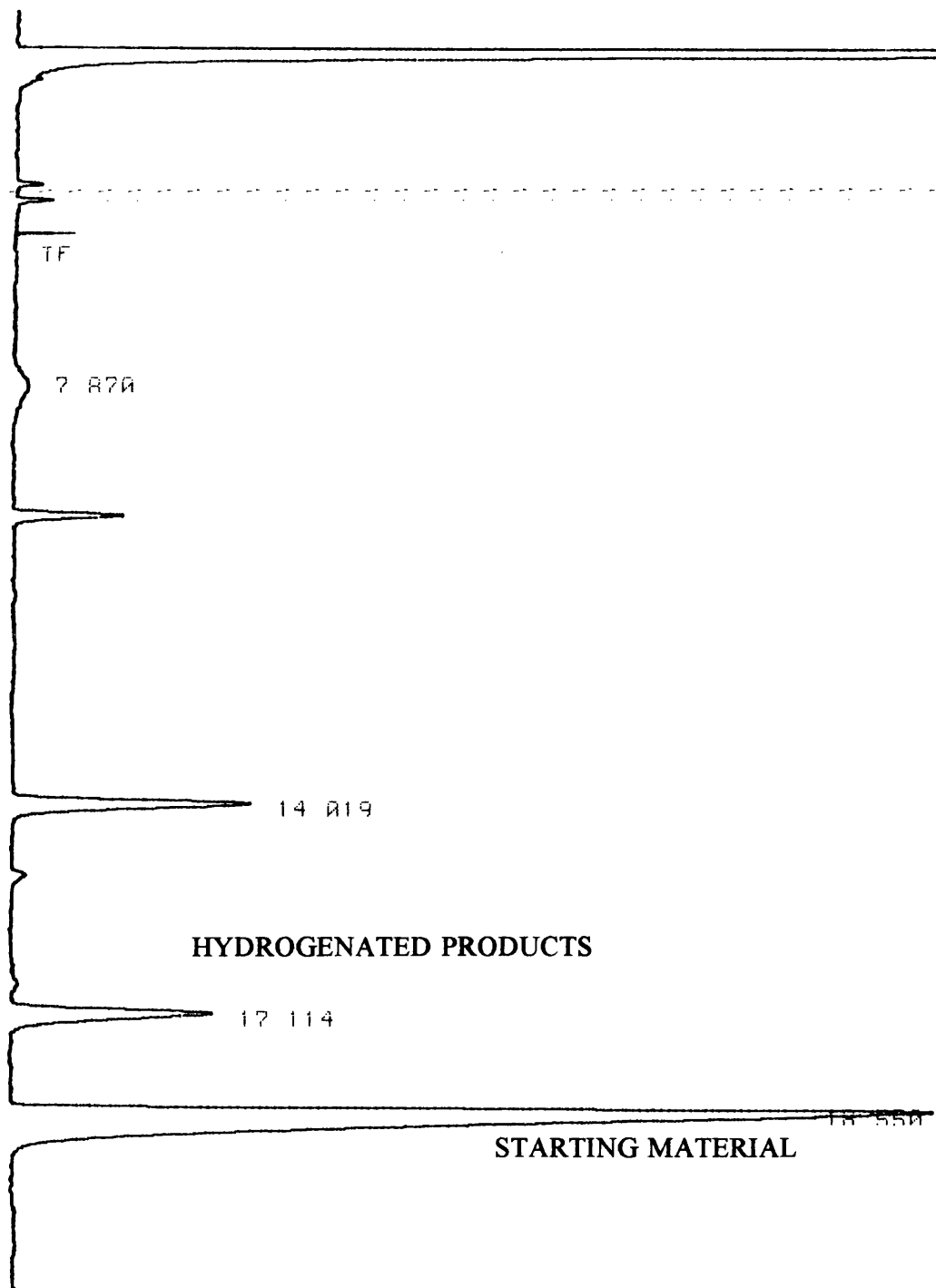


FIGURE 3.10.2: TYPICAL CHROMATOGRAPH OF 4-TRIFLUORO, 2-METHYL 2-BUTENOIC ACID ETHYL ESTER

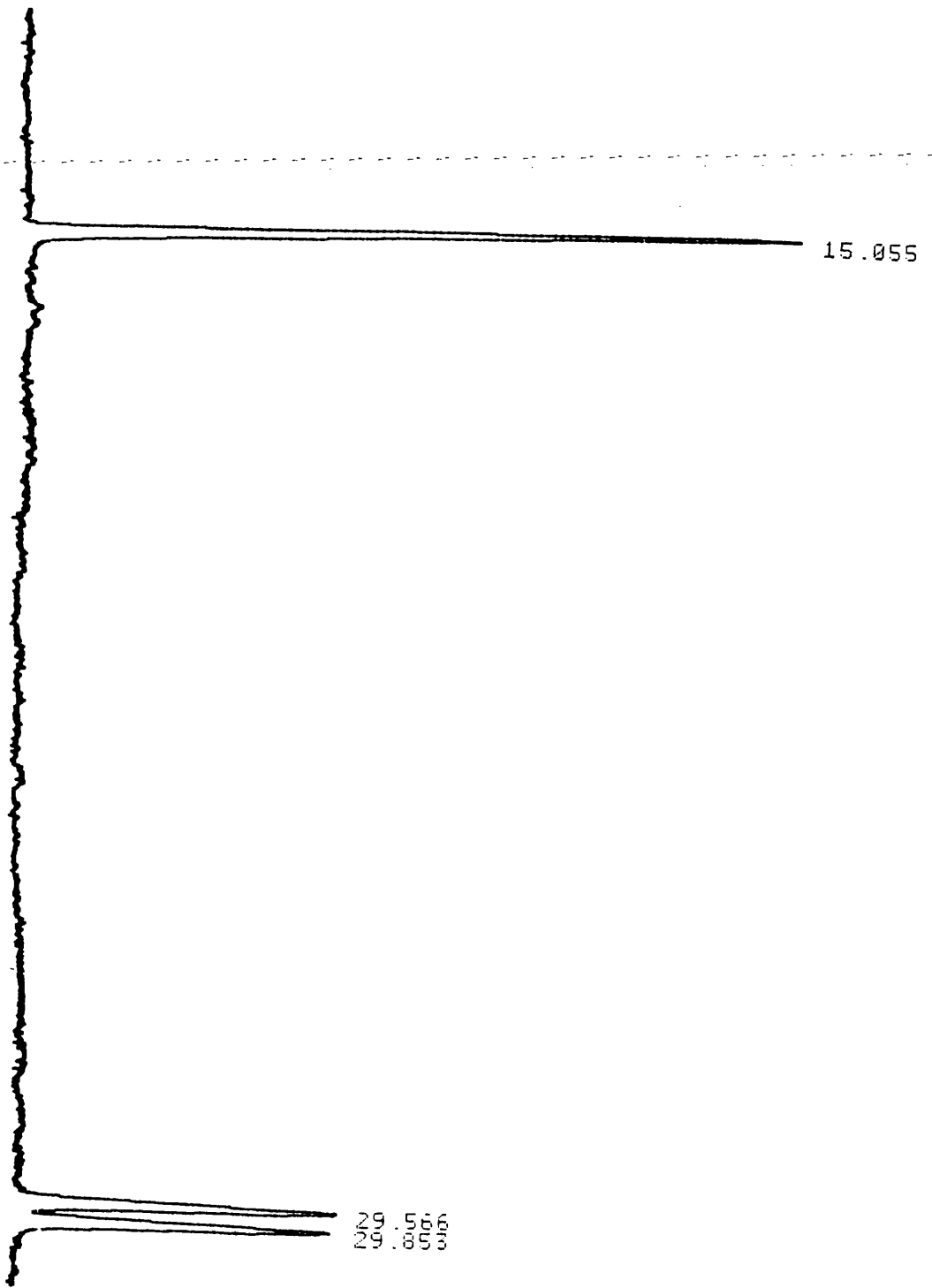


FIGURE 3.10.3: TYPICAL CHROMATOGRAPH OF 3-COUMARANONE.

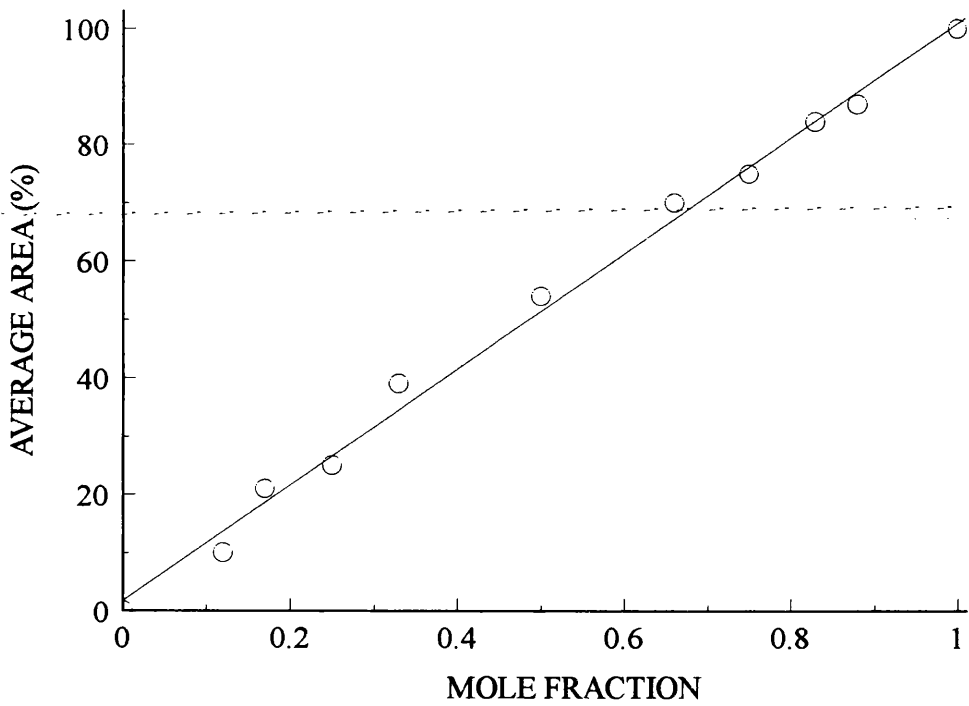


FIGURE 3.10.4: GC CALIBRATION FOR METHYL TIGLATE

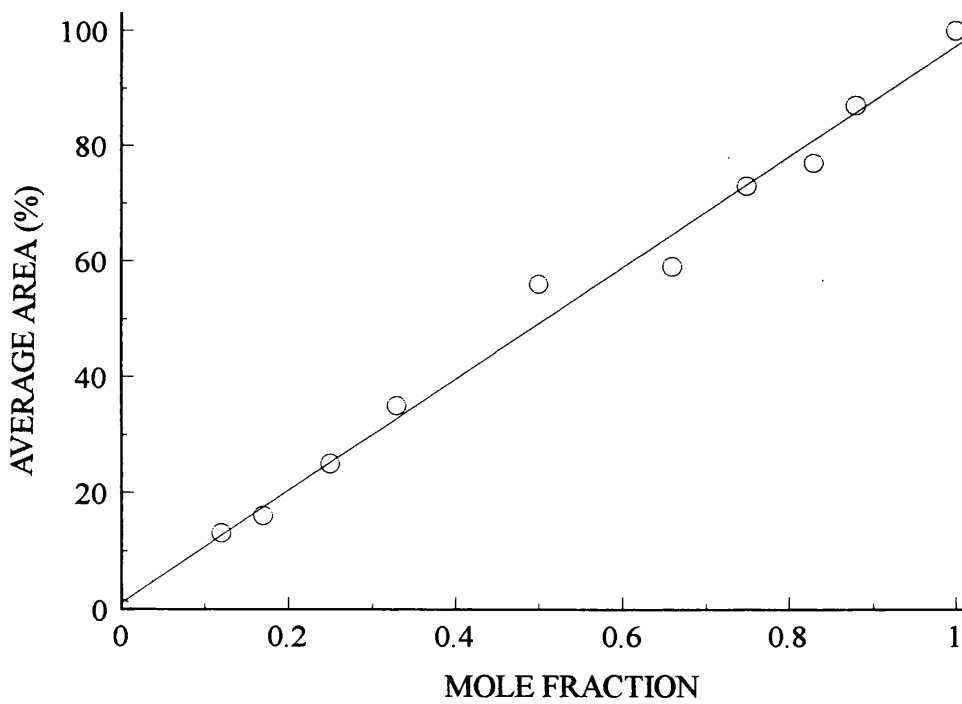


FIGURE 3.10.5: GC CALIBRATION FOR 2-METHYL BUTYRIC ACID METHYL ESTER

The enantiomeric excess of the products is then defined as:

$$\% e. e. = \frac{MF_{E1} - MF_{E2}}{\sum MF_{E1 + E2}} \times 100 \quad \text{Eq 3.10.3}$$

where E1 and E2 represent respectively the major and minor enantiomers produced.

The error on the enantiomeric excess was calculated as  $\pm 2\%$  and as such no e.e. values were quoted below 3%.

### 3.10.2: GAS CHROMATOGRAPHY-MASS SPECTROMETRY

#### (GC-MS).

Analyses were carried out with a Hewlett-Packard 5971 mass selective detector interfaced to a 5890 series II gas chromatograph and computer (Vectra QS/16S). Separations were effected with an HP1 fused silica capillary column (12.5 m x 0.2 mm x 0.33  $\mu\text{m}$ ). The injector was operated in split mode (50:1) and the helium carrier and make up gas flow rates were 2 ml min<sup>-1</sup> and 25 ml min<sup>-1</sup> respectively. The column temperature was programmed from 80°C (2 min) to 265°C (1 min) at 5° min<sup>-1</sup>. The respective injection port and detector temperatures were 255°C and 260°C. Retention times from the total ion current (TIC) traces practically matched those of the initial FID chromatograms. Mass spectra (70eV) were recorded in continuous scanning mode.

## **CHAPTER FOUR**

### **RESULTS**

## 4.1 INTRODUCTION

The adsorption work was principally performed on the nickel and palladium catalysts supported on Grace silica and the palladium/carbon catalyst. Both the Pd and Ni/Cab-O-Sil catalysts were prepared and introduced to the scheme of work at a much later date. The 1% Pd/Cab-O-Sil catalyst was initially introduced after the Pd/Grace silica C30 catalyst was found to have aged after ~18 months into the adsorption work, see Section 4.8, which rendered it unreliable for subsequent hydrogenation studies. The Ni/Cab was then prepared for two reasons: i) as a precaution against the possibility of both the Ni/Grace silica catalysts ageing in a similar manner and ii) to overcome the reduction problems that arose with both these Grace silica catalysts in the hydrogenation reactor, see Section 4.9. Hence, due to this subsequent catalyst ageing and reducibility problems within the Grace silica systems, the hydrogenation studies proceeded mainly with the Cab-O-Sil supported catalysts and the Pd/C.

## 4.2: PREPARED CATALYSTS

The prepared catalysts are listed below, along with their abbreviated nomenclature used throughout the work for ease of discrimination between them.

Catalyst	Nomenclature
Pd/Carbon	Pd/C
Pd/Grace silica C30	Pd/C30
Ni/Grace silica C30	Ni/C30
Ni/Grace silica C10	Ni/C10
Pd/ Cab-O-Sil silica	Pd/Cab
Ni/ Cab-O-Sil silica	Ni/Cab

The surface area data for each of the supports used is shown below in table 4.2.2.

Support	Surface Area (m <sup>2</sup> g <sup>-1</sup> )
Cab-O-Sil silica	194
Grace silica C30	106
Grace silica C10	307
Carbon Norit RX3 Extra	>600

The Grace silica supports used, i.e. C30 and C10, are both porous silica structures which have been observed to have a high content, > 50% surface coverage, of strained three-membered ring structures within their network. As shown in figure 4.2.1, the three-membered rings are able to interconvert with vicinal silanol groups and have been shown to be energetically unstable. Evidence from other workers<sup>113</sup> has shown that catalysts supported on such a silica can have very high activities which led to the initial interest of these supports for potential asymmetric catalysts. The difference between the C30 and C10 supports was the mean pore diameters, 315Å and 99Å respectively, and the resultant surface areas, see table 4.2.2. Both catalysts were supplied as a bead form of approximately 5 mm diameter, which was not predicted to decrepitate upon impregnation or reaction.

Cab-O-Sil silica was a very fine, low density powder. It was a microspheroidal silica which was virtually non-porous, thus circumventing any diffusion limitations during experimental studies that could have been associated with the porosity of the support. This silica was prepared by a different route than the Grace silica and as such the surface structures are different. The Cab-O-Sil support was comprised mainly of

relatively stable, inert, large rings containing six or more Si atoms with < 1% surface coverage of strained three membered rings.<sup>114</sup>

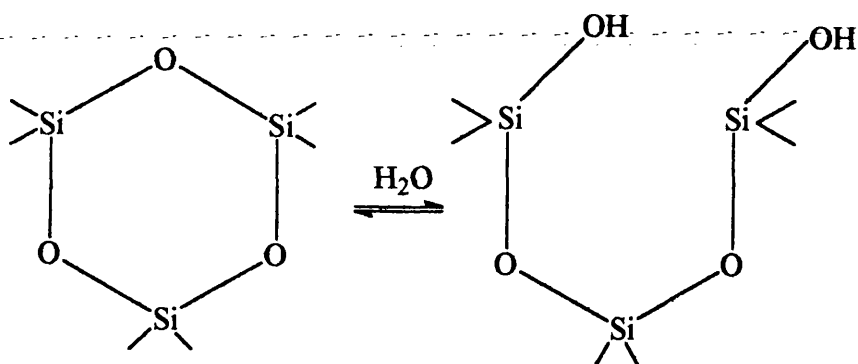


FIGURE 4.2.1: THREE-MEMBERED SILOXANE RING SPECIES

The Carbon Norit RX3 Extra support, an activated carbon, was a black particulate solid. Carbon supports have an oxidised surface with the oxygen bound in several ways. Figure 4.2.2 has been proposed to account for the range of groups with different acidity.

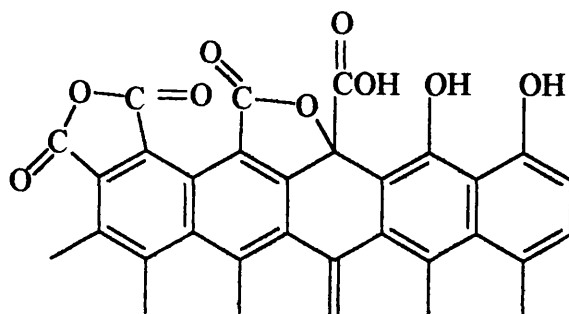


FIGURE 4.2.2: CARBON SUPPORT SURFACE

## 4.3: CHARACTERISATION

### 4.3.1: TEMPERATURE PROGRAMMED REDUCTION.

Table 4.3.1 shows the  $T_{MAX}$  values ( the temperature at each peak maximum) obtained for each catalyst, together with the temperature for complete reduction,  $T_{FINAL}$ , of the predominant species. Figures 4.3.1 to 4.3.6 show the temperature profiles, of hydrogen consumption (arbitrary units) as a function of temperature, obtained for each individual catalyst. These traces show the marked effect of the support in producing a number of peaks as opposed to, for example, the single peak obtained for the reduction of bulk nickel oxide by Robertson *et al.*<sup>1</sup>

The TPR apparatus was restricted to a lower temperature limit of 0°C, below which the programmer would not operate. This represented an experimental difficulty in obtaining a detailed temperature profile for the reduction of the 1% Pd/Cab. The trace shown was obtained by flowing the catalyst sample in 6% H<sub>2</sub>/N<sub>2</sub> isothermally at 0°C. However, no specific  $T_{MAX}$  or  $T_{FINAL}$  temperatures could be defined.

The numbers in ( ) represent shoulders on the main peak, whilst { } denotes high temperature peaks, above the adopted standard reduction temperature. Thus for Ni/Cab the reduction temperature of 450°C was a functional temperature; resulting in a defined, though incompletely reduced state of the catalyst.

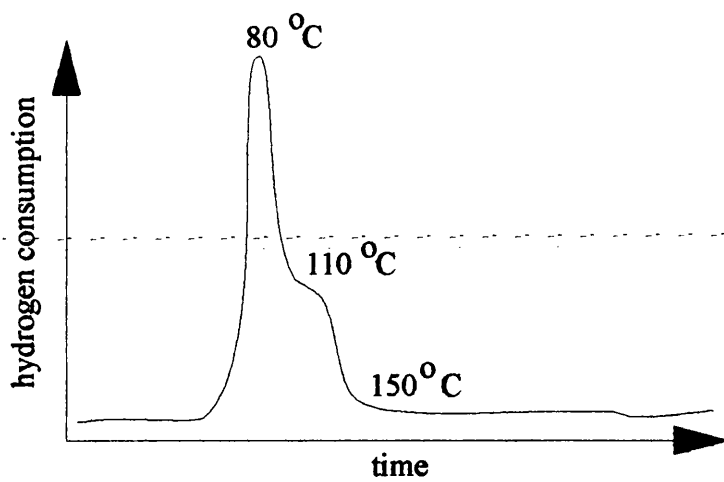


FIGURE 4.3.1: Pd/-C30 TPR

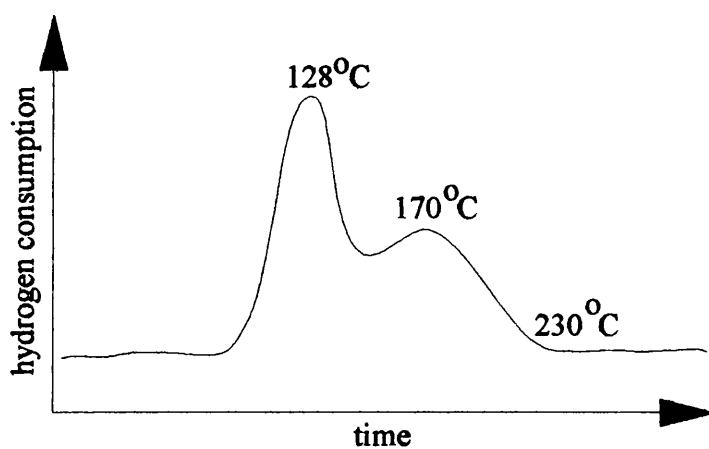


FIGURE 4.3.2: Pd/C TPR

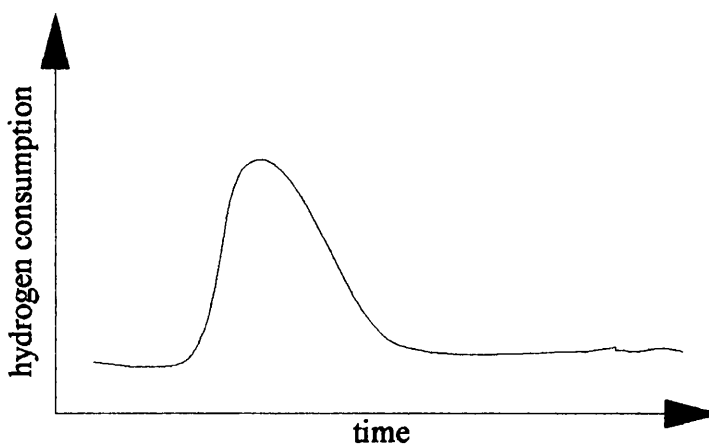


FIGURE 4.3.3: Pd/Cab TPR  
ISOTHERMAL REDUCTION AT 0°C.

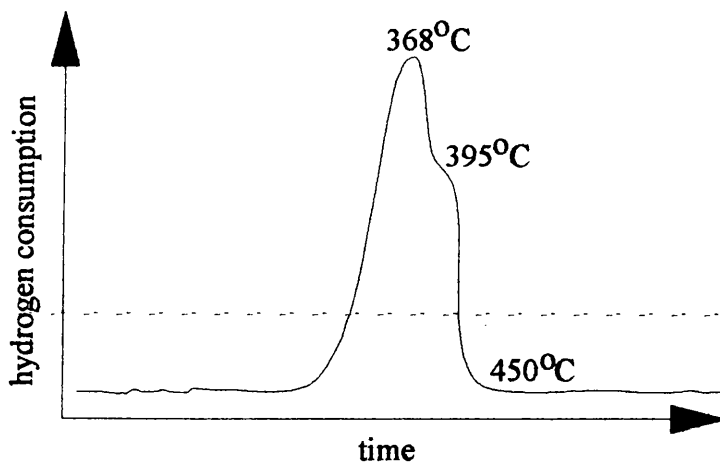


FIGURE 4.3.4: Ni/-C30 TPR

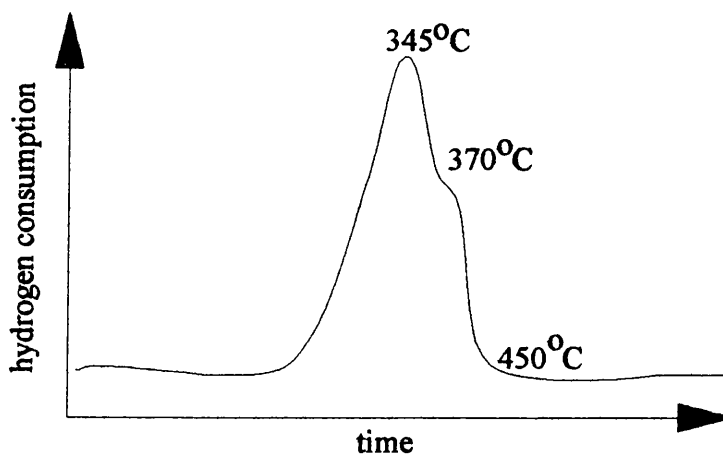


FIGURE 4.3.5: Ni/-C10 TPR

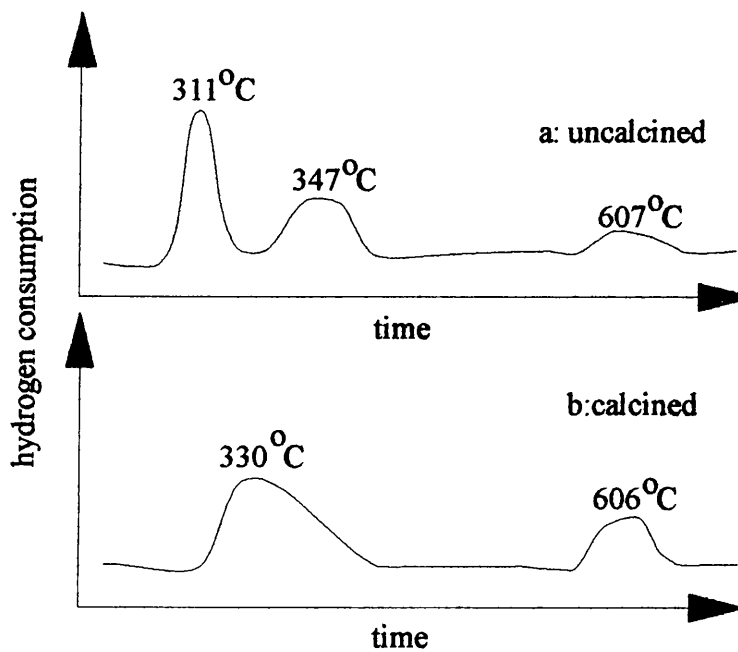


FIGURE 4.3.6: Ni/Cab TPR

TABLE 4.3.1: TPR RESULTS.		
Catalyst	T <sub>MAX</sub> (°C)	T <sub>FINAL</sub> (°C)
Pd/C30	80,110	150
Pd/C	128,170	230
Pd/Cab	< 0	< 0
Ni/C30	368, (395)	450
Ni/C10	345, (370)	450
Ni/Cab uncalcined	311, 347, {607}	420
Ni/Cab calcined	330, {606}	430

#### 4.3.2: ATOMIC ABSORPTION.

The palladium and nickel loadings of each catalyst, as determined by atomic absorption, are shown in table 4.3.2.

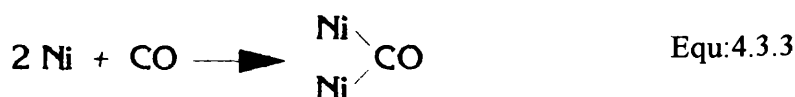
TABLE 4.3.2: ATOMIC ABSORPTION RESULTS.	
Catalyst	% w/w Metal Loading
Pd/C	1.9
Pd/C30	1.8
Pd/Cab	1.0
Ni/C30*	8.4
Ni/C10*	9.2
Ni/Cab	6.8

\* - Catalysts analysed after prewash procedure.

The total amount of nickel deposited on in the Ni/Cab catalyst could have been increased with an extended precipitation time during the initial preparation.<sup>115</sup>

### 4.3.3: CHEMISORPTION STUDIES

In order to translate the uptakes of each gas into dispersion figures the following stoichiometries for each adsorption experiment were assumed:



where M = Ni and Pd.

that is, both metals were assumed to adsorb molecular oxygen dissociatively.<sup>116</sup> Ni was assumed to adsorb carbon monoxide as a bridged species<sup>2</sup> whereas adsorption onto Pd was assumed to be mainly linear.<sup>117</sup> The dispersion values were then calculated as described in Section 3.3.3., equation 3.3.1.

The volumes of the loop sizes used to deliver a pulse of gas were determined as 4.70 cm<sup>3</sup> for the full loop and 2.68 cm<sup>3</sup> for the half loop

Table 4.3.3 shows the dispersion values calculated, as well as the average number of surface metal atoms exposed during a standard reduction per gram of catalyst. These values were used to determine the number of surface metal sites available for catalysed reactions.

TABLE 4.3.3: CHEMISORPTION RESULTS			
Catalyst	% Dispersion		No. Surface Metal Atoms x 10 <sup>18</sup> per gram Catalyst
	CO	O <sub>2</sub>	
Ni/C30 <sup>Δ</sup>	2.09	2.77	23.76
Ni/C30 <sup>α</sup>	0.98	1.23	9.24
Ni/C10 <sup>Δ</sup>	1.99	1.86	17.96
Ni/C10 <sup>α</sup>	0.45	0.62	5.19
Ni/Cab	18.04	19.71	137.39
Pd/C30	6.88	10.69	10.67
Pd/C	11.14	8.87	11.84
Pd/Cab	6.72	7.39	4.00

Δ-before prewash.    α-after prewash.

Both metals have been shown to adsorb both CO and O<sub>2</sub> strongly. Figures 4.3.7 and 4.3.8 show representative adsorption isotherms.

The discrepancy between CO and O<sub>2</sub> dispersion values for Pd/C30 signified that the CO was not adsorbed onto this catalyst as a solely linear species, that is,



where  $X > Y$ , indicating a combination of both bridged and linear species.

**FIGURE 4.3.7: ADSORPTION OF CO ON Ni/C10**

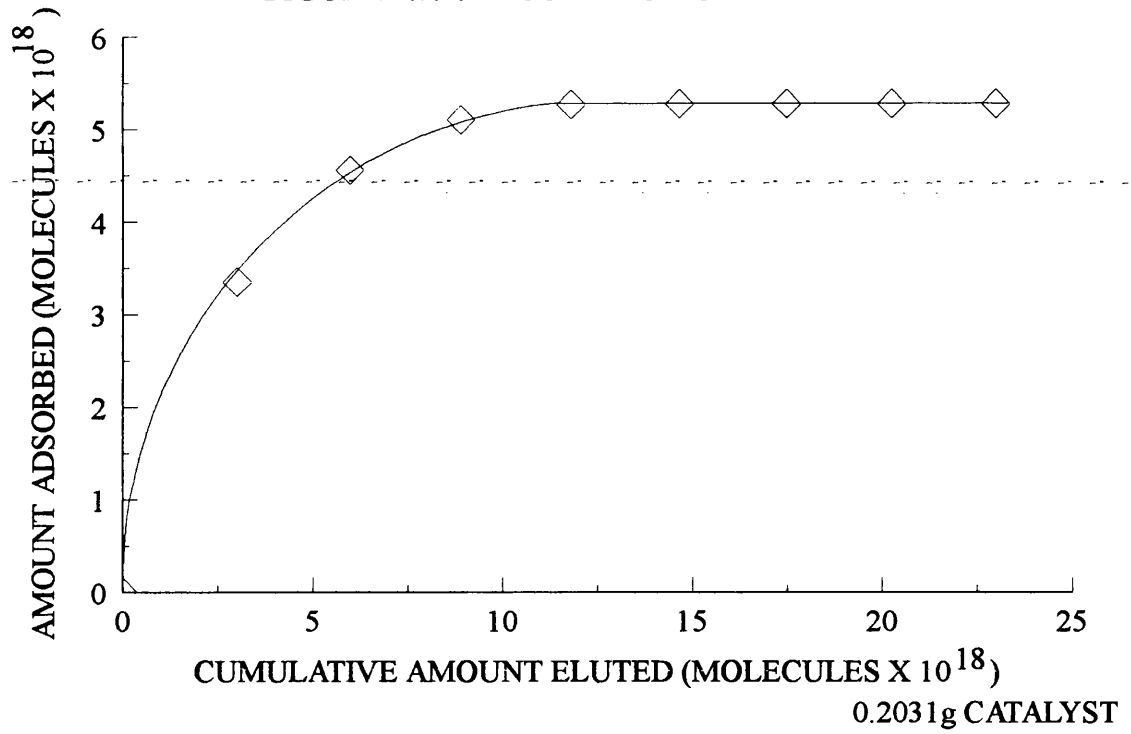
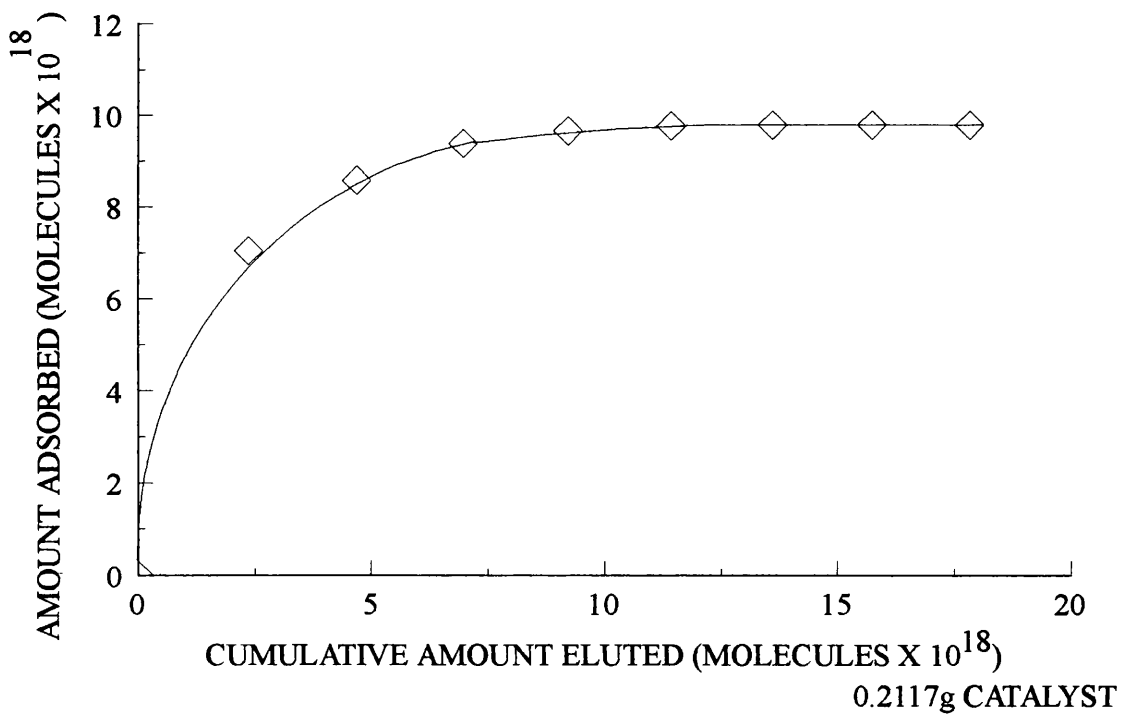


**FIGURE 4.3.8: ADSORPTION OF CO ON Ni/C30**



The correlation of dispersion values for the nickel catalysts was in better agreement. For the Grace silica catalysts these results clearly showed that a large proportion of the surface metal atoms were lost during the catalyst prewash. The final dispersion values would appear to be low but are in fact quite typical for catalysts prepared by wet impregnation.<sup>118</sup> Sintering can occur quite easily during the calcination step, and more particularly, the reduction<sup>119</sup>, leading to the formation of large crystallites.

#### 4.3.4: TRANSMISSION ELECTRON MICROSCOPY.

Reduced and passivated samples of the calcined catalysts were examined by transmission electron microscopy (TEM). Several different areas were scanned by this technique and micrographs of these areas recorded. Representative electron micrographs of each catalyst are shown below in figures 4.3.9 to 4.3.13. The Ni/C10 and Ni/C30 catalysts appeared to have large, regularly shaped Ni particles dispersed over the silica support. For Ni/Cab the micrograph was quite different. In places where free silica was detected the pure support exhibited a granular texture, otherwise the support appeared to be covered by a compound which spread out in the form of fine sheets or as filaments. This structure was the result of the strong chemical interaction between the nickel compound and the silica support with the partial formation of a nickel hydrosilicate. This hydrosilicate can form in almost two dimensional arrays because of very poor adhesion between the platelets of the compound.<sup>120</sup> Individual platelets can become folded or rolled to give the impression that filaments had formed. The overall consequence was the turbostratic effect shown. The Pd/Cab was more regular with small particles apparently clustered together to

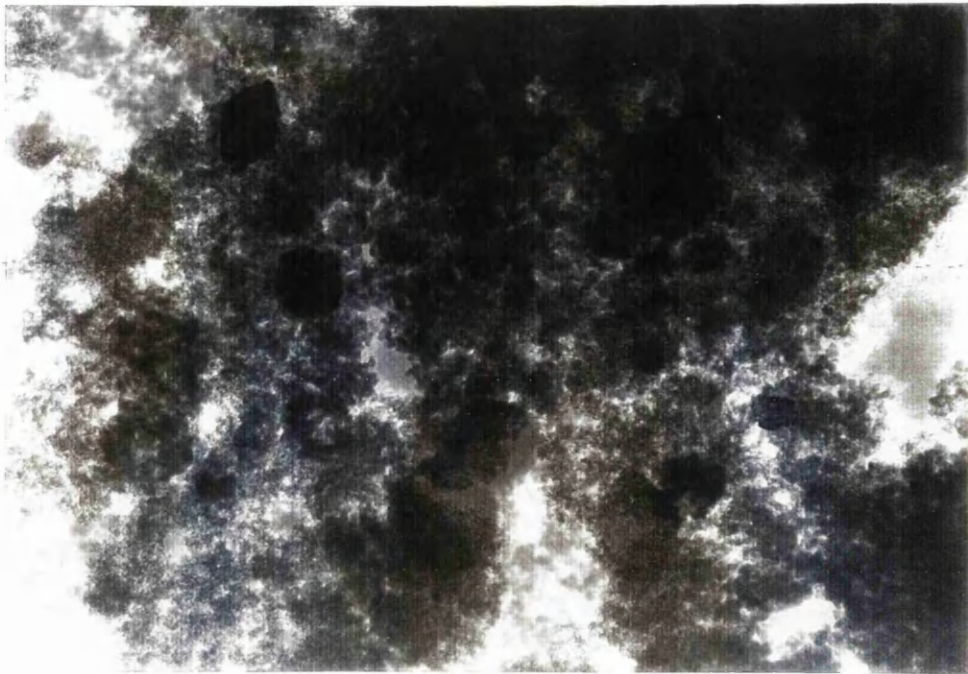


FIGURE 4.3.9: Ni/C10 MICROGRAPH, 1cm:147nm

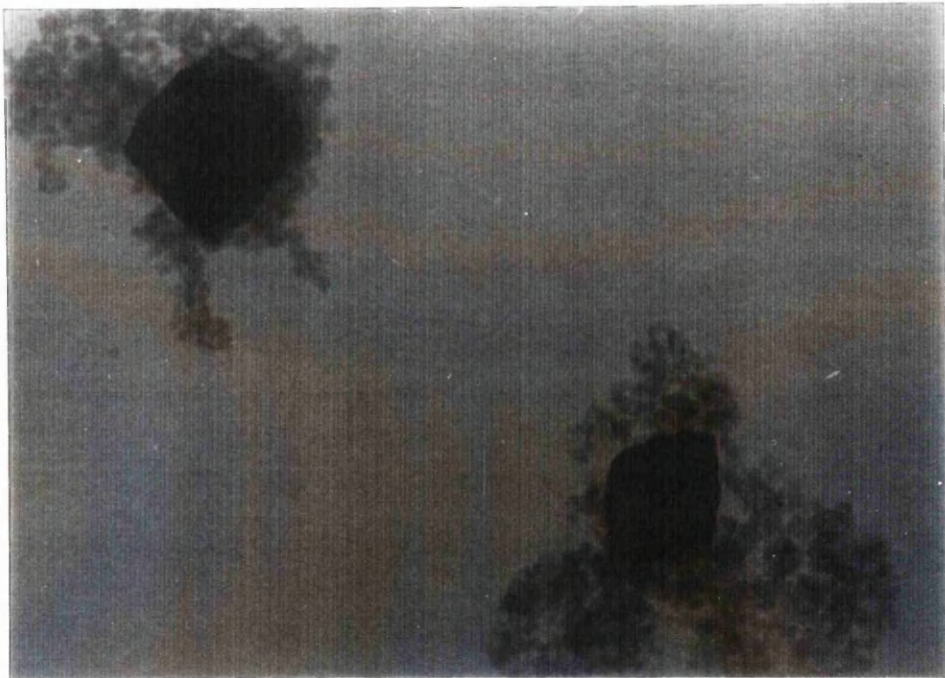


FIGURE 4.3.10: Ni/C30 MICROGRAPH, 1cm:294nm



FIGURE 4.3.11: Ni/Cab MICROGRAPH, 1cm:19nm

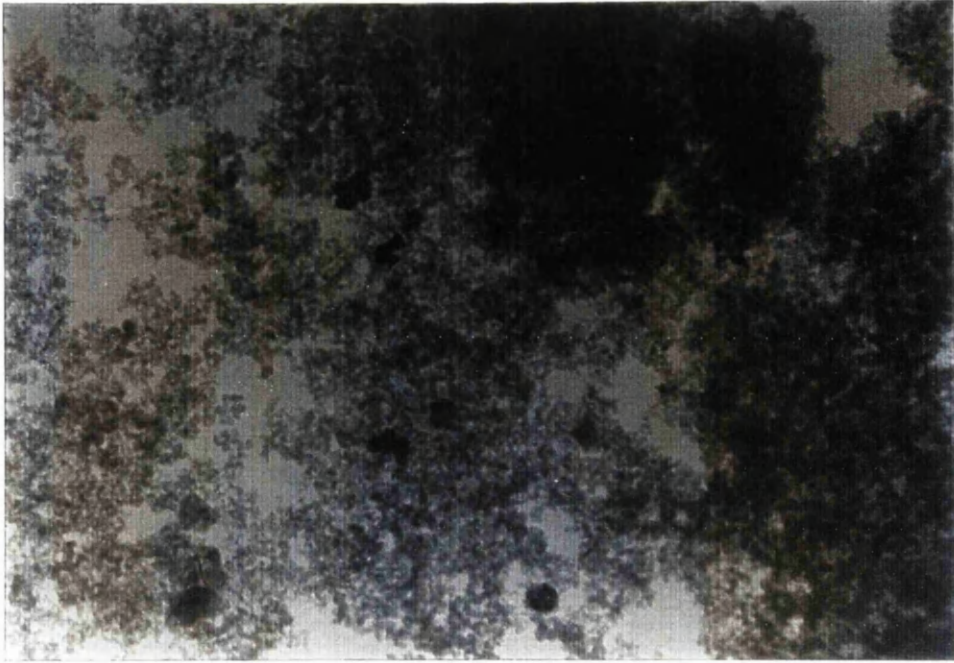


FIGURE 4.3.12: Pd/Cab MICROGRAPH, 1cm:167nm

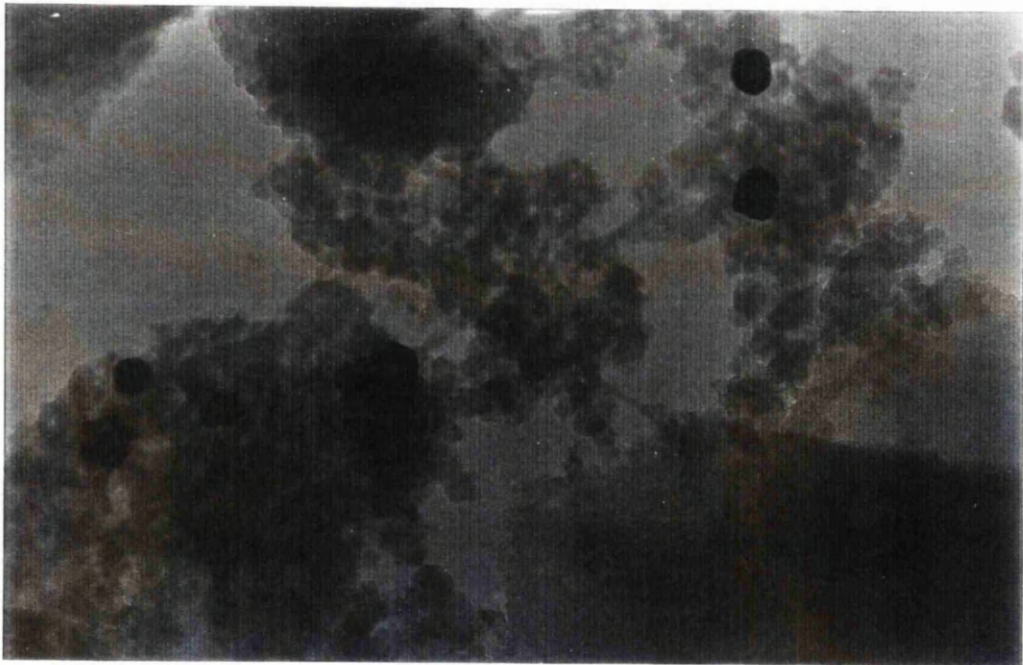


FIGURE 4.3.13: Pd/C MICROGRAPH, 1cm:63nm

form larger associated clumps. The Pd/C micrograph was similar to the Pd/Cab, with clusters of small metal particles dispersed over the support. The diameters of a large number of separate particles were then measured from all the electron micrographs and table 4.3.4 shows these resultant average particle sizes obtained by this technique.

TABLE 4.3.4: AVERAGE PARTICLE SIZES FROM T.E.M.	
Catalyst	Average particle diameter (nm)
Ni/C10	207
Ni/C30	106
Ni/Cab	7
Pd/Cab	21
Pd/C	30

The results showed that there was a large variation in the particles sizes, especially for the respective nickel catalysts prepared by different techniques. These parameters can be directly compared against the analogous values determined from CO and O<sub>2</sub> chemisorption experiments, Section 5.1.2.

#### **4.4: ADSORPTION STUDIES.**

##### **4.4.1: DIOL ADSORPTION**

The work commenced with the adsorption of the diol modifier on Ni/C30, Ni/C10, Pd/C30 and Pd/C. Tables 4.4.1 and 4.4.2, along with figures 4.4.1 and 4.4.2 show typical adsorption isotherms constructed over an extended period of time. All values throughout are quoted as per gram of catalyst sample.

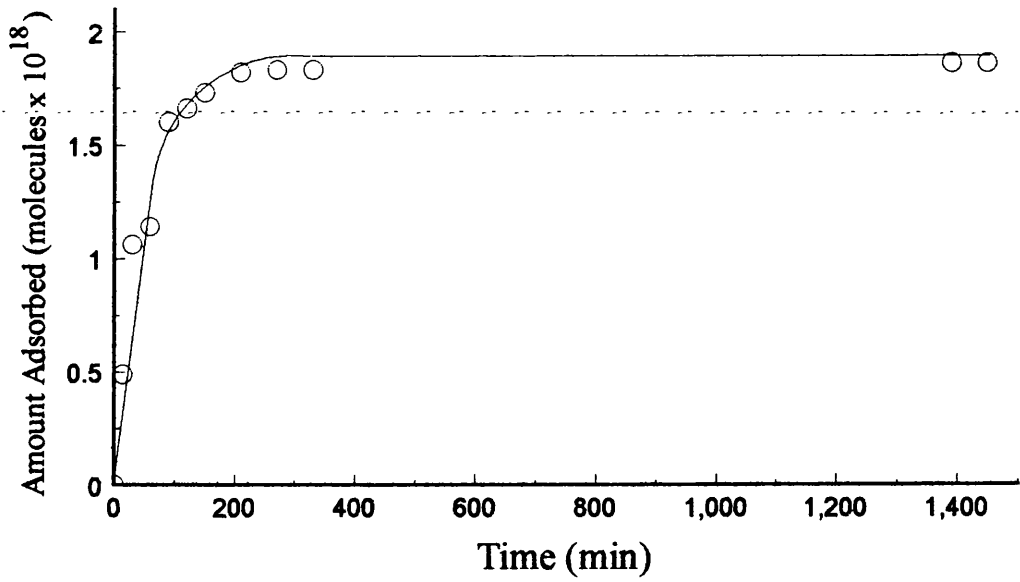


FIGURE 4.4.1: ADSORPTION OF DIOL ON TO Pd/C30

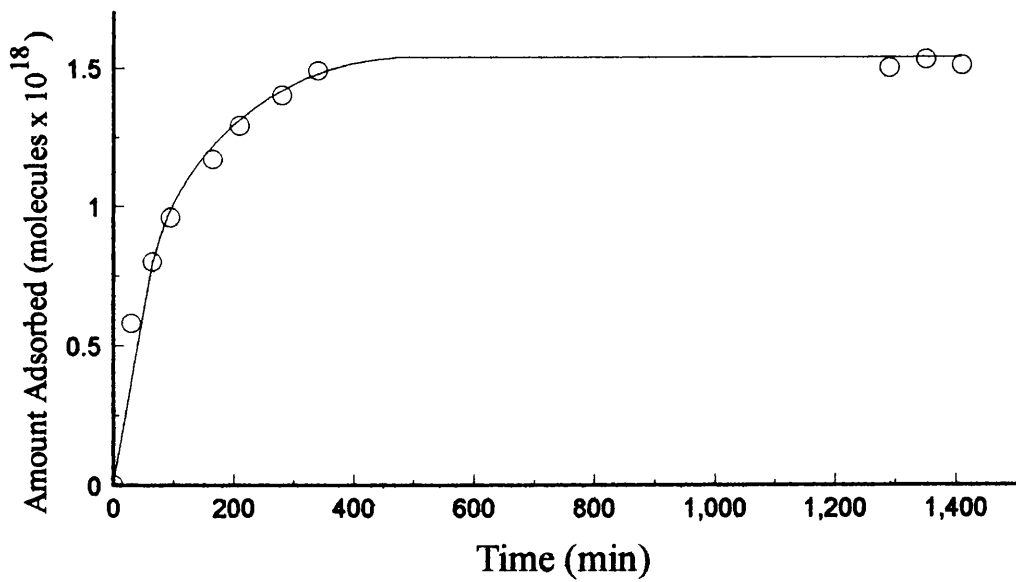


FIGURE 4.4.2: ADSORPTION OF DIOL ON TO Pd/C

TABLE 4.4.1: ADSORPTION OF CHIRAL DIOL ON Pd/C30	
Modification Time (mins)	No. Modifier Molecules Adsorbed $\times 10^{18}$
0	0
15	0.49
30	1.06
60	1.41
90	1.60
120	1.66
150	1.73
210	1.82
270	1.83
330	1.83
1390	1.86
1450	1.86
Initial No. Modifier Molecules Added = $2.38 \times 10^{18}$	

TABLE 4.4.2: ADSORPTION OF CHIRAL DIOL ON Pd/C	
Modification Time (mins)	No. Modifier Molecules Adsorbed $\times 10^{18}$
0	0
30	0.58
65	0.80
95	0.96
165	1.17
210	1.29
280	1.40
340	1.49
1290	1.50
1350	1.53
1410	1.51
Initial No. Modifier Molecules Added = $2.15 \times 10^{18}$	

Within all these catalyst systems the amounts adsorbed initially increased very rapidly and then, as time elapsed, the adsorption appeared to slow down and level out at a plateau value beyond which no further adsorption occurred. This plateau value did not represent a monolayer saturation of the catalyst surface, but was instead, an equilibrium region, the value being very dependent on the initial modifier concentration, see figure 4.4.3. Tables 4.4.3 to 4.4.6 summarise the diol adsorption results for each of these catalyst systems. The final column in each of these tables corresponds to the ratio of modifier molecules adsorbed per surface metal atom and is calculated from the number of modifier species divided by the number of surface metal atoms present in the sample as calculated from selective chemisorption studies.

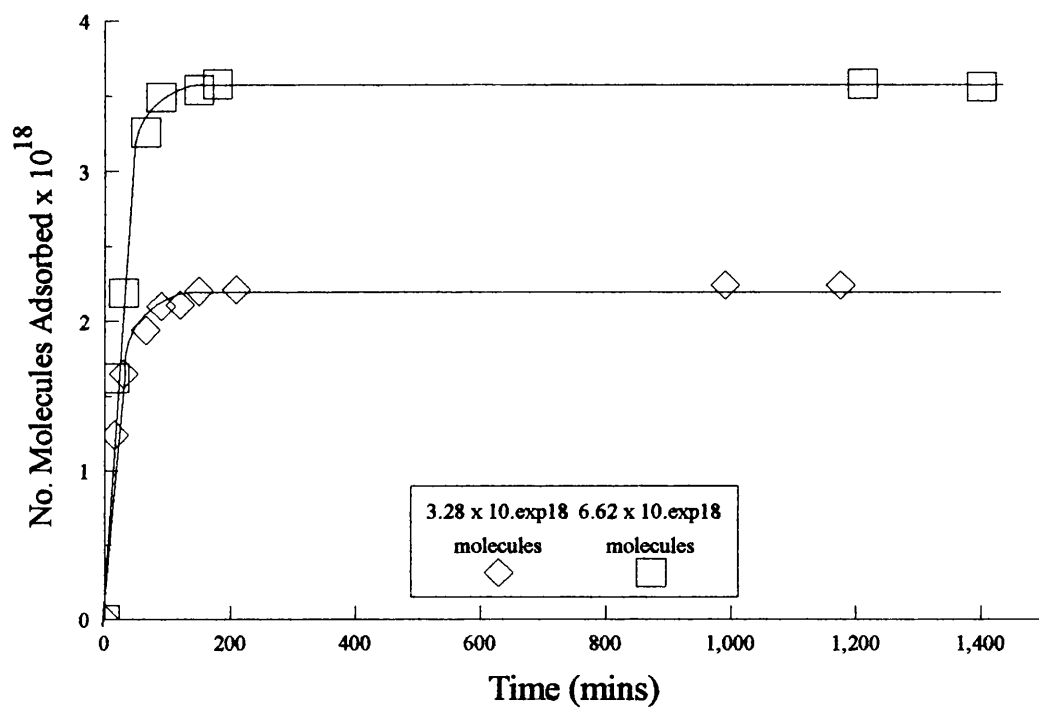


FIGURE 4.4.3: ADSORPTION OF DIOL ON Ni/C10

TABLE 4.4.3: ADSORPTION OF CHIRAL DIOL ON Pd/C30

No. Modifier Molecules Added $\times 10^{18}$	No. Modifier Molecules Adsorbed $\times 10^{18}$	Ratio Molecules Adsorbed per Surface Metal Atom
0.32	0.15	0.01
2.38	1.86	0.17
3.19	2.23	0.21
5.65	2.84	0.27
6.37	3.38	0.31
8.24	5.41	0.51
8.56	3.85	0.36
9.93	4.98	0.47
10.07	4.98	0.47
10.95	4.98	0.47
27.67	5.80	0.54
28.73	6.47	0.60

TABLE 4.4.4: ADSORPTION OF CHIRAL DIOL ON Pd/C

No. Modifier Molecules Added $\times 10^{18}$	No. Modifier Molecules Adsorbed $\times 10^{18}$	Ratio Molecules Adsorbed per Surface Metal Atom
1.63	1.11	0.09
2.18	1.67	0.14
5.86	3.21	0.27
6.76	1.01	0.09
6.82	4.57	0.39
7.98	2.38	0.20
10.54	2.78	0.23
11.18	2.62	0.22
11.20	2.25	0.19
12.20	2.70	0.23
13.38	3.80	0.32
21.72	4.25	0.36
27.72	4.57	0.39
29.97	6.39	0.34

**TABLE 4.4.5: ADSORPTION OF CHIRAL DIOL ON Ni/C30**

No. Modifier Molecules Added $\times 10^{18}$	No. Modifier Molecules Adsorbed $\times 10^{18}$	Ratio Molecules Adsorbed per Surface Metal Atom
1.64	1.11	0.12
2.87	2.27	0.25
7.46	2.42	0.26
8.71	3.51	0.38
9.15	3.82	0.41
9.21	3.17	0.34
9.96	3.92	0.42
11.12	5.11	0.55
11.14	5.05	0.55
27.77	4.05	0.44

**TABLE 4.4.6: ADSORPTION OF CHIRAL DIOL ON Ni/C10**

No. Modifier Molecules Added $\times 10^{18}$	No. Modifier Molecules Adsorbed $\times 10^{18}$	Ratio Molecules Adsorbed per Surface Metal Atom
3.28	0.78	0.15
4.50	0.32	0.06
4.56	0.52	0.10
4.94	2.24	0.43
6.26	3.56	0.68
14.22	4.42	0.85

The final amounts adsorbed were measured after the system had been left to equilibrate for ~24 hr. Figure 4.4.4 shows how the total amount adsorbed increased along with the increase in modifier concentration for Pd/C30, a general trend for each of the catalysts. In all the diol modifier solutions left in contact with the Grace silica catalysts a colour was noted to develop over a period of time which was dependent on the nature of the supported metal, see Section 4.7. No such colour developed in the diol solutions left in contact with the Pd/C catalyst.

Basic molecular modelling, figure 4.4.5, proposed that each binaphthol molecule may obscure between 5 and 10 surface metal atoms, depending on the nature of the metal and the mode of adsorption. This implied that, for a single overlayer of adsorbed modifier species on the metal component of the catalysts, the maximum possible ratio of molecules adsorbed per surface metal atom would have been, very approximately, 0.2. However looking at the ratio figures in the final column in each table, it can be clearly seen that the adsorption very often exceeded this value. An experiment was performed with a very low concentration of modifier species, where the initial amount of diol molecules added was less than that predicted for a possible monolayer coverage. This adsorption occurred very quickly, table 4.4.7 and figure 4.4.6. However, even at such low concentrations total adsorption of the modifier solution still did not occur, with a small proportion always being retained in solution.

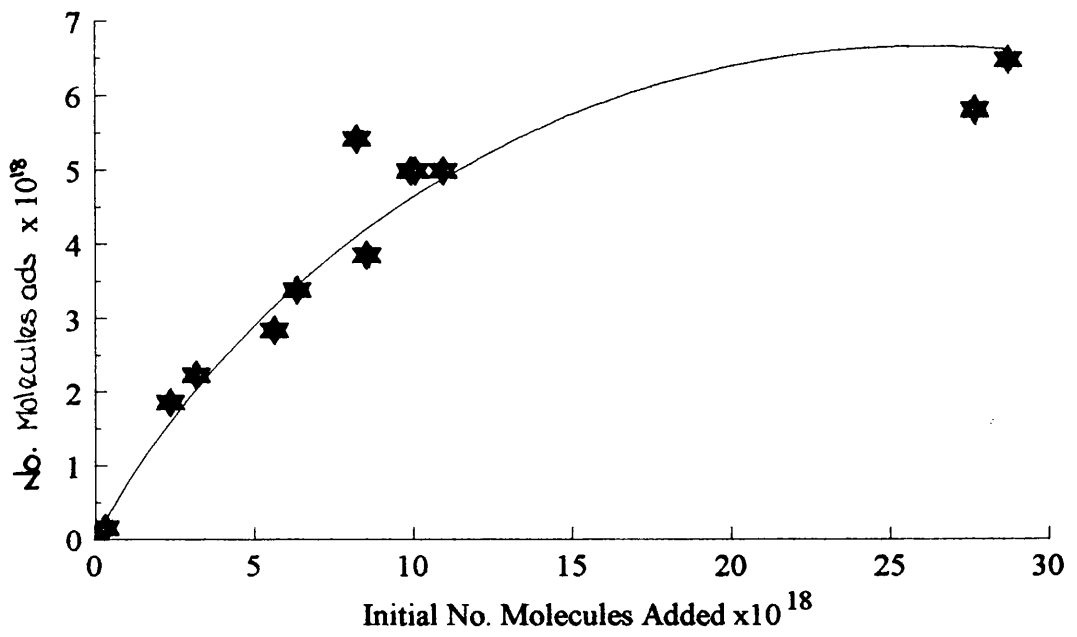


FIGURE 4.4.4: ADSORPTION OF DIOL ON Pd/C30

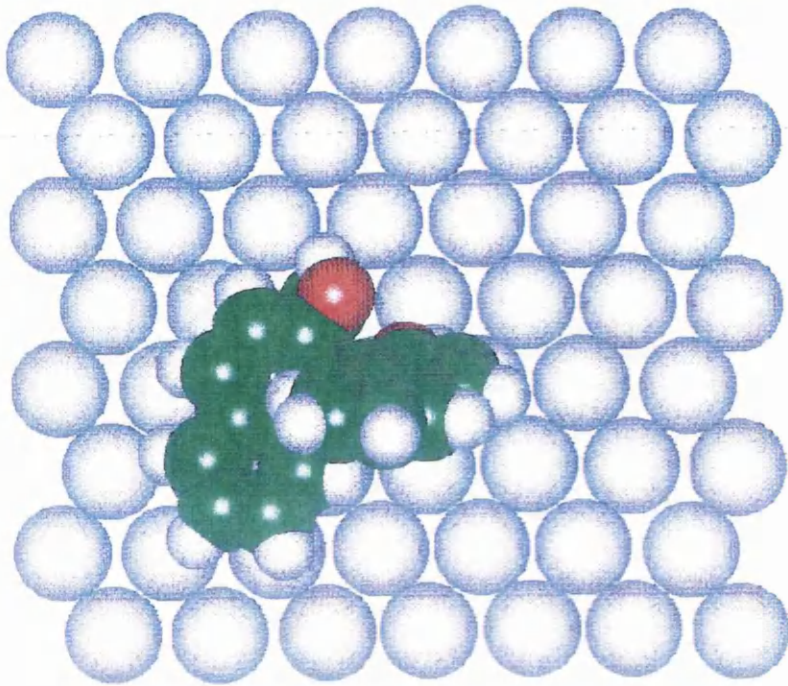


FIGURE 4.4.5: MOLECULAR MODEL SHOWING A BINAPHTHYL  
MODIFIER MOLECULE ADSORBED ON A PLANAR METAL  
SURFACE.

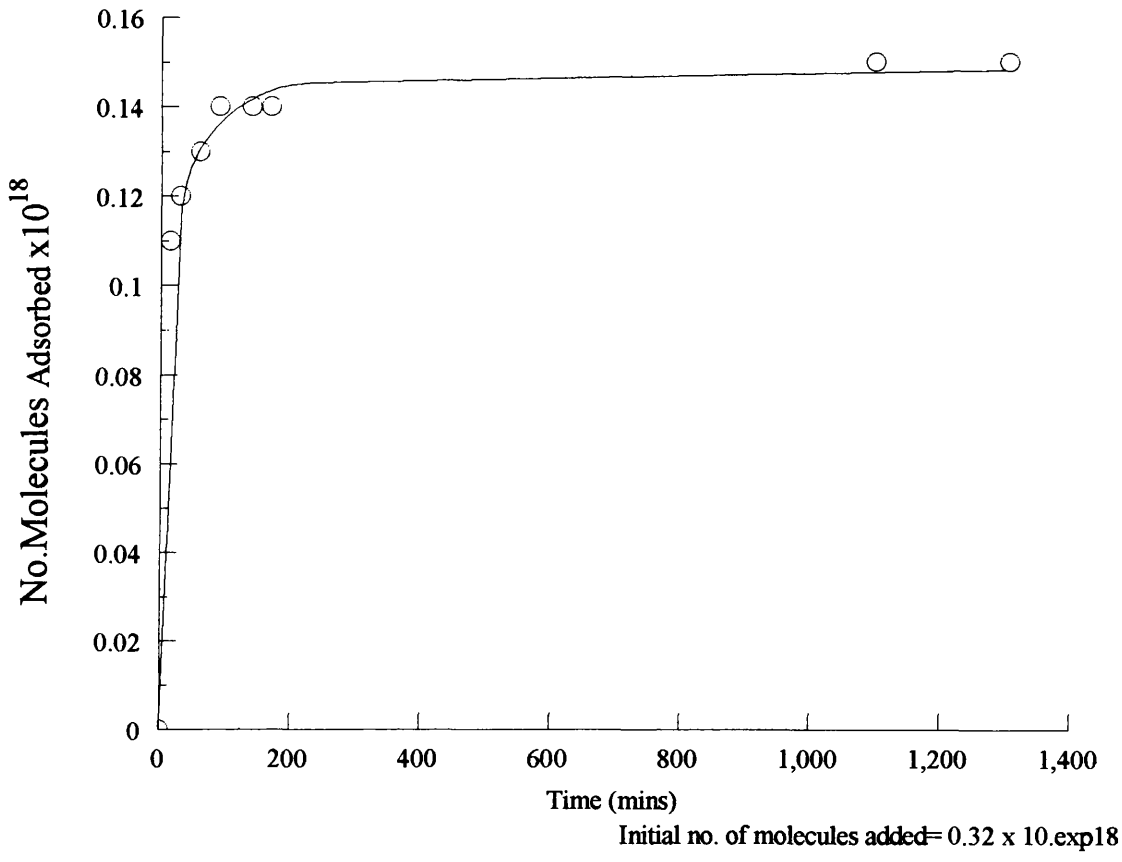


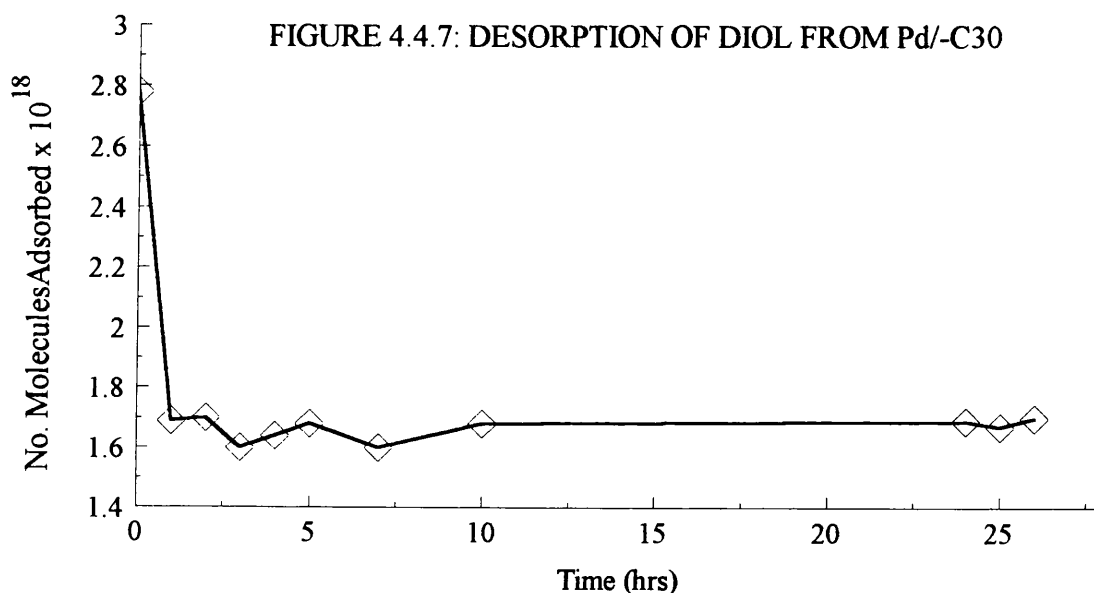
FIGURE 4.4.6:- ADSORPTION OF DIOL ON Pd/C30

TABLE 4.4.7 ADSORPTION OF R-DIOL ON Pd/C30	
Modification time (mins)	No. Modifier Molecules Adsorbed $\times 10^{18}$
0	0
15	0.10
30	0.12
60	0.13
90	0.13
140	0.14
170	0.14
1150	0.15
1305	0.15
Initial No. Modifier Molecules Added = $0.32 \times 10^{18}$	

After a standard modification, Section 3.7, the modified catalysts were washed. The resultant solution, after a standard 24hr modification, was removed from the reactor by syringe to maintain the catalyst in an inert atmosphere. Fresh solvent, 10ml, was added and the initial concentration of the modifier in the prewash solution determined. The solution and catalyst were stirred to investigate the removal of weakly adsorbed species.

The solution and catalyst was stirred over an extended time period at ambient temperature to investigate the variation in the extent of desorption with time. Figure 4.4.7 shows that most of the removable modifier species were desorbed within the first

hour of washing. After this time there was little further variation and as such, a 1 hour washing procedure was adopted as a standard procedure prior to hydrogenation reactions, unless otherwise stated. Incorporation of this wash step attempted to eliminate any weakly associated molecules, to result in only strongly adsorbed modifier species retained on the catalyst surface. This was to ensure that subsequent asymmetric hydrogenation proceeded at the heterogeneous surface modified with a strongly adsorbed chiral adlayer and not via a homogeneous asymmetric reaction.



The variation of the amount of strongly adsorbed modifier retained on the catalyst surface as the reaction temperature was increased, was also investigated. The reaction was initially stirred for 1 hour at ambient temperature and the concentration of modifier in solution analysed. The process was then repeated as the temperature was increased. The upper temperature limit was restricted to less than 66°C, the boiling point of THF. The results of typical temperature controlled desorption experiments are shown in tables 4.4.8 to 4.4.11.

**TABLE 4.4.8: DESORPTION OF DIOL FROM Pd/C30**

Temperature (°C)	Total No. Molecules Adsorbed ( $\times 10^{18}$ )	Ratio Molecules Adsorbed per Surface Metal Atom
Before wash	5.80	0.54
20	4.31	0.40
45	4.29	0.40
56	5.25	0.49
62	5.62	0.53
66	5.53	0.52
Initial No. Modifier Molecules Added = $27.67 \times 10^{18}$		

**TABLE 4.4.9: DESORPTION OF DIOL FROM Pd/C**

Temperature (°C)	Total No. Molecules Adsorbed ( $\times 10^{18}$ )	Ratio Molecules Adsorbed per Surface Metal Atom
Before wash	6.39	0.54
20	5.27	0.45
41	4.48	0.38
51	3.71	0.31
56	3.27	0.28
60	2.72	0.23
66	1.48	0.13
Initial No. Modifier Molecules Added = $29.97 \times 10^{18}$		

TABLE 4.4.10: DESORPTION OF DIOL FROM Ni/C10

Temperature (°C)	Total No. Molecules Adsorbed ( $\times 10^{18}$ )	Ratio Molecules Adsorbed per Surface Metal Atom
Before wash	4.42	0.85
20	4.11	0.79
36	4.06	0.78
44	4.20	0.81
51	4.27	0.82
62	4.31	0.83
66	4.40	0.83
Initial No. Modifier Molecules Added = $14.22 \times 10^{18}$		

TABLE 4.4.11: DESORPTION OF DIOL FROM Ni/C30

Temperature (°C)	Total No. Molecules Adsorbed ( $\times 10^{18}$ )	Ratio Molecules Adsorbed per Surface Metal Atom
Before wash	3.51	0.38
23	3.25	0.35
38	3.24	0.35
47	3.25	0.35
60	3.26	0.35
66	3.31	0.36
Initial No. Modifier Molecules Added = $8.71 \times 10^{18}$		

The amounts desorbed from the Grace silica-supported catalysts were minimal and indicated that the excess binaphthol was not adsorbed as weak, physically adsorbed layers above the chemisorbed species.

It is an important requirement of chirally modified catalysts, designed for asymmetric hydrogenation experiments, that the modifier molecules are strongly adsorbed, or to be more exact, are adsorbed more strongly than the reactant molecules, intermediates, or products, otherwise these molecules could displace the chiral overlayer, losing any possibility of chiral inducement and attainment of enantiomerically enriched products.

The Pd/C results were quite different. Much larger amounts of modifier were desorbed, indicating a difference in the adsorption influenced by the supports, and indeed diol adsorption studies on the blank supports showed that the carbon support itself could independently adsorb the diol modifier although the silica support could not, table 4.4.12.

Support	No. Modifier Molecules Added $\times 10^{18}$	No. Modifier Molecules Adsorbed $\times 10^{18}$
Carbon	21.25	7.66
Silica	21.70	0

When compared against a similar Pd/C modified reaction, the blank support adsorbed an amount in excess of that adsorbed by the catalyst and as such, the palladium crystallites have obviously obscured support surface area which was previously available for adsorption.

The amount of modifier strongly retained on the washed Pd/C catalyst (corresponding to a ratio of 0.13) could possibly correspond to a strongly bonded single overlayer on the palladium metal phase, with the modifier species adsorbed on the carbon support through a weaker interaction, being easily desorbed.

#### 4.4.2: DIMETHOXY ADSORPTION.

Investigations with the dimethoxy modifier showed absolutely no adsorption on any of the Grace silica-supported catalyst systems, even after a few days, with the modifier solutions remaining clear and colourless.

As the dimethoxy derivative showed no apparent adsorption on the Pd/C30 system, to ensure that the adsorption sites had not in some way been obscured, the dimethoxy experiment was repeated and left for twenty-four hours to enable any possible adsorption to occur. After this period of time a similar number of diol molecules was injected into the system and the subsequent adsorptions monitored. Figure 4.4.8 shows the results. Adsorption began to occur immediately the diol solution was added and followed an identical adsorption pattern to that observed before with the dimethoxy modifier remaining unaffected. The total amount adsorbed correlated with the equivalent direct binaphthol adsorption experiment. No colouration was noted in the modifier solution until the binaphthol was added and then the familiar yellow again appeared.

Conversely the Pd/carbon system did adsorb the dimethoxy modifier.

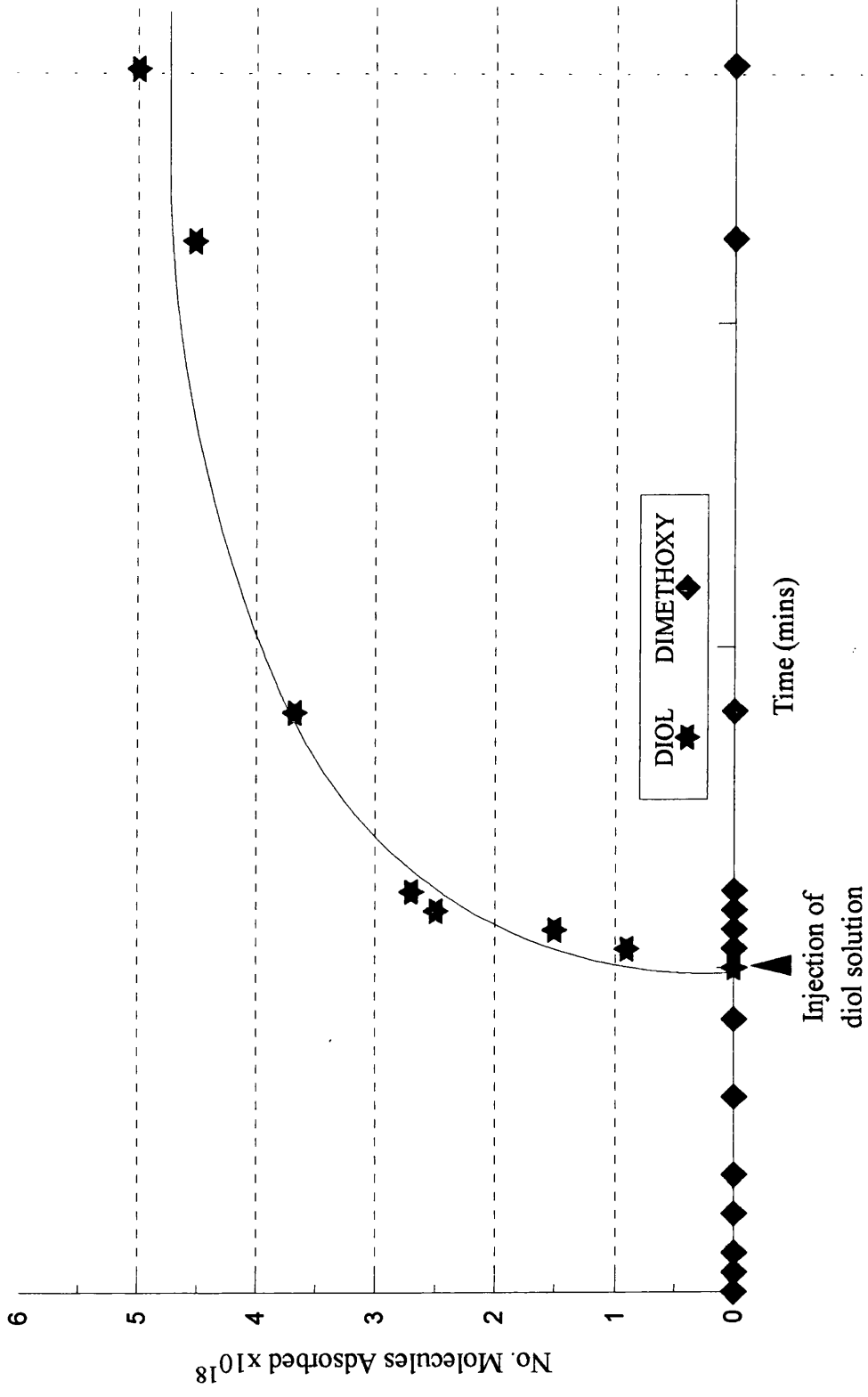


FIGURE 4.4.8: ADSORPTION OF DIMETHOXY FOLLOWED BY DIOL ON Pd/C30

TABLE 4.4.13: ADSORPTION OF DIMETHOXY ON Pd/C.		
Initial No. Molecules Added ( x 10 <sup>18</sup> )	Total No. Molecules Adsorbed (x 10 <sup>18</sup> )	Ratio Molecules Adsorbed per Surface Metal Atom.
1.00	0.41	0.03
10.21	2.21	0.19
14.48	2.49	0.21
21.83	3.96	0.33

As the silica-supported metals did not adsorb this modifier it would again appear that the carbon support was the important factor and, when compared against the blank support, the extent of adsorption was very similar.

TABLE 4.4.14: ADSORPTION OF DIMETHOXY ON Pd/C AND C		
Adsorbate	Initial No. Molecules Added (x 10 <sup>18</sup> )	Total No. Molecules Adsorbed (x 10 <sup>18</sup> )
Pd/C	1.00	0.41
C	1.00	0.44

Desorption of the dimethoxy from the Pd/C was very substantial, as far as the extreme case where all the modifier species were desorbed.

TABLE 4.4.15: DESORPTION OF DIMETHOXY FROM Pd/C		
Temperature (°C)	Total No. Molecules Adsorbed ( $\times 10^{18}$ )	Ratio Molecules Adsorbed per Surface Metal Atom.
Before wash	2.21	0.19
18	1.45	0.12
38	1.00	0.08
66	0.00	0.00
Initial No. Molecules Added = $10.21 \times 10^{18}$		

TABLE 4.4.16: DESORPTION OF DIMETHOXY FROM Pd/C		
Temperature (°C)	Total No. Molecules Adsorbed ( $\times 10^{18}$ )	Ratio Molecules Adsorbed per Surface Metal Atom.
Before wash	6.63	0.56
18	5.12	0.43
38	4.03	0.34
54	2.12	0.18
66	1.15	0.10
Initial No. Molecules Added = $29.70 \times 10^{18}$		

These results, taken together, show that adsorption of the dimethoxy modifier is purely a weak support interaction exclusively with the carbon support.

#### 4.4.3: DIAMINE ADSORPTION.

The same adsorption technique was then used to investigate the extent of modification using the diamine modifier. Tables 4.4.17 to 4.4.20 summarise these results.

TABLE 4.4.17: ADSORPTION OF DIAMINE ON Ni/C30		
Initial No. Molecules Added ( $\times 10^{18}$ )	Total No. Molecules Adsorbed ( $\times 10^{18}$ )	Ratio Molecules Adsorbed per Surface Metal Atom.
1.56	0.22	0.02
3.06	0.30	0.03
8.56	0.57	0.06
9.44	0.78	0.08
11.51	1.09	0.12
12.80	1.30	0.14
26.60	1.63	0.18

TABLE 4.4.18: ADSORPTION OF DIAMINE ON Ni/C10		
Initial No. Molecules Added ( $\times 10^{18}$ )	Total No. Molecules Adsorbed ( $\times 10^{18}$ )	Ratio Molecules Adsorbed per Surface Metal Atom.
1.53	0.38	0.07
5.27	1.22	0.23
5.32	1.23	0.24
8.56	0.84	0.16
26.60	1.01	0.19

For both Ni/Grace silica catalysts, a comparison with the equivalent diol adsorption experiments shows that much less diamine modifier was adsorbed. As the ratio values were much smaller, even when the initial number of molecules added was considerable, it may suggest that the adsorption occurred only on to the surface metal sites to form up to a single chiral overlayer. Once again, adsorption of the diamine modifier on to the blank silica supports did not occur.

Adsorption of the chiral diamine modifier on to the Pd/C30 catalyst proved to be much less reliable than that previously found for the diol. Whereas the earlier diol adsorption results were reproducible, the diamine proved to be much harder to adsorb, to such an extent that often no adsorption occurred at all, without any alterations in the experimental technique. This was the first indication of the catalyst ageing, as further described in Section 4.8. The results that were obtained are shown below.

TABLE 4.4.19: ADSORPTION OF DIAMINE ON Pd/C30		
Initial No. Molecules Added ( $\times 10^{18}$ )	Total No. Molecules Adsorbed ( $\times 10^{18}$ )	Ratio Molecules Adsorbed per Surface Metal Atom.
10.91	1.82	0.17
11.45	1.54	0.14

Again the figures for the amounts of diamine adsorbed were much lower than those for the comparable diol experiments.

The amounts of diamine adsorbed by the Pd/C catalyst were however, much greater than that adsorbed on any of the Grace silica-supported catalysts.

TABLE 4.4.20: ADSORPTION OF DIAMINE ON Pd/-C

Initial No. Molecules Added ( x 10 <sup>18</sup> )	Total No. Molecules Adsorbed (x 10 <sup>18</sup> )	Ratio Molecules Adsorbed per Surface Metal Atom.
1.14	1.01	0.08
2.95	2.32	0.20
6.11	4.60	0.39
8.61	5.70	0.48
8.98	6.74	0.57
9.48	7.24	0.61
10.23	7.65	0.65
11.19	9.77	0.83
11.92	9.56	0.81
21.90	11.15	0.94
22.77	14.94	1.26
24.05	15.91	1.34
34.19	22.10	1.87
34.85	21.19	1.79

To ensure that the adsorption was not just an interaction with the support, the same diamine modifier solution was adsorbed on the catalyst and support in separate experiments. These results are shown in table 4.4.21 along with figure 4.4.9.

Modification Time (mins)	No. Modifier Molecules Adsorbed $\times 10^{18}$	
	Pd/C	C
0	0	0
60	2.41	/
120	2.68	2.32
180	3.51	3.07
235	4.38	3.75
285	4.91	4.01
360	/	4.51
1350	9.62	6.05
1550	9.56	6.01

The results clearly show that the Pd/C catalyst adsorbed much more than the support itself, indicating that there is also adsorption on the active metal sites and not just the support. For all the Grace silica catalysts the diol modifier was adsorbed to the greatest extent, with values exceeding the predicted monolayer coverage, whereas the diamine appeared to adsorb only up to single overlayer. For Pd/C this order was reversed. A comparison of the figures in tables 4.4.4, 4.4.13 and 4.4.20 shows that the dimethoxy, which was adsorbed only on to the support, and the diol modifier, were adsorbed to a much lesser extent than the diamine. Thus the carbon support must

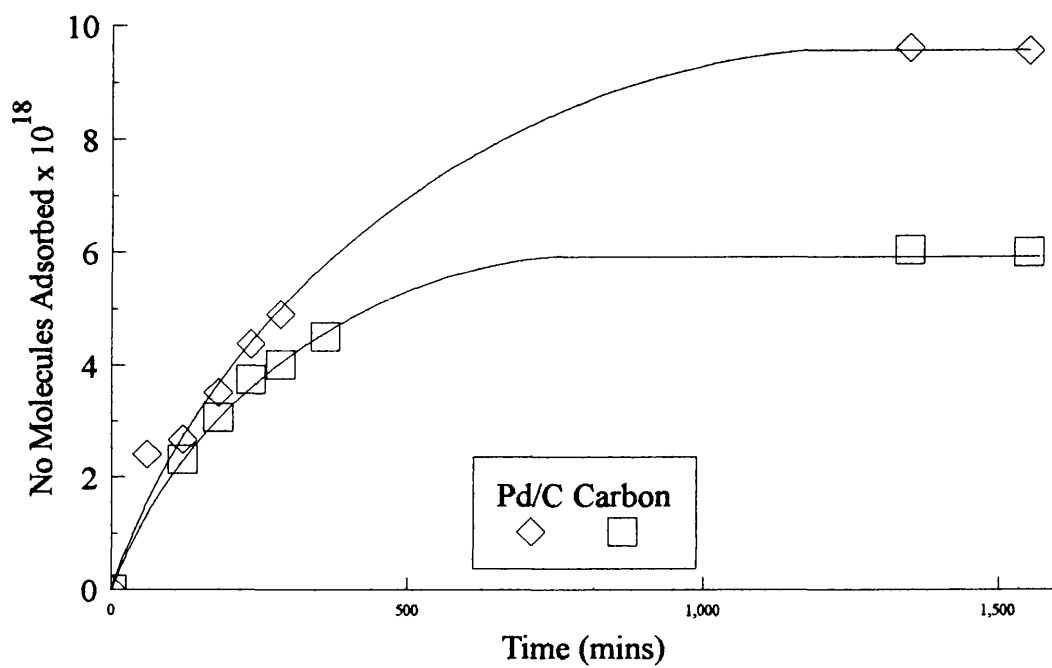


FIGURE 4.4.9: ADSORPTION OF DIAMINE ON Pd/C AND C

preferentially adsorb the diamine modifier, which may be due to the mixed acid groupings on the surface of this support, as explained in Section 4.2, interacting with the basic amine substituents, as opposed to adsorption via the aromatic moieties.

After a 1 hr wash process the amounts remaining adsorbed on each catalyst were as shown below.

TABLE 4.4.22: DESORPTION OF DIAMINE FROM CATALYSTS			
Catalyst	Initial No. Modifier Molecules Added $\times 10^{18}$	Initial No. Modifier Molecules Adsorbed $\times 10^{18}$	Final No. Modifier Molecules Adsorbed $\times 10^{18}$ After 1hr Wash
Ni/C10	1.53	0.68	0.37
	5.27	1.22	1.04
	5.32	1.23	1.02
Ni/C30	1.56	0.22	0.20
	9.44	0.78	0.23
	12.80	1.30	0.89
Pd/C	1.14	1.01	1.01
	1.58	1.58	1.58
	8.61	5.70	5.70
	11.19	9.77	9.77
	21.90	11.15	9.71
	24.05	15.91	15.48
	34.19	22.10	21.58
	34.85	21.19	19.30

Very little was desorbed from either of the nickel catalysts, indicating that the modifier was mainly adsorbed through a strong interaction with the metal phase of the catalyst. For the Pd/C catalyst the fraction of diamine desorbed within the 1 hr wash was very minimal, even with larger concentrations of starting material and initial amounts adsorbed, whereas the diol and dimethoxy modifiers had been easily desorbed. Hence adsorption of each of the diol, dimethoxy and diamine modifiers was very different over the various supported metal catalysts.

#### 4.4.4: ADSORPTION OF THE BINAPHTHALENE OPTICAL ISOMERS

The relative extents of adsorption of each of the diol and diamine enantiomers was investigated.

**TABLE 4.4.23: ADSORPTION OF THE OPTICAL ISOMERS OF BINAPHTHALENE DERIVATIVES ON Ni/GRACE- SILICA.**

Catalyst	Modifier	No. Molecules Added $\times 10^{18}$	Initial No. Molecules Adsorbed $\times 10^{18}$	Final No. Molecules Adsorbed After Wash $\times 10^{18}$
C30	R-diol	11.14	5.05	4.71
C30	S-diol	11.12	5.11	4.96
C30	R-diamine	11.51	1.09	1.02
C30	S-diamine	12.80	1.30	0.89
C10	R-diamine	5.32	1.23	1.04
C10	S-diamine	5.27	1.22	1.02

TABLE 4.4.24: ADSORPTION OF THE OPTICAL ISOMERS OF  
BINAPHTHALENE DERIVATIVES ON Pd/C

Modifier	No. Molecules Added $\times 10^{18}$	Initial No. Molecules Adsorbed $\times 10^{18}$	Final No. Molecules Adsorbed After Wash $\times 10^{18}$
S-diol	8.08	1.80	1.31
R-diol	8.15	1.78	0.91
S-diol	11.20	2.70	1.80
R-diol	11.18	2.62	2.01
S-diamine	11.24	10.22	9.95
R-diamine	11.19	9.77	9.77
S-diamine	34.19	22.10	21.58
R-diamine	34.85	21.19	19.30

These results show that, within the limits of experimental error, these catalysts do not preferentially adsorb either optical isomer of the diol or diamine modifier.

#### 4.4.5: HYDROXYMETHOXY ADSORPTION.

This modifier was introduced in an attempt to understand more about the mode of adsorption of the diol modifier. The adsorption results are shown in table 4.4.25.

Catalyst	No. Molecules Added $\times 10^{18}$	No. Molecules Adsorbed $\times 10^{18}$	Ratio Molecules Adsorbed per Surface Metal Atom
Ni/C30	4.55	0.83	0.09
Ni/C30	9.11	0.67	0.07
Ni/C10	4.56	0.34	0.07
Pd/C	1.54	0.73	0.06
Pd/C	14.49	4.84	0.41
Pd/C	21.16	2.94	0.25

Once again the amounts adsorbed on to the Ni/Grace silica catalysts did not exceed the predicted monolayer coverage. These results are compared with those obtained for the diol and diamine modifiers in table 4.4.26.

TABLE 4.4.26: COMPARISON OF THE ADSORPTION OF BINAPHTHYL  
MODIFIERS

Catalyst	Modifier	No. Molecules Added $\times 10^{18}$	No. Molecules Adsorbed $\times 10^{18}$	Ratio Molecules Adsorbed per Surface Metal Atom
Ni/C30	R-diol	9.96	3.92	0.42
Ni/C30	S-diamine	9.44	0.78	0.08
Ni/C30	Hydroxymethoxy	9.12	0.67	0.07
Ni/C10	R-diol	4.94	1.78	0.34
Ni/C10	R-diamine	5.27	1.22	0.24
Ni/C10	Hydroxymethoxy	4.56	0.34	0.07
Pd/C	R-diol	21.72	3.75	0.32
Pd/C	R-diamine	21.90	5.91	1.34
Pd/C	Hydroxymethoxy	21.16	2.94	0.25

When compared against the amount of diol adsorbed on to the Ni/silica catalysts the amount of hydroxymethoxy adsorbed was much lower, suggesting that only up to a monolayer of this species was adsorbed on the active metal surface, as previously proposed for the diamine modifier. The amount of hydroxymethoxy adsorbed was also less than that of the diamine species, possibly as a result of the hydroxymethoxy only being able to adsorb through one substituent group. Hydroxymethoxy was adsorbed to a lesser extent than either the diamine or diol modifiers on the Pd/C catalyst.

#### 4.4.6: CO-ADSORPTION STUDIES.

Co-adsorption of the diol and diamine binaphthyl derivatives was performed to investigate the relative effect of the presence of a second modifier species and to see if there was competitive adsorption between these modifiers. Two different techniques were used; sequential and concurrent co-adsorption.

For the sequential co-adsorption studies, the modification was carried out as for single modifier adsorption with only one modifier present in solution, during the first 24 hours, and the extent of adsorption was monitored. The second modifier solution was then introduced to the reaction medium without removal of the original solution. The concentration was immediately determined and the reaction then followed for a further 24 hour period.

After modification for 24 hours with the diamine modifier, solutions containing the diol modifier were then directly added. The results are shown in tables 4.4.27 to 4.4.29.

TABLE 4.4.27: ADSORPTION OF DIAMINE FOLLOWED BY DIOL ON Ni/SILICA CATALYSTS				
CATALYST	C30	C30	C30	C10
No.Molecules Diamine Added $\times 10^{18}$	8.56	11.51	26.60	8.56
Initial No. Diamine Molecules Adsorbed $\times 10^{18}$	0.57	1.09	1.63	0.84
Initial Ratio of Diamine Molecules Adsorbed per Surface Metal Atom	0.06	0.12	0.18	0.16
No. Molecules Diol Added $\times 10^{18}$	12.90	11.38	10.05	10.05
Final No. Diamine Molecules Adsorbed $\times 10^{18}$	0.48	0.45	2.21	1.01
Final Ratio of Diamine Molecules Adsorbed per Surface Metal Atom	0.05	0.05	0.24	0.19
Final No. Diol Molecules Adsorbed $\times 10^{18}$	0.57	0.94	1.72	2.31
Final Ratio of Diol Molecules Adsorbed per Surface Metal Atom	0.06	0.10	0.19	0.46
Total No. Molecules Adsorbed $\times 10^{18}$	0.78	1.39	3.93	4.12

In the first two experiments with Ni/C30, addition of the diol modifier resulted in the desorption of an amount of the original diamine, indicating that in these experiments it is the diol that is preferentially adsorbed. In each of these first two experiments the amount of diamine remaining adsorbed was very similar. However, in the last two experiments, where a greater amount of diamine was initially adsorbed, addition of the diol modifier seemed to enhance the extent of diamine adsorption and was itself also adsorbed to a greater extent than in the previous two experiments.

Both the Pd/Cab and Pd/C catalysts were also modified with the diamine molecule followed by addition of the diol.

EXPT.	A	B
No. Molecules Diamine Added $\times 10^{18}$	10.91	8.56
Initial No. Diamine Adsorbed $\times 10^{18}$	1.82	0
Initial Ratio of Diamine Molecules Adsorbed per Surface Metal Atom	0.17	0
No. Molecules Diol Added $\times 10^{18}$	18.94	9.63
Final No. Diamine Adsorbed $\times 10^{18}$	3.37	0
Final Ratio of Diamine Molecules Adsorbed per Surface Metal Atom	0.31	0
Final No. Diol Adsorbed $\times 10^{18}$	3.31	0.93
Final Ratio of Diol Molecules Adsorbed per Surface Metal Atom	0.31	0.09
Total No. Molecules Adsorbed $\times 10^{18}$	6.68	0.93

In expt A with the Pd/C30 catalyst the diamine modifier was adsorbed and subsequent addition of the diol seemed to further enhance this adsorption with a substantial amount of the diol itself also adsorbed. However, in the second experiment there was no apparent diamine adsorption and only very small amounts of diol were subsequently adsorbed. As the diol itself was not extensively adsorbed, the catalyst sample appeared to show irregular behaviour. This was later attributed to the catalyst ageing, as discussed in Section 4.8.

TABLE 4.4.29: ADSORPTION OF DIAMINE FOLLOWED BY DIOL ON Pd/C	
No. Molecules of Diamine Added $\times 10^{18}$	11.92
Initial No. Diamine Molecules Adsorbed $\times 10^{18}$	9.65
Initial Ratio of Diamine Molecules Adsorbed per Surface Metal Atom	0.81
No. Molecules of Diol Added $\times 10^{18}$	11.71
Final No. Diamine Molecules Adsorbed $\times 10^{18}$	9.71
Final Ratio of Diamine Molecules Adsorbed per Surface Metal Atom	0.82
Final No. Diol Molecules Adsorbed $\times 10^{18}$	1.86
Final Ratio of Diol Molecules Adsorbed per Surface Metal Atom	0.16
Total No. of Molecules Adsorbed $\times 10^{18}$	11.75

Addition of diol initially resulted in the desorption of some diamine but over a period of time this displaced diamine was re-adsorbed. The final amount adsorbed remained approximately constant, but tended to fluctuate very slightly between the individual amounts of diol and diamine. See figure 4.4.10.

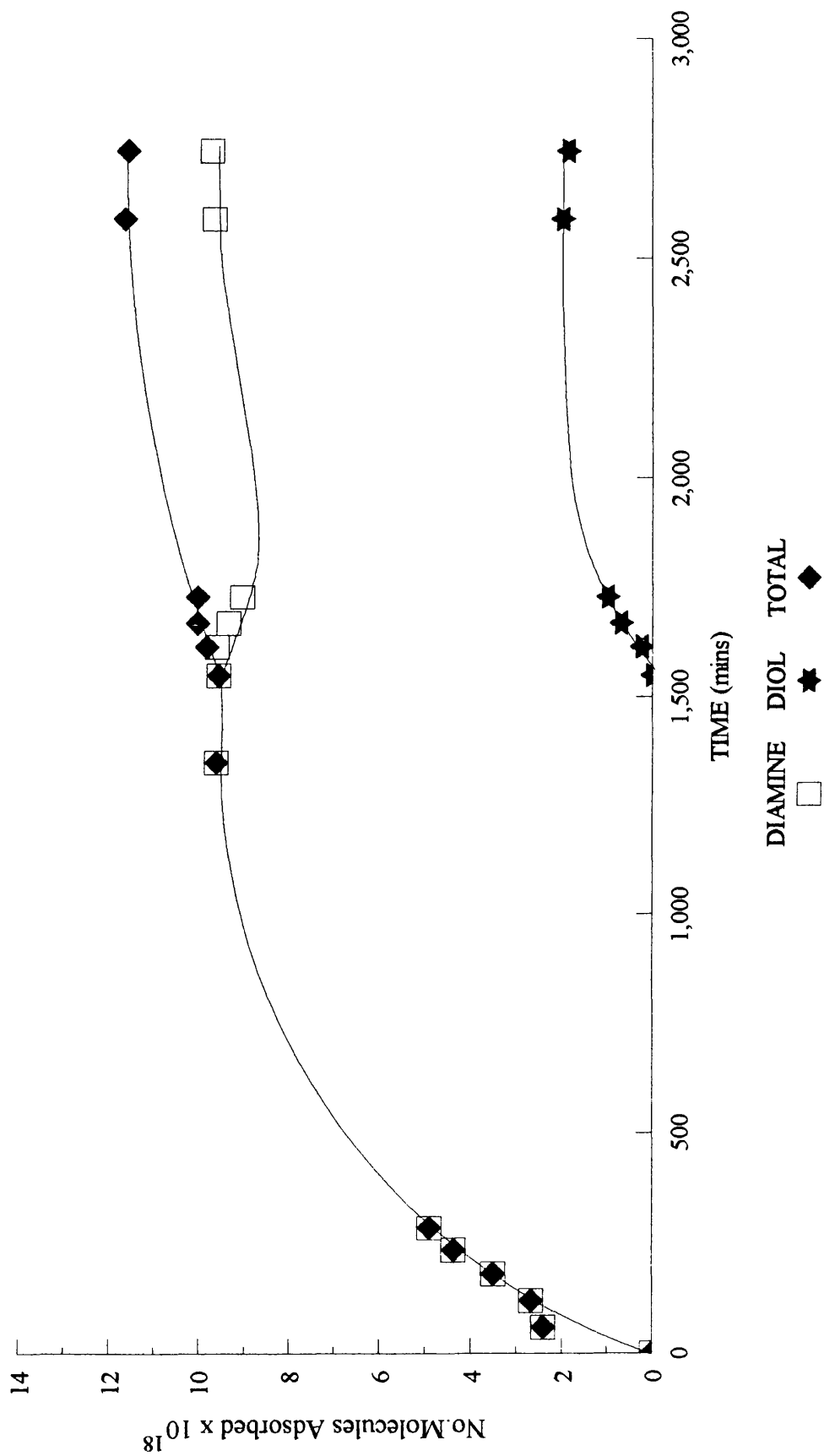


FIGURE 4.4.10: CO-ADSORPTION OF DIAMINE AND DIOL ON Pd/C

Using the Ni/C30 catalyst the experimental procedure was reversed; the diol being added first, followed by the diamine.

TABLE 4.4.30: ADSORPTION OF DIOL FOLLOWED BY DIAMINE ON Ni/C30	
No. of Molecules of Diol Added $\times 10^{18}$	9.15
Initial No. of Diol Molecules Adsorbed $\times 10^{18}$	3.82
Initial Ratio of Diol Molecules Adsorbed per Surface Metal Atom	0.41
No. of Molecules of Diamine Added $\times 10^{18}$	9.64
Final No. of Diol Molecules Adsorbed $\times 10^{18}$	3.44
Final Ratio of Diol Molecules Adsorbed per Surface Metal Atom	0.37
Final No. of Diamine Molecules Adsorbed $\times 10^{18}$	0.24
Final Ratio of Diamine Molecules Adsorbed per Surface Metal Atom	0.03
Total No. of Molecules Adsorbed $\times 10^{18}$	3.68

This time the addition of diamine resulted in the desorption of a small percentage of the diol and this led to the final total amount of molecules adsorbed being less than had originally been the case with only the diol modifier present.

In concurrent co-adsorption experiments the modifier solution added to the catalyst contained both diol and diamine species. The competitive adsorption of these two species on a freshly reduced catalyst surface could thus be investigated. Experiments were performed with the addition of a modifier solution containing similar amounts of both diol and diamine molecules over each catalyst.

Catalyst	C30	C10
No. of Diamine Molecules Added $\times 10^{18}$	5.19	5.08
No. of Diol Molecules Added $\times 10^{18}$	5.20	5.07
No. of Diamine Molecules Adsorbed $\times 10^{18}$	0.35	0.37
Ratio of Diamine Molecules Adsorbed per Surface Metal Atom	0.04	0.07
No. of Diol Molecules Adsorbed $\times 10^{18}$	1.78	1.57
Ratio of Diol Molecules Adsorbed per Surface Metal Atom	0.19	0.30
Total No. of Molecules Adsorbed $\times 10^{18}$	2.14	1.94

Figure 4.4.11 shows how the adsorption proceeded for both of the modifier species on the Ni/C10 catalyst.

Adsorption of mixed modifier solutions on both the Pd/Cab and Pd/C catalysts was also investigated.

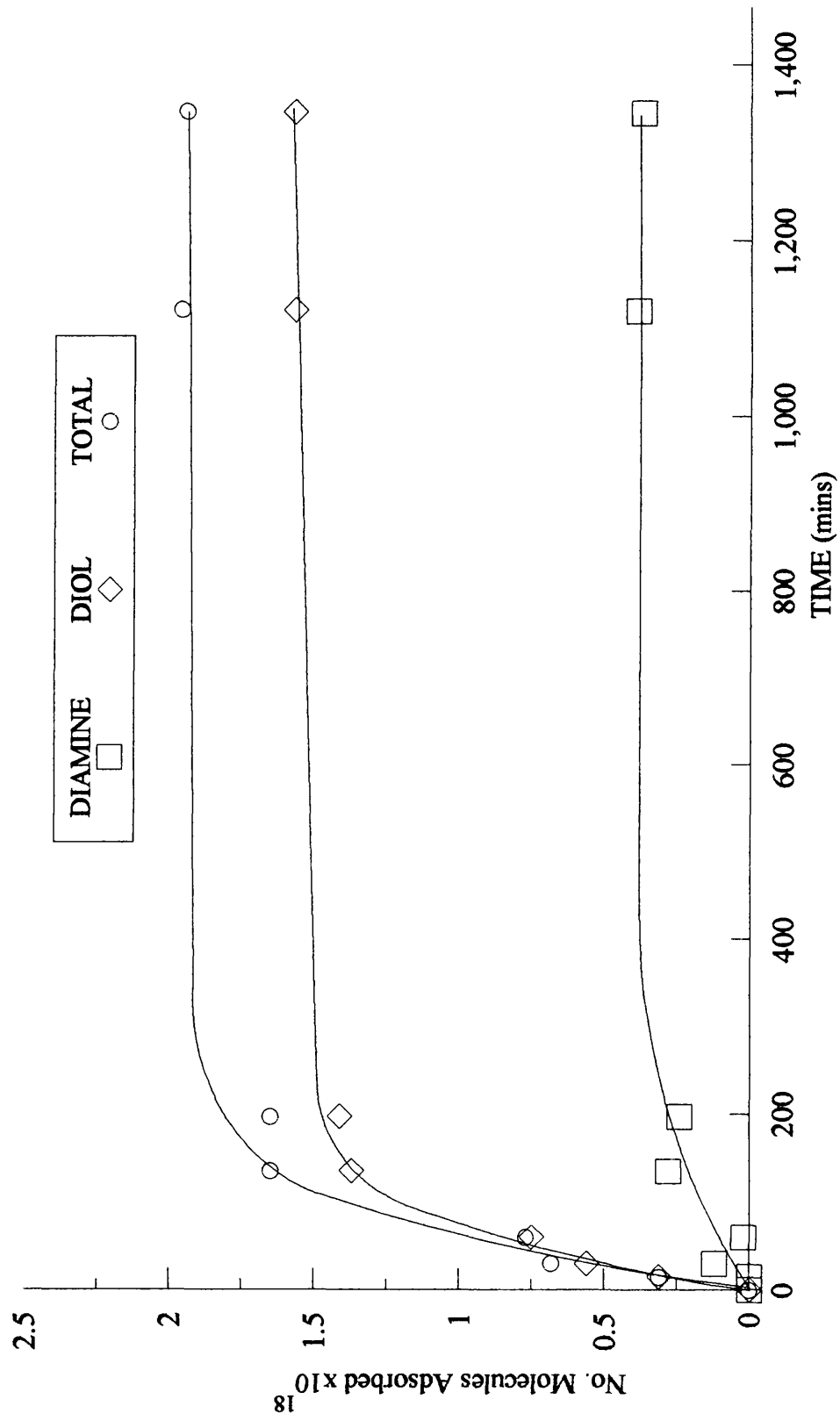


FIGURE 4.4.11: CO-ADSORPTION OF DIOL AND DIAMINE ON Ni/C10

TABLE 4.4.32: CONCURRENT ADSORPTION OF DIOL AND DIAMINE ON Pd/C30					
Experiment	A	B	C	D	E
No. of Diamine Molecules Added $\times 10^{18}$	2.99	3.12	4.98	5.33	5.38
No. of Diol Molecules Added $\times 10^{18}$	2.89	3.02	4.96	5.32	5.37
No. of Diamine Molecules Adsorbed $\times 10^{18}$	0.33	0.29	0.07	0.41	0.29
Ratio of Diamine Molecules Adsorbed per Surface Metal Atom	0.03	0.03	0.01	0.04	0.03
No. of Diol Molecules Adsorbed $\times 10^{18}$	0.50	0.23	0.24	1.93	0.76
Ratio of Diol Molecules Adsorbed per Surface Metal Atom	0.05	0.02	0.02	0.18	0.07
Total No. of Molecules Adsorbed $\times 10^{18}$	0.83	0.52	0.31	2.34	1.05

By monitoring the adsorption in these experiments it was discovered that both modifiers adsorbed in the first sixty minutes and then as the diol continued to increase the diamine appeared to be temporarily displaced until, when left overnight, it was again re-adsorbed and increased to its maximum value, figure 4.4.12.

The ratio figures show that the amount of diamine adsorbed in each experiment was fairly similar, but the same figures for the extent of diol adsorption show a much greater variation. The results for the Pd/C catalyst are shown in table 4.4.33.

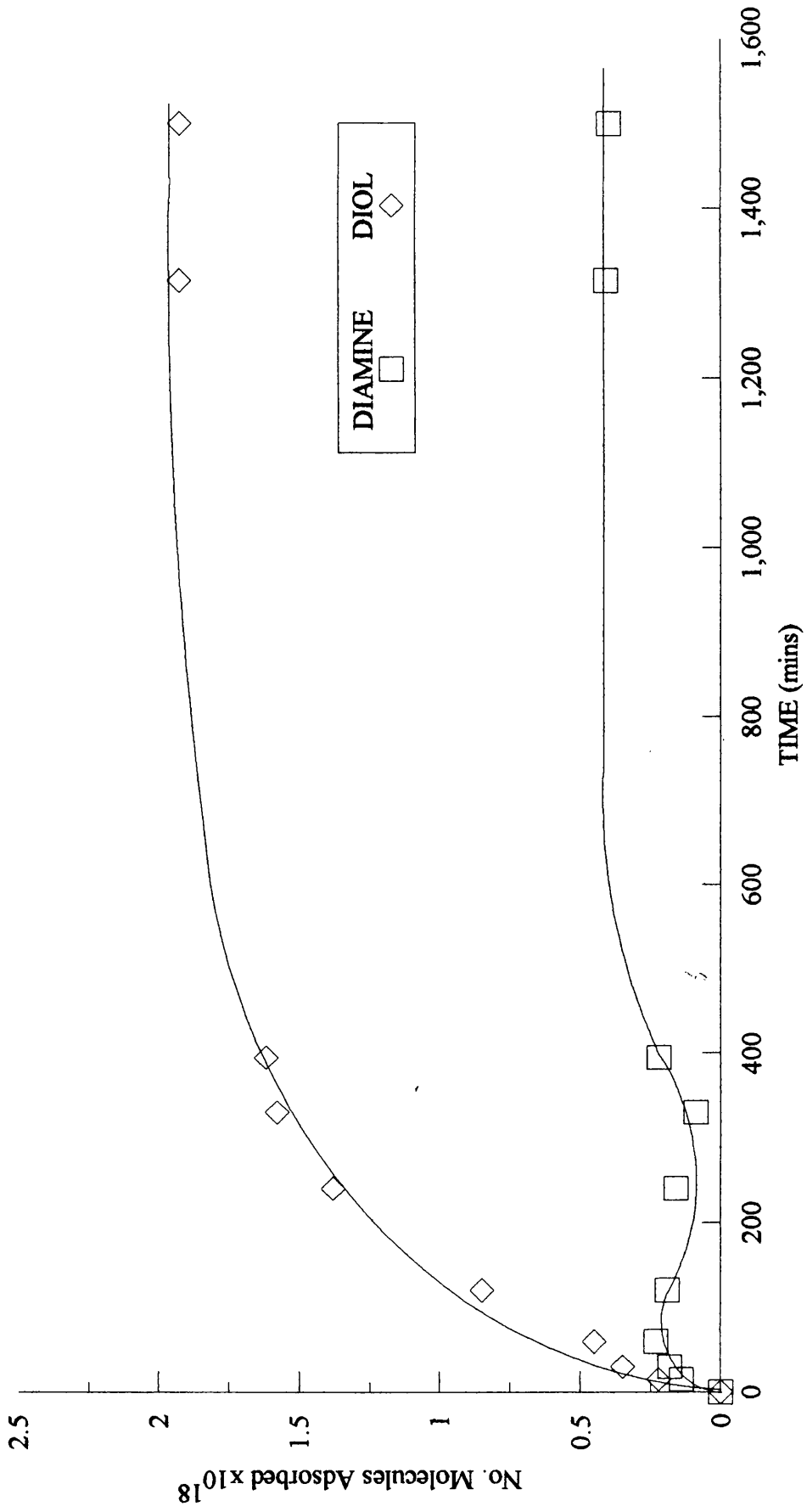


FIGURE 4.4.12: CO-ASORPTION OF DIAMINE AND DIOL ON Pd/C30

TABLE 4.4.33: CONCURRENT ADSORPTION OF DIOL AND DIAMINE ON Pd/C	
No. of Diamine Molecules Added $\times 10^{18}$	2.88
No. of Diol Molecules Added $\times 10^{18}$	2.78
No. of Diamine Molecules Adsorbed $\times 10^{18}$	2.28
Ratio of Diamine Molecules Adsorbed per Surface Metal Atom	0.19
No. of Diol Molecules Adsorbed $\times 10^{18}$	0.69
Ratio of Diol Molecules Adsorbed per Surface Metal Atom	0.06
Total No. of Molecules Adsorbed $\times 10^{18}$	2.97

Clearly the diamine is preferentially adsorbed over the diol even in a mixed modifier medium. The amount of diol adsorbed was less than that in an equivalent single modifier experiment.

#### 4.4.7: TETRAOL ADSORPTION.

The tetraol molecule, see figure 3.6.1, with four hydroxyl substituents at the 2, 2', 7 and 7' positions, was briefly investigated, to try and further elucidate the mode of adsorption of the diol modifier species.

TABLE 4.4.34: ADSORPTION OF TETRAOL

Catalyst	No. Molecules Added $\times 10^{18}$	No. Molecules Adsorbed $\times 10^{18}$	Ratio Molecules Adsorbed per Surface Metal Atom	No. Molecules Remaining Adsorbed $\times 10^{18}$	Ratio Molecules Adsorbed per Surface Metal Atom
Ni/C10	4.05	0.67	0.13	0.51	0.10
Ni/C30	5.66	0.54	0.06	0.37	0.03
Pd/C	5.79	0.42	0.04	0.28	0.02

The tetraol was adsorbed to a much smaller extent than was found for the diol in equivalent experiments on the nickel catalysts, Section 4.4.1. No colouration developed in the modifier solution as the adsorption progressed. For the Pd/C catalyst, a timed adsorption analysis showed that all the adsorption had occurred within the first thirty minutes after contact of the active catalyst with the modifier solution. This was unlike the diol systems where adsorption was shown to gradually build up to a plateau level over several hours. The number of tetraol modifier molecules adsorbed was found to be less than that for the diol.

#### 4.4.8: ADSORPTION OF BINAPHTHALENE DERIVATIVES ON Cab-O-Sil SUPPORTED CATALYSTS.

Although the majority of the adsorption work was initially performed on the Grace silica and carbon-supported catalysts, the Ni/Cab and Pd/Cab were also examined to determine the extent of diol and diamine adsorption. Once again, neither catalyst was

found to adsorb the dimethoxy modifier.

TABLE 4.4.35: ADSORPTION OF DIOL ON Pd/Cab

No. Modifier Molecules Added $\times 10^{18}$	No. Modifier Molecules Adsorbed $\times 10^{18}$	Ratio Molecules Adsorbed per Surface Metal Atom
1.27	0.13	0.03
4.66	0.34	0.08
5.99	0.25	0.06
7.65	0.32	0.08
14.35	0.29	0.07
19.90	0.41	0.10
28.17	0.56	0.14

TABLE 4.4.36: ADSORPTION OF DIAMINE ON Pd/Cab

No. Modifier Molecules Added $\times 10^{18}$	No. Modifier Molecules Adsorbed $\times 10^{18}$	Ratio Molecules Adsorbed per Surface Metal Atom
1.08	0.08	0.02
4.57	0.38	0.09
6.69	0.54	0.13
8.19	0.43	0.11
9.97	0.36	0.09
11.30	0.55	0.14
25.11	0.77	0.19

For Pd/Cab the amounts of diol adsorbed were much lower than those found in the comparable Pd/C30 experiments. Both the diol and the diamine modifiers would appear not to adsorb in excess of the amounts required for monolayer coverage of the metal.

TABLE 4.4.37: ADSORPTION OF DIOL ON Ni/Cab		
No. Modifier Molecules Added $\times 10^{18}$	No. Modifier Molecules Adsorbed $\times 10^{18}$	Ratio Molecules Adsorbed per Surface Metal Atom
1.26	0.77	0.01
3.00	0.58	0.00
5.97	1.35	0.01
13.24	1.85	0.01
14.11	1.08	0.01

TABLE 4.4.38: ADSORPTION OF DIAMINE ON Ni/Cab		
No. Modifier Molecules Added $\times 10^{18}$	No. Modifier Molecules Adsorbed $\times 10^{18}$	Ratio Molecules Adsorbed per Surface Metal Atom
1.09	0.83	0.01
4.71	0.89	0.01
9.01	2.16	0.02
11.99	2.92	0.02
29.40	4.09	0.03

For the Ni/Cab catalyst, very low ratio figures were obtained for the amounts of each modifier strongly adsorbed.

#### 4.4.9: TFAE ADSORPTION.

The TFAE modifier molecule consists of a chiral arm, with -CF<sub>3</sub> and -OH substituents, attached to a planer, aromatic anthracene unit. The adsorption results are shown below, table 4.4.39.

TABLE 4.4.39: ADSORPTION OF TFAE.					
Catalyst	No. Molecules Added x10 <sup>18</sup>	No. Molecules Adsorbed x10 <sup>18</sup>	Ratio Molecules Adsorbed per Surface Metal Atom	No. Molecules Remaining Adsorbed After 1hr Wash x10 <sup>18</sup>	Ratio Molecules Adsorbed per Surface Metal Atom After 1hr Wash
Ni/C10	7.24	3.52	0.67	3.52	0.67
	16.18	1.21	0.23	0.56	0.11
Ni/C30	3.52	0.37	0.04	0.08	0.01
Pd/C	8.88	8.10	0.72	7.70	0.65
	9.92	9.92	0.84	9.75	0.82
Carbon	9.59	8.71	/	/	/

Adsorption was found to occur, to varying extents, on all the catalyst samples. For the nickel catalysts, the amounts initially adsorbed and then retained after washing, appeared to have no direct correlation with the initial amounts of modifier added. There was no substantial adsorption on the blank silica. For Pd/C there was a slight increase in the amount adsorbed as the initial concentration increased. The difference between the amount adsorbed on the carbon support and the Pd/C catalyst showed that

adsorption had occurred on both the metal and support phases of the catalyst.

#### 4.4.10: ADSORPTION OF UNCHELATED MACROCYCLES.

Two unchelated macrocycles, (the structures are shown in figure 3.6.2), referred to as C<sub>5</sub> and C<sub>6</sub> due to the respective sizes of the carbon chain bridging the macrocycle, were also used for adsorption studies with the Ni/Cab, Pd/Cab and Pd/C.

Catalyst	No. Modifier Molecules added x10 <sup>18</sup>	No. Modifier Molecules Adsorbed x10 <sup>18</sup>	No. Modifier Molecules Remaining Adsorbed x 10 <sup>18</sup>
Ni/Cab	1.18	0.15	0.15
Ni/Cab	2.80	0.43	0.49
Ni/Cab	5.51	2.75	2.05
Pd/Cab	1.22	1.15	/
Pd/Cab	2.41	0.26	/
Pd/Cab	2.68	0.33	0.81
Pd/Cab	2.74	1.58	1.54
Pd/Cab	5.81	0.43	0.40
Pd/C	1.21	0.55	0.50
Pd/C	2.43	1.50	1.50
Pd/C	5.73	1.64	1.24
Carbon	1.22	0.75	0.69
Carbon	2.44	1.14	1.02
Carbon	2.89	1.25	1.12

TABLE 4.4.41 ADSORPTION OF C <sub>6</sub> UNCHELATED MACROCYCLE.			
Catalyst	No. Modifier Molecules added x10 <sup>18</sup>	No. Modifier Molecules Adsorbed x10 <sup>18</sup>	No. Modifier Molecules Remaining Adsorbed x 10 <sup>18</sup>
Ni/Cab	1.18	0.10	/
Ni/Cab	1.14	0.19	/
Ni/Cab	4.52	0.00	0.00
Pd/Cab	2.41	0.00	0.00
Pd/Cab	2.44	0.48	0.45
Pd/Cab	4.90	0.57	0.14
Pd/C	1.19	0.82	/
Pd/C	1.16	0.59	/
Pd/C	2.40	0.69	0.61
Carbon	1.20	0.69	0.66

No adsorption of either macrocycle occurred on the blank Cab-O-Sil support. Adsorption of the C<sub>5</sub> macrocycle, on both the Ni/Cab and the Pd/C, appeared to show a direct correlation between the amount added and the amount adsorbed. The Pd/Cab catalyst was less predictable. The blank carbon support was sometimes shown to adsorb more than the Pd/C catalyst and sometimes less, and as such it is not clear whether or not adsorption on the catalyst occurs on both the metal phase and the support or solely on to the support. The amounts of the C<sub>6</sub> macrocycle adsorbed were irreproducible on all the catalyst surfaces. Where adsorption of either macrocycle did occur, subsequent washing removed various proportions of modifier but there was always an amount strongly retained by the catalyst.

## 4.5: ADSORPTION BY-PRODUCTS.

Adsorption of the diamine modifier molecules on to the Pd/Cab catalyst did, at times, yield by-products that were detectable in the resultant modifier solution. This effect was unique to this catalyst system and did not occur within any of the other systems or with the diamine modifier solution in the absence of the catalyst. HPLC and HPLC-MS were used to elucidate the unknown structures.

### 4.5.1: HPLC RESULTS.

In one typical adsorption study of R-diamine on Pd/Cab the resultant colourless solution produced the HPLC trace shown in figure 4.5.1.

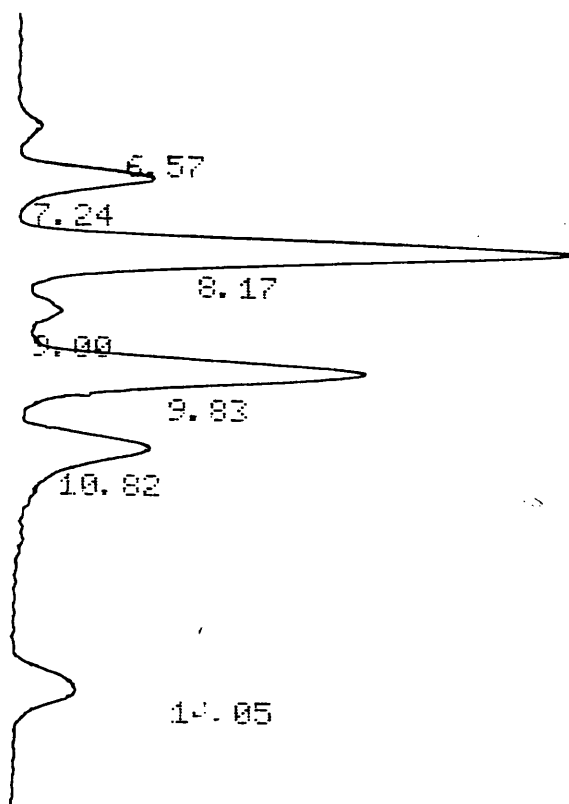


FIGURE 4.5.1: HPLC TRACE.

A maximum of seven species were detectable in any one reaction during an adsorption study, see table 4.5.1. The first three peaks were recognised as the diol, aminol and diamine respectively, as identified by the retention times on the column

and the added reassurance of spiking samples of the solution with known standards of each of these molecules. Thus, by contact of the diamine modifier with the Pd/Cab catalyst, it is possible to convert the  $-NH_2$  substituents to  $-OH$  groups through a stepwise conversion to result in the diol species, figure 4.5.2.

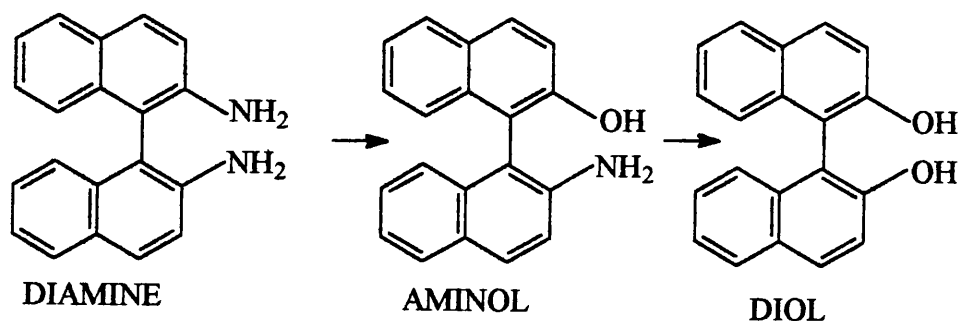


FIGURE 4.5.2: AMINOL INTERCONVERSION

HPLC-MS was used to identify the four remaining by-products, referred to as unknown 1 (UK1) through to unknown 4 (UK4).

TABLE 4.5.1: ELUTION ORDER OF INTERCONVERSION PRODUCTS FROM HPLC		
Product Number	Retention Time (mins)	Product Name
1	6.49	DIOL
2	7.62	AMINOL
3	8.27	DIAMINE
4	9.19	UK1
5	10.11	UK2
6	11.15	UK3
7	14.42	UK4

Coadsorption of the diol with the diamine again resulted in the interconversion of the diamine to the aminol and an excess of the diol species but appeared to prohibit any formation of the additional by-products, UK1-4. Figure 4.5.3 shows the changes in concentration of each of these species with time. This occurred to such an extent that, after 68 hrs, the diamine was virtually all consumed. This decrease in the amount of diamine present in solution was far too large to be attributed only to adsorption on the catalyst surface. Tables 4.5.2 to 4.5.9 detail some of the adsorption results obtained from experiments where by-product formation had occurred. In addition, an aminol adsorption result was included where only direct adsorption was observed to have occurred. No weight can be placed on this singular result and no conclusions can be drawn about whether or not two diamine groups must be present in the initial modifier molecule to initiate interconversion to other species. However, the synthesis of this aminol species was complicated and severely limited the amount of modifier available and as such any further aminol adsorption work was not possible.

N.M.R. analysis of the resultant modifier solution was swamped with too many peaks for any clear evidence of detailed structural changes. Nevertheless, the presence of an additional component with three contiguous methylene groups, such as in  $\text{OCH}_2\text{CH}_2\text{CH}_2\text{O}-$  was detected, which may have in some way arisen from the THF solvent.

The phenomenon appeared to be an entirely random effect and no variable was clearly isolated which could be controlled to alter either direct adsorption or interconversion. One variable that was considered was the dryness of the THF solvent. However, using freshly degassed solvent that had been purposely flushed with air made no difference to the results.

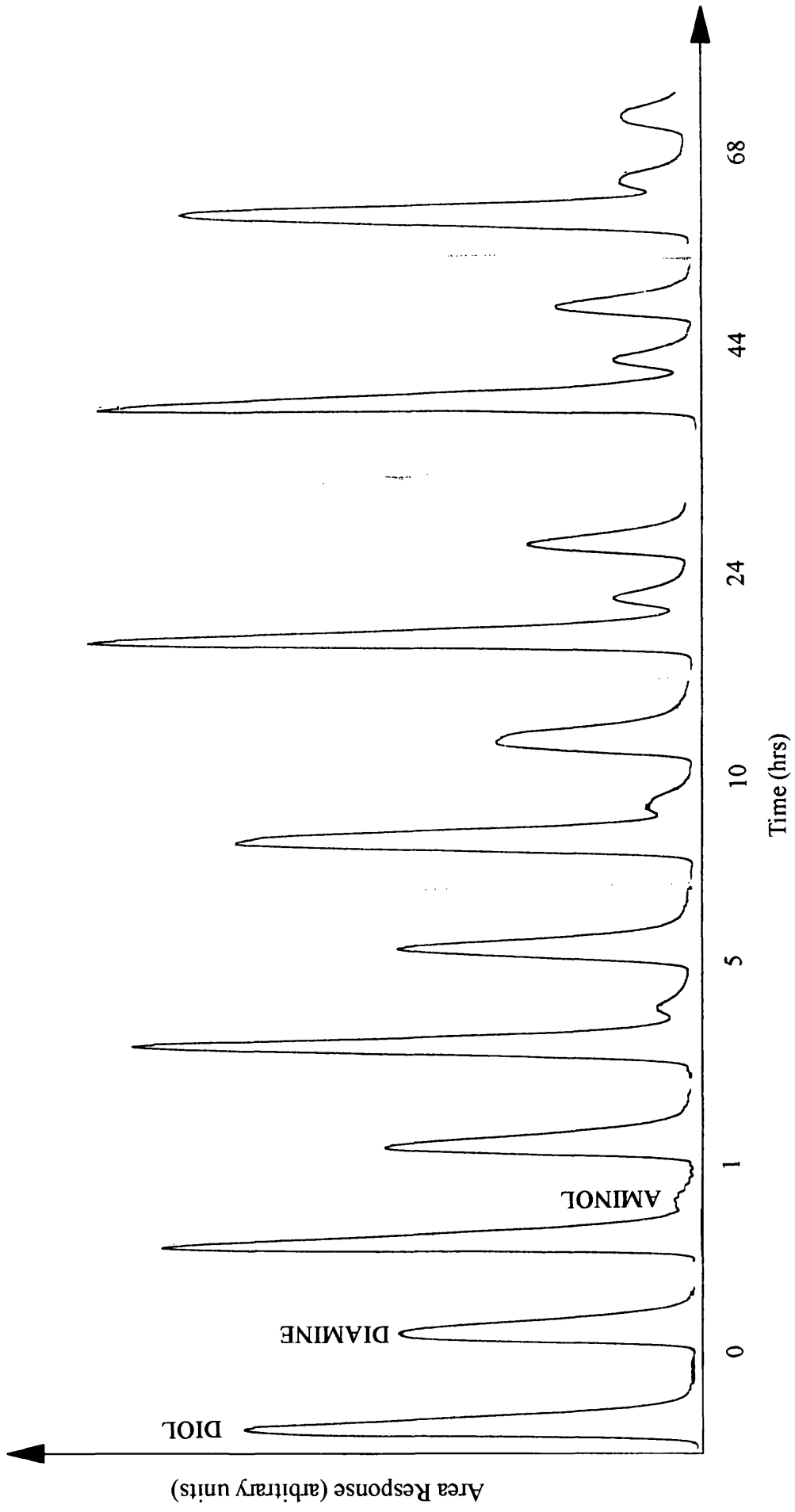


FIGURE 4.5.3: CO-ADSORPTION OF DIOL AND DIAMINE ON Pd/Cab.

TABLE 4.5.2: SINGLE ADSORPTION OF DIAMINE

No. molecules added $\times 10^{18}$	Products after 20 hrs			
	Product Number	Area	No molecules $\times 10^{18}$	Difference from starting solution (molecules $\times 10^{18}$ )
8.23	1	254	0.06	0.06 $\uparrow$
	2	4112	1.01	1.01 $\uparrow$
	3	22947	5.75	2.58 $\downarrow$
	4	0	0	0
	5	1845	\	\
	6	1034	\	\
	7	344	\	\

TABLE 4.5.3: SINGLE ADSORPTION OF DIAMINE

No. molecules added $\times 10^{18}$	Products after 20 hrs			
	Product Number	Area	No molecules $\times 10^{18}$	Difference from starting solution (molecules $\times 10^{18}$ )
11.37	1	386	0.09	0.09 $\uparrow$
	2	5951	1.47	1.47 $\uparrow$
	3	29693	7.62	3.75 $\downarrow$
	4	0	0	0
	5	2082	\	\
	6	733	\	\
	7	622	\	\

TABLE 4.5.4: SINGLE ADSORPTION OF DIAMINE

No. molecules added $\times 10^{18}$	Products after 44 hrs			
	Product Number	Area	No molecules $\times 10^{18}$	Difference from starting solution (molecules $\times 10^{18}$ )
11.37	1	368	0.08	0.08↑
	2	5772	1.42	1.42↑
	3	23552	6.04	5.33↓
	4	579	\	\
	5	6252	\	\
	6	3007	\	\
	7	1424	\	\

TABLE 4.5.5: SINGLE ADSORPTION OF DIAMINE

No. molecules added $\times 10^{18}$	Products after 68 hrs			
	Product Number	Area	No molecules $\times 10^{18}$	Difference from starting solution (molecules $\times 10^{18}$ )
11.37	1	402	0.09	0.09↑
	2	3459	0.85	0.85↑
	3	16267	4.17	7.20↓
	4	1245	\	\
	5	11297	\	\
	6	5075	\	\
	7	2380	\	\

TABLE 4.5.6: SINGLE ADSORPTION OF DIAMINE

No. molecules added $\times 10^{18}$	Products after 20 hrs			
	Product Number	Area (units)	No molecules $\times 10^{18}$	Difference from starting solution (molecules $\times 10^{18}$ )
45.83	1	4887	1.13	1.13 $\uparrow$
	2	49544	12.22	12.22 $\uparrow$
	3	116881	30.92	14.91 $\downarrow$
	4	0	0	0
	5	3038	\	\
	6	1086	\	\
	7	0	0	0

TABLE 4.5.7: SINGLE ADSORPTION OF AMINOL

No. molecules added $\times 10^{18}$	Products after 20 hrs			
	Product Number	Area	No molecules $\times 10^{18}$	Difference from starting solution (molecules $\times 10^{18}$ )
1.10	1	0	0	0
	2	743	0.26	0.84 $\downarrow$
	3	0	0	0
	4	0	0	0
	5	0	0	0
	6	0	0	0
	7	0	0	0

**TABLE 4.5.8: CO-ADSORPTION OF DIAMINE AND DIOL**

No. molecules added $\times 10^{18}$	Products after 20 hrs			
	Product Number	Area	No molecules $\times 10^{18}$	Difference from starting solution (molecules $\times 10^{18}$ )
Diol 12.72	1	59641	13.74	1.04 $\uparrow$
	2	11576	2.84	2.84 $\uparrow$
	3	40611	10.64	2.86 $\downarrow$
Diamine 13.57	4	0	0	0
	5	0	0	0
	6	0	0	0
	7	0	0	0

**TABLE 4.5.9: CO-ADSORPTION OF DIAMINE AND DIOL**

No. molecules added $\times 10^{18}$	Products after 44 hrs			
	Product Number	Area	No molecules $\times 10^{18}$	Difference from starting solution (molecules $\times 10^{18}$ )
Diol 12.72	1	65949	15.22	2.50 $\uparrow$
	2	22116	5.20	5.20 $\uparrow$
	3	26050	6.86	6.71 $\downarrow$
Diamine 13.57	4	0	0	0
	5	0	0	0
	6	0	0	0
	7	0	0	0

#### 4.5.2 : HPLC-MS RESULTS.

HPLC-MS was performed at Zeneca-Macclesfield. Unfortunately the main drawback from this analysis was that the HPLC columns at each centre were different, and even though all other conditions were identical, the retention times within the column and, more important, the order of elution may have varied. Nevertheless, the mass spectra provided important information on the species present. The mass spectrometry technique of electrospray ionisation emphasises the  $MH^+$  peak.

1/ The most prominent species had  $MH^+ = 285$ , (molecule A), and was clearly the original diamine molecule (mass = 284 a.m.u.) .

2/ The next peak had  $MH^+ = 286$ , the aminol, (Molecule Bi) and  $MH^+ = 269$  which could infer the formation of a strained furan ring via the elimination of  $NH_3$ .

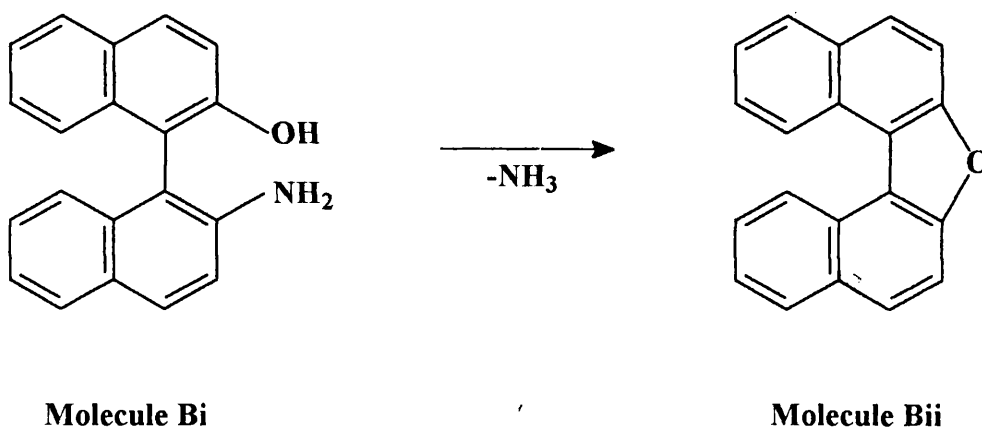


**FIGURE 4.5.4: MOLECULE B**

However the furan ring would not be planar due to the chiral tilt of the naphthalene rings and as such would not retain the stability of a planar aromatic system.

3/ Molecule C, the next to elute, had  $MH^+ = 298$  which could be the diamine and 14H, where ring hydrogenation had occurred.

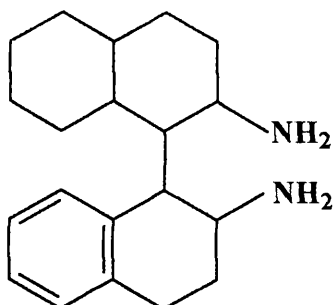
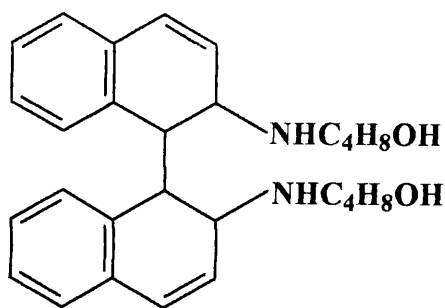


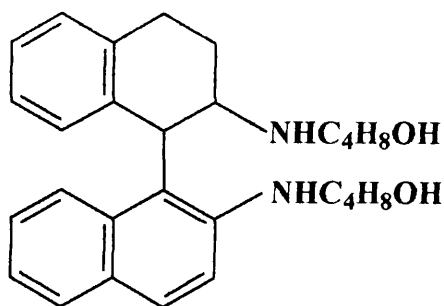
**FIGURE 4.5.5: MOLECULE C**

It was possible that one naphthalene ring initially sat planar to the catalyst surface and in this orientation it was completely hydrogenated to form the decalin ring structure. The second naphthyl group was directed in a more vertical orientation relative to the surface during adsorption. The lower end of the aromatic moiety was then within a sufficient proximity of the surface such that hydrogenation of two alkene bonds could be achieved. However, the remaining benzene ring was then lifted even further from the surface by the new cyclohexene ring, where it remained intact and could not be hydrogenated, leaving the tetralin structure.

4/ Molecule D has the parent ion  $MH^+ = 433$ , the heaviest molecule detected, which was equivalent to diamine plus two THF fragments (= 72 mass units each), and 4H. The possible structures are shown in figure 4.5.6.



**Molecule Di**



**Molecule Dii**

**FIGURE 4.5.6: MOLECULE D**

where the diamine groups have attacked the solvent molecules, forcing a ring opening of the THF to form linear alcohol substrates. This is an effect found with several of the other species. Molecule Dii, where hydrogenation had occurred within the same ring and had only reduced the aromaticity of one unit to form one tetralin and one naphthalene unit, was the most favourable.

5/ Molecule E had  $MH^+ = 361$ , diamine plus 1THF and 4H, and could possibly have been:

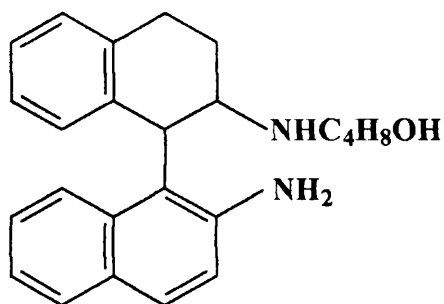


**FIGURE 4.5.7: MOLECULE E**

due to the same reasoning as molecule Dii. This molecule supports the idea that as the aromaticity of the ring system is reduced, the basicity of the amine is correspondingly increased, leaving the lone pair free to attack the THF molecule.

6/ Molecule F had  $MH^+ = 289$  and was likely to be an isomer of the structure;

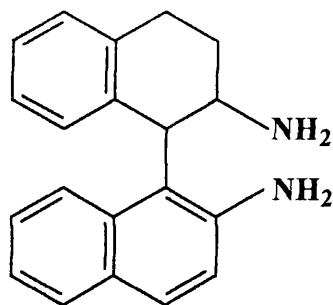
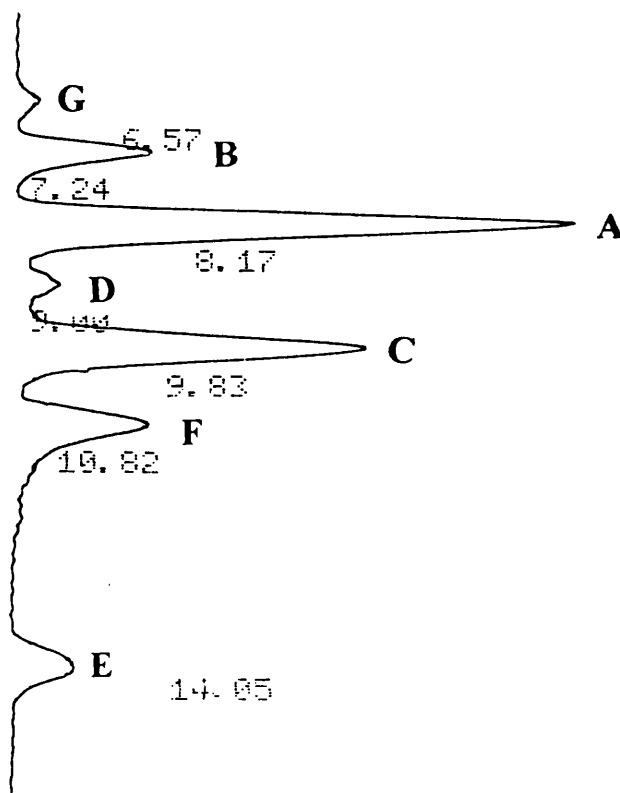


FIGURE 4.5.8: MOLECULE F

7/ The only remaining unidentified peak, G, eluted before the diamine, indicating a more polar species, and had  $MH^+ = 287$ . This would have been the diol structure.

Considering the relative intensities and order of elution, the peaks in the original trace were assigned thus:



From the adsorption figures it would appear that ring hydrogenation occurred preferentially over solvent interaction. The addition of THF increased over an extended period of time, possibly after all the surface hydrogen had been consumed. There was no evidence of THF interaction or ring hydrogenation in the diol or aminol species.

#### **4.6: RETENTION OF CHIRALITY.**

Polarimetry was used for initial investigations into the possibility of racemisation of the modifier molecules by each of the catalysts. From these experiments it was established that neither the Ni/silica catalysts nor the Pd/silica catalyst systems racemised the chiral diol or diamine to any detectable extent. The catalyst of main concern was the Pd/C, as carbon itself is known to act as a catalyst for binaphthyl racemisation<sup>121</sup> but it would appear that the extent of the increase in the barrier to rotation of the binaphthyl molecule by addition of the two -OH or -NH<sub>2</sub> groups was sufficient to prohibit this racemisation.

#### **4.7: COLOURATION OF MODIFIER SOLUTIONS**

During the adsorption studies with the diol modifier, a colour was often noted to develop in the modifier solution. This occurred within all the silica-supported systems (predominantly the Grace silica but also the Cab-O-Sil systems) but not in the Pd/carbon system.

Pd/silica-C30.....YELLOW

Ni/silica-C30.....ORANGE → YELLOW / GREEN

Ni/silica-C10.....PALE ORANGE →YELLOW / GREEN

Visually, the strength of the colour appeared to be concentration and time dependent. A modification experiment was also performed on the blank silica-C10 support to see if this colouration was due to an impurity present in the silica but the solutions remained colourless throughout the entire experiment, thus indicating that the colour must have resulted from metal ions in solution. After washing the modified catalyst, there was no resultant colouration.

U.V. spectra of the coloured solutions were run after the modification process had been left to reach equilibrium. The resultant spectra are shown in figure 4.7.1 and summarised in table 4.7.1.

TABLE 4.7.1: U.V. ABSORPTION BANDS OF COLOURED MODIFIER SOLUTIONS	
Catalyst	Wavelength (nm)
Pd/silica-C30	440
	410
	385
Ni/silica-C30	440
	400
	377
Ni/silica-C10	438
	395
	370

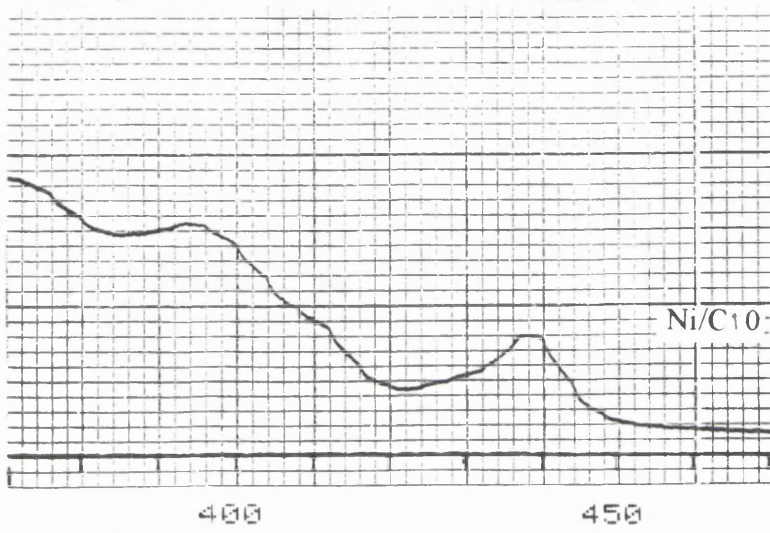
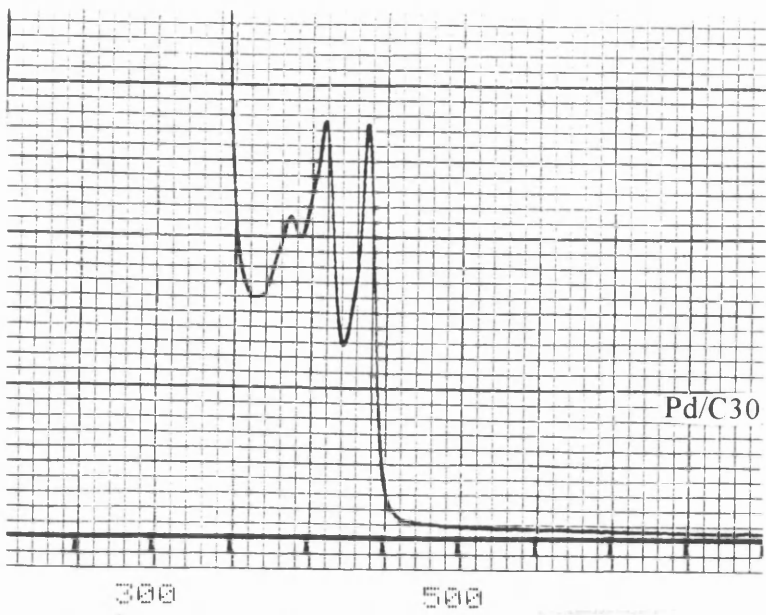


FIGURE 4.7.1: UV ABSORPTION SPECTRA

Each sample clearly showed the presence of metal ions in solution. All these bands are believed to be internal d-electron transitions. Any possible charge-transfer bands would occur further towards the ultra-violet end of the spectrum, overlapping with the binaphthol absorption bands.

Atomic adsorption studies were performed to analyse the metal content in solution. However, these experiments were unsuccessful as the amount of either palladium or nickel detected was so low as to fall within the background noise region, regardless of the strength of the modifier solution.

#### **4.8: CATALYST AGEING.**

There was a loss of reproducibility during adsorption studies on the Pd/C30 catalyst. Subsequent repeated characterisations showed a decrease in the number of available surface metal atoms, see table 4.8.1. This effect was unique to this catalyst.

TABLE 4.8.1: CO CHEMISORPTION STUDIES.		
Catalyst	No. Surface Metal Atoms $\times 10^{18}$ per g Catalyst as of APRIL 94	No. Surface Metal Atoms $\times 10^{18}$ per g Catalyst as of NOV.92
Pd/C30	2.50	10.67
Pd/C	11.72	11.84
Ni/C10	5.62	5.19
Ni/C30	10.11	9.24

Within the limits of experimental error the other catalysts appeared unaffected. Thus the Pd/C30 catalyst had aged whilst sitting on the shelf, the palladium particles

had become mainly inaccessible and as such the catalyst activity had been substantially decreased. The transmission electron micrograph of the aged Pd/Cab catalyst showed the presence of two different regions, figure 4.8.1. These micrographs showed that there were very few palladium crystallites present on the amorphous silica structure. Instead the main body of these crystallites appeared to be located either on or within the matrix of a secondary more crystalline silica species that was present in the catalyst.

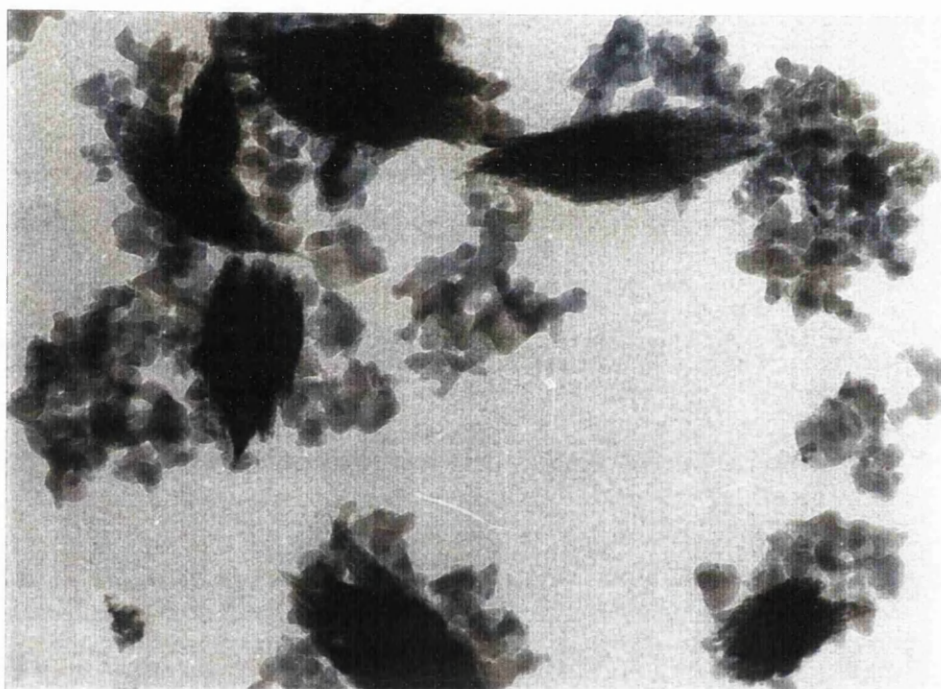


FIGURE 4.8.1: MICROGRAPH OF AGED Pd/C30 CATALYST.

TEM and XRD studies on the blank support showed only the presence of amorphous silica. Thus the ageing process appeared to have advanced by encapsulation of the metal particles due to a restructuring of the support. Hence the palladium crystallites acted as some sort of nucleation sites for the initiation of this recrystallisation, an effect not induced by the nickel crystallites, possibly due to the larger crystallite size or lesser mobility of nickel.

## 4.9: REDUCTION PROBLEMS WITH Ni/GRACE SILICA

### CATALYSTS.

The glass rig designed for the modification and hydrogenation experiments (figure 3.9.1), differed only from the original modification vessel,(figure 3.5.1), in that it had a larger volume and surface area at the bottom well to accommodate the water condenser and hydrogen bubbler for hydrogenation experiments. Regardless of the fact that identical activation conditions were used as before, reduction of the catalysts within this new system was no longer reliable. This was not due to the catalyst ageing, see Section 4.8.

As will be discussed further in Section 5.1, the actual reduction of the nickel oxide precursor to the active metal phase can be fairly ineffective, but this can be counteracted by using a high gas space velocity of hydrogen to carry away any water produced, forcing the equilibrium of the reduction reaction towards the metal side by preventing the back reaction. Consequently, any amount of air or water remaining in the system when it is left to cool after activation will reoxidise the catalyst sample, rendering the experiment void.

Attempts to overcome this problem included:- increasing the flow rate of the hydrogen, heating the top of the reactor, increasing the reduction temperature, altering the fit of the septum caps, evacuating the entire system prior to, during and after reduction and even cooling the system in the reducing gas. These attempts were all unsuccessful and the problem hindered many experiments. Attempts to modify the nickel catalysts in the original adsorption reactor and then transfer the modified system to the larger hydrogenation vessel, whilst maintaining an inert atmosphere, were also unsuccessful. This unreliability of these nickel systems meant that the Ni/C30 and

Ni/C10 catalysts were of no use for the ensuing hydrogenation experiments and as such the hydrogenation studies progressed with the Ni/Cab catalyst.

#### **4.10: HYDROGENATION STUDIES.**

All hydrogenation reactions were carried out as described in Section 3.9, at ambient temperature, unless otherwise stated. No hydrogenation of any reactant occurred in the absence of a catalyst, establishing that a catalyst was essential for hydrogenation to occur.

The work commenced with the hydrogenation of prochiral unsaturated carboxylic esters and figure 4.10.1 shows the two specific reactions that were examined. Methyl tiglate (-CH<sub>3</sub>) was the main prochiral substrate that was investigated and 4-trifluoro, 2-methyl, 2-butenic acid ethyl ester (-CF<sub>3</sub>) was introduced to probe the effect of fluorinated substituents.

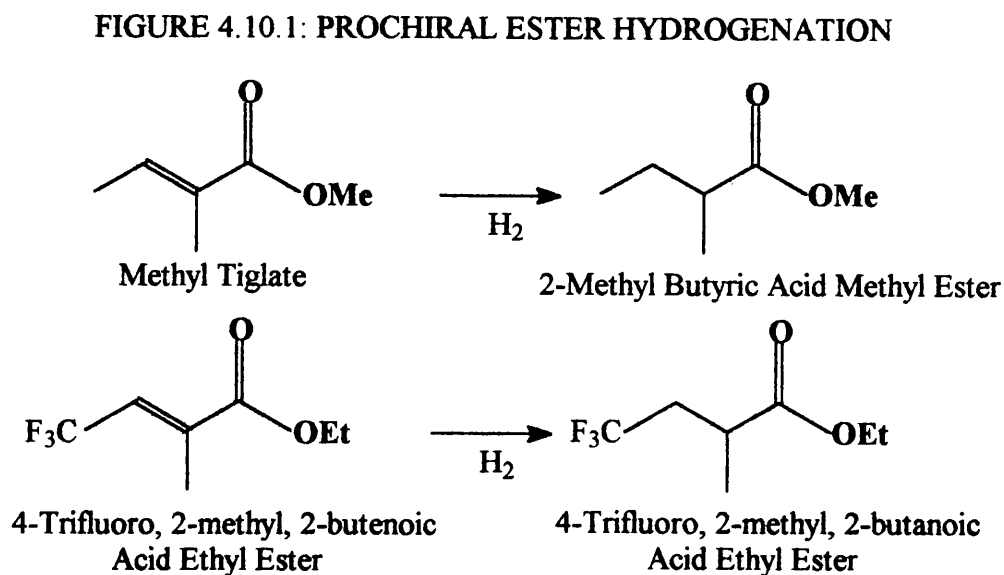


Table 4.10.1 showed that both the Pd catalysts were active for the hydrogenation

of methyl tiglate. With Pd/C an unidentified by-product was also formed, see Section 4.11. The nickel catalyst appeared to be inactive.

TABLE 4.10.1: METHYL TIGLATE HYDROGENATION OVER UNMODIFIED CATALYSTS.		
Catalyst	% Conversion	% Unknown Product Produced
Pd/Cab	93.51	~0
Pd/C	15.07	4.53
Ni/Cab	0.00	0.00

Tables 4.10.2 to 4.10.4 show the results obtained for the hydrogenation of both reactants over the range of catalysts modified with binaphthalene derivatives.

TABLE 4.10.2: METHYL TIGLATE HYDROGENATION OVER Pd/Cab MODIFIED WITH BINAPHTHYL DERIVATIVES				
Modifier	No. Modifier Molecules adsorbed $\times 10^{18}$	% Conversion	e.e.	% Unknown Produced
0	/	93.51	/	1.02
R-diamine	0.36	0	0	0
S-diol	0.41	50.93	0	1.43
S-diamine	0.43	51.91	0	1.56

The binaphthyl derivatives adsorbed on Pd/Cab did not enhance the catalytic activity but only acted to reduce the amount of methyl tiglate hydrogenated. No enantiomeric excess was produced.

TABLE 4.10.3: HYDROGENATION OF ESTER SUBSTRATES OVER Pd/C  
MODIFIED WITH BINAPHTHYL DERIVATIVES

Modifier	No. Modifier Molecules Adsorbed $\times 10^{18}$	Reaction substrate	Temp ( $^{\circ}\text{C}$ )	% Conversion	e.e.	% Unknown Produced
O	0	$-\text{CH}_3$	23	15.07	/	4.53
R-diol	0.91	$-\text{CH}_3$	23	5.42	0	2.61
S-diol	1.31	$-\text{CH}_3$	23	6.78	0	2.83
S-diol	1.37	$-\text{CH}_3$	36	5.87	0	1.37
R-diol	2.57	$-\text{CH}_3$	42	8.05	0	5.68
R-diamine	0.92	$-\text{CH}_3$	42	15.01	0	6.65
S-diamine	5.43	$-\text{CH}_3$	23	7.04	0	2.25
R-diamine	6.08	$-\text{CH}_3$	23	5.34	0	1.92
TFAE	9.75	$-\text{CH}_3$	23	32.97	0	2.26
Tetraol	0.08	$-\text{CH}_3$	23	15.72	0	2.76
TFAE	9.75	$-\text{CH}_3$	23	32.97	0	2.26
O	0	$-\text{CF}_3$	23	80.2	0	10.45
R-diamine	1.58	$-\text{CF}_3$	42	93.17	0	16.58
TFAE	7.70	$-\text{CF}_3$	42	95.03	0	11.57

The Pd/carbon catalyst was active for the hydrogenation of methyl tiglate and 4-trifluoro,2-methyl,2-butenic acid ethyl ester. However, the hydrogenated products were always racemic. The percentage conversions of methyl tiglate were not usually very substantial, only the TFAE modifier was apparently able to improve the extent

of reaction within the standard 20hr hydrogenation time. These results also showed that the Pd/C catalyst modified with either optical isomer of the diol or diamine was able to hydrogenate the methyl tiglate substrate to similar extents within the standard reaction time of 20hrs. No enantioselectivity was observed in the reactions carried out at atmospheric pressure. On the whole, these modifiers reduced the activity of the catalysts towards the hydrogenation of methyl tiglate and as such were thought to be partially poisoning the active metal surface, obscuring potential hydrogenation sites.

For the tetraol modifier, the small amount which was adsorbed did not confer any enantioselectivity on the reaction and did not appear to either increase or decrease the % conversion of methyl tiglate, leading to some doubts about adsorption actually occurring on the active metal surface. It could possibly be adsorbing exclusively on the carbon support. An unknown by-product was produced in each reaction.

**TABLE 4.10.4: HYDROGENATION OF ESTER SUBSTRATES OVER Ni/Cab MODIFIED WITH BINAPHTHYL DERIVATIVES**

Modifier	No. Modifier Molecules Adsorbed $\times 10^{18}$	Reaction substrate	Temp ( $^{\circ}\text{C}$ )	% Conversion	E.E
0	0.00	0	23	0	/
0	0.00	0	44	0	/
Diol	0.26	-CH <sub>3</sub>	23	0	/
Diamine	0.37	-CH <sub>3</sub>	44	0	/
TFAE	3.52	-CH <sub>3</sub>	23	0	/
0	0.00	-CF <sub>3</sub>	44	0	/
Diamine	0.20	-CF <sub>3</sub>	44	0	/

Table 4.10.4 clearly shows that the nickel catalyst was totally inactive for the hydrogenation of methyl tiglate and 4-trifluoro, 2-methyl, 2-butenic acid ethyl ester, even when the reaction temperature was raised to 44°C. Thus the nickel catalyst was not further investigated for these reactions.

In the vast majority of these reactions with the palladium catalysts, the results indicate that the modifier species has served only as a surface poison and precluded metal sites previously available for racemic hydrogenation. No enantioselectivity was induced by these modifiers for the hydrogenation of either prochiral unsaturated carboxylic ester reactant.

Both the Pd/Cab and Pd/C catalysts were modified with a range of the alternative modifiers, tables 4.10.5 and 4.10.6. Adsorption studies with these modifiers were not investigated, the various molecules were simply screened against the hydrogenation of methyl tiglate to see if they could induce enantioselectivity. The modification and washing techniques were identical to those used for the binaphthyl studies. For the modified Pd/Cab catalyst, table 4.10.5, no enantiomeric excess was obtained in any reaction but both DMPEA and MTFMPAA did increase the % conversion of methyl tiglate, to the extent of taking the reaction to completion within the standard reaction time of 20hrs. With this Pd/Cab catalyst the amount of substrate rearrangement that occurred to form the unknown by-product was much less than for the Pd/C system, see table 4.10.6.

TABLE 4.10.5: METHYL TIGLATE HYDROGENATION OVER Pd/CAB  
 MODIFIED WITH ALTERNATIVE DERIVATIVES

Modifier	No. Modifier Molecules Added $\times 10^{18}$	% Conversion	e.e.	% Unknown Produced
0	0	93.51	/	0
PhGly	15.10	41.22	0	1.49
His	80.75	~0	0	~0
PhAla	32.98	7.91	0	~0
Pseudoeph	9.77	50.74	0	1.30
Pseudoeph	89.37	57.17	0	~0
DMPEA	82.32	97.14	0	0
DMPEA	185.43	100.00	0	~0
MTFMPAA	3.56	100.00	0	0

**TABLE 4.10.6: METHYL TIGLATE HYDROGENATION OVER Pd/C  
MODIFIED WITH ALTERNATIVE DERIVATIVES**

Modifier	No.Modifier Molecules Adsorbed $\times 10^{18}$	% Conversion	e.e.	% Unknown Produced
O	0	15.07	/	4.53
PhGly	15.63	4.38	0	2.71
PhAla	29.95	8.24	0	2.91
Trp	12.74	13.08	0	2.41
DMPEA	189.65	8.41	0	3.03
MTFMCAA	10.18	11.69	0	2.75
Pseudoeph	10.17	19.95	0	2.53
Pseudoeph	20.34	20.80	0	2.45

The amount of modifier added was varied as it is known that the percentage surface coverage of the catalyst can effect the resultant enantiomeric excess. This is not a consistent value but is entirely dependent on the specific modifier molecule under investigation.<sup>53</sup> However, once again no enantioselectivity was induced.

Tiglic acid, a prochiral unsaturated carboxylic acid, was then hydrogenated over the range of unmodified and modified catalysts, see figure 4.10.2, again to investigate the asymmetric hydrogenation of a prochiral C=C.

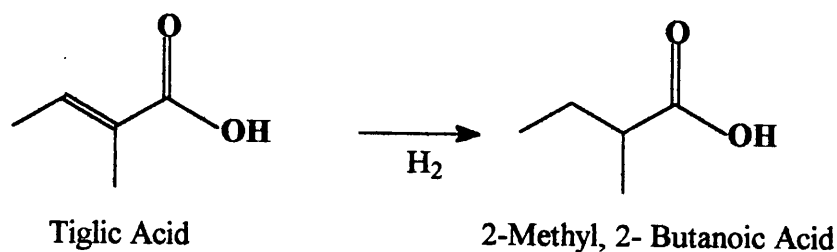


FIGURE 4.10.2: TIGLIC ACID HYDROGENATION

TABLE 4.10.7: TIGLIC ACID HYDROGENATION OVER UNMODIFIED CATALYSTS.

Catalyst	% Conversion	% Unknown Product Produced
Pd/Cab	52.10	0.00
Pd/C	13.23	0.00
Ni/Cab	45.63	0.00

All the catalysts were active for the hydrogenation of tiglic acid and no by-products were detected.

The hydrogenation of tiglic acid was carried out using the Pd/Cab catalyst modified with both the diol and diamine binaphthyl molecules separately and also when co-adsorbed.

TABLE 4.10.8: TIGLIC ACID HYDROGENATION OVER Pd/Cab MODIFIED WITH BINAPHTHYL DERIVATIVES.			
Modifier	No. Modifier Molecules Adsorbed $\times 10^{18}$	% Conversion	e.e.
0	/	52.10	/
R-diol	0.25	0.00	/
S-diamine	0.64	16.12	13
Coads-S	3.31 <sup>a</sup> / -0.48 <sup>b</sup>	3.96	0
Coads-R	0.52 <sup>a</sup> / -0.34 <sup>b</sup>	0.00	/

a-Diamine, b-Diol

In the reactions where interconversion of the original diamine modifier resulted in the production of excess diol, the activity of the modified Pd/Cab catalyst was reduced, the diol species poisoning active metal sites. The same effect was observed in the reaction where the catalyst was modified with the diol alone. Enantiomeric excess (13%) was successfully induced in the reaction where direct adsorption of the diamine on to the catalyst surface had occurred, with no interconversion by-products produced. Diamine molecules that were involved in interconversion did not induce e.e.

TABLE 4.10.9: TIGLIC ACID HYDROGENATION OVER Pd/CARBON MODIFIED WITH BINAPHTHYL DERIVATIVES.			
Modifier	No. Modifier Molecules Adsorbed x10 <sup>18</sup>	% Conversion	e.e.
O	/	13.23	/
R-diamine	4.60	0.00	/
S-diamine	7.65	19.18	4
R-diamine	9.44	4.27	4
S-diamine	9.47	14.80	2
R-diamine	10.00	4.89	3
R-diamine	14.74	16.83	5
R-diamine	14.94	19.21	0
R-diamine*	Adsorption and hydrogenation were run simultaneously	16.81	3

\*- No washing

The Pd/C system was the most reliable catalyst for obtaining optical yields of 2-methyl, 2-butanoic acid, although only small enantiomeric excesses were induced. There was no correlation between the amounts adsorbed and the % conversions. An experiment was then attempted whereby the modifier solution was added to the freshly reduced catalyst and the solution degassed *in situ*. The tiglic acid was then injected after 10 mins and the hydrogenation commenced, that is, the normal 20hr modification and the 1hr washing was by-passed. This experiment resulted in an increase in the catalytic activity compared with the unmodified reaction and an e.e was successfully obtained.

TABLE 4.10.10: TIGLIC ACID HYDROGENATION OVER Ni/CAB MODIFIED WITH BINAPHTHYL DERIVATIVES.			
Modifier	No Modifier Molecules Adsorbed $\times 10^{18}$	% Conversion	e.e.
0	/	45.63	/
R-Diamine	0.54	5.40	0
S-Diamine	0.56	0.00	/
R-Diamine	0.83	7.27	3
R-Diamine	1.13	0.00	/
R-Diamine	2.38	11.95	0
S-Diamine	2.92	0.53	3
S-Diamine	3.09	0.00	/
Coads-R	0.09 <sup>a</sup> / 0.00 <sup>b</sup>	2.89	7
Coads-R	0.29 <sup>a</sup> / 1.52 <sup>b</sup>	3.64	3
Coads-S	0.61 <sup>a</sup> / 1.56 <sup>b</sup>	17.28	0

a-Diamine b-Diol

The Ni catalyst proved to be a very unreliable system for hydrogenation of tiglic acid. The % conversions were not reproducible for very similarly modified catalysts, the reactions that had originally proceeded often appearing completely poisoned when repeated. This was not a result of a interconversion of the modifier as the diamine species appears to remain intact, with no by-product formation, once adsorbed on the Ni/Cab.

Co-adsorption of the diol and diamine, with direct adsorption of both, did, on occasion, induce a slight e.e. As the amount of each modifier adsorbed increased, so

did the % conversions, but there was a corresponding decrease in the e.e. Thus the diol, which appeared to be predominantly adsorbed must have hindered the asymmetric reaction sites.

In each of the reactions where enantioselectivity was induced, the opposite enantiomers of the chiral diamine modifier produced opposite enantiomers of the chiral product, that is, the (S)-diamine produced (S)-2-methyl, 2-butanoic acid, and *vice versa* for the (R)-diamine.

Both the C<sub>5</sub> and the C<sub>6</sub> macrocycles, which had previously been analysed for extents of adsorption, were investigated as potential chiral modifiers during the hydrogenation of tiglic acid.

TABLE 4.10.11: TIGLIC ACID HYDROGENATION OVER Pd CATALYSTS MODIFIED WITH UNCHELATED MACROCYCLE.

Catalyst	Modifier	No. Modifier Molecules Adsorbed x10 <sup>18</sup>	% Conversion	e.e.
Pd/Cab	0	/	52.10	/
Pd/Cab	C <sub>6</sub>	0.14	14.92	/
Pd/Cab	C <sub>6</sub>	0.81	6.53	0
Ni/Cab	0	/	45.63	/
Ni/Cab	C <sub>5</sub>	2.05	6.67	0
Ni/Cab	C <sub>5</sub>	0.49	16.59	0
Ni/Cab	C <sub>5</sub>	0.15	6.63	0
Ni/Cab	C <sub>6</sub>	0.19	0.00	/

No e.e. was induced in any of these reactions, the macrocycles again only acting as surface poisons.

In all the prochiral olefin hydrogenations the catalysts were selective for the hydrogenation of the C=C and did not additionally hydrogenate the C=O functionality in either the tiglic acid or its ester derivatives.

3-Coumaranone was investigated for the asymmetric hydrogenation of the prochiral C=O functionality. Figure 4.10.3 shows the reaction scheme.

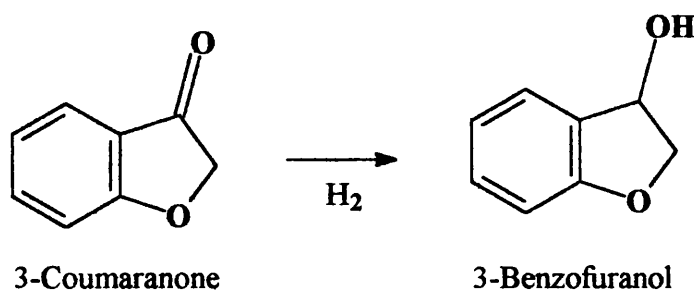


**FIGURE 4.10.3: 3-COUMARANONE HYDROGENATION**

As noted above, neither the Grace silica nor Cab-O-sil nickel catalysts could hydrogenate either methyl tiglate or 4-trifluoro, 2-methyl,2-butenic acid ethyl ester. However, although these catalysts were inactive for alkene hydrogenation with the esters, hydrogenation of the carbonyl group in 3-coumaranone, to form benzofuranol, would be predicted to be more successful since a nickel/silica catalyst system, modified with tartaric acid, has been found to be the best asymmetric catalyst for the hydrogenation of methyl acetoacetate to methyl 3-hydroxy butyrate.<sup>49</sup> The results for the hydrogenation of 3-coumaranone with the unmodified catalysts are reported in table 4.10.12.

Catalyst	% Conversion	% Unknown Product Produced
Pd/Cab	32.23	0.00
Pd/C	6.26	0.00
Ni/Cab	4.75	0.00

In this reaction, all the catalysts were active but the activity of the Pd/C and Ni/Cab was very low resulting in small % conversions after 20 hr of reaction.

Catalyst	Modifier	% Conversion
Ni/C10 <sup>a</sup>	0	0.00
Ni/Cab <sup>b</sup>	0	4.75

a = Reduced in the modification reactor at 450°C, solvent then added followed by transfer to the hydrogenation reactor.

b= Reduced *in situ* in hydrogenation reactor at 450°C for 3 hrs.

The Ni/Cab catalyst, which was reduced and then used for hydrogenation without any possible exposure to the air, showed that the reaction to produce benzofuranol could be catalysed using a nickel system, and it may be concluded that, the Grace silica catalysts are being reoxidised during transfer between reactors, with loss of the active metal sites.

Numerous hydrogenation experiments were carried out using the Pd/Cab catalyst, both the reaction temperature and modifier being varied. See table 4.10.14 for results.

TABLE 4.10.14: 3-COUMARANONE HYDROGENATION OVER Pd/Cab  
MODIFIED WITH BINAPHTHYL DERIVATIVES

Modifier	No. Modifier Molecules Adsorbed x10 <sup>18</sup>	% Conversion	e.e.
None	/	32.23	/
None †	/	2.49	/
R-diol*	0.34	8.61	0
S-diol	0.56	24.03	0
R-diol†	0.79	1.47	0
R-diamine	0.55	1.93	3
S-diamine	0.96	1.33	19
S-diamine*	1.38	2.45	0
R-diamine*	1.97	1.38	6
		4.62 <sup>A</sup>	9 <sup>A</sup>
R-diamine*	0.36	0.92	0
R-diamine	Interconversion occurred	0.00	/
R-diamine	Interconversion occurred	0.92	0
TFAE*	2.83	5.78	0
TFAE	2.79	2.91	0

\*-No washing, †-Reaction at 0°C, A-Reaction after 44 hrs.

The first point to be noted from the results shown in the table, is the steep decrease in the % conversion with the decrease in reaction temperature from ambient to 0°C. This was not unexpected. In addition, any partial poisoning effects by modifier

molecules could decrease the conversion values to such an extent that very few figures could be measured. Hence very few low temperature experiments were performed.

As with the methyl tiglate hydrogenation, the diol molecules act as partial surface poisons to the active hydrogenation sites, lowering the % conversions at both ambient and 0°C, without producing any e.e.

The unwashed R-diol experiment was analysed as having less modifier strongly adsorbed on the surface of the catalyst than the washed S-diol experiment, performed at the same temperature. However, the catalytic activity of the R-diol modified catalyst was lower than the washed S-diol modified system, hence retaining the excess diol modifier molecules in solution during the hydrogenation blocked further reaction sites. Modification with the diamine molecule proved to be more troublesome, due to the tendency of the modifier molecule to interconvert to additional species. In the experiments where direct adsorption did occur, enantiomeric excess was occasionally obtained with both washed and unwashed modified samples. The unwashed R-diamine modified experiment was extended for an additional 24hrs to improve % conversions and the e.e. was noted to increase correspondingly. The maximum e.e. observed was 19% .

In the experiments where a prior interconversion of the chiral diamine had occurred during the modification stage, very little or no hydrogenation occurred and no e.e. was obtained.

Once again the opposite enantiomers of the chiral diamine modifier produced opposite enantiomers of the chiral benzofuranol product. Unfortunately, the individual enantiomeric products could not be assigned a chiral configuration as a standard homochiral form of benzofuranol was not available commercially and could not be

successfully synthesised within the time-scale of the project.

The chiral group of the TFAE modifier was insufficient to enantioselectively direct 3-Coumaranone hydrogenation.

Modifier	No. Modifier Molecules Adsorbed $\times 10^{18}$	% Conversion	E.E
O	/	6.26	/
O <sup>†</sup>	/	0	/
S-diol <sup>**†</sup>	1.01	0	/
S-diamine <sup>**†</sup>	6.72	0	/
S-diamine <sup>*</sup>	8.27	0	/
R-diamine <sup>*</sup>	16.45	1.21	0

\*-No washing, †-Reaction at 0°C

The Pd/C catalyst was active for the hydrogenation of 3-Coumaranone but the reaction was very slow at atmospheric pressure. Owing to this, very few successful results were obtained. Only one modified experiment produced any benzofuranol after 20hrs. In this experiment the catalyst was modified with diamine, without washing. No e.e. was induced. The other reactions, with a lower concentration of adsorbed species, were all unsuccessful and no hydrogenation occurred.

TABLE 4.10.16: 3-COUMARANONE HYDROGENATION OVER Ni/Cab MODIFIED WITH BINAPHTHYL DERIVATIVES.

Modifier	No. of Modifier Molecules Adsorbed x 10 <sup>18</sup>	% Conversion	e.e.
O	/	1.75	/
O <sup>†</sup>	/	0	/
R-diol <sup>*</sup>	0.58	0	/
R-diamine	0.77	0	/
R-diamine <sup>*</sup>	1.05	2.65	0
S-diamine <sup>*</sup>	1.97	0	/
		1.83 <sup>Δ</sup>	0
S-diamine <sup>†*</sup>	2.16	0	/

\* - no wash, † - Reaction carried out at 0°C, Δ- % Conversion after 44 hr

The conversions values for the hydrogenations over Ni/Cab were very low and once again the unmodified reaction at 0°C was so slow, that, after 20hrs, no conversion was recorded. This temperature was thus not investigated any further. After the standard 20hrs of reaction, at ambient temperature, only 1 experiment had successfully recorded any % conversion but with no enantiomeric excess. As a result the next reaction was allowed to proceed beyond the 20hrs and after 44hrs a conversion figure was eventually recorded. This showed that the reaction could proceed but the catalytic activity was very low. No product other than benzofuranol was detected in any reaction.

In the enantio-differentiating hydrogenation of 2-alkanones T.Osawa *et al*<sup>122</sup> reported that the addition of a carboxylic acid to the reaction medium, (TA-NaBr-

MRNi), was an indispensable factor for obtaining high optical yields. 2-Alkanones have only one C=O functionality which limits the polar interactions between the modified catalyst and the substrate. However, upon the addition of a carboxylic acid, the tartaric acid modifier formed an additional complex with this carboxylic acid via hydrogen bonding which was essential to improve the intrinsic enantioselectivity via the additional steric effect from the carboxylic acid. This was an effect only applicable to 2-alkanones. Hence the idea of a possible acid-base enhancement induced by co-adsorption of diol in the presence of diamine was investigated. The 3-Coumaranone hydrogenation results are shown below. In addition, also included are the results from a reaction where acetic acid was added in place of diol.

TABLE 4.10.17: 3-COUMARANONE HYDROGENATION OVER Pd/Cab CO-MODIFIED WITH BINAPHTHYL DERIVATIVES

Modifier	No. Modifier Molecules Adsorbed $\times 10^{18}$		% Conversion	e.e.
	Diamine	Diol		
Coads-R	1.36	-1.70	0	/
Coads-R	3.98	-0.34	0	/
Coads-R	2.68	-1.16	0	/
Coads-S	0.82	0.04	4.47	0
Coads-R <sup>Δ</sup>	1.08	0.00	1.25	7 <sup>A</sup>
Coads-R <sup>⊖</sup>	0.69	3.32	2.28	11 <sup>A</sup>
S-diamine + Acetic Acid	8.19	-1.13	1.54	4 <sup>B</sup>

\*- no wash, A- 1st enantiomer formed, B- 2nd enantiomer formed.

Δ- Surface initially preconditioned with diol before diamine adsorption. No Interconversion.

⊖- Surface initially preconditioned with diamine before diol adsorption. No Interconversion

In the reactions where excess diol was produced from the conversion of diamine via aminol, no hydrogenation of the 3-coumaranone resulted.

In the reactions where the S-enantiomers of both the diol and diamine were directly adsorbed, there was no e.e. Therefore the diol did not successfully enhance the enantioselectivity of the diamine when they were simultaneously coadsorbed.

The two most successful reactions both contained diol and diamine in the reaction medium, but they had each been introduced into the reactor separately during the modification. In the first reaction the catalyst surface was preconditioned with the diol modifier over a 24hr period before the diamine solution of a similar concentration was introduced and the system left for an additional 24hrs. The diamine appeared to displace all the preadsorbed diol. The subsequent hydrogenation of 3-coumaranone with the modified catalyst resulted in an e.e of 7%. No interconversion of the diamine species to form any by-products was apparent.

In the second reaction the reverse modification procedure was followed, the diol being added after the diamine. The diol was adsorbed to a greater extent and displaced around half of the preadsorbed diamine. This diol in no way hindered the reaction and an e.e. of 11% was obtained. It is possible that either the diol interacts with the diamine to enhance the enantioselective sites or, alternatively, it has displaced non-enantioselective diamine molecules that may have been adsorbed in a different orientation and, as such, reduced the number of racemic sites.

Addition of acetic acid with the diamine modifier prevented the production of any hydrogenated by-products but did not stop the production of diol and aminol from the diamine modifier. However, the hydrogenation of 3-coumaranone was still able to proceed and an e.e of 4% was obtained. Interconversion of the diamine to aminol and

diol must proceed favourably under mildly acidic conditions.

Experiments with the alternative modifiers were then undertaken. The washing procedure was omitted and the modifier molecules left in excess in solution.

**TABLE 4.10.18: 3-COUMARANONE HYDROGENATION OVER Pd/Cab MODIFIED WITH THE ALTERNATIVE MODIFIERS**

Modifier	% Conversion	e.e.
O	32.23	/
PhAla <sup>*a</sup>	3.23	10
PhAla <sup>*b</sup>	0.00	/
DMPEA*	0.00	/
His*	0.00	/
Trp*	0.00	/
Pseudoeph*	0.00	/
MTFMPAA*	2.51	0
MTFMPAA*	10.98	0

\* -no washing

a -initial no. of molecules added =  $14.68 \times 10^{18}$

b -initial no. of molecules added =  $34.62 \times 10^{18}$

The majority of the modifiers served only to completely prevent the hydrogenation reactions. Phenylalaninol appeared to be promising with a small e.e. being detected in the first experiment. However, increasing the amount of PhAla added in an attempt to increase the e.e. was unsuccessful and only resulted in poisoning the hydrogenation.

MTFMPAA was the only other modifier where hydrogenation of 3-coumaranone did occur but no e.e. was induced.

As the Pd/Cab catalyst modified with phenylalaninol had shown some enantioselectivity, further experiments using this modifier, and the related diphenyl structure, were carried out.

TABLE 4.10.19 : 3-COUMARANONE HYDROGENATION OVER Pd/CAB MODIFIED WITH THE ALTERNATIVE MODIFIERS.

Modifier*	No. Modifier Molecules Added x10 <sup>18</sup>	% Conversion	e.e.
PhAla	5.86	0	/
PhAla	14.68	3.23	10
PhAla	28.00	3.80	4
PhAla	27.98	0	/
DiPhAla	4.81	0.82	0
DiPhAla	5.01	0.67	0
DiPhAla	18.31	0	/

\* - no wash

Enantioselectivity with the Pd/Cab catalyst modified with phenylalaninol was unpredictable and irreproducible, as the modifier often entirely poisoned the metal sites and prohibited any hydrogenation. If, however, the hydrogenation reaction was able to proceed, enantioselectively was induced. The DiPhAla derivative was not successful. Even in the reactions where there was some catalytic activity, no e.e was produced.

Final hydrogenation studies investigated the hydrogenation of 3-coumaranone with the Pd catalysts modified with the unchelated macrocycles.

TABLE 4.10.20: 3-COUMARANONE OVER Pd CATALYSTS MODIFIED WITH UNCHELATED MACROCYCLE.				
Catalyst	Modifier	No. Modifier Molecules Adsorbed $\times 10^{18}$	% Conversion	e.e.
Pd/Cab	0	/	32.23	/
Pd/Cab	C <sub>5</sub>	0.26	0.00	/
Pd/Cab	C <sub>5</sub>	1.14	4.19	0
Pd/C	0	/	6.26	/
Pd/C	C <sub>6</sub>	0.59	1.23	0

There was no enantiomeric excess in any of the reactions.

#### **4.11: BY-PRODUCT FORMED DURING ESTER**

#### **HYDROGENATIONS.**

Hydrogenation of both methyl tiglate and the fluorinated derivative (4-Trifluoro, 2-methyl, 2-butenic acid ethyl ester) resulted in a by-product detected on the GC trace which always appeared as a single peak (indicative of an achiral material). With methyl tiglate, this product was eluted between the enantiomers and for 4-trifluoro,2-

methyl, 2-butenic acid ethyl ester, the unknown product was eluted after all other identified reactants and products, see table 4.11.1 for the relative retention times and figures 4.11.1 and 4.11.2.

REACTANT	Retention time of unknown by-product (mins)
Methyl Tiglate	13.7
4-Trifluoro,2-methyl, 2-butenic acid ethyl ester	18.7

Achiral GC-MS, see Section 3.10.2, was used in an attempt to identify these unknowns. Transmittance I.R. and Attenuated Total Reflectance (A.T.R.) I.R. were also used in an attempt to identify the nature of the molecules adsorbed on the catalyst surface. However, the spectra obtained from the catalyst surface immediately after hydrogenation were dominated by residual solvent. After drying the catalyst to remove any remaining solvent, no differences in the spectra were detectable between the used catalyst and the blank. The number of molecules adsorbed on the surface may have been too small to detect above the background noise or, alternatively, the species under investigation may have desorbed during removal from the reactor environment.

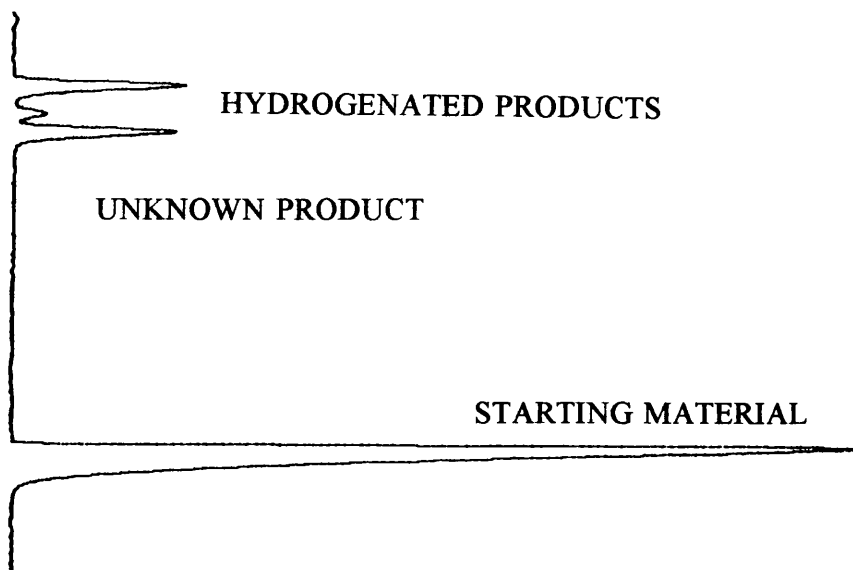


FIGURE 4.11.1: BY-PRODUCT FORMED DURING METHYL TIGLATE HYDROGENATION.

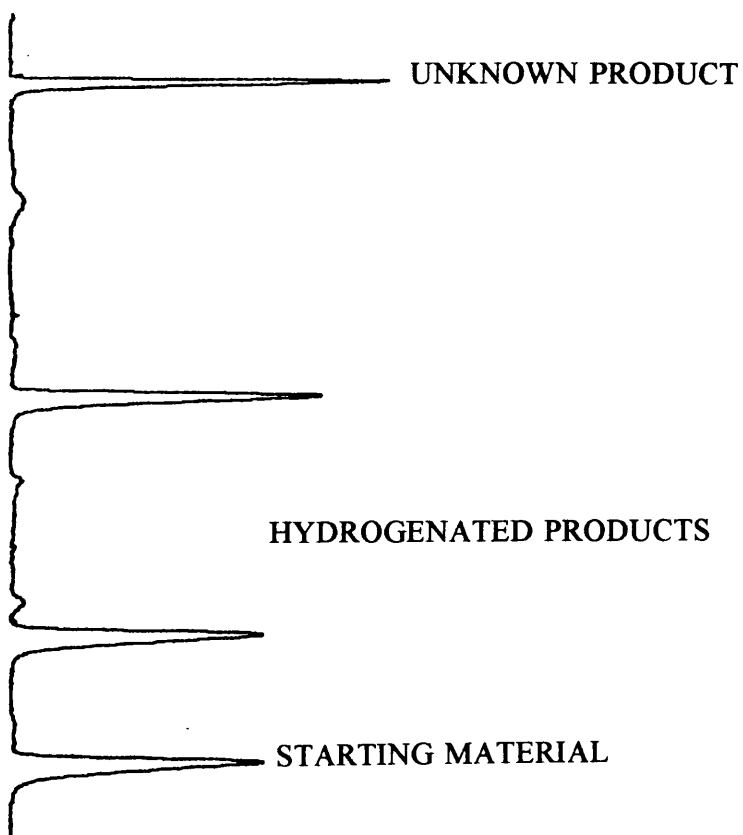


FIGURE 4.11.2: BY-PRODUCT FORMED DURING 4-TRIFLUORO, 2-METHYL 2-BUTENOIC ACID ETHYL ESTER HYDROGENATION.

**CHAPTER FIVE**

**DISCUSSION**

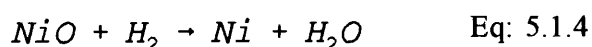
## 5.1:CHARACTERISATION.

### 5.1.1: TEMPERATURE PROGRAMMED REDUCTION.

It is important to have information regarding the reducibility of the metal. This can help to establish the availability of the metal oxide (or metal) on the surface and the extent of interaction with the support. These factors vary with the method of catalyst preparation and have an important part in determining the catalytic activity of the metal oxide-support combination.

Both the Pd/C and the Pd/C30 have two reduction peaks, shown in figures 4.3.1 and 4.3.2. These peaks are attributed to the reduction of PdO and PdO<sub>2</sub>. The single low temperature peak obtained for the 1% Pd/Cab indicates the presence of only a very easily reducible PdO species.

The nickel C10 and C30 catalysts produced very similar reduction profiles: one main peak with a slight shoulder at a higher temperature. The main peak in each case is assigned to the reduction of large nickel oxide<sup>1</sup> particles according to equation 5.1.4:



The overlapping shoulder occurring at slightly higher temperatures in both catalysts indicates the presence of a nickel species that is slightly harder to reduce. This could be either a species with an appreciable interaction with the silica or nickel oxide

present as very small particles which were hard to reduce.<sup>123</sup> XRD work performed at ICI Wilton did not show any evidence of a nickel silicate species within these catalysts.

The TPR profiles for the Ni/Cab catalyst, prepared by precipitation, are shown before and after calcination in figure 4.3.6. Before calcination there are two distinct peaks at 311°C and 347°C indicating the presence of both the hydroxide and the oxidic species. After calcination all the hydroxide had decomposed to leave only a single NiO species. A small, additional high temperature peak is also detected, prior to calcination, at 607°C, which increases slightly in size after the additional air treatment. This compound is stable and remains unreduced at the activation temperature of 450°C, indicating a strong association between the metal and support.

During the preparation of catalysts by homogeneous precipitation-deposition, the slow decomposition of urea acts as a source of hydroxyl ions. In the presence of nickel ions these hydroxyls combine to precipitate nickel hydroxide slowly and homogeneously throughout the suspension. Under these conditions the nickel hydroxide can further combine with the silica to form a nickel hydrosilicate complex, which is sufficiently immobile to be resistant to surface coalescence.<sup>124</sup> As early as 1946 de Lange and Visser<sup>125</sup> postulated the occurrence of chemical interactions between silica supports and nickel compounds, with formation of basic silicates, as the main reason for difficult reducibility of silica-supported nickel catalysts. Many later investigations have substantiated this nickel hydrosilicate formation on catalysts prepared by the precipitation technique, though to varying degrees depending on the precipitation conditions, nickel/silica ratio and silica support reactivity.<sup>115</sup> A sheet like

structure of nickel antigorite can be formed by replacing, on one side of the nickel hydroxide, an array of hydroxyl ions by a network of interlinked  $\text{SiO}_4$ -tetrahedra. Thus a layer of antigorite forms an ideal "glue" between the silica support and nickel hydroxide, an ideal foundation for epitaxial attachment of further nickel hydroxide, which fits perfectly on the hydroxide side of the antigorite layer.

During calcination the amount of hydrosilicate formation appeared to increase, due to the increase in size of the high temperature peak. This is in agreement with other supported catalyst systems, such as alumina<sup>126</sup>, where calcination promotes the formation of an interaction between the support and the catalyst precursor, but is in contrast to the work of Richardson and Dubus<sup>115</sup>, who reported no significant alteration of the hydrosilicate during the air treatment.

Thus, the homogeneous precipitation-deposition method used for the preparation of Ni/Cab-O-Sil catalyst used in this work has led to the partial formation of a nickel hydrosilicate layer. As a result, the reduction of the catalyst in hydrogen tends to be incomplete at 450°C.

### 5.1.2: CHEMISORPTION STUDIES.

Section 4.3.3 shows the average % dispersion values obtained from both CO and O<sub>2</sub> chemisorption experiments. To obtain particle sizes from dispersion data, assumptions must be made concerning particle shape, that is, it was assumed that the supported metal particles were spheres of equal diameter (d). The dispersion of a metal (D) varies as the reciprocal of the average particle size, and as such the larger the value of D the smaller the average particle size<sup>127</sup>, equation 5.1.5:-

$$\% \text{ Dispersion} = \frac{A \times 6}{\rho \times S_a \times N_a \times d} \times 100 \quad \text{Eq: 5.1.5}$$

where

- A = atomic weight
- $\rho$  = density of metal
- $S_a$  = average surface area occupied by 1 active atom
- $N_a$  = Avogadro's number
- d = average particle diameter

This equation is identical to that used by Smith, Thrower and Vannice.<sup>128</sup> It is equally valid for cubic particles with edges of length d. Hence for each metal:

Metal	Ni	Pd
A (a.m.u.)	58.69	106.42
$\rho$ (g nm <sup>-3</sup> )	$8.90 \times 10^{-21}$	$12.02 \times 10^{-21}$
$S_a$ (nm <sup>2</sup> )	0.0651	0.0806
d (nm)	101/D	109/D

Table 5.1.1 shows the average particle diameters thus calculated.

TABLE 5.1.1: AVERAGE PARTICLE SIZES FROM CHEMISORPTION	
Catalyst	Average Particle Diameter (nm)
Ni/C10	184
Ni/C30	94
Ni/Cab	5
Pd/C30	12
Pd/Cab	16
Pd/C	10

For the Ni/Grace silica catalysts, prepared by wet impregnation, such large crystallite sizes and low dispersion values would not normally be of much use in most catalytic processes, however asymmetric catalysis has been shown to be very effective on large crystallites<sup>129</sup> and as such these catalysts may be very useful.

Chemisorption provides only a measure of the mean particle diameter and does not differentiate between large and small particle sizes. Preparation of catalysts by impregnation can lead to inhomogeneous crystallite sizes generally due to the porous structure of the support, with the resultant uneven distribution of nickel precursor. This can lead to a poor nickel dispersion and a broad crystallite size distribution in the reduced catalyst. This range of sizes can change the activity and selectivity in

subsequent reactions such as enantioselective hydrogenation. Thus, preparation of catalysts with a narrow crystallite size distribution is an important consideration and catalysts prepared by homogeneous precipitation/deposition exhibit such a uniform dispersion of nickel particles. Thus, the Ni/Cab-O-Sil catalyst had a more homogeneous dispersion of precipitate over the support with a narrow crystallite size distribution. These smaller metal particles were highly dispersed and were more resistant to coalescence due to the additional hydrosilicate layer.

When compared against the TEM values for average particle sizes in Section 4.3.4, it can be seen that there was fairly good agreement, in most cases, between the figures calculated by selective chemisorption and electron microscopy. TEM, although providing a direct size measurement and additional information on particle shape, texture and size distribution, can miss very small particles, which would explain the slightly larger average particle size values determined by this technique.

## **5.2: ADSORPTION STUDIES.**

The structure of the binaphthyl molecule is relatively simple when compared against many of the other modifier species discussed in Section 1.4.2. The rotation about the C(1)-C'(1)  $\sigma$ -bond in this molecule and its derivatives is sufficiently hindered that optical isomers can be separated<sup>130</sup> and it is this steric hinderance induced by the substituents in the 2,2' positions that is responsible for the axial chirality. Racemisation could occur through a *syn* inversion path with close contacts of the 2,2' substituents or an *anti* process in which the positions 2,8' and 2',8 must pass each other and would appear less hindered, figure 5.2.1.

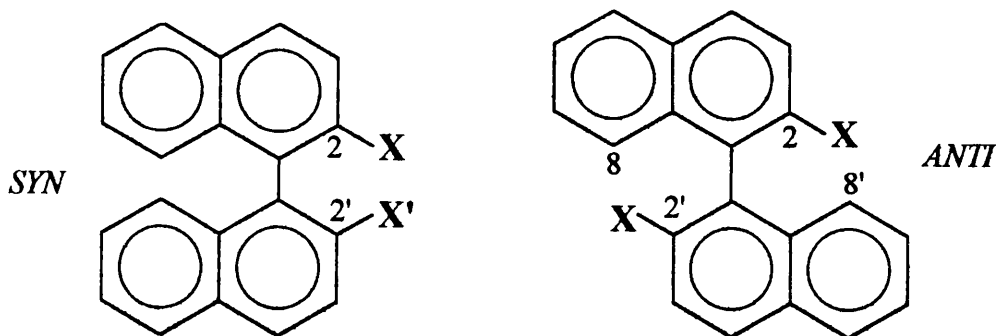


FIGURE 5.2.1: RACEMISATION PATHS OF BINAPHTHYL MOLECULES

However, polarimeter studies showed that  $-OH$ ,  $-NH_2$  are both sufficiently large substituents to prohibit any racemisation. Thus, the simple axial chirality and rigidity of the naphthalene ring systems meant that binaphthyls are very interesting potential new modifier molecules for asymmetric hydrogenation studies, which could be used to provide an insight into the necessary requirements for asymmetric induction.

The Pd/C, Pd/C30, Ni/C30 and Ni/C10 catalysts have all been shown to adsorb the diol and diamine modifier species, to varying extents. Only the Pd/C was able to adsorb the dimethoxy modifier. In the experiments where modifier species were adsorbed on to the catalyst species, the amount adsorbed gradually built up to a plateau level. This final level did not simply represent a saturated, monolayer coverage of modifier species on the metal phase, as the final amount adsorbed varied with the initial amount of modifier present in solution and very often exceeded the number of modifier molecules predicted for adsorption of up to a monolayer. Thus this final adsorption figure would appear to be an equilibrium value, with a steady state being established between adsorption and desorption, where some modifier was retained in

solution. Even when the initial modifier solution contained fewer modifier molecules than predicted for monolayer coverage, complete adsorption from solution did not occur, with some modifier species always detected in the resultant modifier solution.

The binaphthyl molecules could have adsorbed in two different modes. The adsorption could occur with a naphthyl unit parallel to the surface (horizontal mode) resulting in an interaction between the aromatic  $\pi$ -system and the catalyst surface. This type of interaction has been previously noted for the adsorption of benzene on palladium films.<sup>131</sup> Alternatively the adsorption could occur by dissociation of H from the -OH or NH<sub>2</sub> groups (near vertical mode), such as is the case for example, of the adsorption of formic acid on nickel/iron alloy surfaces.<sup>132</sup>

Basic molecular modelling, Section 4.4.1, was used to show that each binaphthyl could possibly obscure between 5 and 10 surface metal atoms, depending on the nature of the metal and the mode of adsorption. This implies that, for a single overlayer of adsorbed modifier species, close packed on the surface of the metal component of the catalysts, the maximum possible ratio of molecules adsorbed per surface metal atom would have been approximately 0.2.

For the Pd/C30, Ni/C30 and Ni/C10 the amount of diol modifier adsorbed exceeded the predicted monolayer coverage. From the washing experiments it was clear that, even though a small amount of diol modifier was desorbed, the majority of the adsorbed species were strongly bound to the catalyst. This indicates that the excess of diol was not physically adsorbed as weakly bound multilayers on top of the initial strongly chemisorbed monolayer. The blank silica supports were shown to be unable to independently adsorb any modifier species, however, as explained in Section 1.1, any support that does not chemically adsorb a reactant in the absence of a metal

cannot be assumed to still not adsorb the reactant when the metal is present. Surfaces can behave very differently when they are part of a composite catalyst and as such, the combined system can supply a greater adsorption area than the individual components were able to provide. Therefore, taking all the diol adsorption results into account, it is proposed that the diol modifier molecules adsorb on to the metal surface and very quickly achieve the 0.2 ratio value, corresponding to an entire single layer coverage of packed modifier molecules. Further molecules may then surface-diffuse or "spillover" at the edges of the metal clusters to form a chemisorbed species on the support itself, where they were retained as a strongly adsorbed species. This presence of additional modifier species retained on the support may be beneficial for subsequent hydrogenation studies. The reservoir of spillover species could act to replenish the metal surface with fresh modifier if any diol was lost to the reaction solution during hydrogenation, via a reverse spillover process. Although the spillover of molecular species was briefly discussed in Section 1.1, there has been no evidence reported for the spillover of molecules as large as the binaphthyl fragments.

The small fraction of modifier which was easily washed off is attributed to minimal amounts of diol that are weakly associated with the catalyst, either physically adsorbed on the chemisorbed layer or chemisorbed species with a very low heat of adsorption.

Comparison of ratio figures (the ratio of the number of modifier molecules adsorbed per surface metal atom) for the nickel catalysts, suggests that the Ni/C10 system, with fewer surface metal atoms and a smaller pore size, adsorbed the diol to a greater extent than the Ni/C30 catalyst under comparable conditions, an effect predominant at higher concentrations of modifier solutions. This may be due to the

greater surface area of the silica C10, see table 5.2.1, which can provide a much larger area on which spillover can occur.

<b>TABLE 5.2.1: CHARACTERISTICS OF NICKEL/ GRACE SILICA CATALYSTS</b>				
<b>Catalyst</b>	<b>No. Diol Molecules Adsorbed <math>\times 10^{18}</math></b>	<b>No. Surface Metal Atoms <math>\times 10^{18}</math></b>	<b>Average Pore Diameter (<math>\text{\AA}</math>)</b>	<b>Surface Area (<math>\text{m}^2/\text{g}</math>)</b>
Ni/-C10	3.56	5.19	99	307
Ni/-C30	2.42	9.24	315	106

From the diamine adsorption figures, the amounts adsorbed appeared to be limited to monolayer coverage on the metal. Hence the presence of the amine grouping in the molecule was insufficient for spillover to occur and, therefore, such a mechanism would appear to require the presence of hydroxyl substituents within the molecule. No evidence of spillover of amines was found from the literature and indeed the molecular species that were reported to be able to spillover were all adsorbed through an oxygen substituent, as shown by detailed infrared studies.<sup>12,13</sup>

The three Grace silica-supported systems were unable to adsorb the dimethoxy modifier and were also unable to adsorb naphthalene itself.<sup>133</sup> Thus, adsorption on the metal phase cannot have occurred through the aromatic ring systems. As the dimethoxy, diamine and diol molecules are very similar in shape, the only difference arising from the relative sizes of the substituents, this is thought to be mainly a steric effect. The chiral twist of the binaphthyl molecule to alleviate steric overcrowding between naphthyl units is more than sufficient to prevent a near planar adsorption of

one or more of the naphthyl ring units. An alternative adsorption through a lone pair interaction on the substituent grouping with the metal surface would have been much weaker in nature and modifier species would have been relatively easily desorbed. Hence it is proposed that adsorption of the diol and diamine on to the active metal sites may occur via dissociation of one or more of the O-H or N-H substituent bonds to result in the molecule strongly adsorbed in a near vertical mode, with the chiral twist of the aromatic systems directed up and away from the surface, figure 5.2.2. This mode of adsorption would create an adlayer that would appear chiral to molecules approaching from the fluid phase. The dimethoxy was not adsorbed in this way as the adsorption was not sufficiently energetic to dissociate the O-CH<sub>3</sub> substituent bond. Each of the substituent groups, -OH, -NH<sub>2</sub> and -OCH<sub>3</sub>, would have activated the aromatic systems through inductive effects. Hence the lack of adsorption of the dimethoxy modifier cannot be attributed to a deactivation of the naphthyl rings due to electron withdrawing substituents, decreasing the electron density available to  $\pi$ -bond with the surface. From the available evidence it is concluded that adsorption of binaphthyl modifiers on the Grace silica-supported catalysts, the aromatic rings played no direct part in the metal-modifier interaction.

Reduction of the catalysts in deuterium instead of dihydrogen was used in an attempt to investigate the possibility of -OH, -OD exchange at the substituent group. However, both NMR and mass spectroscopic analysis of the resultant modifier solutions were inconclusive. The experiment may have been more informative if deuterated THF had also been used as the solvent, as THF could act as a source of hydrogen in the presence of a catalyst, which would further limit the possible amount of -OD species present.

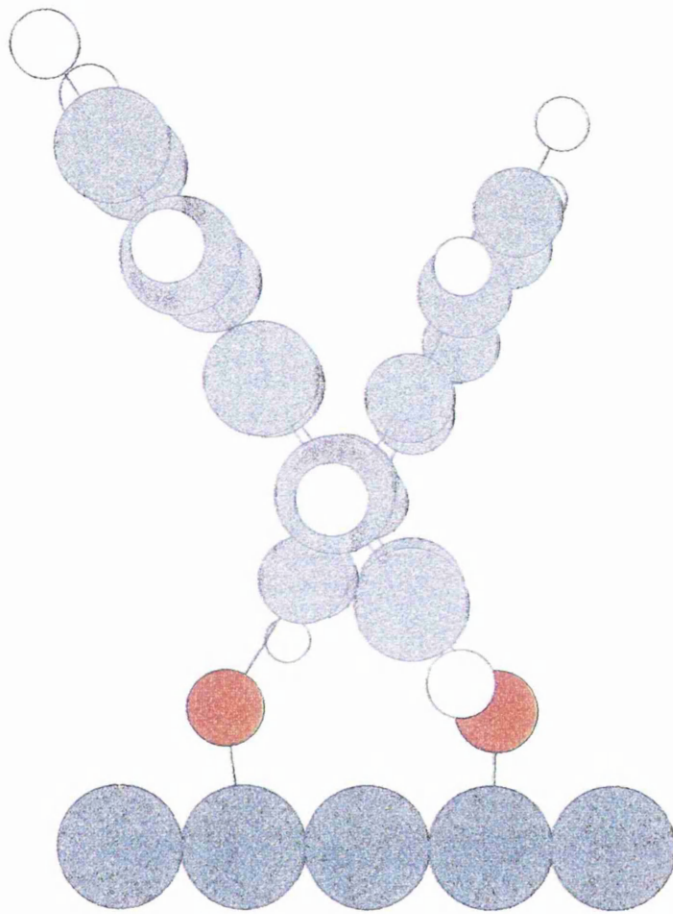


FIGURE 5.2.2: VERTICAL MODE OF ADSORPTION

Although it was not clear from the experimental evidence whether or not the modifiers adsorb through dissociation of both substituents or just one, by considering the relative sizes of the metal atoms compared with the distance between each of the substituent arms, it would appear that adsorption through one substituent will hold the second grouping very close to the metal surface, where a secondary dissociative adsorption would have been expected to occur. Use of spacefilling models shows that a geminal adsorption of both substituents could occur simultaneously on a metal atom. Further work with the adsorption of a binaphthyl derivative such as  $X = X' = -NH(CH_3)$  would be required to define whether only one N-H was cleaved during adsorption of the diamine modifier or both hydrogens were lost.

Adsorption of diol on Pd/C was found to exceed the predicted monolayer coverage of the metal. However, with this modifier-catalyst system, the amounts desorbed were more substantial, such that, often only a residual monolayer equivalent was retained. In addition, the carbon support was also able to adsorb the diol species. Therefore, it is concluded that the palladium crystallites were able to strongly adsorb a monolayer of diol species which is retained even after desorption experiments at elevated temperatures. The excess amounts adsorbed by the catalyst can be attributed to direct adsorption on the carbon support. This adsorption on the support was much weaker in nature than adsorption on the metal or the spillover adsorption that occurred on the Grace silica supports.

From the adsorption and desorption results, adsorption of the dimethoxy modifier is purely a weak interaction with the support. The amount of dimethoxy adsorbed on the blank carbon support was equivalent to the amount of diol adsorbed in a similar experiment. Hence with the carbon system, adsorption can also occur onto the support

itself, independent of the metal, to result in a species weakly bound to the support by adsorption via the aromatic rings, horizontal mode, figure 5.2.3, and as such, all the binaphthyl modifiers were able to adsorb on this system. This is in agreement with existing results which have shown the adsorption of anthracene and naphthalene on the carbon support.<sup>133</sup>

For Pd/C the adsorption of diamine vastly exceeded that of the diol and dimethoxy and the fraction of diamine desorbed within the 1 hr wash was minimal, even with larger concentrations of starting material and initial amounts adsorbed. This may be the result of an acid-base interaction between the acidic groups on the support surface, Section 4.2, and the amine substituents on the modifier, and must be a fairly strong interaction to maintain the adsorption during washing; in contrast to the diol and dimethoxy modifiers which were easily desorbed.

The hydroxymethoxy modifier was introduced in an attempt to understand more about the mode of adsorption of the diol species. This modifier had one -OH and one -OCH<sub>3</sub>, and as such could only adsorb through dissociation of the single -OH substituent, assuming that the mode of adsorption was the same as for the diol. When compared against the adsorption of diol and diamine modifier, of similar initial concentrations, on the Ni/C30 and Ni/C10, the hydroxymethoxy was adsorbed to a much lesser extent than the diol, and slightly less than the diamine. Hence it is possible that the hydroxymethoxy modifier is unable to adsorb as strongly, and pack as tightly on the metal surface, as it can only adsorb through one substituent group. This would result in a single pivotal bond, anchoring the modifier to the catalyst surface, around which the bulky binaphthalene grouping could then rotate, hindering

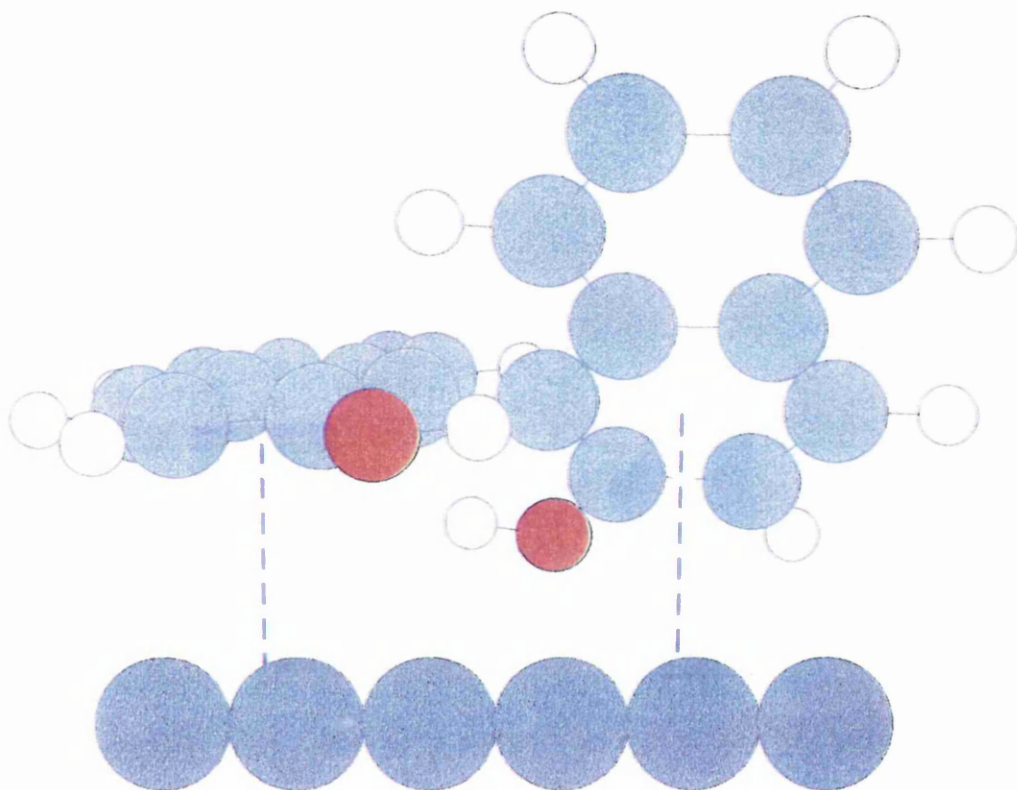
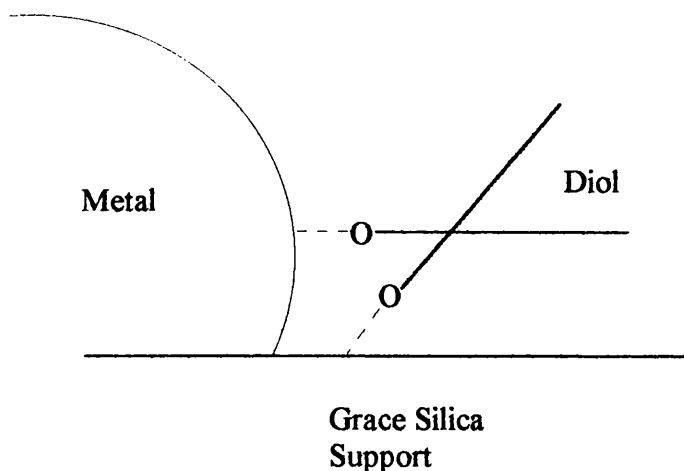


FIGURE 5.2.3: HORIZONTAL MODE OF ADSORPTION

the further adsorption of additional modifier molecules within a close proximity. Alternatively, adsorption of the diol and diamine, through a simultaneous dissociative adsorption of both substituents, would maintain the modifier in a more rigid conformation on the metal surface, permitting a more ordered and close packing of molecules. This is in agreement with the modelling experiments previously discussed. The adsorption of the hydroxymethoxy on the Pd/C catalyst was also less than the amount of diol adsorbed. Therefore, in addition to a similar adsorption through the aromatic rings on the carbon support, the hydroxymethoxy adsorbs less on the palladium metal than the diol.

No spillover of the hydroxymethoxy molecule was observed for Ni/C30 or Ni/C10 and it would thus appear that the spillover mechanism requires two hydroxyl substituents, possibly via a bridging species that can simultaneously adsorb on the support and metal phases, figure 5.2.4.



**FIGURE 5.2.4: BRIDGING BINAPHTHOL SPILLOVER SPECIES**

Co-adsorption experiments did not provide conclusive evidence as to the extent of competitive adsorption of the diol and diamine. In most cases with the Pd/C30, Ni/C30

and Ni/C10 catalysts, it appeared that the diol was initially preferentially adsorbed, with diamine adsorption occurring later. Figure 4.4.12 shows a clear example of this. On addition of both modifiers to the freshly reduced catalyst surface, initial adsorption of both modifiers occurred until the surface coverage reached  $\sim 0.5$ . At this stage the diol appeared to be preferentially adsorbed and partially displaced the diamine. This preference is thought to be the result of adsorption at spillover sites, whereby the diol can access more of the support surface than the diamine. The diamine adsorption was suppressed until the diol appeared to have almost reached its equilibrium value. At this point spillover was thought to have attained its maximum value, and further adsorption of both modifiers was occurring on the available surface metal sites, where an equilibrium was then established between adsorption and desorption. Thus, disregarding spillover, direct adsorption on the metal surface of either modifiers did not appear to favour either species.

For the Pd/C catalyst the initial effects were again reversed, with the diamine always preferentially adsorbed over the diol due to the acidic nature of the support surface. Sequential co-adsorption of the diamine followed by the diol, showed that the introduction of the diol species to the catalyst already modified with diamine temporarily desorbed a small percentage of the diamine species, possibly that weakly adsorbed on the metal surface. This small amount was however, re-adsorbed over a period of time. The final total number of modifier species adsorbed remained constant but fluctuated between the individual amounts of diol and diamine as, when one species was desorbed from the metal surface, either species could be adsorbed.

The tetraol molecule was initially considered as a possible modifier molecule as the additional hydroxyl substituents in the 7,7' positions would maximise the chirality

of the binaphthyl molecule due to increased steric repulsion and these additional substituents could also play an important role in the asymmetric induction during hydrogenation. During adsorption studies it was found that the tetraol was adsorbed to a much lesser extent than the diol on each of the Ni/C30, Ni/C10 and Pd/C catalysts and that this adsorption occurred very rapidly. Knowing that the diol was dissociatively adsorbed via both the hydroxy substituents, it is safe to assume that adsorption of tetraol on the metal surface of the catalysts was likely to arise through all four -OH groupings, to result in the molecule being held in, as near as possible, a planar *syn* or *anti* mode. The 7,7' substituents served only to lock the binaphthyl molecules down on the surface with the naphthalene rings in a near parallel orientation. Such a mode of adsorption blocked many metal sites and reduced the packing efficiency of the binaphthyl molecules, thereby reducing the amounts of modifier adsorbed. With the molecule adsorbed through all four substituent groups no spillover on either nickel catalyst had ensued, as the modifier was unable to achieve the correct orientation for spillover to occur.

It was at this stage, having encountered the adsorption reproducibility problems with the diamine and co-adsorption studies, that the ageing of the Pd/C30 catalyst was realised. As explained in Section 4.8, the available active metal area had diminished over a period of time. This effect was unique to the palladium metal and the Grace silica support and is an effect of the active support surface structure. Figure 4.2.1 shows how the strained three-membered siloxane rings present in this silica are able to interconvert with vicinal silanol groups. Expanding the siloxane ring size by incorporating palladium oxide would act to lower the ring strain, figure 5.2.5.

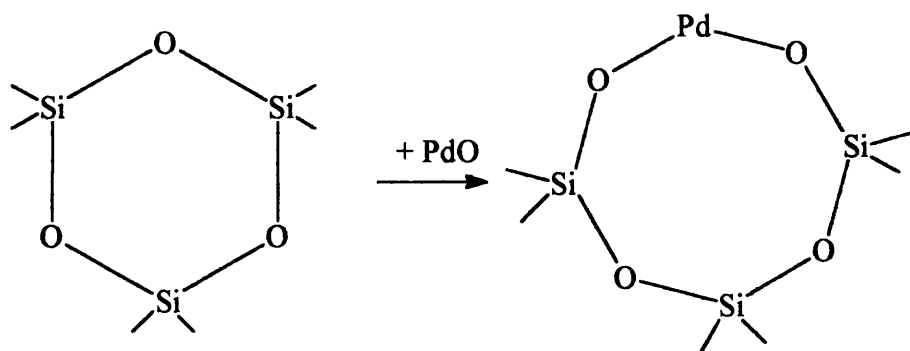


FIGURE 5.2.5: STRAIN RELEASE IN THREE-MEMBERED SILOXANE RING

Consequently, if the palladium has become involved in the surface support structure, it is no longer available for catalytic reaction. The nickel catalyst did not age in a similar manner for a number of possible reasons; the lesser mobility of nickel compared with palladium, incorrect energetics for incorporation of a nickel oxide species or the much larger crystallites may have prevented a similar inclusion. Thus only the small palladium crystallites were able to induce a partial restructuring of the silica support surface. The variation in the number of available surface metal atoms for Pd/C30 meant that a quantitative study of the amounts adsorbed, as well as the subsequent catalytic activity, would have been inconsistent and unconvincing. In addition, the irreproducibility of the reduction of both the nickel catalysts in the hydrogenation reactor meant that all the catalysts supported on Grace silica were abandoned for further studies.

Both the Pd/Cab and Ni/Cab catalysts, were able to adsorb the diol and diamine modifiers and not the dimethoxy, which indicated that the same mode of adsorption, as predicted for Pd/C30, Ni/C30 and Ni/C10, due to dissociation of the O-H or N-H

bonds, occurred on the metal phase. For Pd/Cab the amounts adsorbed of both the diol and diamine did not exceed the amount required for monolayer coverage on the metal, hence spillover of the diol species did not appear to occur on this catalyst. This result is in agreement with that of Gladden et al<sup>134</sup>, who found that strained siloxane rings could act as spillover sites in silica-supported catalysts such as Ni/C10, Ni/C30 and Pd/C30. However, in the absence of such strained rings, in a silica support such as Cab-O-Sil, NMR showed only the presence of silanol species with no additional spillover hydrogen. This work shows that different processing techniques can affect the proportion of spillover sites in a catalyst system. Thus, a support can be selected to optimise or minimise the number of spillover sites depending on the nature of the catalytic application.

For the Ni/Cab catalyst the amounts adsorbed of each modifier gave very low adsorbed modifier molecule to surface metal atom ratio values. This was attributed to the very small particles, highly dispersed over the support and the additional nickel hydrosilicate layer, both a result of the preparation technique. The large bulky binaphthyl groups were unable to pack as efficiently on the smaller metal particles as compared to the larger, more planar crystallites of Ni/Grace silica. In addition the extra 'glue' layer may have inhibited adsorption. Once again spillover of the diol species on to the Cab-O-sil support or the hydrosilicate layer did not occur.

In conclusion, adsorption of the diol and diamine modifiers is now thought to occur on the metal components of each catalyst through a dissociative adsorption of hydrogen at both substituents, to hold the binaphthyl species in a near vertical mode. Adsorption via the naphthalene ring system does not create the active species in this work. Whilst these adsorption studies cannot be claimed to have unequivocally defined

the nature of the adsorbed chiral adlayer, they have provided a clear picture as to the possible mode of adsorption and extent of coverage of the catalyst surface, which is invaluable as part of any explanation of asymmetric hydrogenation.

### 5.3: ADSORPTION BY-PRODUCTS

Adsorption of the diamine modifier on to the Pd/Cab catalysts could occasionally facilitate an interconversion of this molecule to other related species. This interconversion was not found to occur on any of the other catalysts, Section 4.5. Figure 5.3.1 shows all the various products which were obtained from the original diamine modifier.

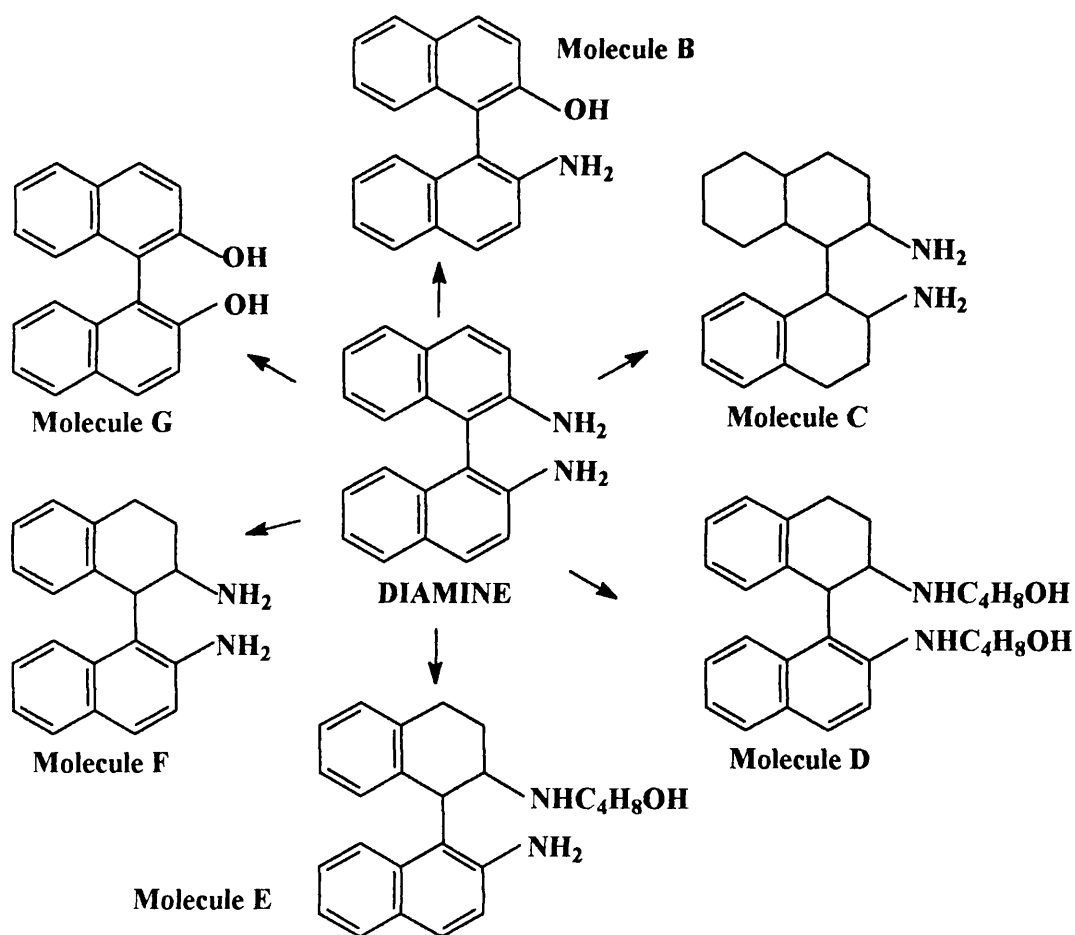


FIGURE 5.3.1: DIAMINE INTERCONVERSION PRODUCTS.

These results showed that over a period of time ring hydrogenation can occur around the naphthalene ring systems to varying extents before the modified molecules desorb and are detected in solution. Hence the Pd/Cab must activate this ring addition process compared against the other systems, where no such reaction was apparent and the presence of surface hydrogen would appear to be a likely prerequisite to this reaction.

Naphthols can be synthesised from naphthyl amines by direct hydrolysis under acidic conditions, a reaction that does not work for benzene derivatives, figure 5.3.2.

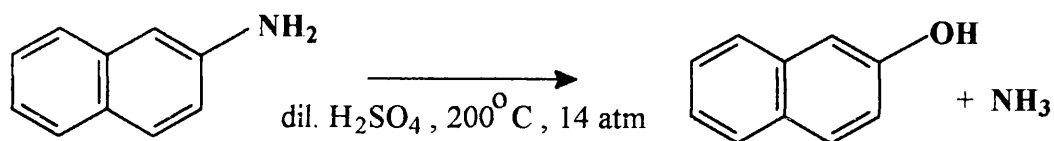


FIGURE 5.3.2: NAPHTHOL FORMATION

The conditions required for this reaction were very severe with high temperatures, high pressures and an acidic medium. Thus interconversion of diamine stepwise via aminol to diol may proceed over the Pd/Cab catalyst which lowered the energetics necessary for the reaction to occur. When acidic conditions are increased, such as during the coadsorption studies with the diol, interconversion was enhanced and ring hydrogenation was quenched.

There was also a very definite interaction between the THF solvent and the diamine molecules, showing that the solvent must have a distinct adsorption interaction with the catalyst surface. If these secondary amines were still retained, adsorbed onto the catalyst as modifiers, the alkyl chain could cause severe steric hinderance to any possible asymmetric hydrogenation or, in an extreme case, the

alcohol group could completely alter the mode of adsorption of the binaphthalene group by preferential adsorption via the hydroxyl group. This highlights the importance of solvent choice in asymmetric hydrogenation.

#### **5.4: COLOURATION OF MODIFIER SOLUTIONS**

During the adsorption studies with the diol modifier, a colour was often noted to develop in the modifier solution. This occurred within all the silica-supported systems (predominately the Grace silica but also the Cab-O-Sil systems) but not in the Pd/carbon system.

Use of UV-Vis spectroscopy to analyse this resultant colouration gave palladium spectra which had three clear peaks, indicative of a  $d^8$  species. For such a  $Pd^{2+}$  species the majority of compounds are four co-ordinate and square planar. From the literature<sup>135</sup> there are three allowed d-d transitions corresponding to transitions from the three lower lying d levels to the empty  $d_{x^2-y^2}$  orbital.

Similarly, with the Ni catalysts, three absorption bands arose, again indicative of a  $d^8$  species which is  $Ni^{2+}$ . Such  $Ni^{2+}$  compounds are often six or four co-ordinate. However, the yellow colouration and the absence of any electronic transitions below  $10000\text{cm}^{-1}$  ( $>1000\text{nm}$ ) may suggest a square planar complex.

The presence of unreduced metal in the catalyst samples, which was chelated out into solution, required the presence of ligands or counterions. Infrared spectra of the binaphthol were recorded before and after the modification to investigate any variation

in the O-H stretching mode. The solutions were initially directly analysed in a liquid cell but the absorption bands arising from the T.H.F. swamped the spectra. The samples were then heated to dryness to remove all the solvent, and the remaining powder was then analysed as a nujol mull and a KBr disc, however any changes were again unnoticeable as the bulk of the binaphthol remaining in solution was not expected to have been altered, as it had already been shown that there was only small amounts of metal ions in solution. Much higher and lower concentrations of binaphthol solutions were then investigated to respectively try and maximise the counterion concentration, or minimise the bulk unadsorbed binaphthol but once again these experiments both failed to produce any identifiable variation between the initial and final infrared spectra.

In conclusion the diol modifier appeared to slightly corrode the metal catalysts. As there was no similar effect from the basic diamine modifier, this may have been an acidic effect induced by the diol. The colours that appeared were due to a small amount of metal ions being taken into solution, and were a consequence of internal electronic transitions. It definitely did not arise from a silica impurity. As the amounts of these ions was so microscopic any possible side reaction initiated by them would have required an immensely fast turnover rate to compete in any way with the hydrogenation reactions, and as such this may eliminate their importance. However, after washing there was no further colouration in the modifier solutions, and as such only modifier species adsorbed on the heterogeneous surface were able to act as the chiral catalytic site.

## 5.5: ASYMMETRIC HYDROGENATION.

### 5.5.1: ASYMMETRIC HYDROGENATION WITH MODIFIED CATALYSTS.

As the % conversions for all the reactions over the binaphthalene modified catalysts, either with or without resultant enantioselectivity, are substantially reduced, the binaphthyl molecules must be quite close-packed to preclude such a proportion of active metal sites. These binaphthyl molecules would have packed so as to minimise the surface energetics. No substantial amount of modifier is displaced by any of the substrates during hydrogenation reactions, which reinforces the proposed mode of adsorption of both the diol and diamine modifiers through dissociative chemisorption to form a strongly adsorbed chiral adlayer.

#### 5.5.1.1: PROCHIRAL C=C HYDROGENATION

The initial investigation of the hydrogenation of methyl tiglate over the catalysts modified with binaphthyl derivatives, did not produced any enantiomeric excess. Similar attempts by Tungler *et al*<sup>136</sup> to hydrogenate dimethyl itaconate, a prochiral unsaturated carboxylic ester, over Pd/carbon catalysts modified with a range of chiral modifiers, such as (S)-proline, also met with no enantioselectivity. The binaphthyl modifiers act only as surface poisons and reduce the % conversions. The catalysts are however, totally selective for the hydrogenation of C=C and did not further reduce the carbonyl bond. This regioselectivity is also true for the reduction of tiglic acid but on occasion stereoselectivity is also implemented on this substrate. This shows that the presence of the acid grouping in the reactant was essential for asymmetric induction. Experimentally, no optical yields were achieved with catalysts modified with diol. Only the diamine modifier is successful at inducing enantioselectivity and as such the amine grouping must also be mandatory for asymmetric hydrogenation with binaphthyl

modified catalysts.

As the binaphthyl modifiers were predicted to pack closely, thereby reducing the amount of free surface area, the tiglic acid molecules that are adsorbed in the near vicinity of the modifier species, are adsorbed on the unmodified active surface metal sites, via a dissociation of the acidic proton, in a vertical orientation which results in some extent of delocalisation extended throughout the reactant structure. After the primary mode of adsorption is established, this molecule then migrates to reach the lowest energy conformation possible. Stabilisation can be achieved by interaction with the binaphthyl modifier at two recognition sites, through a combination of a  $\pi$ - $\pi$  stacking interaction and hydrogen bonding, to form a co-adsorbed species. The  $\pi$ -system of the tiglic acid is aligned over one naphthalene ring to allow a  $\pi$ - $\pi$  stacking interaction to occur, binding the reactant to the modifier. An optimum interaction results when the cofacial arrangement is off-set, such that the relative atoms of each molecule are not aligned.<sup>137</sup> Substituents such as the amine and the hydroxy would have both activated the naphthalene ring systems, improving the strength of such  $\pi$ - $\pi$  interactions. In addition, with the prochiral substrate in the correct orientation, an additional hydrogen bonding interaction can be established between the substituent of the modifier and the C-O of the tiglic acid to further stabilise the reactant, as shown in figures 5.5.1. and 5.5.2. Figure 5.5.3 shows the other possible cofacial arrangement, where the substrate has interacted with the  $\pi$ -system of the modifier via the opposite prochiral face, and in this orientation cannot achieve the necessary additional hydrogen bonding interaction with the diamine modifier substituent. Similar interactions are commonly found in systems where binaphthyl molecules are used as chiral recognition agents.<sup>138,139</sup> The steric influence thus only establishes the specific orientation of the

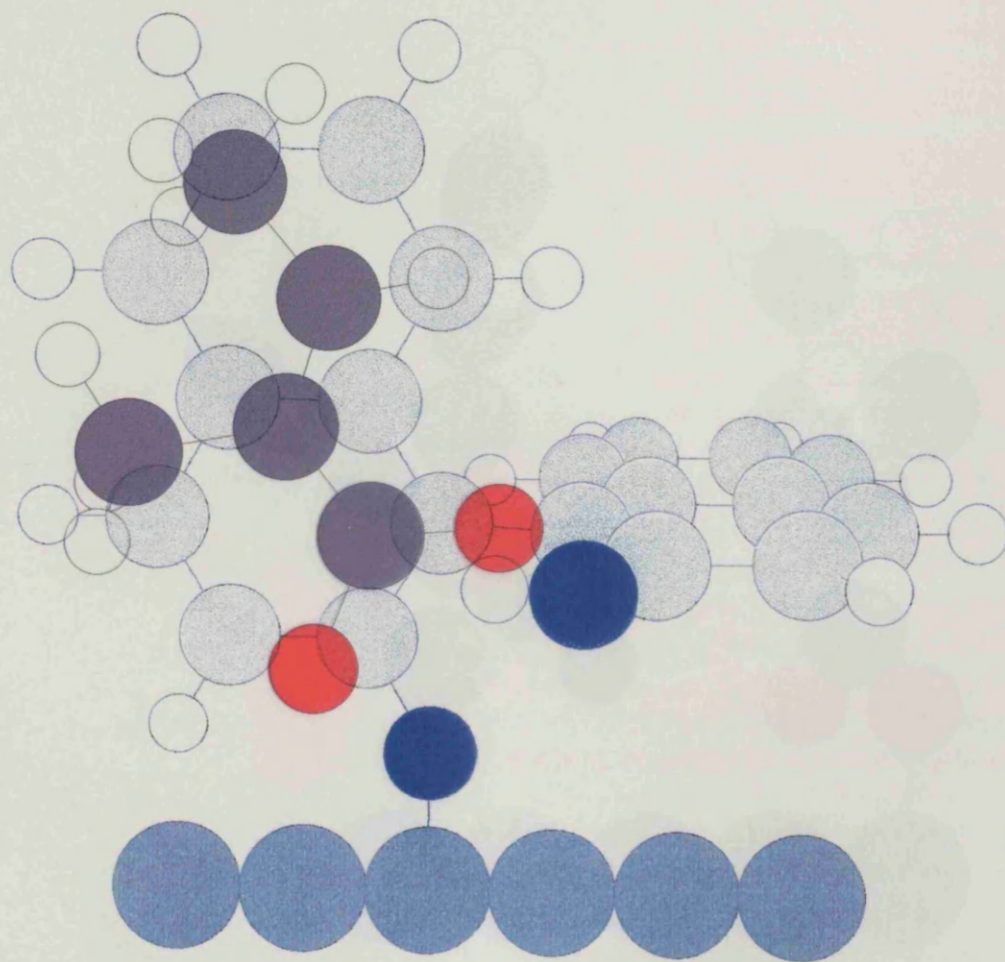
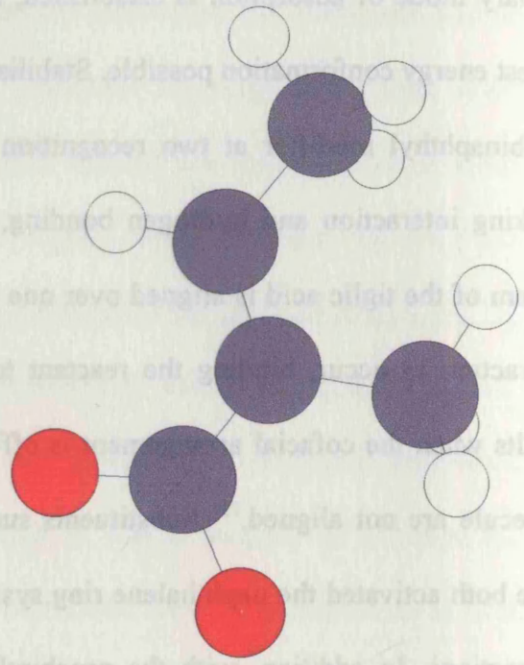


FIGURE 5.5.1: DIAGRAM SHOWING THE  $\pi$ - $\pi$  STACKING AND HYDROGEN BONDING INTERACTIONS BETWEEN TIGLIC ACID AND DIAMINE.

As the bisphthalyl modifiers were predicted to pack closely, thereby reducing the amount of free surface area, the rigid acid molecules that are adsorbed in the near vicinity of the modifier species are adsorbed on the unmodified active surface metal sites, via a dissociation of the acidic proton, in a vertical orientation which results in some extent of delocalization extended throughout the reaction structure. After the primary mode of adsorption is established, the molecule then migrates to reach the lowest energy configuration possible. Stabilization can be achieved by interaction with the bisphthalyl moiety in two locations either through a combination of a  $\pi$ - $\pi$  stacking interaction or through hydrogen bonding to form a co-adsorbed species. The  $\pi$ - $\pi$  stacking system of the rigid acid is arranged over one neighbor to allow a  $\pi$ - $\pi$  stacking interaction with the modifier. An optimum interaction results in such that the relative sizes of each molecule are not aligned.



have both activated the reaction by systems, improving the strength of such  $\pi$ - $\pi$  interactions. In addition, with the product substrate in the correct orientation, an additional hydrogen bonding interaction can be established between the substrate of the modifier and the C-O of the rigid acid to further stabilize the reactant, as shown in figures 2.2.1, and 2.2. Figure 2.2.3 shows the other possible cofacial arrangement where the substrate has interacted with the  $\pi$ -system of the modifier via the opposite prochiral face, and in this orientation cannot achieve the necessary additional hydrogen bonding interaction with the diamine modifier substrate. Similar interactions are commonly found in systems where bisphthalyl molecules are used as chiral recognition agents.<sup>12,13</sup> The steric influence that only establishes the specific orientation of the

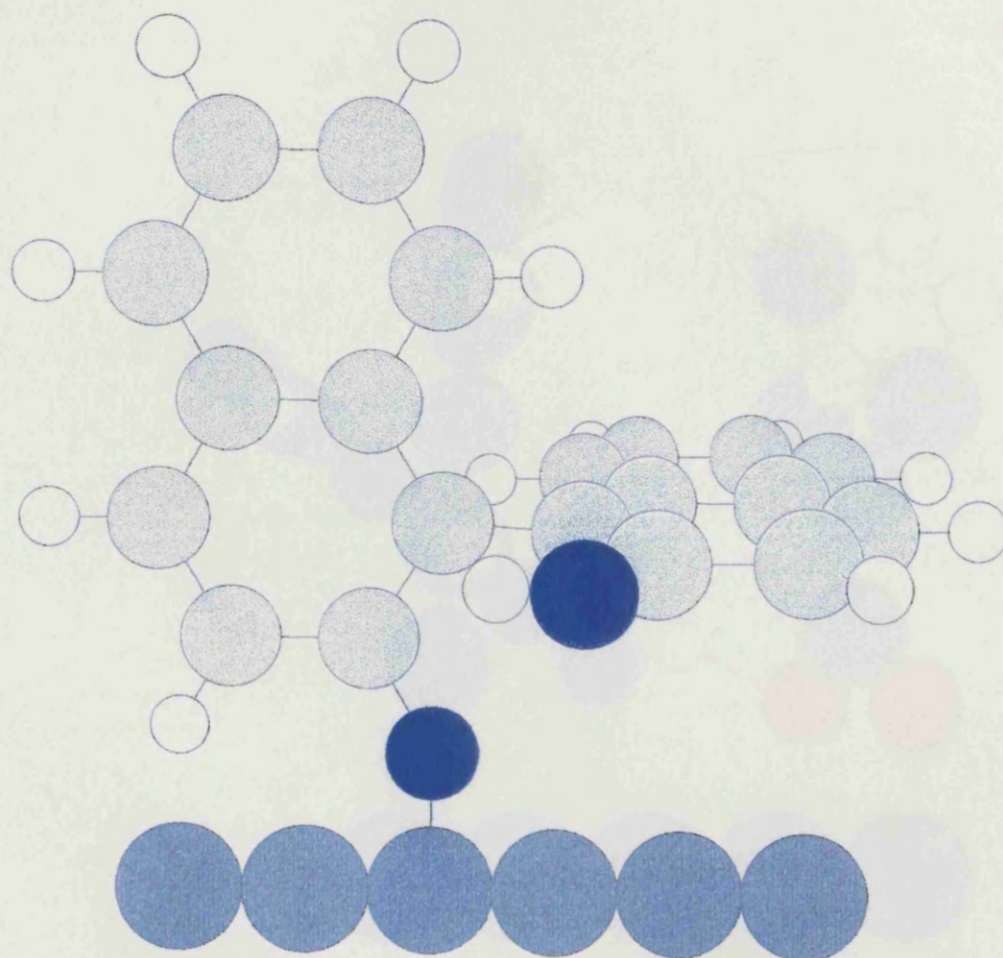


FIGURE 5.5.1: DIAGRAM SHOWING THE  $\pi$ - $\pi$  STACKING AND HYDROGEN BONDING INTERACTIONS BETWEEN TIGLIC ACID AND DIAMINE.

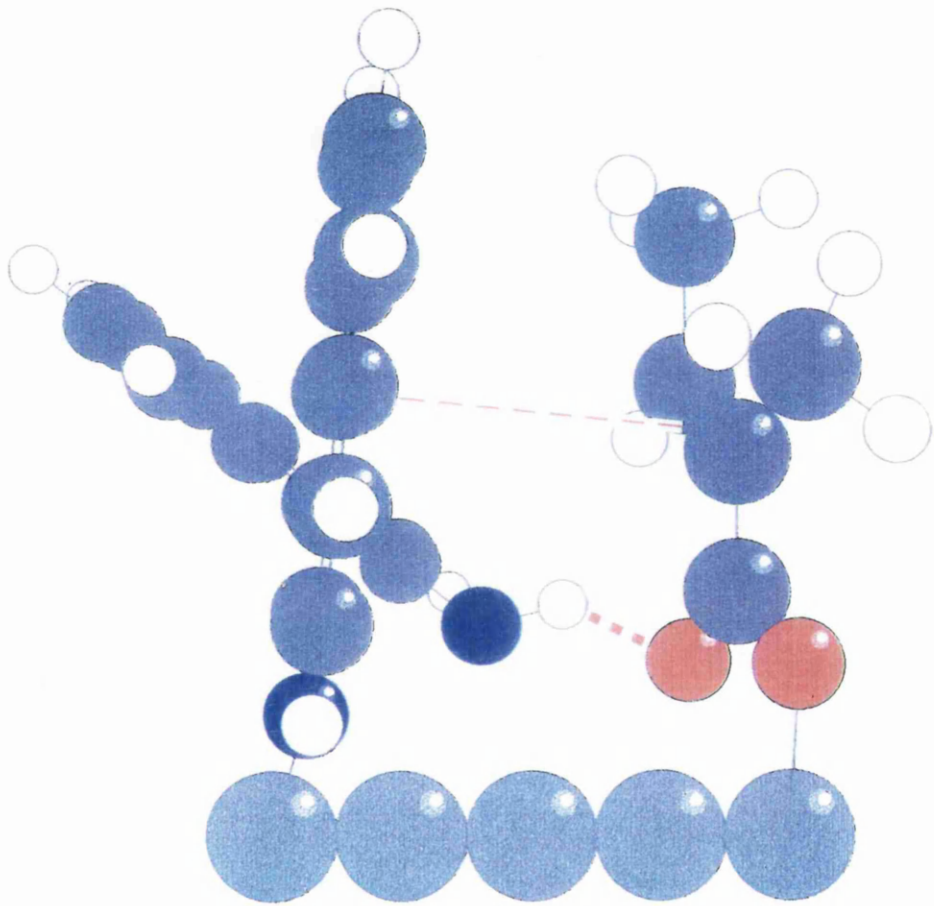
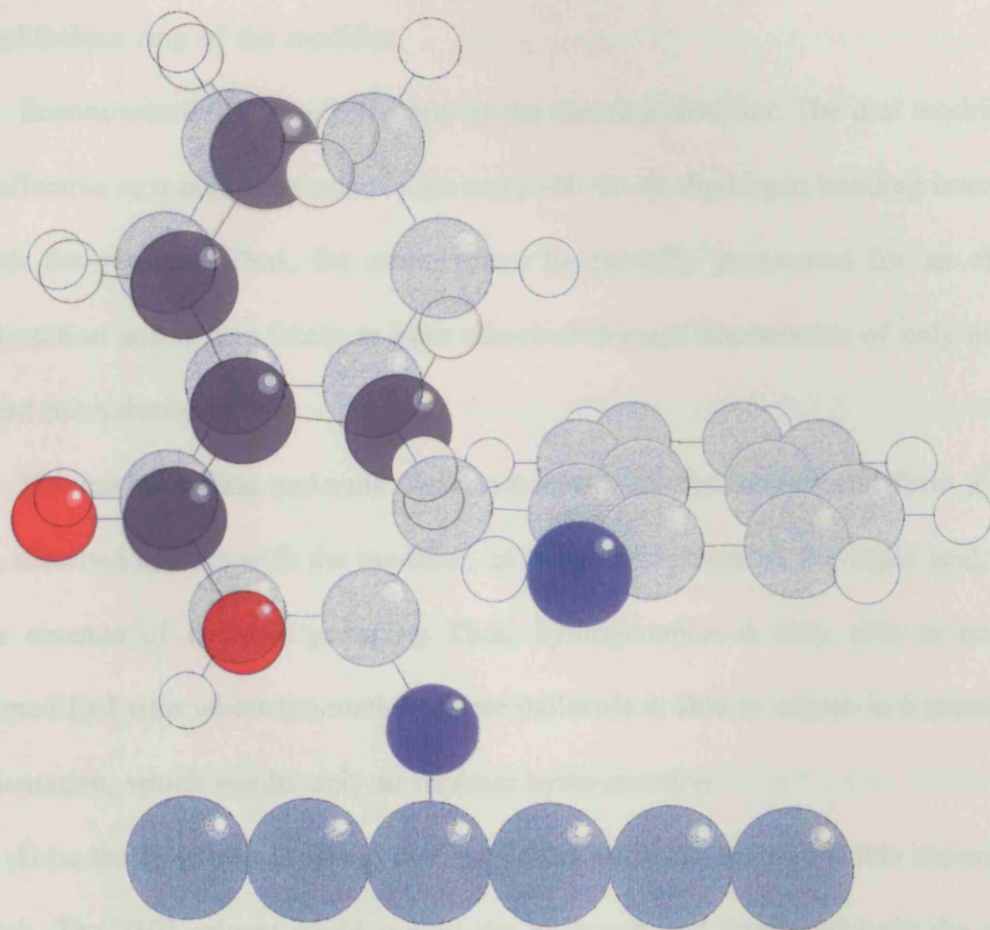


FIGURE 5.5.2: SIDE VIEW OF THE INTERACTION BETWEEN TIGLIC ACID AND DIAMINE.



**FIGURE 5.5.3: OPPOSITE COFACIAL ARRANGEMENT BETWEEN TIGLIC ACID AND DIAMINE WHERE NO HYDROGEN BONDING CAN OCCUR.**

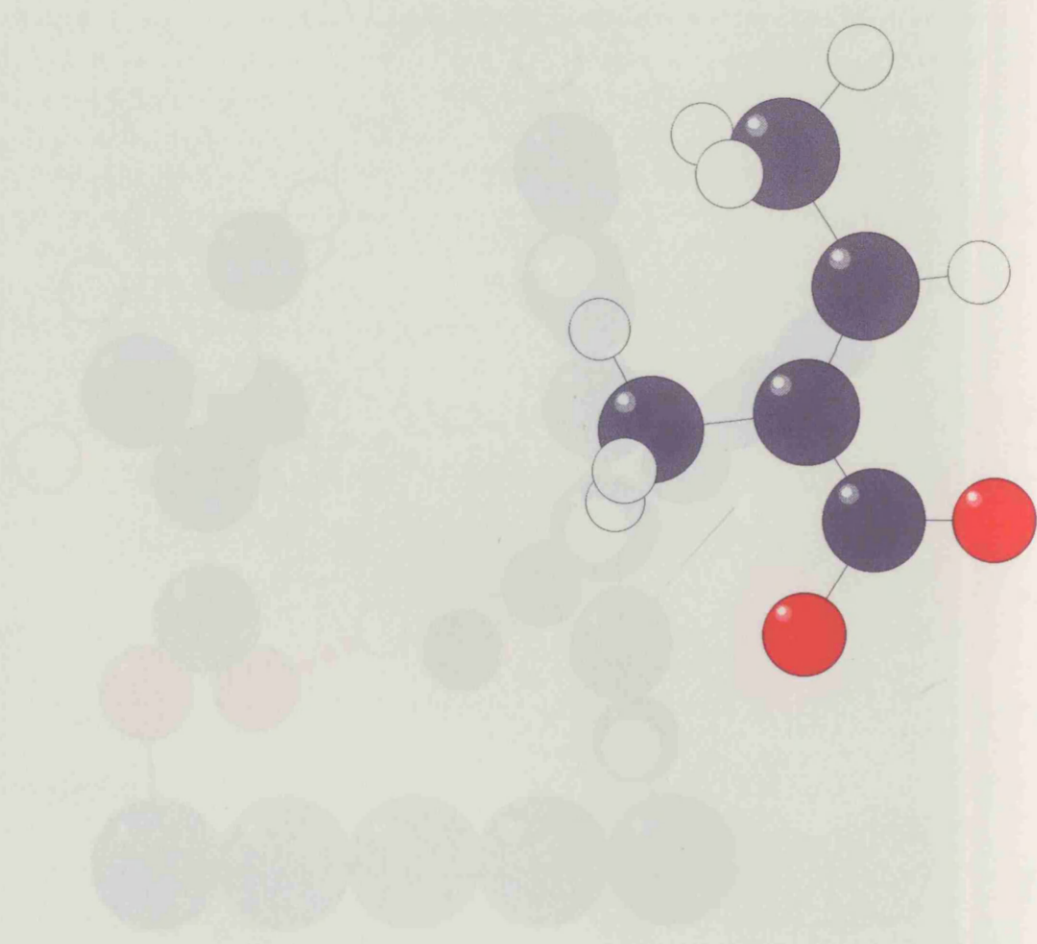
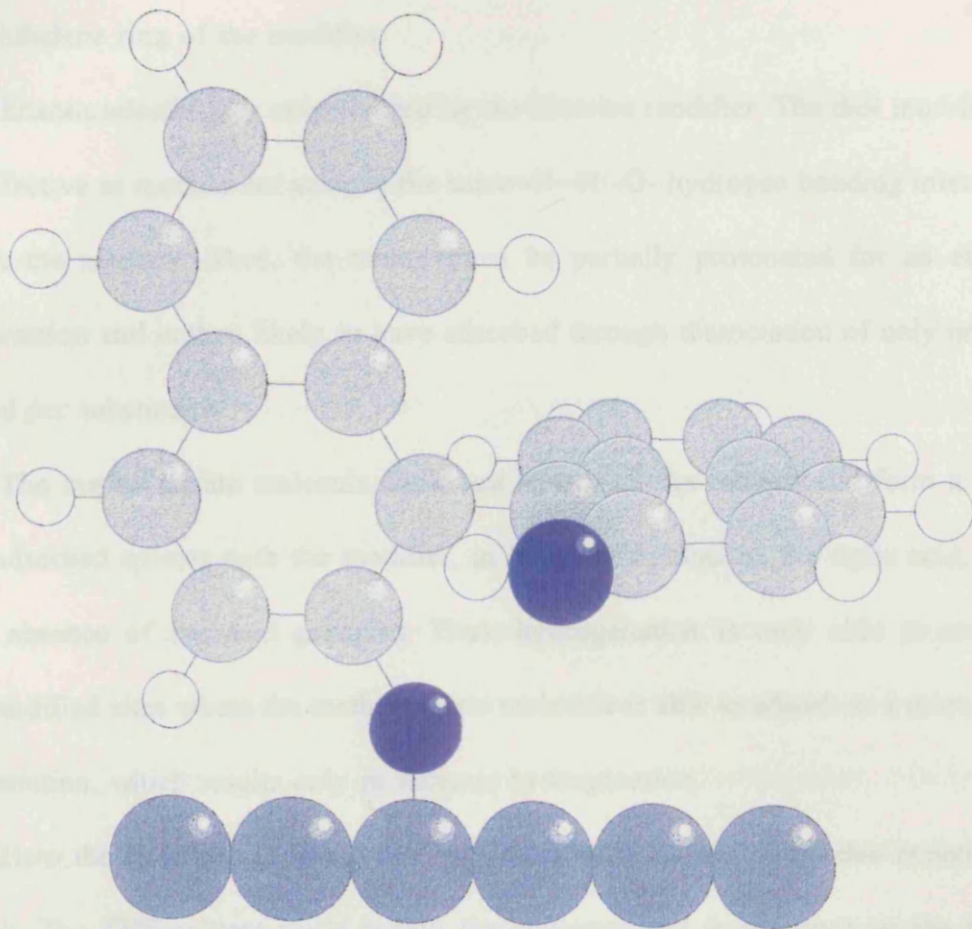


FIGURE 2.1. SIDE VIEW OF THE INTERACTION BETWEEN URACIL ACID AND CYTOSINE.



**FIGURE 5.5.3: OPPOSITE COFACIAL ARRANGEMENT BETWEEN TRIGLIC ACID AND DIAMINE WHERE NO HYDROGEN BONDING CAN OCCUR.**

co-adsorbed species. Subsequent hydrogenation is then controlled by orbital symmetry limitations which will only allow a cis addition of the hydrogen to the open face of the C=C bond which results in the observed enantiodifferentiation. Upon hydrogenation of the olefin bond the product molecule is then desorbed from the catalyst surface due to the loss of the  $\pi$ - $\pi$  stacking interaction, along with steric repulsion due to the bulky methyl groups of the reactant forced back towards the naphthalene ring of the modifier.

Enantioselectivity is only exerted by the diamine modifier. The diol modifier was ineffective as it could not achieve the same -N...H...O- hydrogen bonding interactions with the reactant. Thus, the amine must be partially protonated for an effective interaction and is then likely to have adsorbed through dissociation of only one N-H bond per substituent.

The methyl tiglate molecule could not adsorb on the catalyst and form a similar co-adsorbed species with the modifier, in the same manner as the tiglic acid, due to the absence of the acid grouping. Thus, hydrogenation is only able to occur on unmodified sites where the methyl tiglate molecule is able to adsorb in a more planar orientation, which results only in racemic hydrogenation.

How the hydrogen is added has not been clearly defined from this experimental work. The THF solvent could supply the hydrogen and then adsorb on the catalyst surface where it could itself be rehydrogenated. The solvent has already been shown to be able to adsorb on the metal surface where it can be activated for further reaction as seen from the aminol interconversion work. Hence, looking at different solvents would help to elucidate this idea. Alternatively, the hydrogen could be transferred from the metal surface through the delocalised system of the adsorbed reactant.

However, a concerted, thermal addition, either from direct impact or a weak complex of molecular dihydrogen, does not satisfy the Woodward-Hoffman rules for a cis addition, and as such can be ruled out. The presence of a nitrogen atom in many modifiers could possibly also be important for the addition of hydrogen. When compared against the diol, the amine has an additional valency which maybe able to assist in a hydrogen transfer, whereas the oxygen compound would again be ineffective.

Hydrogenation over the Pd/Cab catalyst modified with the diamine, where the modifier had subsequently undergone interconversion to the diol via the aminol or partial hydrogenation of the naphthalene units, is completely racemic. Thus, both the extended  $\pi$ -system and amine grouping are essential for asymmetric hydrogenation. This is in agreement with other workers who also concluded that these two structural elements were crucial, however, the reasoning is slightly different. Heinz *et al*<sup>140</sup> have stated that they believe their modifiers are adsorbed through the aromatic grouping to anchor these species to the catalyst surface, and the chiral amino side chain, in the protonated form, then interacts with the substrate. However, in the binaphthyl modified systems the modifiers are not adsorbed through the naphthalene rings, mainly due to steric hinderance. Alternatively, the naphthalene rings and the amine substituents are vital for the formation of the co-adsorbed complex between the modifier and the reactant and loss of either of these interaction sites does not result in any subsequent enantiodifferentiation during hydrogenation.

#### 5.5.1.2: PROCHIRAL C=O HYDROGENATION.

The same theory can be applied to the hydrogenation of 3-coumaranone, which already has an extent of delocalisation around the entire molecule, including the 5-

membered ring. Thus, the initial geometric requirements were such that the 3-coumaranone was able to form a co-adsorbed species with the binaphthyl modifier, again by a  $\pi$ - $\pi$  stacking interaction with a naphthalene moiety. To establish this essential binding interaction, the extended  $\pi$ -system in both rings of the 3-coumaranone interacts with the extended aromatic system of one naphthalene ring of the modifier. This in return orientates the C-O toward the amine substituent of the other naphthyl system to achieve a weak hydrogen bonding interaction, figure 5.5.4. Figure 5.5.5 shows the opposite cofacial arrangement where, once again, the hydrogen bonding interaction is not possible. Having once again geometrically orientated the substrate to form a specific co-adsorbed species, hydrogenation then proceeds by the enantioselective cis addition of hydrogen to the open face of the C=O bond, as controlled by the orbital symmetry. Thus, the reactant once again formed a co-adsorbed species with the binaphthyl modifier, but in this case, the 3-coumaranone is not directly interacting with the metal surface. Hence, enantioselective hydrogenation need not involve the reactant directly adsorbed on the metal surface, but rather the asymmetric catalytic site is defined by the entire metal:modifier:reactant complex. Looking at modifier molecules that have previously been successful in other reaction systems, although not all have had extended aromatic systems, many of them have had some  $\pi$ -system which could have been used to stabilise the substrate through the proposed  $\pi$ - $\pi$  stacking interaction to form a co-adsorbed species.

Thus a 1:1 specific interaction between the modifier and the substrate establishes the enantioselective site. The enantiomeric excess values obtained in each reaction are moderate, a result of overcrowding of modifier species which were packed quite tightly. Steric blocking by a neighbouring binaphthalene molecule hinders access of

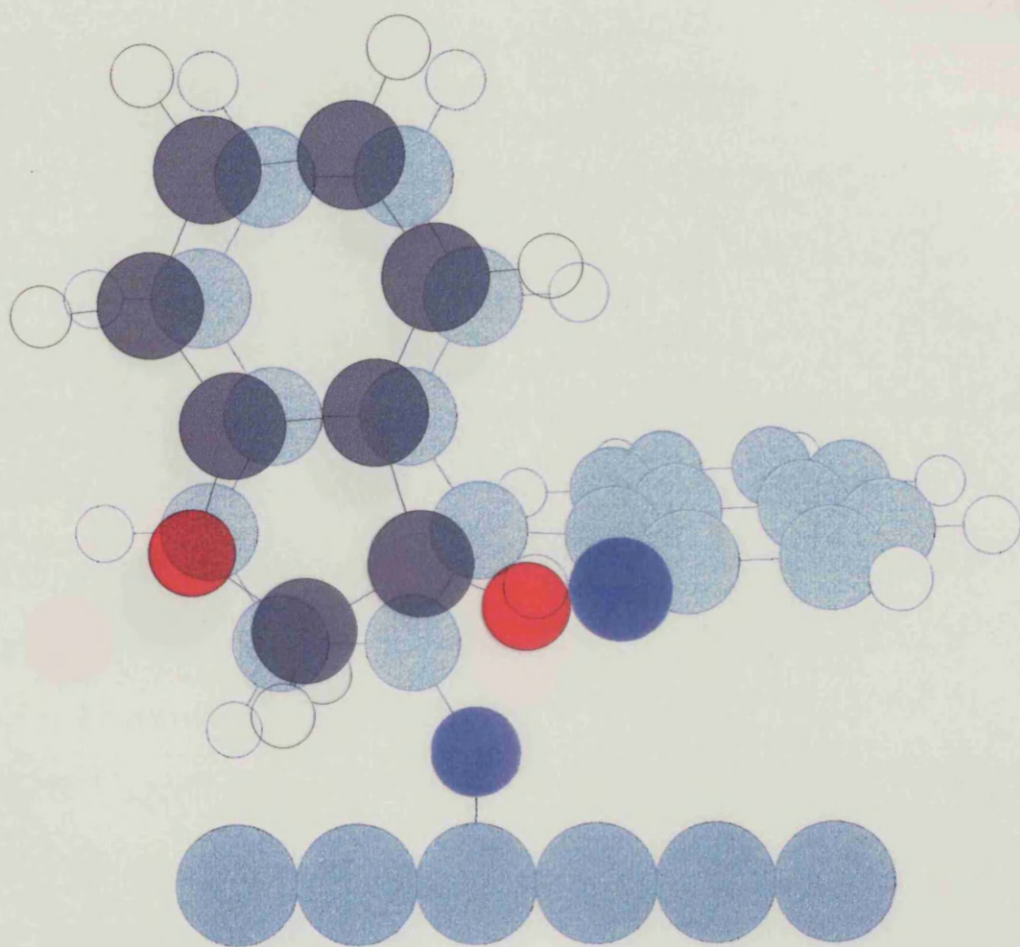
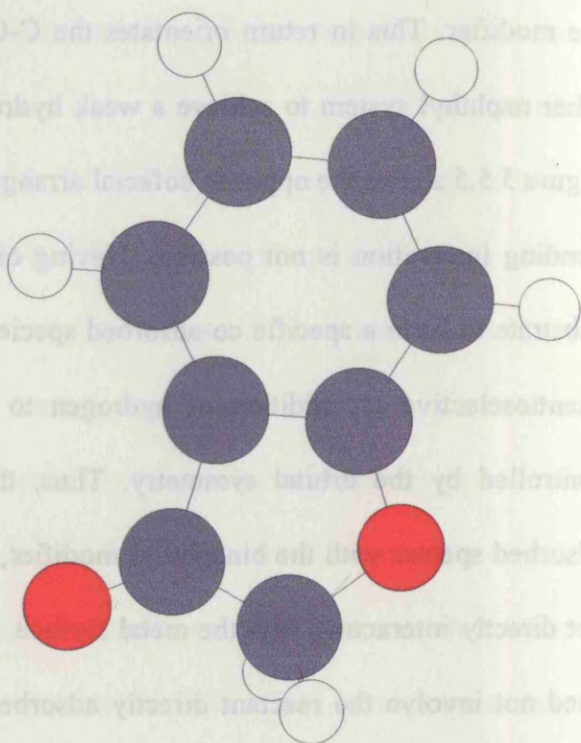


FIGURE 5.5.4: DIAGRAM SHOWING THE  $\pi$ - $\pi$  STACKING AND HYDROGEN BONDING INTERACTIONS BETWEEN 3-COUMARANONE AND DIÁMINE.

coordinated ring. Thus, the initial geometric requirements were such that the 3-  
 component was able to form a co-adsorbed species with the bimetallic modifier.  
 again by a  $\pi$ - $\pi$  stacking interaction with a neighboring moiety. To establish the  
 essential binding interaction, the extended  $\pi$ -system in both rings of the 3-  
 component interact with the extended aromatic system of one neighboring ring of



the modifier. This in turn causes the C-O toward the same substrate of the  
 other neighbor, causing a weak hydrogen bonding interaction. Figure 3.3.4.  
 Figure 3.3.3 shows a ball-and-stick model of the structure of the 3-  
 component. The structure is not perfectly planar, but the geometrically oriented the  
 structure is a specific co-adsorbed species, hydrogenation then proceeds by the  
 anisotropic interaction of the hydrogen to the open face of the C-O bond, as  
 controlled by the initial geometry. Thus, the reaction once again formed a co-  
 adsorbed species with the bimetallic modifier, but in this case, the 3-component is  
 not directly interacting with the metal surface. Hence, consecutive hydrogenation  
 need not involve the reaction directly adsorbed on the metal surface, but rather the  
 subsequent catalytic site is defined by the entire metal-modifier-reactant complex.  
 Looking at modifier molecules that have previously been successful in other reaction  
 systems, although not all have had extended aromatic systems, many of them have had  
 some  $\pi$ -system which could have been used to stabilize the substrate through the  
 proposed  $\pi$ -stacking interaction to form a co-adsorbed species.  
 Thus a 1:1 specific interaction between the modifier and the substrate establishes  
 the catalytic site. The enthalpic excess values obtained in each reaction are  
 modest, a result of overcrowding of modifier species which were packed quite  
 tightly. Steric blocking by a neighboring bimetallic molecule hinders access of

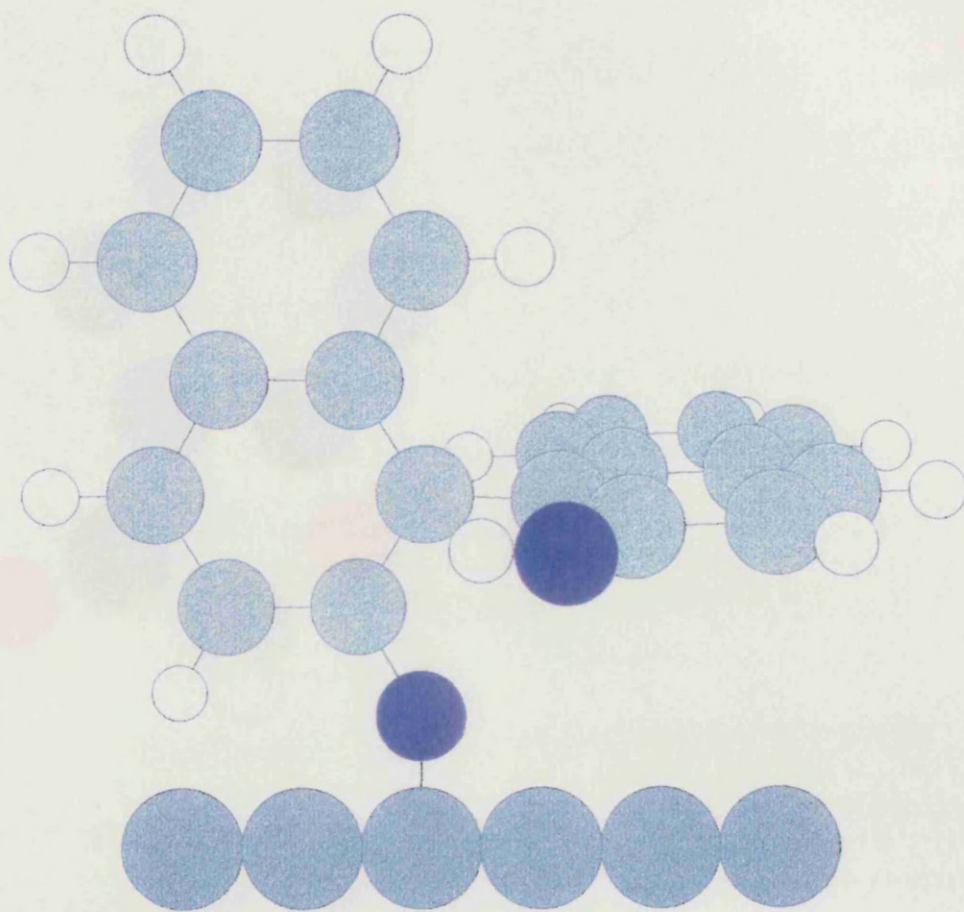


FIGURE 5.5.4: DIAGRAM SHOWING THE  $\pi$ - $\pi$  STACKING AND HYDROGEN BONDING INTERACTIONS BETWEEN 3-COUMARANONE AND DIÁMINE.

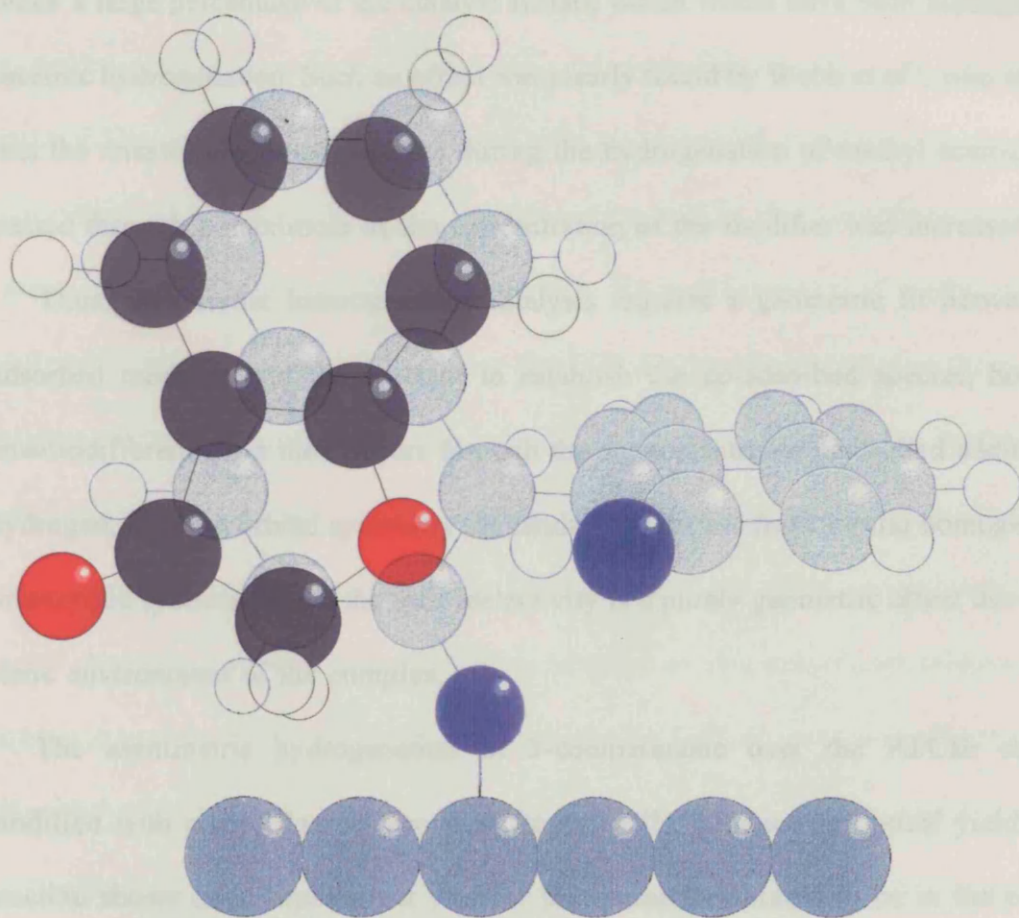


FIGURE 5.5.5: OPPOSITE COFACIAL ARRANGEMENT BETWEEN 3-COUMARANONE AND DIAMINE WHERE NO HYDROGEN BONDING CAN OCCUR.

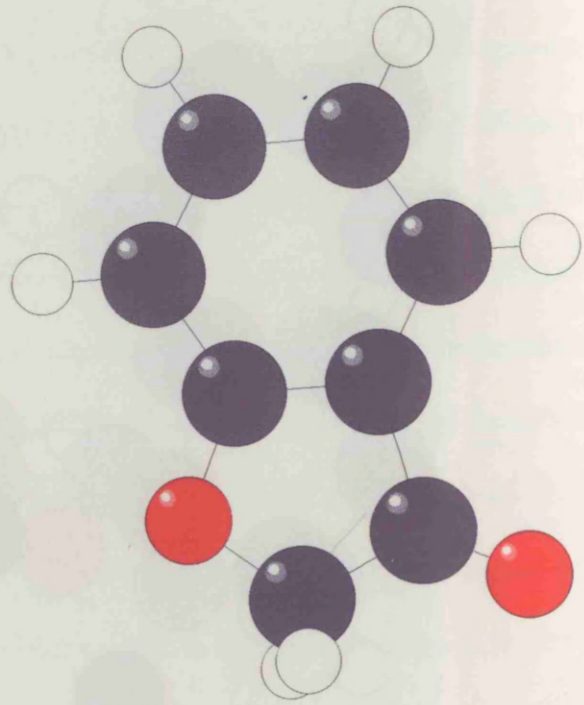
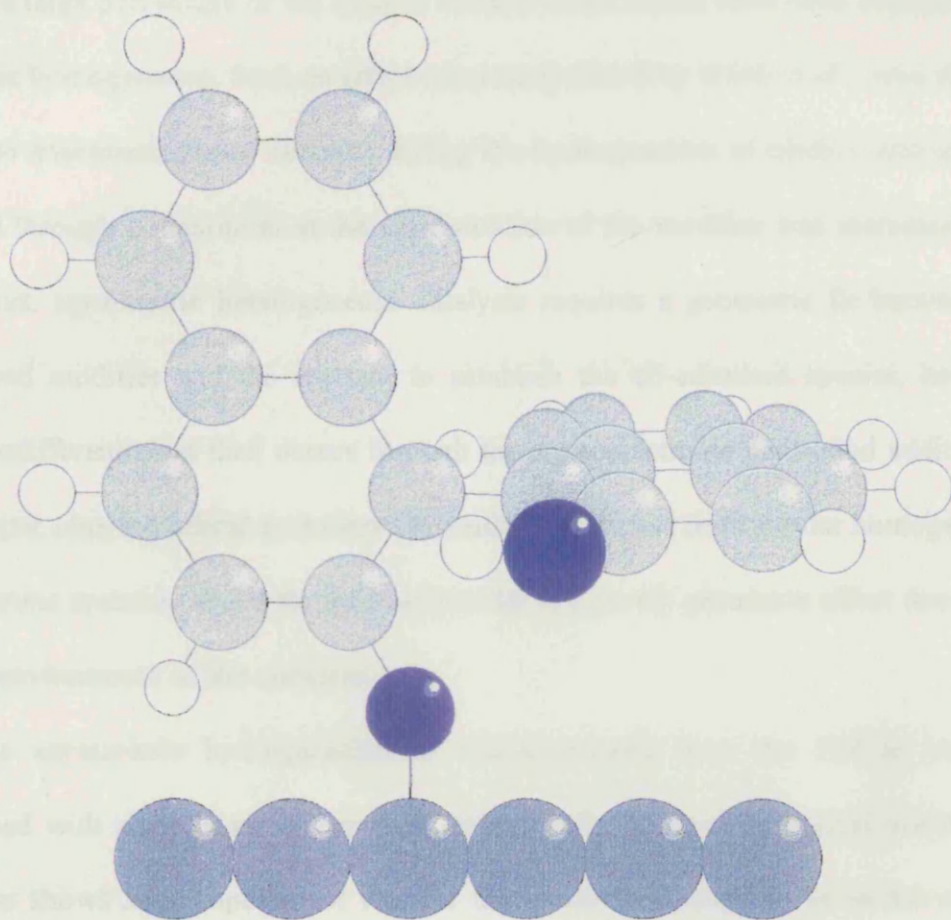


FIGURE 2.1. BALL-AND-STICK MODEL SHOWING THE H-BONDING AND HYDROGEN-BONDING INTERACTIONS BETWEEN 3-OXO-3-PHENYLPROPANOATE AND BENZOIC ACID.



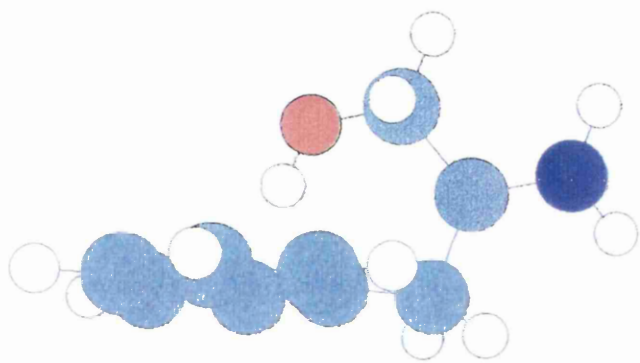
**FIGURE 5.5.5: OPPOSITE COFACIAL ARRANGEMENT BETWEEN 3-COUMARANONE AND DIAMINE WHERE NO HYDROGEN BONDING CAN OCCUR.**

the substrate to the modifier species and prohibits effective formation of the co-adsorbed complex, limiting the number of productive asymmetric sites. Maximum enantioselectivity would be predicted at an optimum surface coverage of modifier species whereby the binaphthyl species are adequately spaced to permit efficient 1:1 interactions between the reactant and the modifier, but sufficiently close packed to block a large percentage of the catalyst surface which would have been accessible for racemic hydrogenation. Such an effect was clearly found by Webb *et al*<sup>53</sup>, who showed that the enantioselectivity obtained during the hydrogenation of methyl acetoacetate, passed through a maximum as the concentration of the modifier was increased

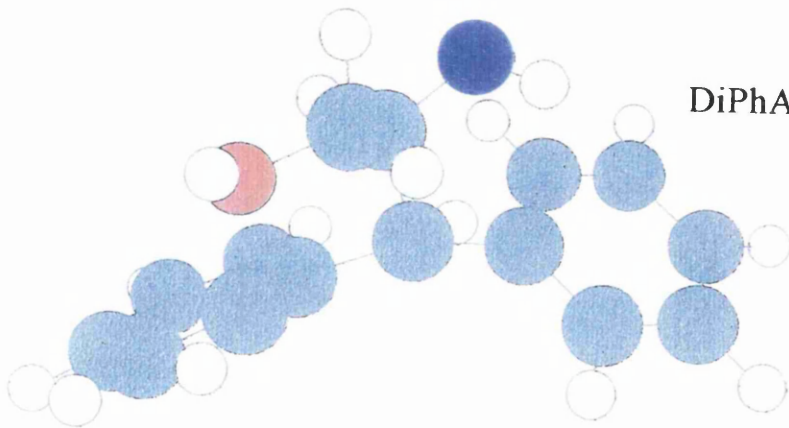
Thus, asymmetric heterogeneous catalysis requires a geometric fit between the adsorbed modifier and the reactant to establish the co-adsorbed species, however enantiodifferentiation then occurs through the stereoelectronic controlled addition of hydrogen, obeying orbital symmetry demands. This differs from similar homogeneous or enzymic systems, where the stereoselectivity is a purely geometric effect due to the steric environment of the complex.

The asymmetric hydrogenation of 3-coumaranone over the Pd/Cab catalyst modified with phenylalaninol can also, occasionally, produce an optical yield. This reaction shows how important it was for the amine substituent to be in the correct position, as the phenylglycinol was an unsuccessful modifier, but the phenylalaninol molecule, with only an additional -CH<sub>2</sub> spacer between the aromatic ring and the chiral centre with the amine substituent, was effective as a chiral modifier. The other molecules which were also attempted as chiral modifiers were unsuccessful as they either did not possess an amine grouping (MTFMPAA, TFAE), the vital amine substituent was not protonated (DMPEA) or was not in the correct place for

interaction and subsequent asymmetric hydrogenation (His, Trp, Pseudo). No information was obtained for the mode of adsorption of these modifiers but, with the aromatic group in each molecule considerably less sterically hindered than the chiral binaphthyls, there is the possibility of interaction between the metal surface and the aromatic group. The DiPhAla molecule was investigated as it was previously shown by Wang *et al*<sup>141</sup> that chiral modifiers which had extended aromatic  $\pi$ -systems, such as naphthalene or quinoline, were superior chiral modifiers to the analogous benzene or pyridine modifiers. They proposed that the extended  $\pi$ -systems improved the adsorption of the modifier on the metal surface and in this orientation substantial enantioselectivity was found to be induced in the hydrogenation of methyl pyruvate over a Pt catalyst. Using this reasoning the DiPhAla was investigated as the presence of two aromatic groups should also have anchored the modifier to the catalyst more effectively. However, basic molecular modelling suggested that steric crowding by the presence of the second benzene group actually forced the chiral amine group up and away from the surface, changing the orientation of this substituent relative to the aromatic system, figure 5.5.6, and consequently the DiPhAla was an ineffective chiral modifier. Using the theories proposed here, it is believed that the naphthalene and quinoline molecules that were found to be superior chiral modifiers to the analogous benzene or pyridine modifiers, were more effective as chiral modifiers, as the extended  $\pi$ -systems provided a superior region for the essential  $\pi$ - $\pi$  stacking interactions with the prochiral substrate, affording a more efficient enantioselective site.



PhAla



DiPhAla

FIGURE 5.5.6: MOLECULAR MODELS OF PhAla AND DiPhAla

### 5.5.2: CHIRAL MACROCYCLES AS MODIFIERS FOR ASYMMETRIC HYDROGENATION.

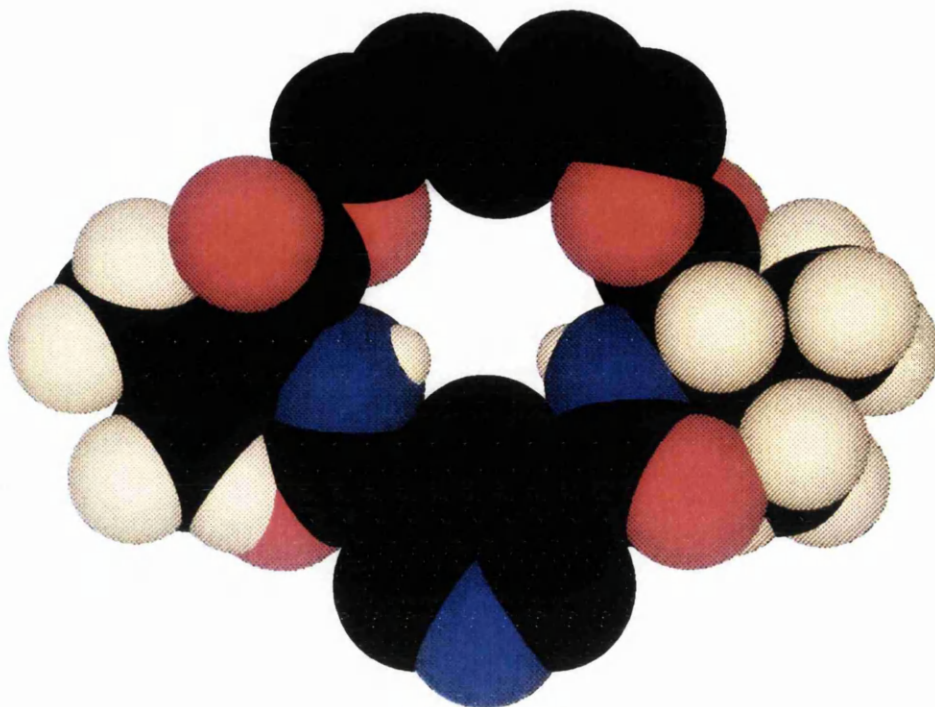
Chiral host molecules, such as a chiral macrocycle, may exhibit chiral recognition properties in the complexation of enantiomers. Such a macrocycle must be optically stable and bind the guest with a marked preference for one of the two enantiomers, relying on binding mechanisms such as hydrogen bonding and dipolar attractive interactions. Thus optical resolution may be possible, for example, the resolution of amino acids can be easily achieved in homogeneous systems. However to overcome the limitations of such homogeneous systems, the chiral macrocycles, previously shown in figure 3.6.2, were adsorbed on the metal surfaces of the catalysts. These macrocycles had the chirality built in through the incorporation of two identical amino acid groups and would appear to have many possible adsorption sites. Where adsorption did occur, this appeared to be a fairly strong interaction, with some modifier retained even after washing, but this adsorption was not reliable. This may have been due to the varied morphology of the catalyst surface. The desired pseudo-planar adsorption orientation would have required a fairly ordered surface for such a large adsorbate.

It was then hoped that the designed macrocycle cavity could preferentially complex the prochiral substrates in a specific orientation and direct them towards the metal surface. The reactant molecules would then reach the surface in a specific conformation which best fitted the spatial geometry of the chiral cavity. Thus the underlying metal could supply dissociated hydrogen and the macrocycle, with such conformational selection, would ensure high chemical and chiral selectivity whilst the physical properties would allow ease of separation and handling. The hydrogenation

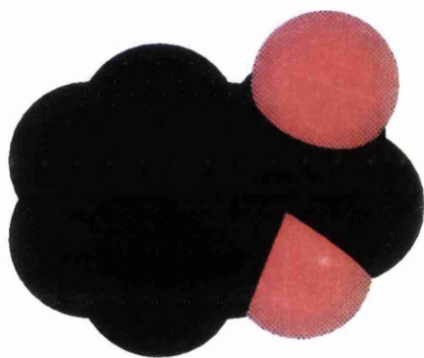
results from both the tiglic acid and 3-coumaranone reactions showed no enantioselectivity. Once again the macrocycle modifiers acted only to block active metal sites and reduce the extent of reaction. Molecular modelling, figure 5.5.7, showed that the actual chiral cavity may have been too small to permit either prochiral reactant access to the metal surface through the central channel. The hydrogenation that did occur was thought to have resulted from the racemic, unmodified metal sites that were not obscured by adsorption of the macrocycle.

Although both these macrocycles were unsuccessful there are many alternatives still available. Increasing the cavity size may permit the reactants easier access to the metal surface, but this cannot be done by simply increasing the number of carbons in the (CH<sub>2</sub>) bridge as the longer such a bridge is, the more flexible the macrocycle becomes and the specific chiral conformation may be lost. Alternatively, the bridging structure could be substituted with a more rigid spacer, such as a naphthalene moiety, to hold the macrocycle in a unique chiral conformation. Such a naphthalene grouping may also improve the adsorption as shown by Wang *et al*<sup>141</sup> who reported that an extended aromatic system, such as naphthalene or quinoline, showed superior adsorption to pyridine or benzene analogues.

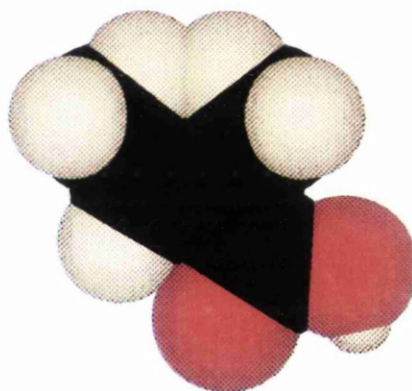
By encapsulating a transition metal ion, the same metal as the catalyst, within the cavity of the C<sub>5</sub> or C<sub>6</sub> macrocycle, a new metal complex could be developed which could then be adsorbed on to the catalysts. In such complexes the prochiral substrates would rest on the macrocycle where chiral recognition would occur and would not enter the now occupied cavity. It has been established that in the presence of metal ions, carbonyl compounds can be enantioselectively reduced by 1,4-dihydronicotinamide derivatives possessing a chiral side arm.<sup>142</sup>



C<sub>5</sub>-MACROCYCLE



3-COUMARANONE



TIGLIC ACID

FIGURE 5.5.7: MOLECULAR MODEL SHOWING THE RELATIVE SIZES OF THE C<sub>5</sub>-MACROCYCLE CAVITY WITH THE TIGLIC ACID AND 3-COUMARANONE SUBSTRATES

Kellog<sup>143</sup> then advanced this work and developed macrocycles, very similar in structure to C<sub>5</sub> and C<sub>6</sub>, which locked the central metal ion in a defined position. The oxygen atom of the carbonyl to be reduced was coordinated to the central metal atom and lay on top of the macrocycle. Steric effects that arose from the chiral substituents on the macrocycle then acted to selectively coordinate the prochiral substrate in one favourable orientation. Hence, the C<sub>5</sub> and C<sub>6</sub> macrocycles of this size may be more use when chelated with a transition metal. Adsorbing these new chiral metal complexes on the metal function of the heterogeneous catalyst could possibly produce a hybrid system which would maximise the benefits of both components.

### 5.3 BY-PRODUCTS FORMED DURING METHYL TIGLATE HYDROGENATIONS.

Achiral GC-MS work showed that both the by-products formed during the hydrogenation of methyl tiglate and 4-trifluoro, 2-methyl, 2-butenic acid ethyl ester have the exact same mass as the initial starting materials, which indicates that a molecular rearrangement has occurred as opposed to an alternative hydrogenation reaction.

Olefin isomerisation can be classed in two groups: 1) double bond migration and 2) cis-trans isomerisation. Dihydrogen is dissociatively adsorbed on a metal surface with the olefin diadsorbed on adjacent sites. A hydrogen atom then adds to one carbon, leaving a monosaturated species; the half hydrogenated state. Such a half hydrogenated state can be a relatively stable intermediate.<sup>144</sup> At this stage a number of reactions are then possible. A second hydrogen can then add to form the saturated molecule, which is desorbed from the surface or, alternatively, the first addition of hydrogen can be reversed. If the half hydrogenated state undergoes a configurational

change before reverting to an olefin, then cis-trans isomerisation may be effected. Double bond migration will occur if the half hydrogenated state returns to a different diadsorbed species than the original. After isomerisation the new olefins can desorb from the surface and be detected in solution or they can undergo further reaction.

From the methyl tiglate results the best data match obtained from the computer data base predicted the unknown to be 3-methyl, 2-butenic acid methyl ester, figure 5.5.8, but had this rearrangement occurred, the ensuing hydrogenation would have resulted in a different, single achiral product peak on the GC chromatogram. If however an internal double-bond migration had occurred two possible rearrangements could have happened, figures 5.5.9 and 5.5.10.

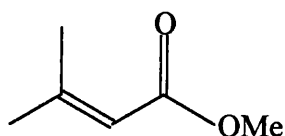


FIGURE 5.5.8

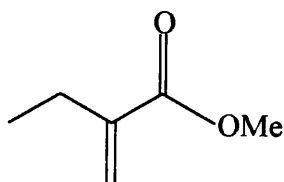


FIGURE 5.5.9

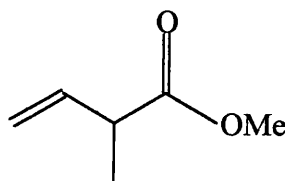


FIGURE 5.5.10

2-Ethyl, 2-propenoic acid methyl ester, figure 5.5.9, is also a prochiral molecule and would have appeared as a single peak on the chiral GC trace. Hydrogenation of this molecule would produce the same methyl 2-methyl butyrate products as the original methyl tiglate. 2-Methyl, 3-butenic acid methyl ester is a chiral molecule and as such two additional peaks would appear on the GC trace. Subsequent hydrogenation

of this molecule would be symmetric and would not in any way alter the predetermined chirality of the products.

Thus, it is then possible that the methyl tiglate molecule is adsorbed on to the metal where it could either be hydrogenated or undergo a double-bond migration. 2-Ethyl, 2-propenoic acid methyl ester could be produced and then either desorbed (and detected as a single peak on the GC trace) or hydrogenated. 2-Methyl, 3-butenic acid methyl ester could also be produced but it could be either permanently adsorbed on the catalyst surface or react very rapidly and is therefore not observed in the reaction solution. If this is the case, the ensuing hydrogenation of this molecule is symmetric, the chirality of the molecule having previously been determined by the double-bond migration step. This transition is unlikely to be stereoselective and would produce a racemic amount of 2-methyl, 3-butenic acid methyl ester for further reaction. No enantioselectivity could then possibly arise in the production of methyl 2-methyl butyrate.

Another possible rearrangement is the formation of methyl angelate, the *Z*-isomer of methyl tiglate, figure 5.5.11. The methyl tiglate could adsorb on to the catalyst surface where, instead of a double-bond migration, the *cis-trans* isomerisation then occurs, followed by desorption in the angelate form. Hydrogenation of methyl angelate would also produce methyl 2-methyl butyrate.

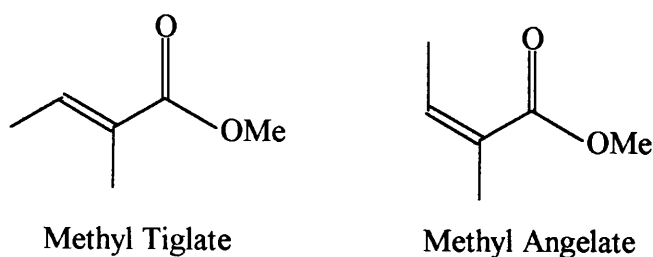


FIGURE 5.5.11

Fragmentation patterns from the mass spectrometry data were very similar for both starting material, products and by-product and did not provide any further information on which rearrangement had occurred.

N.M.R. was then investigated as a secondary technique for the elucidation of the structure detected in solution. Unfortunately the volatility of all the related species present in solution was so similar that separation into the distinct components for individual analyses could not be effected. The resultant N.M.R. trace was thus swamped with peaks from the known materials and any possible structural variations were undetectable.

The methyl angelate product became commercially available and subsequent GC analysis showed a peak concurrent with the unknown product. Hence, a cis-trans isomerisation of methyl tiglate appears to occur. The extent of migration and isomerisation is related to the rate at which the half hydrogenated state species reforms a diadsorbed species relative to the rate at which it adds a second hydrogen. The greater the hydrogen concentration at the catalyst surface, the greater the rate of saturation relative to the rate of reversion. Migration and isomerisation are favoured by a low hydrogen concentration at the catalyst surface. Isomerisation was found to be predominant with the Pd/C catalyst relative to the Pd/Cab where only a slight amount of methyl angelate was detected. Bond and Wells<sup>145</sup> found that the effect on the extent of double-bond migration was a property of the metal itself and was altered very little by the support. It was related to the relative tendency of the half hydrogenated states to reform an unadsorbed olefin. Palladium was found to be much more active for isomerisation than nickel.<sup>146</sup> Although the Pd/C appeared to form more methyl angelate than Pd/Cab, this was only the amount that was desorbed and detected

in solution. The Pd/Cab catalyst has a higher hydrogenation activity and as such the methyl angelate produced may undergo a rapid reaction and is therefore not detected as much.

With the hydrogenation of 4-trifluoro, 2-methyl, 2-butenic acid ethyl ester the possible rearrangements within the starting material are more limited and the fragmentation patterns were more informative. The presence of the terminal  $\text{CF}_3$  grouping restricts the number of possible double-bond migrations. This time the fragmentation pattern of the unknown had an additional peak at  $m/z = 99$ , a species not detected anywhere else. This mass is attributed to the starting material less the  $\text{CH}_2\text{CF}_3$  grouping and thus the unknown structure is assigned as shown in figure 5.5.12. The alternative cis-trans isomerisation may have been hindered by the heavier - $\text{CF}_3$  grouping.

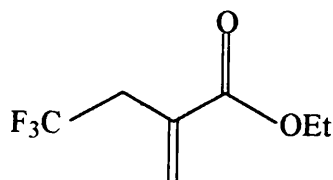


FIGURE 5.5.12

Subsequent hydrogenation of this molecule still has the possibility of being enantioselective. A further replacement of the remaining Me group with an additional  $\text{CF}_3$  may be useful to block this rearrangement further. Thus although isomerisation occurs within both substrates, the alternative olefins could still, potentially, be hydrogenated enantioselectively, to form the same products as the original starting materials.

Such isomerisations can often pass unnoticed, as very often there may be no direct

evidence remaining that rearrangement has occurred. However, conditions can be selected that will influence the reactive pathway, for example, conditions that increase the hydrogen availability, such as increased pressure, agitation and solvent variation can retard the activity of olefin isomerisation. Alternatively, in some reactions such isomerisation can prove favourable. Selective removal of cis homoconjugated dienes and trienes in natural oils, used to make edible hydrogenated fats, depends on prior isomerisation of multiple unsaturation into conjugation under hydrogenation conditions.<sup>147</sup>

## REFERENCES

1. S.D.Robertson, B.D.McNicol, J.H.DeBaas and S.C.Kloet, *J. Catal.*, **37**, 424, (1975).
2. C.H.Bartholomew and R.B.Pannell, *J. Catal.*, **65**, 390, (1980).
3. K.Lu and B.J.Tatarchuk, *J.Catal.*, **106**, 166, (1987).
4. D.G.Mustard and C.H.Bartholomew, *J. Catal.*, **67**, 186, (1981).
5. R.J.Farrauto, *AIChE, Symp. Ser.*, **70**, 143, (1974).
6. J.L.Falconer and W.C.Conner, *Appl. Catal.*, N28, 56, (1989).
7. S.J.Khoobiar, *J. Phys. Chem.*, **68**, 411, (1964).
8. W.C.Conner, "Hydrogen on Metals", (Z.Paál, P.G.Menon, Eds.), Dekker, New York, (1988), p.311.
9. J.F.Cevallos-Candau and W.C.Conner, *J. Catal.*, **106**, 378, (1987).
10. M.Boudart, A.Aldag and M.A.Vannice, *J. Catal.*, **18**, 46, (1970).
11. R.B.Levy, M.Boudart, *J. Catal.*, **32**, 304, (1974).
12. C.Mirodatos, H.Praulaud and M.Primet, *J. Catal.*, **107**, 275, (1987).
13. A.Palazov, G.Kudinov, H.Bonev and D.Shapov, *J. Catal.*, **74**, 44, (1982).
14. T.Bansagi, J.Racko and F.Solymosi, "Studies in Surface Science and Catalysis 17", (G.M.Pajonk, S.J.Teichner and J.E.Germain, Eds.), Elsevier, Amsterdam, (1983), p.109.
15. K.Fujimoto, "Studies in Surface Science and Catalysis 77", (T.Inui, K.Fujimoto, T.Uchijima, M.Masai, Eds.), Elsevier, Kyoto, Japan, (1993), p.9.
16. W.C.Conner, S.J.Teichner and G.M.Pajonk, "Advances in Catalysis", (D.Eley, H.Pines, P.Weisz, Eds.), (1986), Vol. 34, p.1.
17. T.M.Borchkhadze and N.G.Kogoshvili, *Astronomy and Astrophysics*, **53**, 431, (1976).
18. E.L.Malus, *Mem. Soc. d'Arcueil*, **2**, 143, (1809).

19. J.B.Biot, *Bull. Soc. Philomath. Paris*, 190, (1815).
20. L.Pasteur, Two lectures delivered before the Societé Chimique de Paris, Jan. 20th and Feb. 3rd, (1860).
21. L.Kelvin, Baltimore Lectures, p. 436, 619 (1904).
22. J.van't Hoff, *Bull. Soc. Chim. France*, [2], 23, 295, (1875).
23. J.A. Le Bel, *Bull. Soc. Chim. France*, [2], 22, 337, (1874).
24. E.Fischer, *Ber.*, 24, 2683, (1891)
25. J.M.Bijvoet, A.F.Peerdeeman and A.J.Bommel, *Nature*, 168, 271, (1951).
26. R.S.Cahn, C.K.Ingold and V.Prelog, *Agnew Chem. Int. Ed. Engl.*, 5, 385, (1966).
27. L.C.Cross and W.Klyne, *Pure Appl. Chem.*, 45, 11, (1976)
28. FDA's Policy Statement for the Development of New Stereoisomeric Drugs; *Chirality*, 4, 338, (1992).
29. T.Ohta, T.Kimura, N.Sato and S.Nozone, *Tetrahedron Lett.*, 29, 4303, (1988).
30. T.N.Salzmann, R.W.Ratcliffe, B.G.Christensen and F.A.Bouffard, *J. Am. Chem. Soc.*, 102, 6161, (1980).
31. H.B.Kagan and T.P.Dang, *J. Am. Chem. Soc.*, 94, 6429, (1972).
32. W.S.Knowles, B.D.Vineyard, M.J.Sabacky, G.L.Bachman and D.J.Weinkauff, *J. Am. Chem. Soc.*, 99, 5946, (1977).
33. G.Gelbard, H.B.Kagan and R.Stern, *Tetrahedron*, 32, 233, (1976).
34. R.Noyori and H.Takaya, *Acc. Chem. Res.*, 23, 345, (1990).
35. A.Miyashita, H.Takaya, T.Souchi and R.Noyori, *Tetrahedron*, 40, 1245, (1984).
36. H.Muramatsu, H.Kawano, Y.Ishii, M.Saburi and Y.Uchida. *J. Chem. Soc., Chem. Comm.*, 769, (1989)
37. H.Takaya, T.Ohta, N.Sayo, H.Kumobayashi, S.Akutagawa, S.Innoue, I.

- Kasahara and R.Noyori, *J. Am. Chem. Soc.*, **109**, 1596, (1987).
38. R.Noyori, T.Ohkuma, M.Kitamura, H.Takaya, N.Sayo, H.Kumobayashi and S.Akutagawa,, *J. Am. Chem. Soc.*, **109**, 5856, (1987).
39. E.J.Corey and J.O.Link, *J. Am. Chem. Soc.*, **114**, 1906, (1992).
40. I.Ojima, N.Clos and C.Bastos, *Tetrahedron*, **45**, 6901, (1989).
41. J.P.Arhancet, M.E.Davis, J.S.Merola and B.E.Hanson, *Nature*, **339**, 454, (1988).
42. E.G.Kuntz, *CHEMTECH*, **17**, 570, (1987).
43. K.T.Wan and M.E.Davis, *Nature*, **370**, 449, (1994).
44. J.B.Hoke, L.S.Hollis and E.W.Stern, *J. Organomet. Chem.*, **455**, 193, (1993).
45. R.V.Chaudhari, B.M.Bhanage, R.M.Deshpande and H.Delmas, *Nature*, **373**, 501, (1995).
46. G.M.Schwab and L.Rudolph, *Naturwiss*, **23**, 363, (1932).
47. D.Lipkin and T.D.Stewart, *J. Am. Chem. Soc.*, **61**, 3295, (1939).
48. Y.Nakamura, *Bull. Chem. Soc. Jpn.*, **16**, 367, (1941).
49. Y.Izumi, *Adv. Cat.*, **32**, 215, (1983).
50. S.Akabori, Y.Izumi, Y.Fuji and S.Sukurai, *Nature*, **178**, 323, (1956).
51. Y.Orito, S.Imai, S.Niwa and G.H.Nguyen, *J. Synth. Org. Chem. Jpn.*, **37**, 173, (1979).
52. Y.Orito, S.Imai and S.Niwa, *J. Chem. Soc. Jpn.*, 1118, (1979).
53. G.Webb and P.B.Wells, *Catal. Today*, **12**, 319, (1992).
54. I.M.Sutherland, A.Ibbotson, R.B.Moyes and P.B.Wells, *J. Catal.*, **125**, 77, (1990).
55. J.T.Wehrli, A.Baiker, D.M.Monti and H.U.Blaser, *J. Mol. Catal.*, **61**, 207, (1990).
56. Y.Nitta, Y.Ueda and T.Imanaka, *Chem. Lett. Jpn.*, 1095, (1994).

57. H.U.Blaser, S.K.Boyer and U.Pittelkow, *Tetrahedron: Asymmetry*, **2**, 721, (1991).
58. H.U.Blaser, H.P.Jalett, D.M.Monti, J.F.Reber and J.T.Wehrli, *Stud. Surf. Sci. Catal.*, **41**, 153, (1988).
59. K.E.Simons, A.Ibbotson, P.Johnston, H.Plum and P.B.Wells, *J. Catal.*, **150**, 321, (1994).
60. H.U.Blaser, H.P.Jalett, D.M.Monti, A.Baiker and J.T.Wehrli, *Stud. Surf. Sci. Catal.*, **67**, 147, (1991).
61. H.U.Blaser, H.P.Jalett and J.T.Wehrli, *J. Mol. Catal.*, **68**, 215, (1991).
62. P.A.Meheux, A.Ibbotson and P.B.Wells, *J. Catal.*, **128**, 387, (1991).
63. R.L.Augustine, S.K.Tanielyan and L.K.Doyle, *Tetrahedron: Asymmetry*, **4**, 1803, (1993).
64. G.C.Bond, K.E.Simons, A.Ibbotson, P.B.Wells and D.A.Whan, *Catal. Today*, **12**, 421, (1992).
65. M.Garland and H.U.Blaser, *J. Am. Chem. Soc.*, **112**, 7048, (1990).
66. O.Schwalm, B.Minder, J.Weber and A. Baiker, *Catal. Lett.*, **23**, 271, (1994).
67. O.Schwalm, B.Minder, J.Weber and A.Baiker, *J. Quant. Chem.*, **52**, 191, (1994).
68. H.Brunner, M.Muschiol, T.Wishert and J.Wiehl, *Tetrahedron: Asymmetry*, **1**, 159, (1990).
69. D.R.Richards, H.H.Kung and W.M.H.Sachtler, *J. Mol. Catal.*, **36**, 329, (1986).
70. A.Hoek and W.M.H.Sachtler, *J. Catal.*, **58**, 276, (1979).
71. Y.Nitta, T.Imanaka and S.Teranishi, *J. Catal.*, **96**, 429, (1985).
72. Y.Nitta, T.Utsumi, T.Imanaka and S.Teranishi, *J. Catal.*, **101**, 376, (1986).

73. E.I.Klabunovskii, V.I.Neupokoev and Y.I.Petrov, *Izu. Akad. Nauk SSSR, Ser. Khim.*, 2829, (1970).
74. E.I.Klabunovskii, N.P.Sokolova, A.A.Vendenyapin, Y.M.Talanov, N.D.Zubreva, V.P.Polyakova and N.Gorina, *Izu. Akad. Nauk SSSR, Ser. Khim.*, 2361, (1972).
75. A.Tai and T.Harada, In "Tailored Metal Catalysts", (Y.Iwasawa, Ed.), D.Reidel, Dordrecht, (1986), p265-324.
76. A.Tai, T.Harada, Y.Hiraki and S.Murakami, *Bull. Chem. Soc. Jpn.*, **56**, 1414, (1983).
77. M.A.Keane and G.Webb, *J. Mol. Catal.*, **73**, 91, (1992).
78. A.Tai, T.Kikukawa, T.Sugimura, Y.Inoue, S.Abe, T.Osawa and T.Harada, *Bull. Chem. Soc. Jpn.*, **67**, 2473, (1994).
79. M.A.Keane, *Can. J. Chem.*, **72**, 372, (1994).
80. M.A.Keane and G.Webb, *J. Catal.*, **136**, 1, (1992).
81. M.A.Keane and G.Webb, *J. Chem. Soc., Chem. Commun.*, 1619, (1991).
82. E.N.Lipgart, Y.L.Petrov and E.I.Klabunovskii, *Kinet. Catal.*, **12**, 1491, (1971).
83. G.Webb, in "Proc. European Symposium on Chiral Reactions in Heterogeneous Catalysis", (G. Jannes, Ed.), Plenum, (1995), in press.
84. T.Osawa, T.Harada and A.Tai, *J. Catal.*, **121**, 7, (1990).
85. T.Harada and Y.Izumi, *Chem. Lett.*, 1195, (1978).
86. L.J.Bostelaar and W.H.M.Sachtler, *J. Mol. Catal.*, **42**, 387, (1987).
87. H.U.Blaser and M.Muller, in "Heterogeneous Catalysis and Fine Chemicals" (M.Guisnet et al. Eds.), Elsevier, Amsterdam, (1991), p.73.
88. Y.I.Petrov and E.I.Klabunovskii, *Kinet. Catal.*, **8**, 814, (1967).

89. W.M.H.Sachtler, in "Catalysis in Organic Reactions", (L.Augustine, Ed.) Chem. Ind., **22**, 189, (1985).
90. G.Webb, in "Chiral Reactions in Heterogeneous Catalysis" (G.Jannes and V.Dubois, Eds.) Plenum Press, New York, (1995), p.61.
91. S.Akabori, S.Sakurai, Y.Izumi and Y.Fujii, *J. Chem. Soc. Jpn., Ind. Chem. Sec.*, **77**, 798, (1956).
92. J.R.G.Perez, J.Malthête and J.Jacques, *C. R. Acad. Sc. Paris*, **300**, 170, (1985).
93. M. Bartók, G.Wittman, G.B.Bartók and G.Göndös, *J. Organomet. Chem.*, **384**, 385, (1990).
94. Y.Nitta, Y.Ueda and T.Imanaka, *Chem. Lett.*, 1095, (1994).
95. Y.Nitta and K.Kobiro, *Chem. Lett.*, 165, (1995).
96. D.J.Cram and J.L.Mateos, *J. Am. Chem. Soc.*, **81**, 5150, (1959).
97. P.L.Rinaldi, *Prog. Nucl. Magn. Reson. Spectrosc.*, **15**, 291, (1982).
98. R.R.Fraser, "Asymmetric Synthesis", (J.D.Morrison, Ed.), Academic Press, New York, (1983), Vol. 1, Chapter 9, p.173.
99. W.H.Pirkle and D.J.Hoover, *Top. Stereochem.*, **13**, 263, (1982).
100. S.Yamaguchi, "Asymmetric Synthesis", (J.D.Morrison, Ed.), Academic Press, New York, (1983), Vol. 1, Chapter 7, p.125.
101. I.W.Wainer, *Trends Anal. Chem.*, **6**, 125, (1987).
102. C.E.Dalgliesh, *J. Chem. Soc.*, 3940, (1952).
103. R.J.Baczuk, G.K.Landram, R.J.Dubois and H.C.Dehm, *J. Chromatogr.*, **60**, 351, (1971)
104. W.H.Pirkle, D.W.House and J.M.Finn, *J. Chromatogr.*, **192**, 143, (1980)
105. E.Gil-Av, *J. Chromatogr. Libr.*, **32**, 111, (1985).
106. W.A.König, *J. High Resolut. Chromatogr., Chromatogr. Commun.*, **5**, 588,

(1982)

107. V.Schurig, *J. Chromatogr.*, **441**, 135, (1988).
108. V.Schurig and H.P.Nowotny, *Agnew. Chem., Int. Ed. Engl.*, **29**, 939, (1990).
109. F.A.Lewis, "The Palladium Hydrogen System", Academic Press, New York, (1967).
110. E.B.Maxted, *Adv. Catal.*, **3**, 129, (1951).
112. M.Montes, C.Penneman de Bosscheyde, B.K.Hodnett, F.Delannay, P.Gränge and B.Delmon, *Appl. Catal.*, **12**, 309, (1984).
112. D.Hunter, PhD Thesis, University of Glasgow, (1995).
113. P.D.Maniar and A.Navrotsky, *J. Non-Cryst. Solids*, **120**, 20, (1990).
114. L.F.Gladden, M.Vignaux, P.Chiaranussati, R.W.Griffiths, S.D.Jackson, J.R.Jones, A.P.Sharatt, F.J.Robertson, G.Webb, P.Chieux and A.C.Hannon, *J Non-Cryst. Solids*, **139**, 47, (1992).
115. J.T.Richardson and R.J.Dubus, *J.Catal.*, **54**, 207, (1978) .
116. G.C.Bond., in "Heterogeneous Catalysis: Principles and Applications", 2nd edition, Oxford, New York, (1987).
117. J.J.F.Scholten and A.Van Montfoort, *J. Catal.*, **1**, 85, (1962) .
118. C.H.Bartholomew and R.J.Farrouto, *J. Catal.*, **45**, 41 (1976).
119. C.Hoang and V.Kahaya, *Appl. Cat.*, **46**, 281, (1989).
120. J.W.E.Coenen and B.G.Linsen, "Physical and Chemical Aspects of Adsorbents and Catalysts", (B.G.Linsen, Fortuin, Okkerse and Steggerada, Eds.), Academic Press, London, (1970), p.495.
121. R.E.Pincock, W.M.Johnson and J.Haywood-Farmer, *Can. J. Chem.*, **54**, 548, (1976).
122. T.Osawa. T.Harada and A.Tai, *J. Mol., Catal.*, **87**, 333, (1994).

123. B.Mile, D.Stirling, M.A.Zammit, A.Lovell and M.Webb, *J.Catal.*, **114**, 217, (1988) .
124. J.W.E.Coenen, *Appl. Catal.*, **54**, 65, (1989).
125. J.J.de Lange and G.H.Visser, *Ingenieur*, **58**, 24, (1946) .
126. M.Popowicz, W.Celler and E.Treszczanowicz, *Int. Chem. Eng.*, **6**, 63, (1966) .
127. J.L.Lemaitre, P.G.Menon and F.Delannay, in "Characterisation of Heterogeneous Catalysts", (F.Delannay, Ed.), Chemical Industries/15, Marcel Dekker, New York, (1984), p.299-365.
128. J.S.Smith, P.A. Thrower and M.A.Vannice, *J.Catal.*, **56**, 236, (1979) .
129. Y.Nitta, F.Sekine, T.Imanaka and S.Teranishi, *Bull.Chem. Soc. Jpn.*, **54**, 980, (1981) .
130. A.S.Cooke and M.M.Harris, *J. Chem. Soc.C*, 2365, (1963).
131. J.J.Rooney, *J. Catal.*, **2**, 53, (1963).
132. E.M.Silverman,R.J.Madix and C.R.Brundle, *J. Vac. Sci. Technol.*, **18**[2], 616, (1981).
133. N.Young, Unpublished results.
134. P.Chiaranussati, L.F.Gladden, R.W.Griffiths, S.D.Jackson and G.Webb, *Trans. Inst. Chem. Eng.*,**71**, 267, (1993) .
135. F.A.Cotton and G.Wilkinson, "Advanced Inorganic Chemistry". John Wiley and sons, 4<sup>th</sup> edition, (1980).
136. A.Tungler, M.Kajtar, T.Mathe, G.Toth, E.Fogassy and J.Petro, *Catalysis Today*, **5**, 159, (1989).
137. C.A.Hunter and J.K.Sanders, *J. Am. Chem. Soc.*, **112**, 5525, (1990).
138. J.Reeder, P.P.Castro and C.B.Knobler, *J. Org. Chem.*, **59**, 11, (1994).
139. P.Qian, M.Matsuda and T.Miyashita, *J. Am. Chem. Soc.*, **115**, 5624, (1993).

140. T.Heinz, G.Wang, A. Pfaltz, B.Minder, M.Schurch, T.Mallat and A.Baiker, *J. Chem. Soc., Chem. Commun.*, 1421, (1995).
141. G.Wang, T.Heinz, A.Pfaltz, B.Minder, T.Mallat and A.Baiker. *J. Chem. Soc., Chem. Commun.*,2047, (1994).
142. A.Ohno, M.Ikeguchi, T.Kimura and S.Oka, *J. Am. Chem. Soc.*, **101**, 7036, (1979).
143. R.M.Kellog, *Agnew. Chem. Int. Ed. Engl.*, **23**, 782, (1984).
144. G.C.Bond, "Catalysis by Metals", Academic Press, New York, (1962).
145. G.C.Bond and P.B.Wells, *Adv. Catal.*, **15**, 92, (1964)
146. I.V.Gostunskaya, V.S.Petrova, A.I.Leonava, V.A.Mironava, M.Abubaker and B.A.Kazanski, *Neftekhimiya*, **7** (1), 3, (1967).
147. E.N.Frankel, "Topics in Lipid Chemistry", (F.D.Gunstone, Ed.), Logan Press, London, (1970), p.6.

